

CANADIAN THESES ON MICROFICHE

THÈSES CANADIENNES SUR MICROFICHE



National Library of Canada
Collections Development Branch

Canadian Theses on
Microfiche Service

Ottawa, Canada
K1A 0N4

Bibliothèque nationale du Canada
Direction du développement des collections

Service des thèses canadiennes
sur microfiche

7

NOTICE

The quality of this microfiche is heavily dependent upon the quality of the original thesis submitted for microfilming. Every effort has been made to ensure the highest quality of reproduction possible.

If pages are missing, contact the university which granted the degree.

Some pages may have indistinct print especially if the original pages were typed with a poor typewriter ribbon or if the university sent us an inferior photocopy.

Previously copyrighted materials (journal articles, published tests, etc.) are not filmed.

Reproduction in full or in part of this film is governed by the Canadian Copyright Act, R.S.C. 1970, c. C-30. Please read the authorization forms which accompany this thesis.

AVIS

La qualité de cette microfiche dépend grandement de la qualité de la thèse soumise au microfilmage. Nous avons tout fait pour assurer une qualité supérieure de reproduction.

S'il manque des pages, veuillez communiquer avec l'université qui a conféré le grade.

La qualité d'impression de certaines pages peut laisser à désirer, surtout si les pages originales ont été dactylographiées à l'aide d'un ruban usé ou si l'université nous a fait parvenir une photocopie de qualité inférieure.

Les documents qui font déjà l'objet d'un droit d'auteur (articles de revue, examens publiés, etc.) ne sont pas microfilmés.

La reproduction, même partielle, de ce microfilm est soumise à la Loi canadienne sur le droit d'auteur, SRC 1970, c. C-30. Veuillez prendre connaissance des formules d'autorisation qui accompagnent cette thèse.

**THIS DISSERTATION
HAS BEEN MICROFILMED
EXACTLY AS RECEIVED**

**LA THÈSE A ÉTÉ
MICROFILMÉE TELLE QUE
NOUS L'AVONS REÇUE**

ANALYSIS OF DIESEL ENGINE PERFORMANCE
USING
OFF-SPECIFICATION WBRF-FUELS

BY

LUC I. MENARD

THESIS SUBMITTED TO THE SCHOOL OF
GRADUATE STUDIES OF THE UNIVERSITY OF
OTTAWA IN PARTIAL FULFILLMENT OF THE
REQUIREMENTS FOR THE DEGREE

OF

MASTER OF APPLIED SCIENCE

IN

MECHANICAL ENGINEERING

SEPTEMBER, 1984



UNIVERSITÉ D'OTTAWA
UNIVERSITY OF OTTAWA

ACKNOWLEDGEMENT

The author would like to express his deepest gratitude and appreciation to Dr. R.C. Flanagan for his valuable supervision and guidance throughout the work. Also the author wishes to thank the Department of Mechanical Engineering Machine Shop, the University of Ottawa Power Plant Group and the Computing Services for the substantial contribution to this project.

In addition, he wishes to thank Dr. R.C. Flanagan for his financial support from the Department of National Defence (Canada) Contract No. 2SUS1-00088, NSERC Grant No. A1638 and teaching assistantships from the Department of Mechanical Engineering, University of Ottawa.

The author would also like to express his sincere thanks to Mrs. Susan Flanagan for her carefulness and patience in typing this thesis.

ABSTRACT

Canadian diesel fuels could see degradation in fuel properties by the 1990's. This thesis is directed at understanding the effects these off-specification fuels may have on the Canadian Forces AVGP-GM6V53T engine.

To understand these effects, and to develop an R & D base capable of projecting and testing engine specification changes required for operation on these fuels, a program involving not only engine-fuels testing but also indicated performance and combustion monitoring was structured.

For the engine test program, fuel-to-fuel comparisons require combustion monitor and indicated parameter determination. Thus, computerized engine control/data acquisition/data reduction and presentation systems were developed to meet the required precision, repeatability and massive data collection required for such studies. The heart of the data acquisition system is an LS111 computer which controls, monitors and samples engine data and interfaces with the lab computer (HP1000) for both on-line and off-line data analysis which, in turn, interfaces with the mainframe Amdahl and Calcomp model 906 plotter for data presentation and modeling interaction.

Approximately ten million samples of data were collected and analyzed for each fuel tested. Full load and part load brake, indicated and combustion characteristic performance curves are presented plus fuel-to-fuel comparison plots of each parameter. To understand the engine-fuel behaviour, the most informative presentation format was found to be parameter maps contoured over the complete operating range of the engine.

Concern exists over the compatibility of the off-specification fuels due to very high pressure rates and gas vibrations which occur over large operating ranges of the engine. The problems are rooted in the early combustion period and an easy 'fix', eg. derating the engine for operation on these fuels, is not to be expected. This combustion behavior could result in premature component failure and it is advised that controlled "durability and transient duty cycle" tests be performed before implementing any extensive field use of these fuels. However, brake characteristic performance from these off-specification fuels were equal to and better than the reference (high quality) 3GP30 diesel fuel.

TABLE OF CONTENTS

	<u>Page</u>
ABSTRACT	1
TABLE OF CONTENTS	ii
LIST OF FIGURES	v
LIST OF TABLES	x
NOMENCLATURE	xi
CHAPTER 1: INTRODUCTION	1
1.1 BACKGROUND	1
1.2 LITERATURE SURVEY	1
1.3 THESIS OBJECTIVES	3
1.4 THESIS OVERVIEW	4
CHAPTER 2: RESEARCH FACILITY	5
2.1 INTRODUCTION	5
2.2 ENGINE INSTRUMENTATION AND TEST CELL FACILITY	5
2.3 SYSTEM CONTROL AND DATA ACQUISITION	14
2.3.1 System Control	14
2.3.2 Data Acquisition	15
2.4 DATA PROCESSING	17
2.4.1 Hardware	17
2.4.2 On-line Data Processing	18
2.4.3 Off-line Data Processing	18
2.4.4 Amdahl Data Processing	19
2.5 TEST PROCEDURES	20
2.5.1 Brake Performance Tests	20
2.5.2 Combustion and Indicated Performance	21
2.5.3 TDC Location Tests	22
2.5.4 General Test Procedure	22
2.6 FUEL SPECIFICATION	26

	<u>Page</u>
CHAPTER 3: TOP DEAD CENTRE (TDC) ANALYSIS	28
3.1 INTRODUCTION	28
3.2 TDC LOCATIONAL ERROR ANALYSIS	28
3.3 PHYSICAL MEASUREMENT OF DYNAMIC TDC	30
3.4 ANALYSIS OF EXPERIMENTAL RESULTS	31
3.5 CLOSURE	33
CHAPTER 4: ENGINE/FUEL CHARACTERISTIC PERFORMANCE.	35
4.1 BRAKE CHARACTERISTIC CURVES	36
4.2 INDICATED CHARACTERISTIC CURVES	36
4.3 COMBUSTION CHARACTERISTICS	37
4.3.1 Test Methodology/Event Definitions	37
4.3.2 Combustion Characteristic Data.	43
4.4 PRESSURE CURVES	44
CHAPTER 5: ENGINE/FUEL CHARACTERISTIC PERFORMANCE COMPARISONS	78
5.1 BRAKE CHARACTERISTIC PERFORMANCE COMPARISONS	79
5.1.1 Maximum Torque Tests	80
5.1.2 Constant Torque (Part Load) Tests	80
5.2 INDICATED CHARACTERISTIC PERFORMANCE COMPARISON	81
5.3 COMBUSTION PARAMETER CHARACTERISTIC COMPARISON	82
5.3.1 Maximum Torque Tests	82
5.3.2 Constant Torque Tests	85
5.4 PRESSURE CURVE COMPARISONS	87
5.5 CLOSURE	90
CHAPTER 6: ENGINE PERFORMANCE MAPS	152
6.1 BRAKE PERFORMANCE MAPS	153
6.2 INDICATED ENGINE MAPS	153
6.3 COMBUSTION PARAMETER MAPS	154

	<u>Page</u>
CHAPTER 7: CONCLUSIONS	168
7.1 OVERVIEW COMMENTS	168
7.2 ENGINE-FUEL ASSESSMENT	170
BIBLIOGRAPHY	172

LIST OF FIGURES

	<u>Page</u>
Fig. 2.1: Facility/Data Acquisition and Control Overview	6
Fig. 2.2: Data Processing Systems	7
Fig. 2.3: Schematic Layout of the Engine Test Cell Facility	8
Fig. 2.4: Engine (Test Cell)	10
Fig. 2.5: Single Cylinder Testing Hardware	10
Fig. 2.6: Main Operator-Control Panel and Computer Monitor/ Interface Terminal	11
Fig. 2.7: Control/Data Acquisition and Processing Systems	12
Fig. 3.1: Calculated IHP Error vs. TDC Locational Error; 2800 RPM, Full Rack, 3GP30 Fuel	29
Fig. 3.2: Study of TDC Shift at 2200 RPM	34
Fig. 4.1: Engine Brake Performance Characteristics. 6V53T Engine, Full Rack, Fuel 1 (3GP30, reference)	45
Fig. 4.2: Engine Brake Performance Characteristics. 6V53T Engine, Full Rack, Fuel 2, (#2-D)	46
Fig. 4.3: Engine Brake Performance Characteristics. 6V53T Engine, Full Rack, Fuel 3 (Shell, 1990)	47
Fig. 4.4: Engine Brake Performance Characteristics, 6V53T Engine, Full Rack, Fuel 4 (1990)	48
Fig. 4.5: Engine Brake Performance Characteristics, 6V53T Engine, Fuel 1 (3GP30, reference)	49
Fig. 4.6: Engine Brake Performance Characteristics, 6V53T Engine, Part Load, Fuel 2 (#2-D)	50
Fig. 4.7: Engine Brake Performance Characteristics, 6V53T Engine, Part Load, Fuel 3 (Shell, 1990)	51
Fig. 4.8: Engine Brake Performance Characteristics, 6V53 Engine, Part Load, Fuel 4 (1990)	52
Fig. 4.9: Engine Indicated Performance Characteristics, 6V53T Engine, Full Rack; Fuel 1 (3GP30, reference)	53

	<u>Page</u>
Fig. 4.10: Engine Indicated Performance Characteristics, 6V53T Engine, Full Rack, Fuel 2 (#2-D)	54
Fig. 4.11: Engine Indicated Performance Characteristics, 6V53T Engine, Full Rack, Fuel 3 (Shell, 1990)	55
Fig. 4.12: Engine Indicated Performance Characteristics, 6V53T Engine, Full Rack, Fuel 4 (1990)	56
Fig. 4.13: Engine Indicated Performance Characteristics, 6V53T Engine, Part Load, Fuel 1 (3GP30, reference)	57
Fig. 4.14: Engine Indicated Performance Characteristics, 6V53T Engine, Part Load, Fuel 2 (#2-D)	58
Fig. 4.15: Engine Indicated Performance Characteristics, 6V53T Engine, Part Load, Fuel 3 (Shell, 1990)	59
Fig. 4.16: Engine Indicated Performance Characteristics, 6V53T Engine, Part Load, Fuel 4 (1990)	60
Fig. 4.17: Effect of Crank Angle Span on the Calculation of Maximum Pressure Rates	61
Fig. 4.18: Engine Combustion Characteristic Curves, 6V53T Engine, Full Rack, Fuel 1 (3GP30, reference)	62
Fig. 4.19: Engine Combustion Characteristic Curves, 6V53T Engine, Full Rack, Fuel 2 (#2-D)	63
Fig. 4.20: Engine Combustion Characteristic Curves, 6V53T Engine, Full Rack, Fuel 3 (Shell, 1990)	64
Fig. 4.21: Engine Combustion Characteristic Curves, 6V53T Engine, Full Rack, Fuel 4 (1990)	65
Fig. 4.22: Engine Combustion Characteristic Curves, 6V53T Engine, Part Load, Fuel 1 (3GP30, reference)	66
Fig. 4.23: Engine Combustion Characteristic Curves, 6V53T Engine, Part Load, Fuel 2 (#2-D)	67
Fig. 4.24: Engine Combustion Characteristic Curves, 6V53T Engine, Part Load, Fuel 3 (Shell, 1990)	68
Fig. 4.25: Engine Combustion Characteristic Curves, 6V53T Engine, Part Load, Fuel 4 (1990)	69
Fig. 4.26: Ignition and Combustion Delays, 6V53T Engine, Fuel 1 (3GP30), Full Load	70
Fig. 4.27: Ignition and Combustion Delays, 6V53T Engine, Fuel 2 (#2-D), Full Load	71

	<u>Page</u>
Fig. 4.28: Ignition and Combustion Delays, 6V53T Engine, Fuel 3 (Shell, 1990), Full load	72
Fig. 4.29: Ignition and Combustion Delays, 6V53T Engine, Fuel 4 (1990), Full Load	73
Fig. 4.30: Typical Average P-CA Curves (Motored and Fired), 6V53T Engine, Full Load, 2200 RPM	74
Fig. 4.31: Typical Average P-CA Curves (Motored and Fired), 6V53T Engine, Part Load, 2200 RPM	75
Fig. 4.32: Typical Average P-V Diagram, 6V53T Engine, Full Load, 2200 RPM	76
Fig. 4.33: Typical Average P-V Diagram, 6V53T Engine, Part Load, 2200 RPM	77
Fig. 5.1: Brake Horsepower Comparison at Full Load	92
Fig. 5.2: Brake Torque Comparison at Full Load	94
Fig. 5.3: Fuel Consumption Comparison at Full Load	96
Fig. 5.4: Brake Specific Fuel Consumption Comparison at Full Load	98
Fig. 5.5: Brake Thermal Efficiency Comparison at Full Load . .	100
Fig. 5.6: Smoke Number Comparison at Full Load	102
Fig. 5.7: Fuel Consumption Comparison at Part Load (Constant Torque)	103
Fig. 5.8: Brake Specific Fuel Consumption Comparison at Part Load (Constant Torque)	105
Fig. 5.9: Brake Thermal Efficiency Comparison at Part Load (Constant Torque)	107
Fig. 5.10: Indicated Horsepower Comparison at Full Load	109
Fig. 5.11: Indicated Specific Fuel Consumption Comparison at Full Load	111

	<u>Page</u>
Fig. 5.12: Indicated Horsepower Comparison at Part Load. (Constant Brake Torque)	113
Fig. 5.13: Indicated Specific Fuel Consumption Comparison at Part Load (Constant Brake Torque)	115
Fig. 5.14: Mechanical Efficiency Comparison at Full Load	117
Fig. 5.15: Mechanical Efficiency Comparison at Part Load	119
Fig. 5.16: Onset of Combustion Comparison Curves at Full Load	121
Fig. 5.17: Ignition Delay Comparison Curves at Full Load	123
Fig. 5.18: Onset of Rapid Combustion Comparison Curves at Full Load	124
Fig. 5.19: Combustion Delay Comparison at Full Load	126
Fig. 5.20: Maximum Pressure Comparison Curves at Full Load	127
Fig. 5.21: Maximum Pressure Rate Comparison Curves at Full Load.	129
Fig. 5.22: Onset of Combustion Comparison Curves at Part Load	131
Fig. 5.23: Onset of Rapid Combustion Comparison Curves at Part Load	133
Fig. 5.24: Maximum Cylinder Pressure Comparison Curves at Part Load	135
Fig. 5.25: Maximum Pressure Rate Comparison Curves at Part Load.	137
Fig. 5.26: Multi-Span Pressure Rate Comparison Plots	139
Fig. 5.27: Pressure Trace Comparison (2800 RPM, Full Load)	140
Fig. 5.28: Pressure Trace Comparison over TDC (2800 RPM, Full Load)	141
Fig. 5.29: Pressure Trace Comparison (2800 RPM, Part Load)	142
Fig. 5.30: Pressure Trace Comparison over TDC (2800 RPM; Part Load)	143
Fig. 5.31: Pressure Trace Comparison (1500 RPM, Full Load)	144
Fig. 5.32: Pressure Trace Comparison over TDC (1500 RPM, Full Load)	145

	<u>Page</u>
Fig. 5.33: Pressure Trace Comparison (1500 RPM, Part Load) . .	146
Fig. 5.34: Pressure Trace Comparison over TDC (1500 RPM Part Load	147
Fig. 5.35: Cracked Head Gasket. Cylinder Number Two, Right Bank.	148
Fig. 5.36: View of the Head and Block. Failed Right Cylinder Bank	149
Fig. 5.37: View of the Head and Block. Left Cylinder Bank (Unfailed)	150
Fig. 5.38: Instantaneous Pressure Rate/Combustion Development Period Relationship	151
Fig. 6.1: B.S.F.C. Map Comparison	157
Fig. 6.2: Brake Thermal Efficiency Map Comparison	158
Fig. 6.3: Fuel Consumption Map Consumption Map Comparison. . .	159
Fig. 6.4: Indicated Specific Fuel Consumption Map Comparison .	160
Fig. 6.5: Indicated Horsepower Map Comparison	161
Fig. 6.6: Indicated Mean Effective Pressure Map Comparison . .	162
Fig. 6.7: Onset of Combustion Map Comparison	163
Fig. 6.8: Onset of Rapid Combustion Map Comparison	164
Fig. 6.9: Maximum Cylinder Pressure Map Comparison	165
Fig. 6.10: Maximum Pressure Rate Map Comparison	166
Fig. 6.11: Maximum Instantaneous Pressure Rate Map Comparison .	167

LIST OF TABLES

	<u>Page</u>
Table 2-1: List of Test Cell Equipment	9
Table 2-2: Test Engine Specifications	13
Table 2-3: Fuel Specification.	27
Table 3-1: Experimental Measurements TDC Location	32
Table 5-1: Numerical Values and Statistical Results. Combustion Parameter Data (Full Load)	83
Table 5-2: Onset of Rapid Combustion Vs. Engine Speed	84
Table 5-3: Numerical Values and Statistical Results. Combustion Parameter Data (Part Load)	86

NOMENCLATURE

AC	Alternating current
BHP	Brake horsepower
BMEP	Brake mean effective pressure
BSFC	Brake specific fuel consumption
BTU	British thermal unit
C.A.	Crank angle
CFM	Cubic feet per minute
CGSB	Canadian General Standard Board
CU. IN.	Cubic inches
DIA	Diameter
°C	Degree celcius
Deg	Degrees
°F	Degree Fahrenheit
FBP	Final boiling point
FT	Feet
Ft-lbs	Foot pounds
GM	General Motores
GMDD	General Motors Detroit Diesel
GPM	Gallons per minute
HP	Horsepower
IBP	Initial boiling point
IHP	Indicated horsepower
IMEP	Indicated mean effective pressure
IN	Inches

I/O	Input/output
ISFC	Indicated specific fuel consumption
KHz	Kilo hertz
MHz	Megal hertz
mS	Milli-seconds
mV	Milli-volts
NRC-FLL	National Research Council Fuel and Lubricant Lab
P	Pressure
P-CA	Pressure vs crank angle
PSI	Pound per square inches
P.T.	Pressure transducer
P-V	Pressure vs volume
RAM	Random access memory
R & D	Research and Development
RPM	Rotation per minute
SAE	Society of Automotive Engineer
TDC	Top dead centre
USGPM	United States gallon per minute
V	Volume
WBRF	Wide boiling range fuel
WOT	Wide open throttle

CHAPTER 1

INTRODUCTION

1.1 BACKGROUND

While Canadian Tar Sands crude oil penetration forecasts vary, it is clear that these vast reserves will eventually provide a significant portion of the Canadian oil demand. It is projected that such penetration will result in off-specification diesel fuels. In this regard, the CGSB fuels panel, through a nation wide survey of the oil industry, concluded that 35 cetane fuel with high end points (to 380°C) could result in the 1990-2000 time frame. It is generally accepted now that this fuel is more likely to see penetration in Canada after the year 2000 and the 1990 fuel will most likely, be a 37 cetane with no significant changes in the end products. As a result, the NRC FLL has produced a 35 cetane fuel, representative of the original 1990 projection, for R & D purposes.

Independent of Tar Sands penetration, the need to develop centers for advanced Canadian R & D into internal combustion engines in general, and compression ignition engines in particular, is becoming increasingly clear. The ability of the Canadian research community to respond to such developments was weak. As observed in a recent paper by Webster [24]: "To date only limited fuel/engine research has been carried out and virtually none directed towards military land and marine powerplants." Further, military requirements make this point even more pressing in that: "military vehicles have a lifetime of 15-30 years, long term engine/fuel compatibility must be designed into new vehicles and modifications made for existing vehicles" [24].

1.2 LITERATURE SURVEY

Diesel engine testing is commonly used to design, rate and monitor pollutants on conventional #2 diesel fuel, but as reported by Whyte and Moyes [23] "Diesel Engines have traditionally been developed and operated on straight run distillates from conventional crude giving cetane numbers in the range 45-55 and little experience is available on the penalties, if any of operating on lower quality fuels".

Preliminary runs were performed on a Detroit Diesel 3-71N, direct injection, two stroke, compression ratio of 18.7 to 1 using standard N65 injectors by Whyte and al. [23]. The fuels used for these tests were blended from various refinery streams to give approximate properties of the 1990-2000 fuels. High cylinder pressure rates and longer than normal ignition delays which might affect engine durability and noise level were of primary concern, whereas the other parameters were within the engine design standards.

Tar sand fuels were run in a Deutz Fil 511D four stroke, naturally aspirated, air cooled, direct injection diesel engine [24] which is representative of future small power plant that may be used by the Canadian Armed Forces. Rated and high output tests were run using 1990-2000 fuels with no part load tests performed. Small differences in brake data were noticed with respect to the data obtained with the high stability reference fuel, with an increase of 7% in BHP for the highest density fuel (Fuel 4). Further, only five engine speeds were tested over the entire engine operating range, thus accurate parameter trends could not be determined. The rates of pressure rise were noted as high but acceptable, although one should examine the method used to calculate them. It consisted of fitting a polynomial to the compression stroke and rapid combustion phase which generated a derived, not measured, value of pressure rate. Derating of the engine was suggested due to high maximum pressures and rates of pressure rise, however it is known that higher pressure rates occur at part load rather than full load engine settings.

Canadian alternate fuels were tested in a 251 Bombardier, 12 cylinder, four stroke, turbocharged, direct injection, marine/rail medium speed diesel engine [25]. The lower engine speed design (maximum 1100 rpm) made it easier to burn off-specification fuels: "None of these test fuels caused any apparent engine operational difficulties over the speed range tested" [25]. The author recommended further tests to monitor cylinder deposits and engine durability.

Light duty automotive diesel engines (as compared to heavy duty military engines) have also been tested (1,26) with fuels close to the same properties as the 1990-2000 fuels with low cetane 30-40 and wider boiling range. Again, pressure rates seem to be the main concern of these studies with acceptable variations of the other parameters.

Tar sands fuels have been tested only in a few industrial type engines whereas simulated tar sands fuels have been tested in a variety of engines. Therefore, a lack of knowledge exists with respect to multi-cylinder high speed turbocharged diesels.

In order to carry out that research, a highly accurate and repeatable data acquisition/control system is required [12, 13, 14; 15]. Such a system was implemented to produce high precision and reliable data without the human factor required to judge equilibrium.

Accurate indicated parameter data can only be achieved with a high precision encoder [1,2] phased to TDC with less than 0.1 C.A. Deg. error. An error of one degree on the location of TDC gives an IHP error of 5-10% [7, 14, 15, 17, 18, 22]. An error of this magnitude would be unacceptable for comparing subtle differences in IHP measurements from fuel to fuel.

1.3 THESIS OBJECTIVES

While diesel engine test codes, procedures and data analysis/presentation are well established for engine to engine performance comparisons; fuel to fuel comparisons on a given engine do not enjoy the same level of procedural, test and interpretation standards. Contrary to the literature reviewed earlier, indicated parameters will also be presented to access fuels. In order to produce reliable indicated data, high precision sampling with an averaging technique to produce average indicator cards is required. As previously mentioned, it is first necessary to accurately locate both static and dynamic top dead center. Moreover, no set procedure had been established, therefore advanced locational methods needed to be developed and TDC measured for the complete RPM range of the engine.

In addition to indicated performance, high precision combustion parameters will also be developed and studied. Further, since combustion parameters are single event data, statistical analysis is required to study the cycle to cycle variation. Also, combustion parameters could become more critical at part load conditions where compression temperatures and pressures are at the minimum. Thus it was decided that indicated performance and combustion parameters, as well as standard brake performance characteristics, should be analyzed at both full and part load characterizations to produce full range maps of all the parameters of interest.

The main objectives of this thesis were to:

- a) Develop an engine test facility that would provide reliable and repeatable brake data to SAE standards.
- b) Study TDC so as to determine and achieve the accuracy necessary for reliable indicated performance studies.
- c) Investigate/define combustion parameters useful for fuel to fuel comparisons.
- d) Investigate the full operating range of the engine for all parameters of interest and explore the possibility of mapping these parameters.

1.4 THESIS OVERVIEW

To meet the preceding objectives, the cell instrumentation was upgraded to SAE standards. However, indicated performance and fuel-to-fuel combustion characterization comparisons required diagnostics well beyond conventional engine testing requirements. To perform the task, it was recognized that repeatable, accurate and extensive amounts of data would have to be collected, handled, reduced and interpreted. Conventionally available data acquisition systems did not provide the perceived capacity nor the vital research component requirement of computer software development flexibility so as to allow investigative 'massaging' of the data. Chapter two gives a summary of the system from the hardware, operation and software points of view.

Indicated performance characterization can be complex. Precision P-CA data, exact TDC location, exact engine physical values and precise numerical integration must come together. Chapter three presents the detailed study conducted so as to precisely define TDC location over the complete engine speed range.

Chapters 4,5 and 6 present the experimentally measured data for the four fuels tested: (i) reference fuel for base comparisons; (ii) commercially available No. 2-D; (iii) an off-specification fuel typical of a best case 1990 product and (iv) a second off-specification fuel typifying the projected 1990 (now 2000) fuel.

Maximum torque and part load characteristic curves of brake, indicated and combustion parameters together with averaged P-CA, P-V and Log P-Log V plots are presented first, for each engine-fuel combination, in Chapter 4.

Multi-fuel comparison plots, for all parameters at both load settings, are presented in Chapter 5 together with a set of single-shot P-CA curves for detailed viewing of fuel combustion characteristics.

In Chapter 6, complete engine maps of all parameters (brake, indicated and combustion), most of which have never been previously viewed, are presented. They provide an exciting insight into engine-fuel behaviour, trending and fuel compatibility evaluation.

CHAPTER 2

RESEARCH FACILITY

2.1 INTRODUCTION

The engine research facility at the University of Ottawa is designed to permit complete engine-fuel performance and comparison tests to SAE standards. A high speed data acquisition and control system allows accurate repeatability from fuel to fuel for brake performance, indicated characteristics and analysis of combustion related parameters. Combustion studies can be performed using the entire engine or, should the fuel under test not be suitable for engine operation, in cylinder #1 only. Further, cylinder #1 instrumentation also allows virtually back-to-back motored/fired P-CA curves to be taken (computer controlled).

On-line statistical analysis of combustion parameters is performed by the HP1000 mini-computer.* Off-line data reduction and processing is performed by the HP and the University mainframe, data transfer being performed by a computer hardware interface. Figures 2.1 and 2.2* give a general overview of the facility, data acquisition, control and data processing systems.

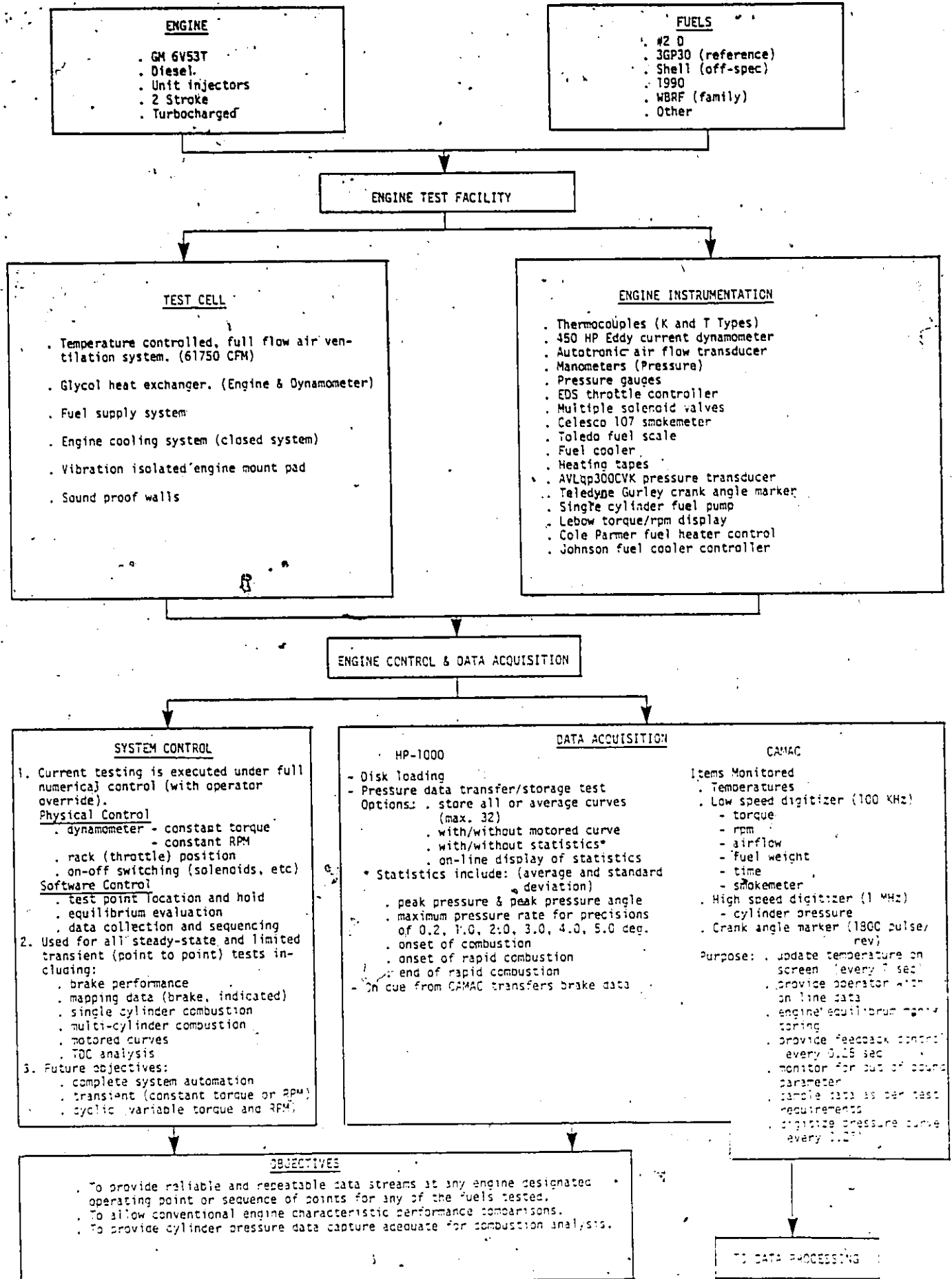
2.2 ENGINE INSTRUMENTATION AND TEST CELL FACILITY

In developing the research test facility, attention was given to the need for high speed data acquisition and precise control for engine-fuel comparisons. Figure 2.3 and Table 2.1 provide a schematic of the facility together with an instrumentation and equipment list. The engine and instrumentation is pictorially presented in Figure 2.4 (engine); Figure 2.5 (single cylinder hardware); Figure 2.6 (control panel) and Figure 2.7 (control/data acquisition and processing systems).

All tests were performed on the AVGP-Canadian Forces Issue - of the 6V53T Detroit Diesel Engine, with specifications as listed in Table 2.2. Of the auxiliary equipment, only the AiResearch turbo charger, air cleaner, fuel filter and engine oil filter are in use. The Canadian Forces personnel carrier vehicle uses an electrically driven fan, thus the fan was removed (as recommended by the SAE code for "Net" brake performance testing). Before any tests were performed, all the equipment instrumentation and engine were calibrated to specification.

* See reference 36.

ENGINE TESTING - CONTROL - DATA ACQUISITION



DATA PROCESSING

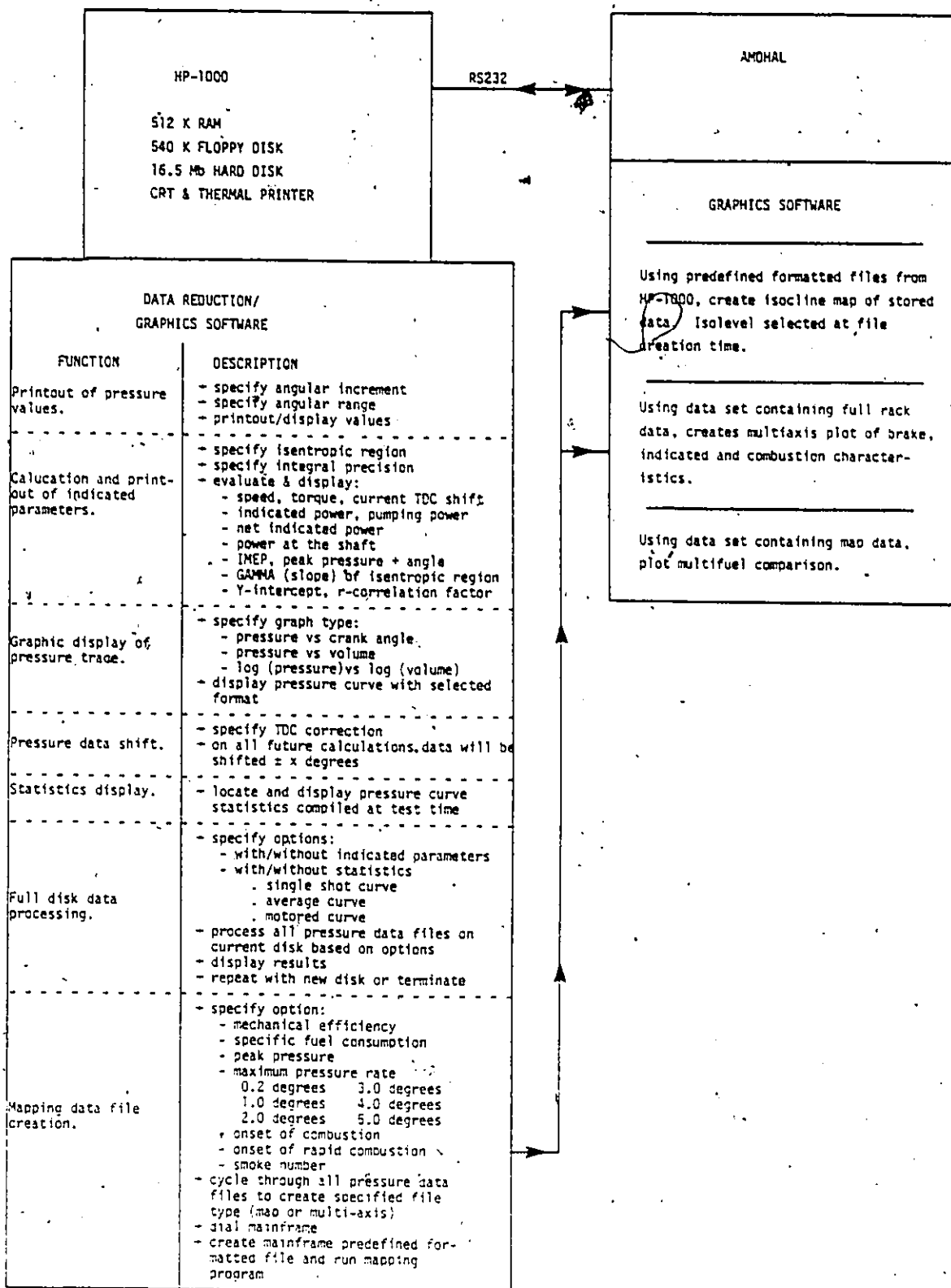


Fig. 2.2: Data Processing Systems

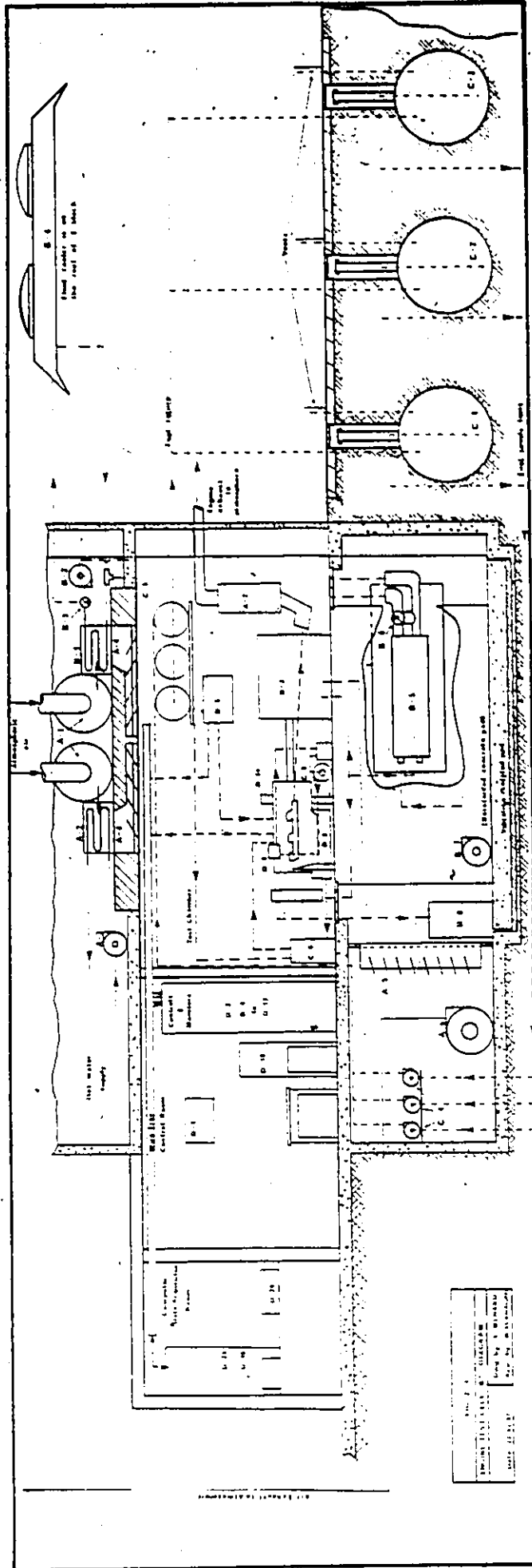


Fig. 2.3: Schematic layout of the Engine Test Cell Facility

Fig. 2.3	Sheet No.	1
Project No.	1000000	
Drawn by	V. Srinivasan	
Checked by	M. Srinivasan	
Date	20/11/2000	

TABLE 2-1: LIST OF TEST CELL EQUIPMENT

LIST OF TEST CELL EQUIPMENT		
ITEM	NAME	NOTES
SYSTEM "A": CELL VENTILATION		
A-1 A-2 A-3 A-4 A-5 A-6	Supply fans (2) Hot water condenser coils Hot water supply pump Supply dampers Exhaust damper Exhaust fan	10 H.P. motors, 61,750 CFM 200 GPM, 2 rows of tubes, 4,000 RPM 2 H.P. motor, 200 GPM, 25 ft. of head Pneumatic controls in D-1 Pneumatic controls in D-1 20 H.P. motor, 61,750 CFM
SYSTEM "B": ENGINE COOLING		
B-1 B-2 B-3 B-4 B-5 B-6 B-7 B-8 B-9	Glycol condenser coils Glycol circulation pump Three-way valve Fluid cooler Heat exchanger Three-way valve Cooling water pump Surge tank Engine cooling tower	200 GPM, 2 rows of tubes, 4,000 MBH 5 H.P. motor, 300 GPM, 52 ft. of head Diverts glycol to B-4 when supply air is hotter than 60°F. 5 H.P. motors (2), forced convection 185 GPM of water, range (190/170°F), 1,850 MBH Diverts glycol into B-5 when cooling water is hotter than the set point adjusted in D-1 1 H.P. motor, 63 GPM, 100 ft. of head 45 gallon drum 22,000 BTU/hr open heat exchanger
SYSTEM "C": FUEL SYSTEM		
C-1 C-2 C-3 C-4 C-5 C-6 C-7 C-8	Gasoline tank WBRF tank Diesel tank Supply pumps (3: Viking) Cell tanks (3) Weigh scale and fuel tank Fuel cooler Auxiliary fuel pump	500 IMP gallons 500 IMP gallons 500 IMP gallons 1/3 H.P. motors, SUSGPM, 60 ft. of head Return lines and vents, piping meets ASTM standards 50 lbs/6 gal. capacity Fuel return cooler - fuel/water Single cylinder monitoring
SYSTEM "D": CONTROL AND MONITORING		
D-1 D-2 D-3 D-4 D-5 D-6 D-6a D-7 D-8 D-9 D-10 D-11 D-12 D-13 D-14 D-15 D-16 D-17 D-18 D-19 D-20 D-21	Honeywell cabinet Dynamometer controls Dynamometer (Dynamatic) RPM counter (Standard) Air flow transducer/analog computer Pressure transducer Single cylinder testing accessories Temperature control Temperature control Smokemeter Amplifier Weight Digital readout Temperature monitors Throttle control Dynamometer control Pressure reading Switches Online combustion space monitor CAMAC crate HP 1000 Thermocouple boards	Controls for systems A and B Engine speed and Eddy current absorption: 450 H.P., 1600-6000 RPM Model SG6,0-6000 ± 10 RPM Autotronic Controls Corporation AVL QP300CVK water cooled Multiple Asco valves Cole Parmer fuel heater control Johnson control fuel cooler control Celeasco model 107 AVL 3059 P.T. amplifier 3130 Toledo scale (fuel) Lebow (RPM, Torque, HP) 3 ELPH Thermo electric E.D.S. SPC 7100 Cte rpm, cte torque Multitype pressure gauges/manometer Tektronix scope

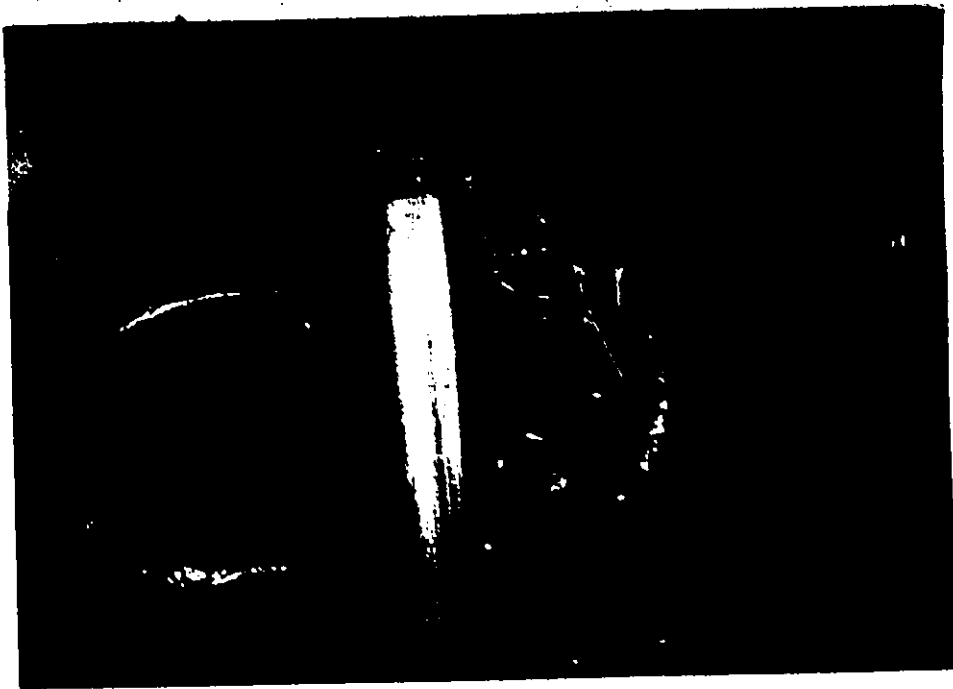


Fig. 2.4: Engine (Test Cell)



Fig. 2.5: Single Cylinder Testing Hardware

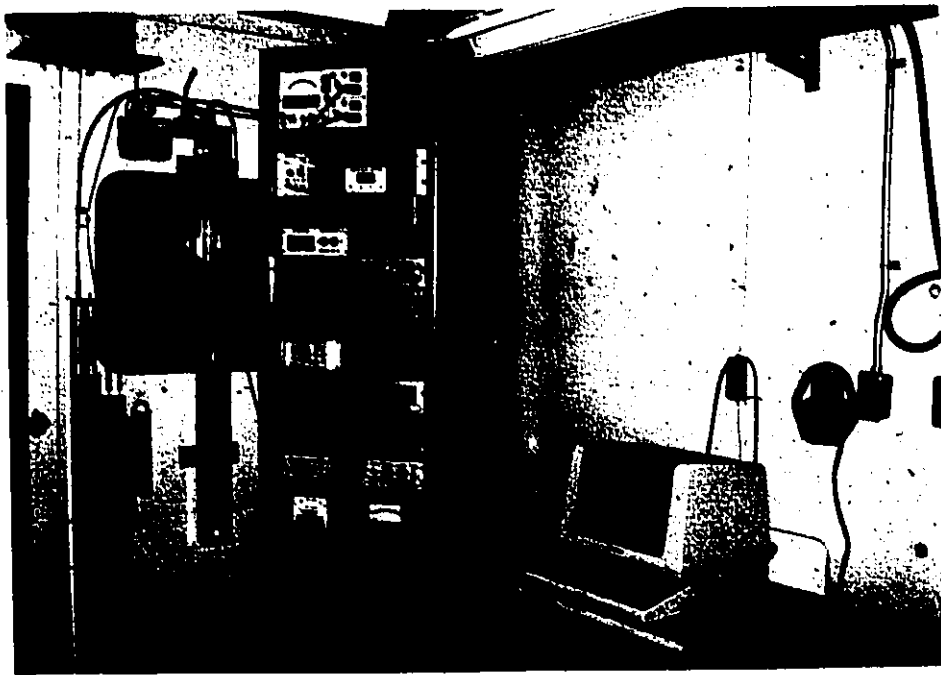


Fig. 2.6: Main Operator Control Panel and
Computer Monitor/Interface Terminal

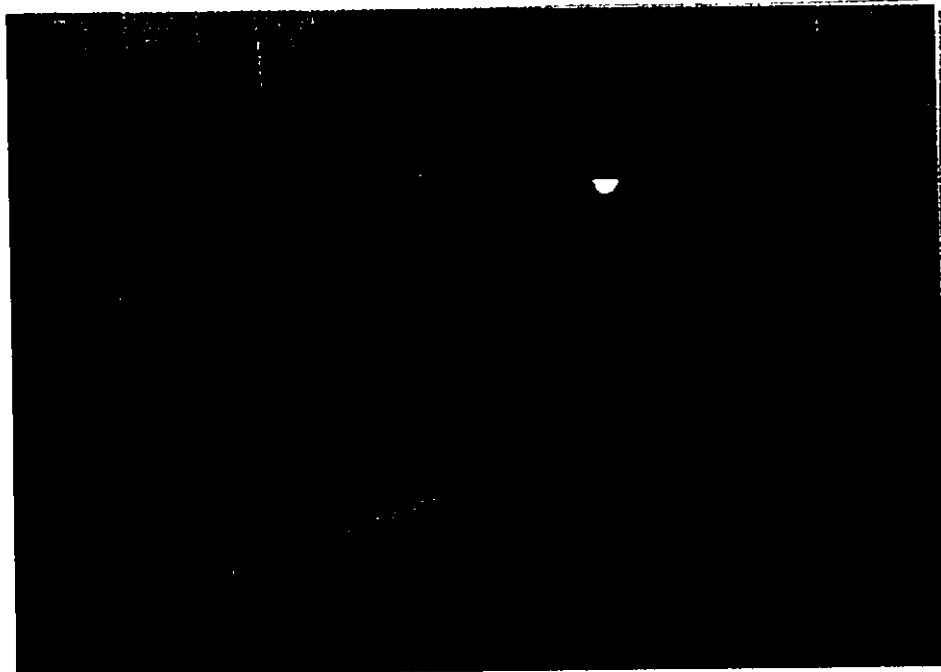
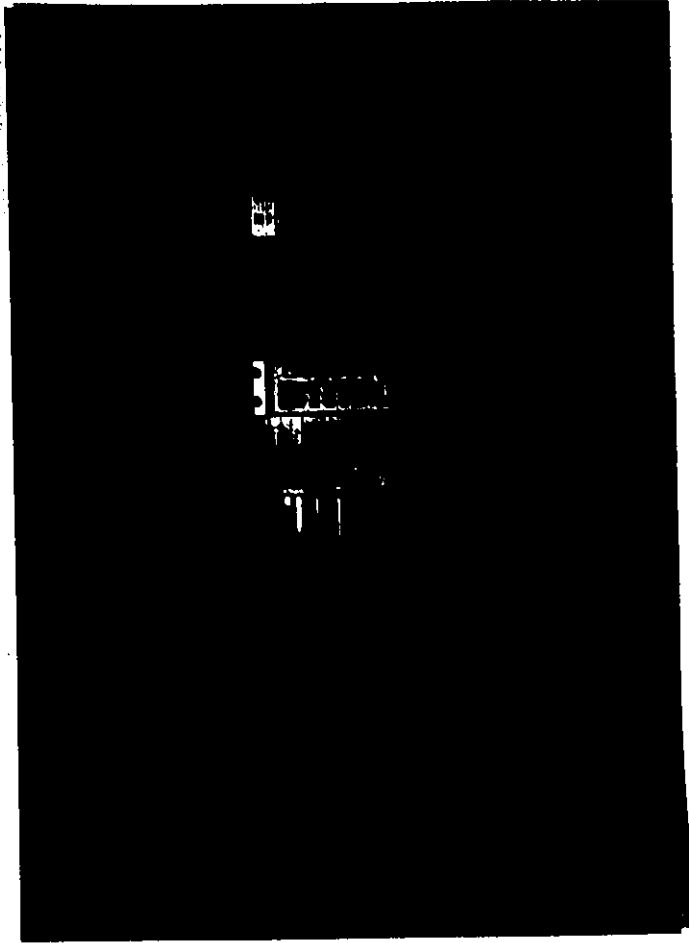


Fig. 2.7: Control/Data Acquisition and Processing Systems

TABLE 2-2

TEST ENGINE SPECIFICATIONS

Manufacturer	Detroit Diesel Allison Division (GMDD)
Model	6V53T (5063-5394), Turbocharged
Type	Two cycle; compression ignition
Compression ratio	17.5:1
Compression pressure	525 psi @ 600 rpm
Idle speed	500-600 rpm
Governed speed	2800 rpm
Number of cylinders	6
Firing order	1L-3R-3L-2R-2L-1R
Rotation	Right hand (clockwise)
Bore	3.875 in (98.4 mm)
Stroke	4.500 in (114.3 mm)
Piston displacement	318 cu. in (5.22 l)
Gross horsepower	275 @ 2800 rpm (nominal)
Valve clearance	cold - 0.026 in. hot - 0.024 in.
Coolant temp.	160 - 180°F (72-82°C)

Auxiliary equipment:

- 100 amp Motorola alternator
- AiResearch turbocharger
- Air compressor
- Hydraulic pump
- Air cleaner
- Fuel filters
- Engine oil filter
- Cold start attachment
- Jacobs brake

2.3 SYSTEM CONTROL AND DATA ACQUISITION

This section provides an overview of the control/data acquisition system (Fig. 2.1) developed for the engine-fuels research objectives.

2.3.1 SYSTEM CONTROL

The control system is divided into three parts, namely:

- i) CAMAC Hardware,
- ii) Test Cell Hardware, and
- iii) Control Software

CAMAC Hardware

The CAMAC controlling hardware consists mainly of two control cards in the crate itself.

The model 3112, eight channel, 12 bit D/A converter is mainly used to proportionally control the dynamometer and throttle controller. The precision on the instrument is 1 part in 4096 on a range of 0-10V which gives a minimum voltage increase of 2.4 mV per unit digit increase.

The model 3080-8 bit output register with AC switches controls the on/off requirements of the system. Being a normally open switch, it provides an easy way to design a failsafe system. The present use of this card is to control the taking of the motored curve.

Test Cell Hardware

The test cell hardware is divided into two groups.

- Proportional control: This section includes both dynamometer controls and the throttle controller. The first dynamometer control sets the desired RPM for the engine whereas the second control applies a constant torque over the entire range of the engine. For its part, the throttle controller sets the injector rack position from a reference signal from the CAMAC.
- On/off control: The engine motored curve facility is controlled in this manner. When the solenoid is activated, the fuel is cut to cylinder #1. This is done at the command of the operator and/or the CAMAC control card.

Control Software

The software resides in the brains of the CAMAC crate, namely the Digital LSI 11/23 micro computer system which contains a dual diskette drive, terminal interface, diskette interface and a crate controller.

The software uses a feedback control system in that it samples the required parameter, makes the necessary correction and sends it to the control card. This correction is performed at 0.25 sec intervals. This feedback control system provides an accuracy of ± 3 RPM and ± 2 ft-lbs. torque for discrete point testing. The software also controls timing for data sampling and the sequencing of the motored curve.

2.3.2 DATA ACQUISITION

The CAMAC data acquisition components process/digitize signals from the engine-dynamometer mounted transducers. The control software, dictated by the requirements of a specific test, identifies the data, rate and sequence of sampling.

The following CAMAC cards are used in the data acquisition portion of the CAMAC crate.

- LeCroy 8210 digitizer with one memory module:
 - Frequency: 1 MHz (MAX)
 - No. of channels: 4
 - Precision: 10 bits
 - Storage: 32 Kword
 - Function: channel 1 - digitize cylinder pressure, triggered by pulse generator (1800 samples per revolution).
 - channel 2-4 - not used

LeCroy 8212 digitizer:

Frequency: 100 KHz (MAX)

No. of channels: 8

Precision: 12 bits

Function: channel 1 - rpm
channel 2 - torque
channel 3 - air flow
channel 4 - fuel flow (weight)
channel 5 - K units (smoke)
channel 6 - opacity (smoke)
channel 7-8 - not used

Two Kinetic Systems 3525 temperature monitors:

Scan time/channel: 175 ms

Update time (16 chan.): 2800 ms

Accuracy: $\pm 0.1^\circ\text{C}$

No. of channels: 16/card

Function: K-type thermocouples:
channel 1 - exhaust before turbo charger
channel 2 - exhaust at smokemeter
channel 3-16 - not used

Function: T-type thermocouples:
channel 1 - oil
channel 2 - air box
channel 3 - coolant left bank
channel 4 - coolant right bank
channel 5 - coolant inlet
channel 6 - inlet fuel
channel 7 - air inlet
channel 8 - fuel tank
channel 9-16 - not used

Kinetic Systems 3655 timing pulse generator:

Frequency: 1 MHz (MAX)

No. of channels: 8

Function: to provide counting system time base

Kinetic Systems 3610 counter:

Frequency: 50 MHz (MAX)

No. of channels: 6

Function: to provide precision timing of events for testing.

2.4 DATA PROCESSING

The bulk of the data reduction and processing is handled by the HP-1000 operating in both on-line and off-line modes. The on-line task consists of uploading P-CA data sampled by the CAMAC, analyzing the combustion related parameters and establishing the statistics, Average fired P-CA curve and motored curve..

Off-line functions include uploading the brake test data, generating and analyzing brake and indicated characteristic performance and isocline map data packages, reformatting and transferring the data to the mainframe for graphical presentation.

2.4.1 HARDWARE

HP 1000:

The usable random access memory (RAM) is 512K partitioned into segments plus two 270K mini floppy disk drives and one 16.5 megabyte Winchester hard disk.

Communication paths are provided firstly to the CAMAC system via two 16 bit parallel I/O cards accessible through system software and secondly to the Amdahl mainframe via an eight port RS-232 serial I/O interface also accessible through system software. It should be noted that only one of the eight ports is used for communication with the mainframe. The remaining seven ports are for use by other terminals attached to the HP-1000.

Data display is effected on the system graphic terminal using, again, system software. A thermal printer is contained in the terminal thus providing a hardcopy of the data present on the screen.

Amdahl:

The usable virtual memory is 2 Megabyte. Mass storage is provided by seven 3350-disk cylinders which yield approximately 3.2 Megabyte in total.

The facilities of the Amdahl include a CALCOMP Model 906 plotter capable of producing plots to a maximum size of 87.5 cm by 100 meters. Extensive software libraries are provided both for the CALCOMP plotter as well as program development support.

2.4.2 ON-LINE DATA PROCESSING

This and the next two sections are used to describe the various data processing capabilities now offered at the University of Ottawa facilities. The term On-line refers to data processed while the test is on-going, specifically:

- Pressure data storage, and
- Statistical evaluation of pressure data

Pressure Data Storage *

This is the main combustion test feature in that pressure digitized data is transferred from the LECROY memory to HP mass storage in two formats. The first stores the entire digitized curve into a permanent RPM and Torque name dependent file. The second is a transient data file containing a specific region of the pressure data to be analyzed statistically once all pressure traces at a given torque and RPM are amassed.

Statistical Evaluation*

The basic objective of the statistical analysis pack is to establish combustion parameter evaluation for individual pressure curves. Once these parameters are evaluated, the mean and standard deviation as well as the mean and standard deviation of the angular occurrence are calculated. A list of the current statistics available are given in Figure 2.2.

2.4.3 OFF-LINE DATA PROCESSING

During an engine-fuel test, only P-CA data is transferred to the HP for on-line analysis thus providing a pressure monitor capability to the test engineer. All other brake and gross parameter data can be monitored directly by the operator on the CAMAC terminal. Both data sets are permanently stored on floppy disk. For off-line processing, the CAMAC stored data is reformatted and forwarded to the HP.

The HP is used for all experimental data analysis. This includes specific investigations (eg. TDC analysis, P-CA data shift, P-V and Log P-Log V, etc.); data reduction (eg. brake performance characteristics, integral P-dV and indicated performance characteristics, etc.); generation of plot and isocline map files* (eg. brake and indicated performance plots - constant torque or full rack; brake, indicated or combustion isocline map files - BSFC, ISFC, peak pressure, pressure rate, etc.); and for the routing of data to the system graphics terminal or to the Amdhal mainframe. The list of functions is outlined in Figure 2.2.

2.4.4 AMDAHL DATA PROCESSING

The HP forwards to the mainframe all reduced data for characteristic plots and isocline maps plus, for each test point, the cylinder pressure traces (1800 points per trace) in three formats: the averaged fired curve, the averaged motored curve and a single shot fired curve.

Graphical presentation by the mainframe takes several forms: engine-fuel performance curves and isocline maps; multi-fuel comparison plots; and experimental-analytical comparison plots.

Characteristic Performance Curves

This program utilizes either brake or indicated parameters and creates multi-axes plots of the engine-fuel characteristic performance at full-rack or at any specified brake torque. Two options exist for the curve fit. Option 1: using cubic regression, a 'smooth' curve is fit to the data points which, in turn, do not necessarily fall on the line. Option 2: using a cubic spline a 'continuous' curve is drawn 'through' all data points. This routing uses a piecewise third-degree polynomial for each set of two adjacent points. The polynomial passes through the plotted points and matches the first and second derivatives of neighboring segments at the points.

Isocline Mapping*

The program is essentially an isocline or contour mapping program applied to a grid matrix. Grid ordinates are engine torque (or BMEP) and engine RPM. Any type of grid data can be used; brake, indicated or combustion parameters - the most common being brake specific fuel consumption to produce an "engine map".

To increase precision, this program first expands the grid data (every 100 RPM and 50 ft-lb brake torque) by interpolation to a matrix of size 101 by 101 from which the operator-specified isoclines are searched, evaluated and plotted.

Pressure Trace Plotting

This software package is responsible for producing high precision/high resolution plots to provide in-depth insight into the character of the fuel burn. From the pressure vs. crank angle trace a wealth of information is obtained: Pressure versus Crank Angle, Pressure vs. Volume, Log (pressure) vs. Log (Volume), pressure rates, peak pressure and location, onset of combustion and rapid combustion, net indicated work and virtually all indicated characteristic parameters.

It should be noted that all of the above information is preprocessed by the HP-1000 and the data transmitted to the Amdahl mainframe via the RS-232 data link.

Multi-Fuel Comparison Plots

This program is used to compare the characteristic performance of the engine when operated on different fuels. Data from each fuel 'file' is read and presented on a common plot. Typically, two operating conditions of the engine are used: full rack or maximum torque and brake torque equal to 250 ft-lbs. Curve plotting options are as discussed previously under 'Characteristic Performance Curves'.

2.5 TEST PROCEDURE

A number of experimental tests were performed to derive the fuel-engine interaction with respect to the four fuels tested namely:

Brake Performance Tests:

- a) Engine characteristic curves (full rack)
- b) Engine mapping (part rack)

Combustion Monitor:

- a) Single cylinder
- b) Multi cylinder
- c) Motored

TDC Location Study:

Proximity probe

2.5.1 BRAKE PERFORMANCE TESTS

Standard characteristic performance tests (full rack or maximum torque) were conducted for each fuel. Readings were taken every 100 RPM from 1500-2800 RPM.

Additionally, each fuel was tested over the complete operating grid used for mapping and intermediate setting performance curves. The grid consists of 149 test points: every 50 ft-lbs of brake torque from 100 to maximum at every 100 RPM from 1500 to 2800 RPM.

2.5.2 COMBUSTION AND INDICATED PERFORMANCE

Three types of combustion monitoring and indicated performance tests were performed:

- a) Single-Cylinder (P-t, P-CA),
- b) Multi-Cylinder (P-t, P-CA on cylinder #1), and
- c) Motoring (P-t, P-CA on cylinder #1).

a) SINGLE-CYLINDER TEST

Single-cylinder combustion tests are used for a number of purposes, viz:

- As a preliminary test to evaluate the fuel's suitability for the engine (eg. observe pressure rates, knock, operability, etc.).
- To perform combustion characteristic studies on fuels that would not otherwise operate in the engine (can be executed at any engine speed chosen by the operator).
- To perform combustion tests on fuels that would harm the standard fuel delivery system of the engine.
- To perform combustion tests on fuels that require higher feed pressures to avoid flashing.
- To perform complete combustion analysis studies on any specialty fuel when brake performance data are either already known or not desired or when specialty fuel supply is limited.

This test is performed using the specialty fuel in cylinder #1 only and #2D or reference fuel in the other five cylinders. Therefore, brake results are meaningless but combustion analysis and data are complete.

A different procedure is used for this type of test. The standard start-up procedure using #2D or reference fuel in all six cylinders is followed. Once the proper operating temperature is reached for the first testing point, the specialty fuel is then switched on for the combustion data recording. This procedure is followed for the required testing points after which the engine is switched back to regular fuel for the cool off period.

b) MULTI-CYLINDER TEST

Multi-cylinder combustion monitoring was carried out for each of the four fuels in the same manner as the Brake Performance tests using the specialty fuel in all six cylinders. A complete set of data, brake and/or combustion, was taken over the full torque-RPM range of the engine. Such a data set is used when fuel supplies are adequate and combustion characteristics suitable for complete engine/fuel analysis.

c) MOTORING TEST

Motoring tests are not independent from any of the above performance or combustion tests described. To perform the test, No. 1 cylinder injector is simply switched to the NO-FUEL position (computer controlled). In this manner, a motored P-t (P-CA) curve can be recorded virtually back-to-back with firing P-t (P-CA) curves, during any of the above test procedures, when desired by the operator. Such tests provide valued data re pumping losses (any engine rpm), indicated performance analysis, engine modeling data correlation and provide a key indicator test on engine condition and wear.

2.5.3. TDC LOCATION TESTS

These tests were used to calibrate the location of the crank-angle marker with respect to dynamic top-dead-centre. Precise measurement of TDC is quite critical due to the sensitivity of indicated performance calculations with respect to TDC location. The general subject is treated in Chapter 3.

To perform the tests, a proximity probe (response to 600,000 RPM) was inserted into the engine in lieu of the pressure transducer, and adjusted so as to provide the closest approach of the piston. The instrumentation of cylinder No. 1 allowed a complete range of TDC tests including: cold motored, hot motored and fired, at any RPM. A total of four probes were used in order to complete all tests.

2.5.4. GENERAL TEST PROCEDURE

A general procedure is used in testing together with 'options' which allow tailoring a test to a specific objective.

General Procedure

Manually start instrumentation for warmup.

- Lebow digital display
- weigh scale (toledo)
- Celesco smokemeter (after warmup verify calibration)

- pressure transducer amplifier
- air flow computer
- throttle controller
- crank angle marker

. Start and boot CAMAC and HP computers

. Verify:

- engine oil level
- coolant flow in pressure transducer
- air flow in smokemeter
- water coolant in smokemeter
- dynamometer bearing oil level
- fuel level in tank

. Open water supply to dynamometer

. Turn on main power switch to dynamometer and engine cooling system

. Turn on engine cooling circulation pump

. Turn on main ventilation system

7 . At this point it is recommended that the system instrumentation and equipment be allowed a thirty minute warm-up period.

. Verify smokemeter calibration - calibrate if necessary

. Turn on dynamometer

. Start main testing programs on HP and CAMAC.

At this time, the CAMAC takes over the test cell and prompts operator assist as required.

. First, the CAMAC executes the following:

- verify if there is enough space on disk to store required test data
- sets initial crate condition (initial cards, set limits....)
- ask the operator if this is a fully automated test or if operator interaction is required (operator interaction is defined as to supplying points to be tested)
- the program now enters the warm-up subroutine, sets the dynamometer and throttle position initial values
- the operator is now asked to start engine and turn on fuel heaters

- . The warm up subroutine will let the engine idle for 1.5 minutes then slowly bring it up to 2000 rpm, 200 ft-lbs until the coolant temperature has reached 70.0°C.
- . The operator is prompted for the different options and the first test point. If the fully automated version was chosen at the start, then the CAMAC will look in a data file to set the required option and test point.
- . Using the feedback control system, the engine is brought to the required test point. The engine is then monitored for critical parameters until the engine has reached equilibrium. (Temperature variation less 2°C in two minutes.)

At this point, the CAMAC takes the required data in sequence. Throughout the data collection sequence, the engine is held at the prescribed test point by monitoring and updating the engine RPM and torque every 0.25 second.

- A complete set of brake, gross parameter and auxiliary (eg. temperatures) data is taken and stored, (set 1).
- A P-CA shot is taken (four consecutive P-CA curves) and a signal sent to the HP to upload the pressure curves, (set 2).
- Set 2 data is repeated eight times in order to provide thirty-two P-CA curves to the HP for statistical analysis (on-line) of the pressure and combustion related parameters.
- Two further samples of set 1 data are taken, the second sample after sixteen pressure curves (mid point) and the third sample at the end.
- During the taking of the cylinder pressure traces, the operator manually takes the different manometer readings and environmental conditions.
- The motored curve is then automatically taken and sent to the HP.
- Set 1 and set 2 data (reduced) are stored on the dual diskette drives of the CAMAC and HP respectively. The HP will display the P-CA combustion data and statistics.

A complete set of data for a discrete test point is now recorded and stored. The CAMAC will now proceed to the next test point or prompt the operator for the next point and the cycle is repeated. When the end of a test sequence is reached, the engine will be set to idle for three minutes then shut-off.

Options

Multiple test options give the test procedure flexibility to accommodate the range of tests performed.

<u>Option No.</u>	<u>Function/Purpose</u>
1	Manually (through keyboard) tell the HP that there is no other pressure curve coming. This is used when the operator finds an error in the system.
2	Will send the actual values of the torque to the HP for file creation during maximum torque test instead of the nominal value given at start of the test.
3	The program will not send any pressure traces to the HP. Used to calibrate instrumentation or to perform a brake test alone.
4	Used to resume sending of pressure traces to HP - nulls option 3.
5	Used to enter new equilibrium time, default value is two minutes.
6	Used to change the number of P-CA traces sent to HP, default value is 32.
7	Used to change equilibrium temperature, default value is 2°C.
8	Equipment calibration test for motored curve.
9	Nulls option 8.
10	Nulls option 2.
11	The cylinder pressure traces are taken by LSI 11/23 and stored on diskette (can do only one test point at a time).
12	Special TDC test with proximity probe, no engine warmup is used. A special code is entered when the operator is prompted for automated or operator control.

2.6 FUEL SPECIFICATIONS

A total of four fuels were tested. Two 'standard or conventional' fuels and two 'off-specification' fuels. A list of fuel specification data is given in Table 2-3.

CONVENTIONAL FUELS

- a) 3GP30 reference fuel (Fuel 1: FLO 79657). This fuel meets the Canadian General Standard Board (CGSB), 3-GP-30 standard for high stability diesel and was selected as the reference fuel.
- b) Commercial grade #2D from a local supplier, (Fuel 2). This fuel was used for all preliminary testing, calibration runs, proofing of the D/A system, etc....and providing commercial grade engine fuel characteristics. Due to the great amount of characteristic variability between each shipment, no complete analysis was performed on this fuel and, therefore, does not appear in Table 2-3.

OFF-SPECIFICATION FUELS

- a) 'Shell' test fuel (Fuel 3) - A blend comprising 40% of a distillate cut from western Canadian tar sands crude with 60% from conventional western Canadian crude both from the St. Boniface Refinery. This fuel provided an example of a best case fuel with a substantial percentage of tar sands derived products.
- b) Low Cetane (Fuel 4) - A blend comprising 78% of a distillate cut from a 50/50 mixture of conventional western Canadian and tar sands crude and 22% of hydrogen treated cracked stock. This provided a fuel containing a substantial level of aromatics and cracked components and is typical of diesel fuel quality predicted for the 1990-2000 time frame.

TABLE 2-3

FUEL SPECIFICATION

PROPERTY	FUEL 1	FUEL 3	FUEL 4
Density @15°C, kg/L (D1298)	.8403	.8463	.8783
Distillation (D86)			
I.B.P., °C	173	171	164
10% recovered, °C	203	196	196
50% recovered, °C	257	236	268
90% recovered, °C	323	287	354
F.B.P., °C	351	306	381
Recovered % vol.	98.0	98.0	98.3
Carbon Residue, % mass (D524)	1.9	1.6	1.8
Cloud Point, °C (D2500)	-12	-43	-8
Pour Point, °C (D97)	-18	-54	-39
Kinematic Viscosity @40°C, mm ² /S (D445)	2.41	1.90	2.78
Ash, % mass (D482)	0.000	0.000	0.002
Water and Sediment, % vol. (D1796)	0.000	0.000	0.000
Sulphur, % mass (D1552)	0.21	0.21	0.53
Nitrogen Content (chemiluminescent)ppm by wt	-	30	-
Flash Point, °C (D93)	57	60	60
Total Acid No. mg KOH/g (D974)	0.03	0.01	0.03
Corrosion, 3 hr. @100°C (D130)	1a	1a	1a
Cetane Number (D613)	46.7	36.9	35.9
Cetane Index, ASTM (D976) CGSB	48.0	40.0	40.0
Aniline Point, °C (D611)	64.4	49.8	46.9
Carbon (By Difference) % mass	86.6	86.39	87.83
Hydrogen Content, % mass (D3701)	13.4	12.08	12.17
C/H-Ratio	6.6	7.15	7.2
Smoke Point, mm (D1322)	17.0	14.7	12.1
Heat of Combustion, MJ/kg (23.4M)	45.63	45.54	44.94
Hydrocarbon Type Analysis			
Saturates and Olefins, %	77.8	60.4	56.02
Poly-Aromatics and Polar Compounds, %	0.9	0.2	1.63
Total Aromatics %	21.3	39.4	42.35

CHAPTER 3

TOP DEAD CENTRE (TDC) ANALYSIS

3.1 INTRODUCTION

Precision in the determination of indicated and combustion parameters are of prime importance for the work related to this thesis. The high precision of these parameters permits close fuel to fuel comparison necessary to properly evaluate each fuel.

Such parameters are difficult to measure and if any validity is to be placed on the experimentally derived values, accuracy must be guaranteed. A number of potential 'traps' exist, all of which can give rise to substantial experimental errors. One of these is the precise determination of TDC for the complete speed range of the engine and the exact correlation between crank angle position and cylinder pressure measurements.

The critical nature of TDC and its potential as a source of large errors, easily rendering all indicated calculations useless, cannot be over emphasized. Because of its importance, together with the difficulty of defining and locating TDC, a number of special studies were conducted prior to any fuels testing. This chapter reports on these special investigations and defines the locational accuracy required and achieved for the 6V53T engine-fuel studies.

3.2 TDC LOCATIONAL ERROR ANALYSIS

To demonstrate and establish the accuracy required in locating TDC, Fig. 3.1 plots the absolute value of the calculated IHP error, i.e. $| \text{IHP (calculated)} - \text{IHP (actual)} |$, against the crank angle degree error in locating TDC. The demonstration plot is at 2800 RPM, full load with Fuel 1.

The results of Fig. 3.1 are somewhat surprising but clearly demonstrate the point in question. For the 6V53T engine, a ± 1.0 crank angle degree error in TDC location results in a calculated IHP error of 31.5 HP ($+1.0^\circ$) to 32.5 HP (-1.0°), or approximately 10% errors.

TOP DEAD CENTER STUDY (IHP CHANGE)

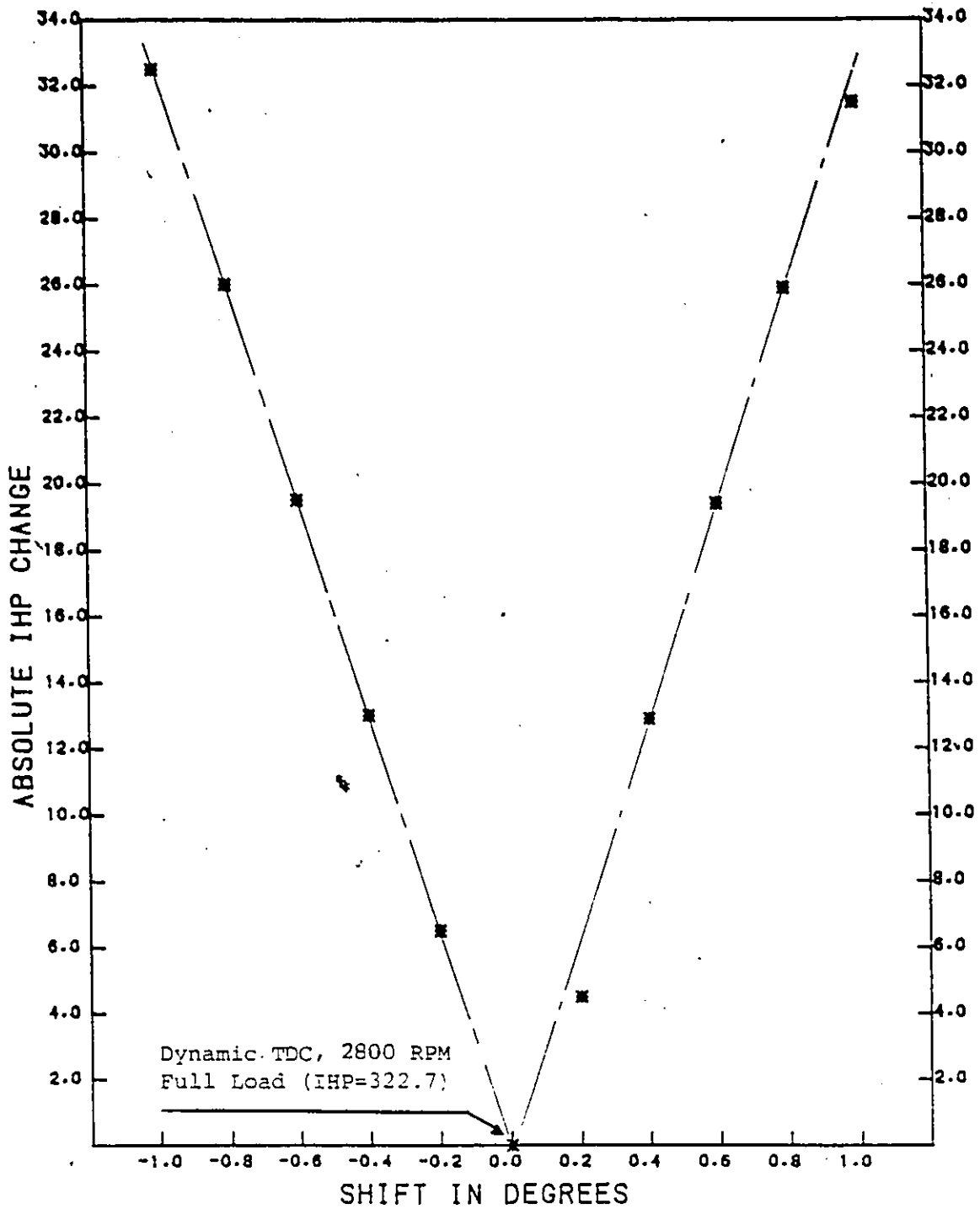


Fig. 3.1: Calculated IHP Error vs. TDC Locational Error, 2800 RPM, Full Rack, 3GP30 Fuel

For fuel-to-fuel comparisons, an error band of 1.0% or less is required. Thus, from the figure, the locational accuracy of TDC must be within ± 0.1 crank angle degree during the dynamic conditions of pressure measurement.

The problem is further complicated since the required accuracy gives rise to the question of static vs. dynamic TDC location. Under dynamic conditions, gas pressures and inertia forces (which maximize over TDC), bearing clearances, component stressing (torsional and elongational strains), etc., can be expected to affect TDC with respect to a static determination. Further, even without this complication, it is virtually impossible to locate static TDC to within ± 0.1 crank angle degrees as this angular motion of the crank represents only about four millionths of an inch in translational motion of the piston.

3.3 PHYSICAL MEASUREMENT OF DYNAMIC TDC

Of the various techniques considered, an in-cylinder non-contact, direct measurement technique was chosen. A Bently-Nevada 7200 Series proximity probe was inserted into the combustion space and adjusted so as to measure the closest approach of the piston (i.e. TDC). Probe sensitivity is 200 mv/mil and can sense proximity of a metallic object (piston) to approximately 1 mv. Frequency response is 0-600,000 RPM. Thus, the probe can sense piston proximity to within ± 0.1 crank angle degree, as required.

It should be noted that thermal drift and linearity were not important to the measurements since only the closest approach of the piston to the probe was being measured, not any actual distances.

The probe system was interfaced with the data acquisition system, the probe signal being fed into the 8210 Lecroy high speed digitizer. The digitizer was triggered by the 1800 pulses/revolution rotational marker used for engine testing. The pulse generator was synchronized with static TDC using the probe and a millivolt meter. Thus, static TDC was set to within ± 0.2 crank angle degrees (accuracy of the pulse generator or crank angle marker).

A total of four probes were used with a burn-out (major problem) of the first probe before any measurements could be made. A series of 107 TDC measurements were taken over the operating speed range of the engine under three operating conditions: (i) cold motored; (ii) hot motored; and (iii) fired. The various conditions were selected to observe the effect of oil viscosity and thermal expansion (cold motored vs. hot motored) and the effect of gas pressures (motored vs. fired) on dynamic TDC location. It should be noted that the instrumentation and physical set-up of cylinder number (Chapter 2) was well suited to these tests, particularly for the fired tests where fuel was injected in the cylinder only during the TDC measurement.

Table 3-1 lists the experimental data measured with each probe and the test condition. Engine RPM was changed for each measurement, i.e. back-to-back measurements at a given RPM were not used. All measurements of TDC location are relative to the static setting of the crank angle marker.

Probe 2 was used for repeat studies/measurements (1200 and 2000 RPM) and for hot-cold comparison studies. The probe three study was conducted differently from probes 2 and 4 in that the engine was started and data collected against increasing RPM until probe burn-out at 2700 RPM. Probe 4 was used to check fired TDC in both the low and high RPM range.

3.4 ANALYSIS OF EXPERIMENTAL RESULTS

From the experimental data (Table 3.1), three important observations can be made:

1. Dynamic TDC for the 6V53T engine did not shift for the various test conditions, viz: cold motored - hot motored - fired.
2. TDC measurements were highly repeatable for all test conditions and test probes.
3. There is a clear TDC 'jump' at 2200 RPM.

TABLE 3-1

EXPERIMENTAL MEASUREMENTS - TDC LOCATION
(Relative to the Crank Angle Marker Static TDC Setting)

RPM	PROBE 1	PROBE 2		PROBE 3	PROBE 4			NOTES
		Cold Motored	Hot Motored		Cold Motored	Hot Motored	Fired	
750	Burnout before vents were made.	0.2,0.0		0.0	0.3	0.3		Average TDC location = 0.20 Standard Deviation = 0.08.
1000		0.2,0.0		0.2 C	0.2	0.1		
1200		0.3,0.2,0.4	0.4,0.3,0.3,0.3,0.3	0.4 L	0.4			
1400		0.2,0.2		0.2 D	0.1,0.2			
1500		0.2,0.3	0.4,0.4	0.3	0.3	0.2,0.2	0.3	
1600		0.2,0.2		0.2	0.3			
1700		0.2,0.4		0.4	0.0,0.0			
1800		0.0,0.2		0.0	0.1,0.0			
1900		0.0,0.3,0.4,0.4		0.4	0.2			
1925		0.2						
1950		0.3						
1975		0.2						
2000		0.2,0.2,0.0,0.2	0.0,0.4,0.0,0.4	0.2	0.1	0.2		
2050		0.2						
2075	0.1			0.0	0.0,0.3			
2100	0.2,0.1							
2200	0.9		1.0	0.8,1.1			Average = 1.00 Std. Dev. = 0.08	
2300	1.2		0.8	1.0,0.8	1.4	1.1		
2400			0.9 H	0.8,0.8				
2500			1.0 O	0.9,0.9				
2600	1.4		1.4 T	0.9,1.0				
2700	0.8			1.0,1.1,0.9				
2800	1.3			1.0,0.9,0.9				

Analysis of the data reveals that from idle to 2100 RPM, dynamic TDC can be considered constant at an average value of 0.20 crank angle degrees (relative to the static setting of the crank angle marker) with a standard deviation of only 0.08. Likewise, from 2200 RPM to maximum (2800 RPM) dynamic TDC is constant at an average value of 1.00 crank angle degrees (relative to static setting) with a standard deviation of, again, only 0.08. Further, linear regression curve fitting to the data shows virtually a straight, near zero slope line with a maximum deviation from the average of 0.03 crank angle degrees.

The experimentally observed shift at 2200 RPM from 0.20 to 1.00 degrees required further investigation to determine whether this was indeed an angular displacement shift, as observed, or just a localized shift (i.e. restricted to the TDC area).

To resolve this, a maximum torque engine test was conducted over the operating speed range of the engine. Brake horsepower and two sets of indicated horsepower were plotted. The first IHP calculations were corrected according to the measured TDC location: namely, shifted by 0.20 crank angle degrees from 1500-2100 RPM then shifted by 1.00 degree from 2200-2800 RPM. The second IHP curve was calculated using a 0.2 degree shift for the full speed range.

Figure 3.2 plots the resulting measured BHP and calculated IHP for the two TDC shift conditions. The smoothness of the BHP curve through this region (2100-2200 RPM) together with the two IHP curves clearly establishes that the observed TDC shift at 2200 RPM is indeed localized at TDC and cannot be used for IHP integration over the complete cycle. Further, the smoothness of the constant 0.2 degree shift IHP curve suggests that the observed shift is very localized and should be ignored for IHP and indicated parameter calculations and that the 0.2 degree shift should be used for the full engine speed range.

3.5 CLOSURE

From this analysis, dynamic TDC for the 6V53T engine was accurately determined within the required ± 0.1 crank angle degrees. Further, TDC does not change with RPM within the bounds of the required accuracy, nor does it change for any dynamic operating condition: namely, cold motored, hot motored or fired.

Further, the maximum difference between static and dynamic TDC that could be inferred from this study is a shift of 0.4 degrees, the minimum change being zero. Although the crank angle marker was zeroed at static TDC using the probe, the setting accuracy of the marker is ± 0.2 crank angle degrees (i.e. the pulse step of the marker). Thus, static and dynamic TDC for the 6V53T engine would appear to be very close.

TOP DEAD CENTER STUDY (IHP)

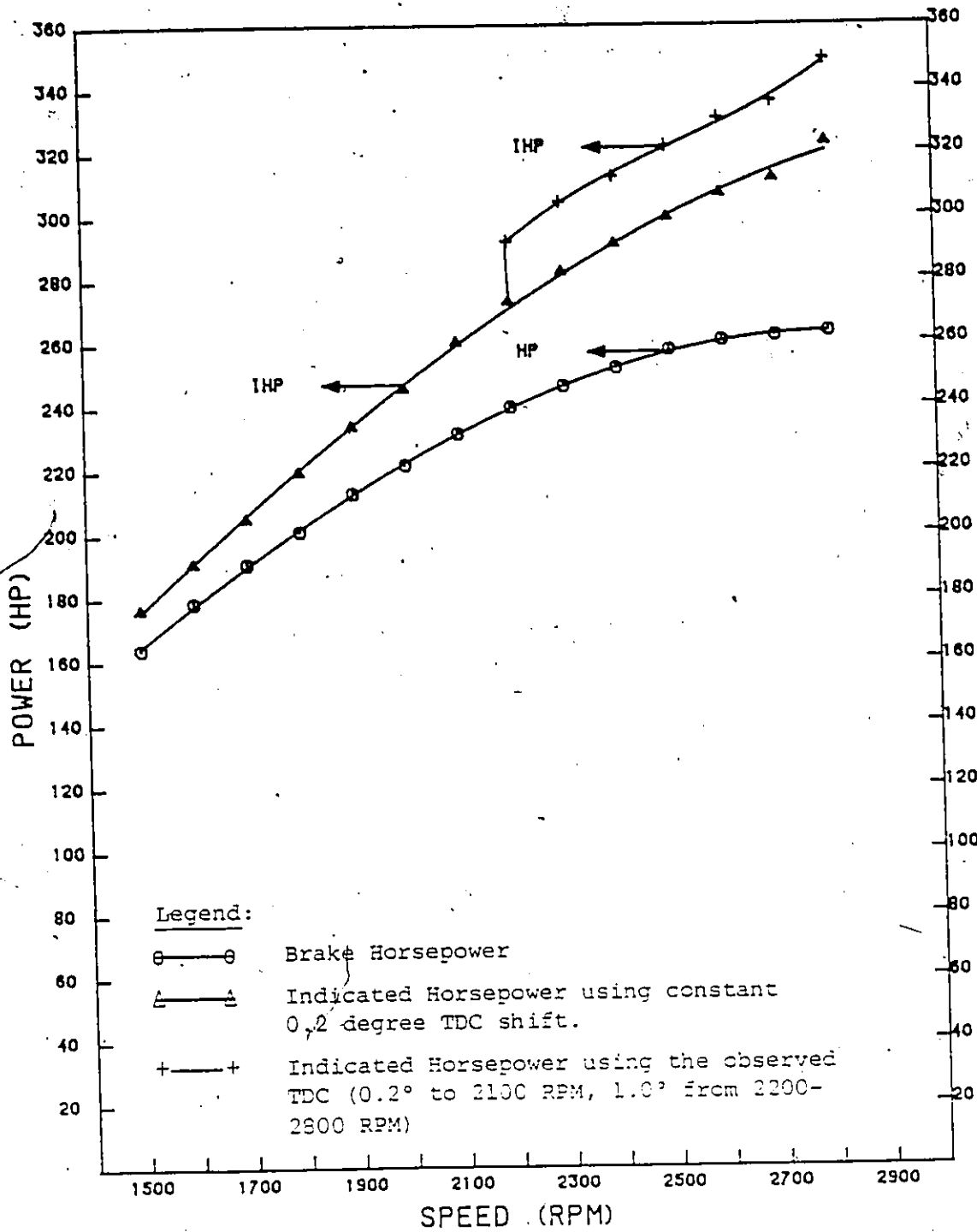


Fig. 3.2: Study of TDC Shift at 2200 RPM

CHAPTER 4

ENGINE/FUEL CHARACTERISTIC PERFORMANCE

Engine brake characteristic curves (full rack or WOT) have become an industry standard for engine 'performance' comparison, and are highly suited for engine-to-engine comparisons when operated on standard fuels. However, the thesis objective is to assess not only engine 'performance' but, in particular, engine operability and fuel suitability to a particular engine (6V53T) with respect to sub-standard fuels. Full rack characteristic performance provides valued, but very limited insight into operability and fuel suitability.

For this objective, approximately ten million samples of data are taken for each fuel tested. This data bank for each fuel allows reduction and presentation in both standard and unconventional formats including: brake, indicated and combustion parameter characteristic presentation at full rack or any selected torque setting; statistical analysis of combustion parameters; ** mapping of all parameters over the operating speed-load range of the engine and the viewing of P-CA, P-V or Log P-Log V curves, averaged, single-shot or motored at any desired operating point.

Brake performance characteristic curves reflect those parameters that a vehicle operator will observe. These are presented for each fuel in section 4.1. Both full rack and part load* characteristic curves are presented. To further understand the characteristic performance behavior, a complete set of indicated characteristic curves, at both load settings, are also presented in section 4.2.

It is believed that combustion characteristics will provide the greatest insight into operability and suitability of each fuel to the engine. As such, combustion characteristics of each fuel are presented in section 4.3 together with P-CA and P-V plots (section 4.4).

The main purpose of this chapter is to 'present' the brake, indicated and combustion characteristics of the engine when operated on each of the four fuels tested, whereas Chapter 5 will present comparison plots and appropriate discussion.

* Part load conditions selected throughout this thesis are at a brake torque equal to 150 ft.lbs. which is about the mid power setting for the engine.

** See reference 10.

4.1 BRAKE CHARACTERISTIC CURVES

Brake characteristic curves are the most commonly used parameters for engine performance comparison. These curves include: brake horsepower, brake torque, brake mean effective pressure, brake specific fuel consumption, brake thermal efficiency and smoke. The first five parameters are corrected for ambient conditions under SAE test code J1349.

Full rack brake performance curves are presented in Figures 4.1-4.4, whereas part load (torque = 250 ft.lb) characteristics are given in Figures 4.5-4.8, for each of the four fuels tested. It should be noted that the commercial grade #2-D (Fuel 2) was used to establish calibration procedures and use of the smoke meter, as such, smoke is not plotted on the #2-D characteristic parameter plots, Figures 4.2 and 4.6.

4.2 INDICATED CHARACTERISTIC CURVES

Indicated performance characteristic curves show what is actually developed within the combustion space of the engine and, as such, provide a clearer insight into engine-fuel performance. Basically, the parameters are the same as their brake counterparts, numerical differences being directly accountable to engine mechanical losses.

However, indicated performance is difficult to measure; the essence of the calculations being the experimentally recorded P-CA data and the accurate location of top dead centre (TDC). For this calculation, data was recorded every 0.2° CA (1800 points per revolution) with a cylinder pressure sensitivity of ± 2 psi. Further, an average P-CA curve, based on 32 single-shot curves, was used for the P-dV numerical integration. Separate tests show very high repeatability on indicated parameter calculations (less than 1% variation on the tests performed).

Indicated characteristic curves include: indicated horsepower, indicated torque, indicated mean effective pressure, indicated specific fuel consumption and indicated thermal efficiency. The plots also show the smoke number recorded. Again, indicated parameters are corrected for ambient conditions under SAE test code J1349.

Figures 4.9-4.12 give the indicated parameters at full rack, figures 4.13-4.16 plot the part load characteristics. The indicated characteristics show expected trends. IHP will reflect the air breathing capacity of the engine. The test engine, being turbocharged, shows a fairly linear IHP curve with RPM (eg. Fig. 4.9) and a moderately flat indicated torque. The roll-off in BHP and brake torque (Fig. 4.1) are principally due to increasing mechanical losses with engine speed. For a naturally

aspired engine, this roll-off will be substantially more pronounced due to the roll-off in volumetric efficiency.

4.3 COMBUSTION CHARACTERISTICS

Combustion characteristic data provides considerable insight into the suitability of a fuel and a means of interpreting characteristic performance results. However, unlike brake performance characteristics, combustion parameters are not well defined and methods of data collection, evaluation and presentation are not an established practice. The combustion characteristic data evaluated in this study are: (i) start of injection; (ii) onset of combustion; (iii) onset of rapid combustion; (iv) maximum pressure rate location; (v) location of maximum pressure; (vi) maximum cylinder pressure and (vii) maximum pressure rate.

4.3.1 TEST METHODOLOGY/EVENT DEFINITIONS

For the seven combustion characteristic events identified above, a test and data collection procedure had to be established. Further, while identification of some of the events is obvious, others, and in particular: start of injection, onset of combustion, onset of rapid combustion, delay period and pressure rate calculations must be clarified or defined.

Test Procedure

It is important to recognize that combustion characteristic data are "instantaneous" events occurring once per revolution of the engine (two-stroke) as opposed to engine performance data which are "average" events, eg. RPM, torque, etc. Further, of particular interest in understanding the combustion behavior of off-specification fuels is the question of cycle-to-cycle repeatability and the variability or scatter of the data set itself. Thus, statistical analysis of the combustion events was considered to be important.

The procedure adopted was to extract all combustion events from 'single-shot' P-CA curves. A total of thirty-two such curves are collected to allow calculation of the average value of the event and the standard deviation. For further clarity, it could be noted that the combustion events are not calculated from the average P-CA curve (an averaged curve would conceal combustion events but is required for indicated performance calculations) but rather from the single-shot curves to provide a data

set of thirty-two samples for each event. Further, a digitizing rate of 0.2 CA degrees was used at all test points (1800 points per revolution) and eight sets of four consecutive single-shot P-CA curves were sequenced and collected as outlined in Chapter 2.

Start of Injection

The 6V53T, being a unit injection design, does not allow easy access for instrumentation in order to monitor fuel injection timing. Various techniques were assessed and reviewed. The following excerpt summarizes:

"I have enclosed a copy of SAE Paper 780161 which describes Detroit Diesel's injection system model. At your request, we have used this model to simulate the N-65 injectors in your 6V-53T engine (model no. 5063-5394) for 14 engine speeds and 5 throttle settings at each speed. The 70 computer outputs showing the injection rate, injection pressure, beginning of injection, etc. are enclosed.

In response to your request to measure the fuel injection timing on an engine, I have reviewed the following methods with our injection group:

- strain-gaged injector tip
- strain-gaged check valve cage
- needle lift indicator
- strain-gaged rocker arm
- load cell on injector follower
- accelerometer on injector body

None of these methods would give you satisfactory accuracy and reliability, so we cannot recommend any of them. For our own combustion simulation work, we use the beginning of injection provided by the injection simulation program with the recognition that it may be in error by a degree or two because of manufacturing and adjustment tolerances.*

For the full-rack (maximum torque) tests, start of injection is taken directly from the GM data supplied. However, for part load conditions, interpolation of the data sets is required and correlated through the mass of fuel injected and engine RPM. The injection model developed interpolates start and end of injection to all crank angle degrees. *This

* From correspondence with Richard E. Winsor, Supervisor, Performance and Modeling, GM-DDA Division, September 19, 1983.

accuracy was found to be somewhat coarse for both the experimental data and therefore, the model is being refined.

Thus, for this study, start of injection is taken directly from the analytical model, the full-rack data being retrieved directly from the GM data supplied while part-load data was interpolated to $\pm 0.5^\circ$ CA.

Onset of Combustion

Onset of combustion is interpreted, in this study, to mean the point where combustion is sufficiently sustained so as to create an appreciable or measurable deviation of the cylinder pressure over that of a purely motored pressure curve.

Depending on the experimental set-up, identification of this point of pressure deviation could be very difficult to measure. However, as outlined in Chapter 2, our cylinder instrumentation allows virtually back-to-back motored/fired pressure measurements to be taken. Further, as detailed in Chapter 3, highly accurate crank angle position phasing for cycle-to-cycle comparison has been achieved.

A number of techniques to identify motored/fired pressure curve deviation were explored. The most reliable indicator for a single-shot pressure curve, which typically exhibit short duration fluctuations, was found to be the slopes of the pressure curves, i.e. instantaneous pressure rates, $\Delta P/\Delta\theta$ where $\Delta\theta = 0.2^\circ$ CA. A set of numerical experiments were conducted to evaluate the 'slope indicator' over the operating range of the engine. The maximum motored instantaneous pressure rate for the 6V53T was found to be 38.5 psi/ $^\circ$ CA with a typical upper range of 34-36 psi/ $^\circ$ CA. Thus, onset of combustion was taken to occur when the fired pressure gradient exceeded 40 psi/ $^\circ$ CA for three consecutive readings (0.6 crank angle degrees). The following observations are also worthy of note:

- (i) The slope indicator used could not be generally applied and would not likely be constant for any throttled engine (Otto), in such cases, direct comparison of the pressure curves (or slopes) at each test point would likely be required.
- (ii) Examination of the pressure data sets suggests that there are elements of combustion occurring earlier than identified by the slope indicator. However, such combustion does not provide a 'sustained, appreciable' affect on the cylinder pressure.

Onset of Rapid Combustion

In a diesel engine, the ignition delay period or onset of combustion is followed by a 'rapid combustion period' characterized by a high rate of energy (heat) release and a corresponding high rate of pressure

rise.* This results from autoignition and flame propagation occurring simultaneously in the spary envelope and is also the 'diesel knock' region. The severity of the pressure rate or knock intensity is roughly proportional to the mass rate of fuel

Thus, the onset of rapid combustion (high heat release rate) is characterized by a high pressure rate and can be identified as that point when pressure rate reaches a 'threshold value'. The difficulty arises in defining the threshold value to be used. Here however, the threshold rate value should be a constant and applicable to all diesel engines, both naturally aspirated and turbocharged. However, no standard values could be found, thus, it again became necessary to define a suitable threshold value. Defining this value became further complicated due to the fact that no standard exists for pressure rate calculations (see following section - Pressure Rate Calculation).

To gain perspective, numerical pressure rate experiments were conducted from which a threshold value of 75 psi/°CA, based on an instantaneous rate calculation, was selected. The basis of the selection is as follows:

- (i) The lowest pressure rates were found to occur at full load and maximum speed for the 6V53T engine. Instantaneous rate values up to about 134 psi/°CA (about 90 psi/°CA using a one degree CA span) were reached.
- (ii) Whenever the pressure rate reached the selected value, all experiments showed that the high energy release period was occurring and maximum cycle rates always followed usually within one crank angle degree. The following data sets, taken from average P-CA curves and representing the two extreme operating regions of the engine, exemplify:

1500 RPM, PART LOAD (T = 250 Ft.Lbs.)	
°CA (TDC = 180)	Instantaneous Pressure Rates
.174.0	54.0
.2	75.5
.4	119.5
.6	158.5
.8	215.0
175.0	215.5
.2	222.5
.4	180.0
.6	111.5

(a)

*Assuming normal ignition delays and injection timing so as to bring on this high energy release period prior to TDC.

2800 RPM, FULL LOAD (T = Max)	
°CA (TDC = 180)	Instantaneous Pressure Rates
168.8	50.0
169.0	57.0
.2	56.5
.4	73.5
.6	97.5
.8	104.5
170.0	96.5
.2	62.5

(b)

Thus, the selected value of 75 psi/°CA, based on an instantaneous rate calculation, is sufficiently above onset of combustion rates for a turbocharged diesel engine yet should be low enough to be suited to a naturally aspirated engine. More importantly, it was a threshold value which always indicated onset of rapid combustion.

For this study, the instantaneous pressure rate is taken to be equal to $\Delta P/\Delta\theta$ where $\Delta\theta = 0.2^\circ\text{CA}$. Clearly, if larger crank angle measurements are used, this basic relationship would no longer be representative of instantaneous rates. As such, other approaches, such as curve fitting, would be required.

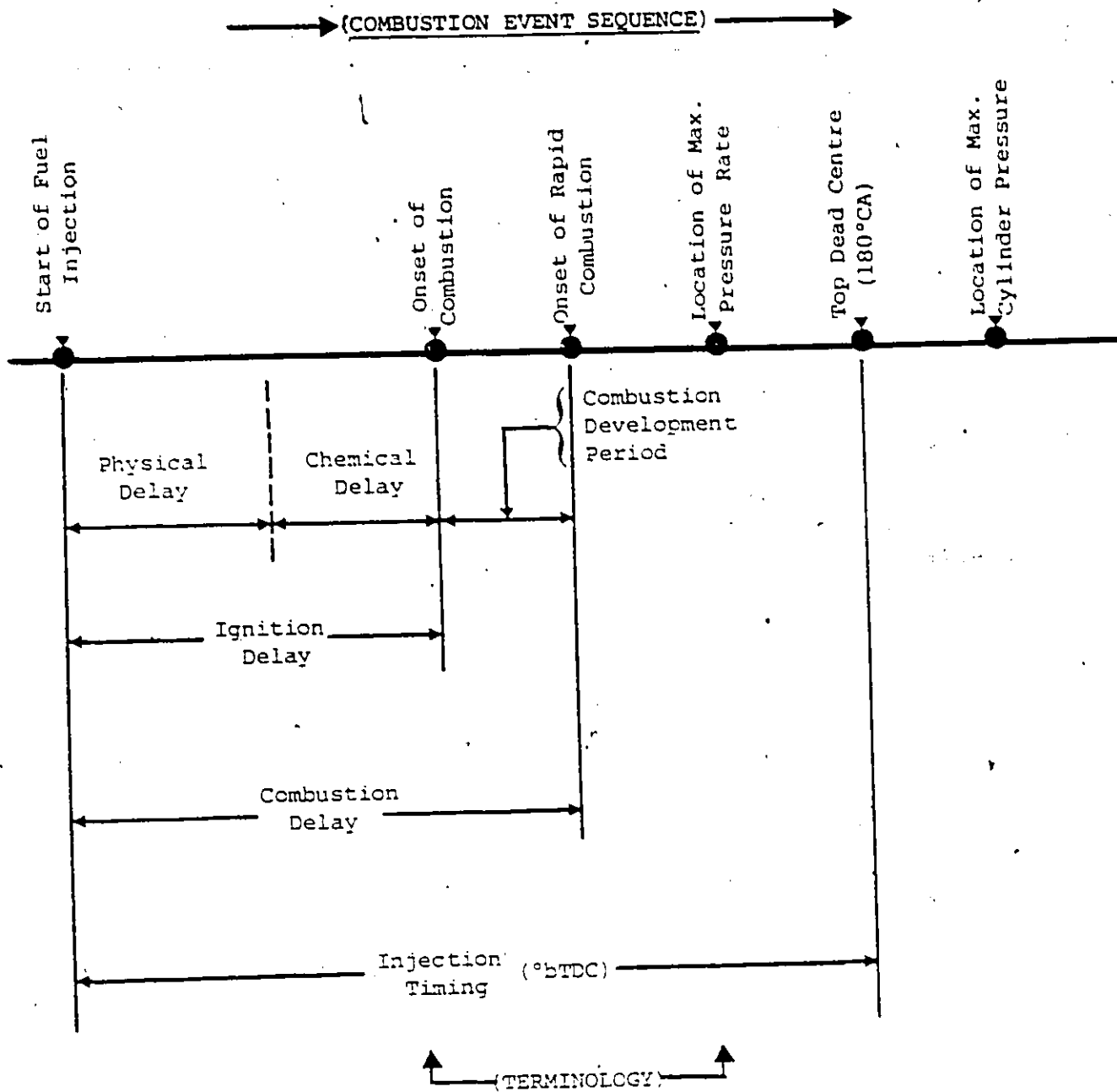
Delay Period Definitions

In studying the combustion event data, it became clear that the classical terminology of 'injection timing' and 'ignition delay' were not adequate to completely describe the observed results. Hence, two new additional terms are used, namely: (i) combustion delay and (ii) combustion development period.

Combustion delay is similar to ignition delay and is the period (measured here in °CA) from injection to the onset of well developed or established combustion in the cylinder. In this study, the onset of established combustion is taken as the 'onset of rapid combustion' defined above.

The period (measured here in °CA) from where combustion is in evidence until combustion is well established is defined here as the 'combustion development period' and is, numerically, simply the difference between combustion delay and ignition delay.

The following sketch, showing the combustion event sequence, pictorially presents the terminology used.



Pressure Rate Calculation

While it is not uncommon to see pressure rate data in the literature, there again does not appear to be a standard established for its calculation. Studies made indicate that the crank angle span (angular displacement over which the rate calculation is made) must be defined.

Figure 4.17 shows, for Fuel 1 (3GP30), typical maximum pressure rates calculated from the same data using crank angle span as a parameter. The search uses, for all spans, a 0.2°CA step. It is clear that this parameter plays an important role in the numerical value determined for pressure rate and must be defined if such rates are to be used in engine/fuel studies.

For this study, pressure rates are calculated using a one degree crank angle span unless noted as instantaneous rates where a 0.2°CA span is used. The choice of 1°CA is somewhat arbitrary however, much smaller spans could be misleading due to rough combustion effects, etc., and larger values tend to conceal the maximum pressure rate region.

4.3.2 COMBUSTION CHARACTERISTIC DATA

Full rack combustion characteristic curves are presented in Figures 4.18-4.21, part load settings are presented in Figures 4.22-4.25, for each of the fuels tested. It is worth noting, at this time, that maximum pressure rate conditions will occur (typically) at low-speed/part-load operation whereas maximum pressures will occur at high-speed/maximum-load settings.

On the right hand ordinate, the plots provide, as a function of RPM, the crank angle position ($\text{TDC}=180^\circ$) where combustion related events occur in the cylinder starting with the location of start of fuel injection (from the model developed with GM data), followed by the onset of combustion, the onset of rapid combustion and ending with the location of maximum pressure. Clearly, the relative position of the first three curves gives directly the ignition and combustion delay periods. In addition, maximum pressure rates (psi/deg) and maximum cycle pressures (psia) are plotted against the left hand ordinate. These parameters are considered to be important in assessing fuel suitability.

Finally, Figures 4.26-4.29 plot directly the ignition and combustion delays, measured in crank angle degrees, for each of the four fuels tested at full rack (maximum torque) conditions. These values are not independently plotted for the part load conditions since the calculation of start of injection ($\pm 0.5^\circ\text{CA}$) was found to be too coarse. However, full insight into their trends and behavior is easily seen from the combustion characteristic plots, Figures 4.22-4.25. It should be noted, at this time, that the combustion delay period ($^\circ\text{CA}$) is very much independent of engine RPM, whereas the ignition delay period is not.

4.4 PRESSURE CURVES

In addition to the combustion data of the preceding section, a study of the pressure trace itself provides valuable insight into the roughness of combustion and knock. Figures 4.30 and 4.31 present typical (2200 RPM) motored and fired P-CA curves for each fuel at full rack and part load settings. The averaged data (32 curves) is used for these plots while Chapter 5 will show single-shot P-CA data plots for fuel-to-fuel comparison.

Figures 4.32 and 4.33 give the corresponding pressure-volume plots (used to calculate indicated parameters). Even from the these averaged curves, it is worth noting the rougher combustion associated with part load operation.

ENGINE BRAKE PERFORMANCE CHARACTERISTICS

TORQUE = MAX FUEL = REFERENCE

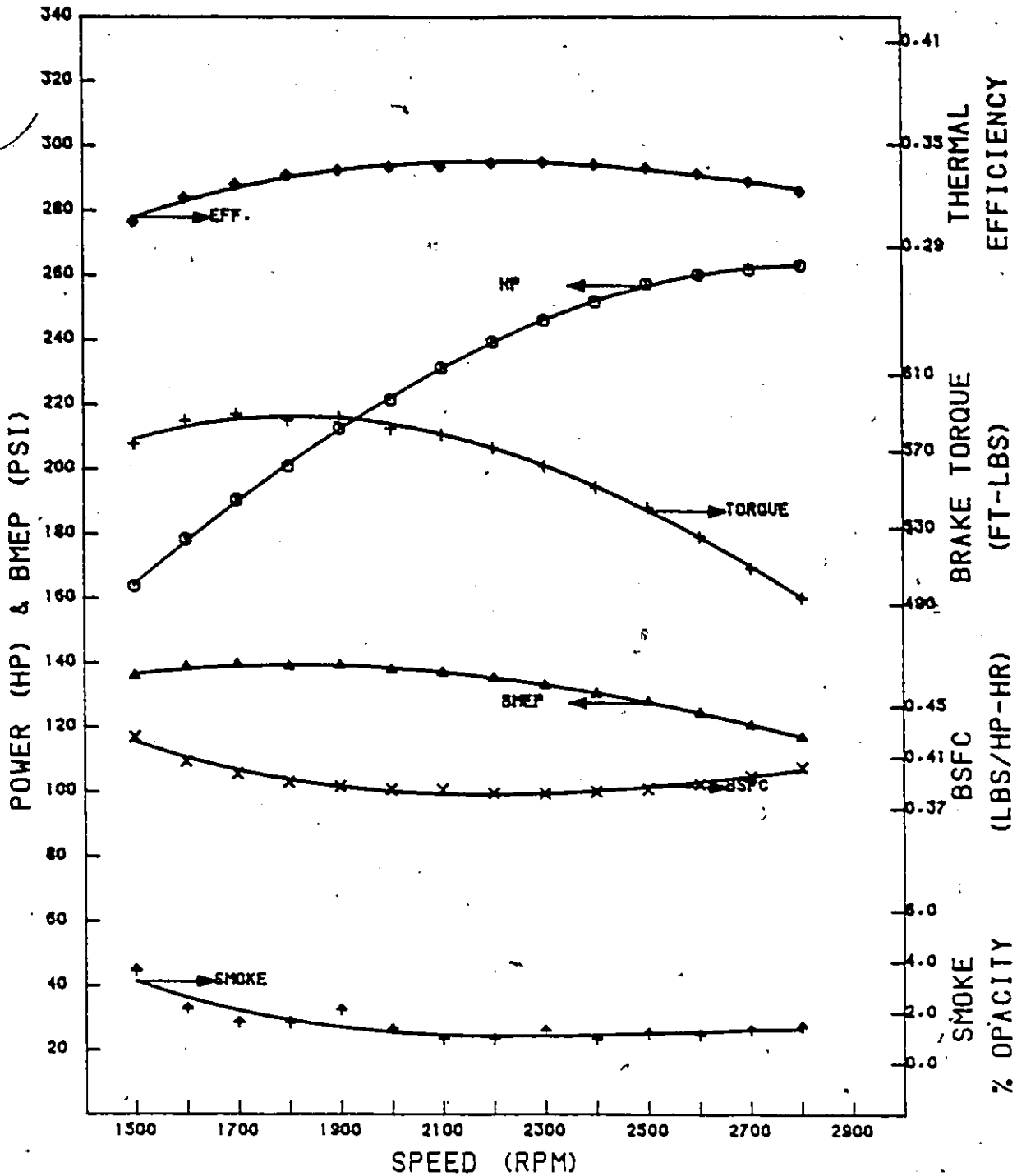


Fig. 4.1: Engine Brake Performance Characteristics.
6V53T Engine, Full Rack, Fuel 1 (3GP30,
reference)

ENGINE BRAKE PERFORMANCE CHARACTERISTICS

TORQUE = MAX FUEL = #2 DIESEL

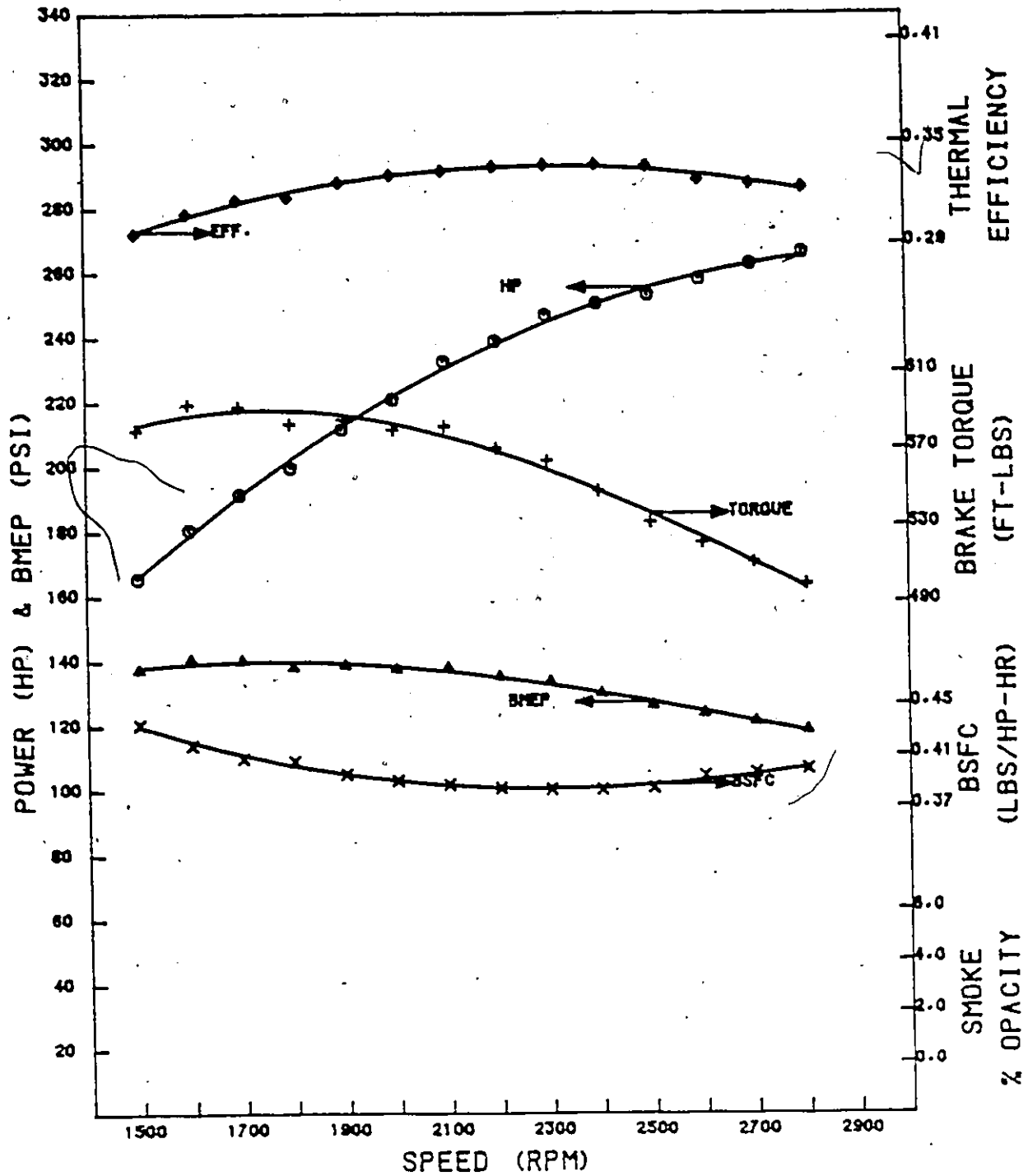


Fig. 4.2: Engine Brake Performance Characteristics.
6V53T Engine, Full Rack, Fuel 2 (#2-D).

ENGINE BRAKE PERFORMANCE CHARACTERISTICS

TORQUE = MAX FUEL = SHELL (BEST CASE)

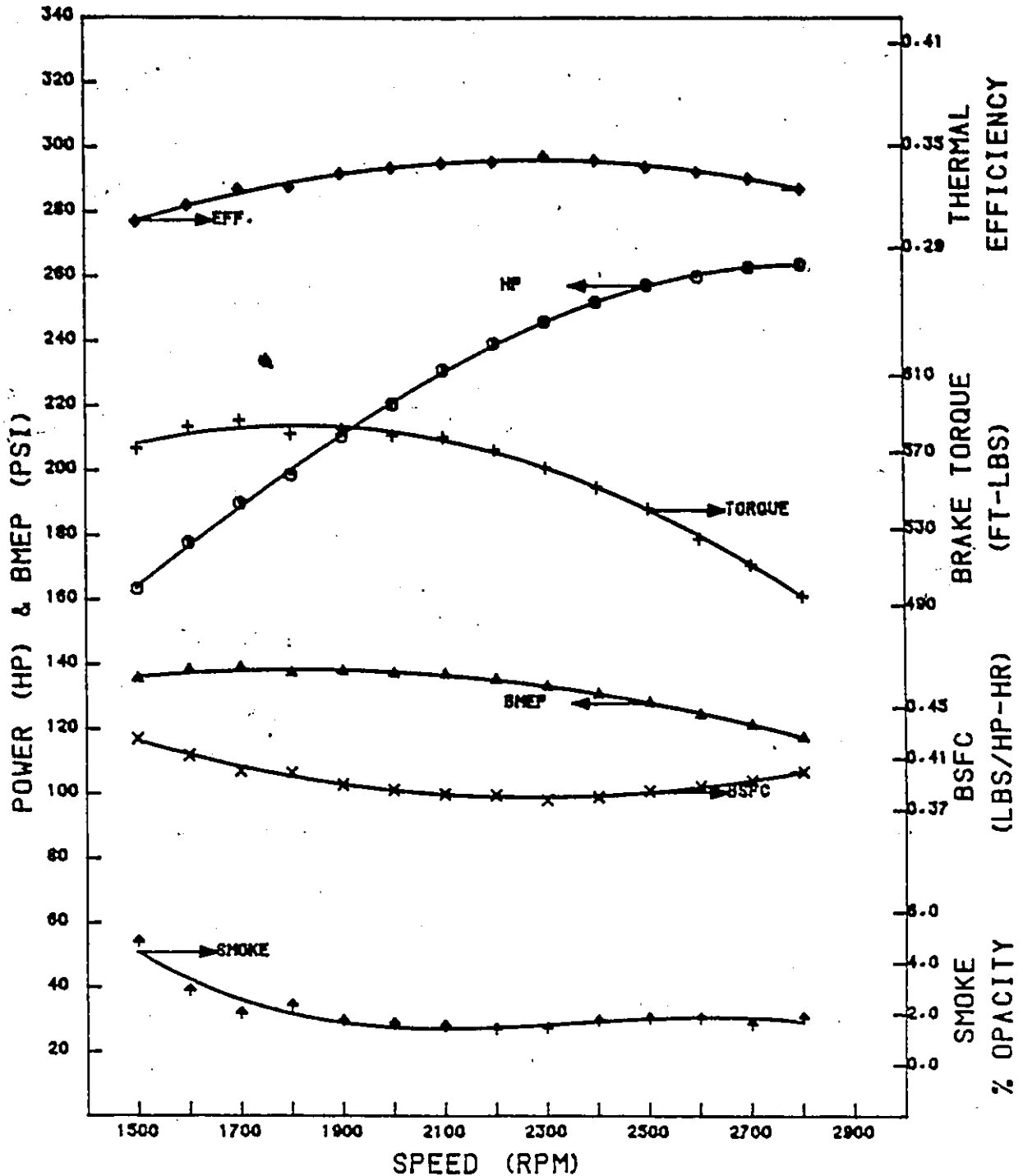


Fig. 4.3: Engine Brake Performance Characteristics.
6V53T Engine, Full Rack, Fuel 3 (Shell, 1990).

ENGINE BRAKE PERFORMANCE CHARACTERISTICS

TORQUE = MAX FUEL = 1990 (WORST CASE)

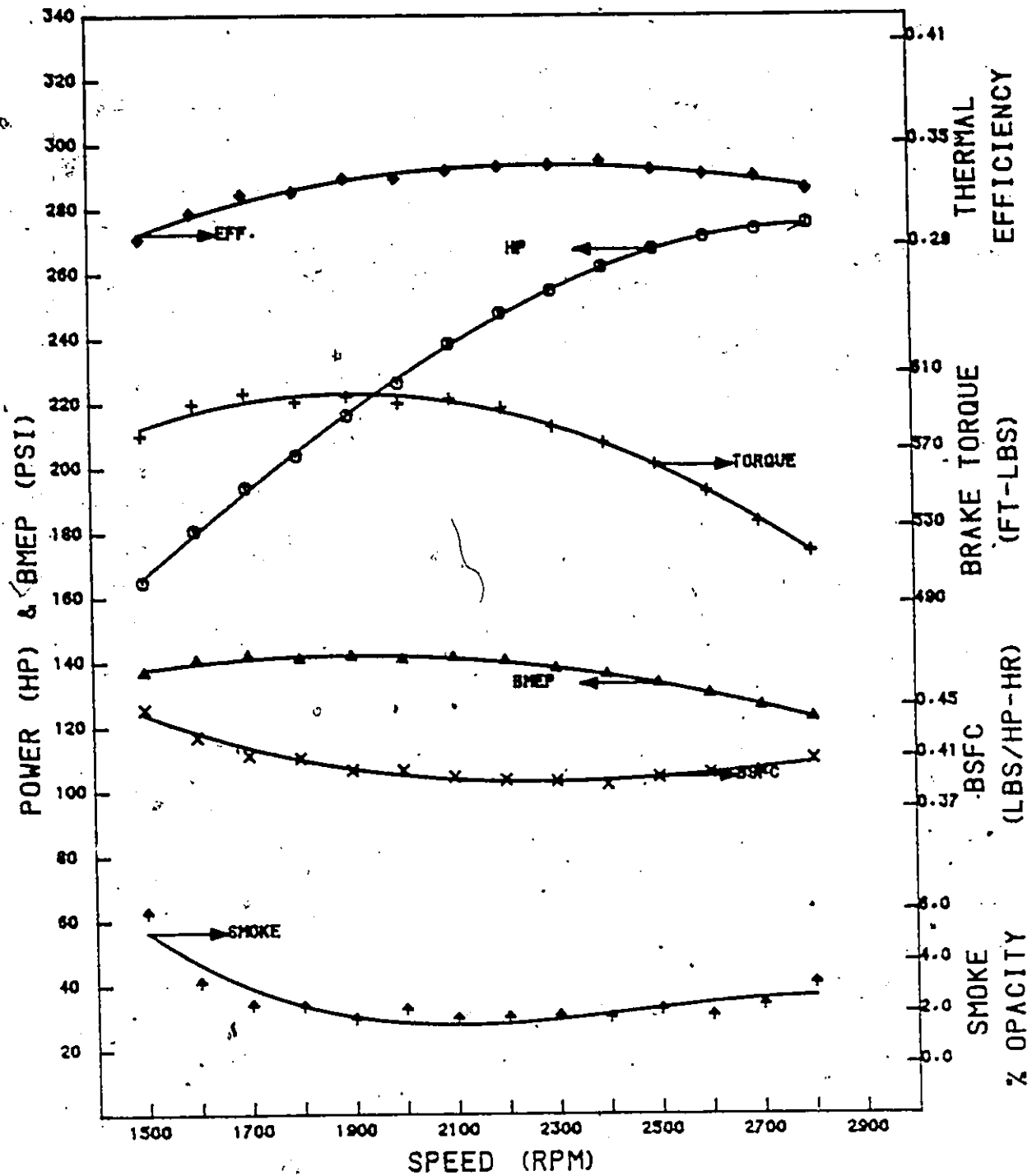


Fig. 4.4: Engine Brake Performance Characteristics. 6V53T Engine, Full Rack, Fuel 4 (1990).

ENGINE BRAKE PERFORMANCE CHARACTERISTICS

TORQUE = 250 FUEL = REFERENCE

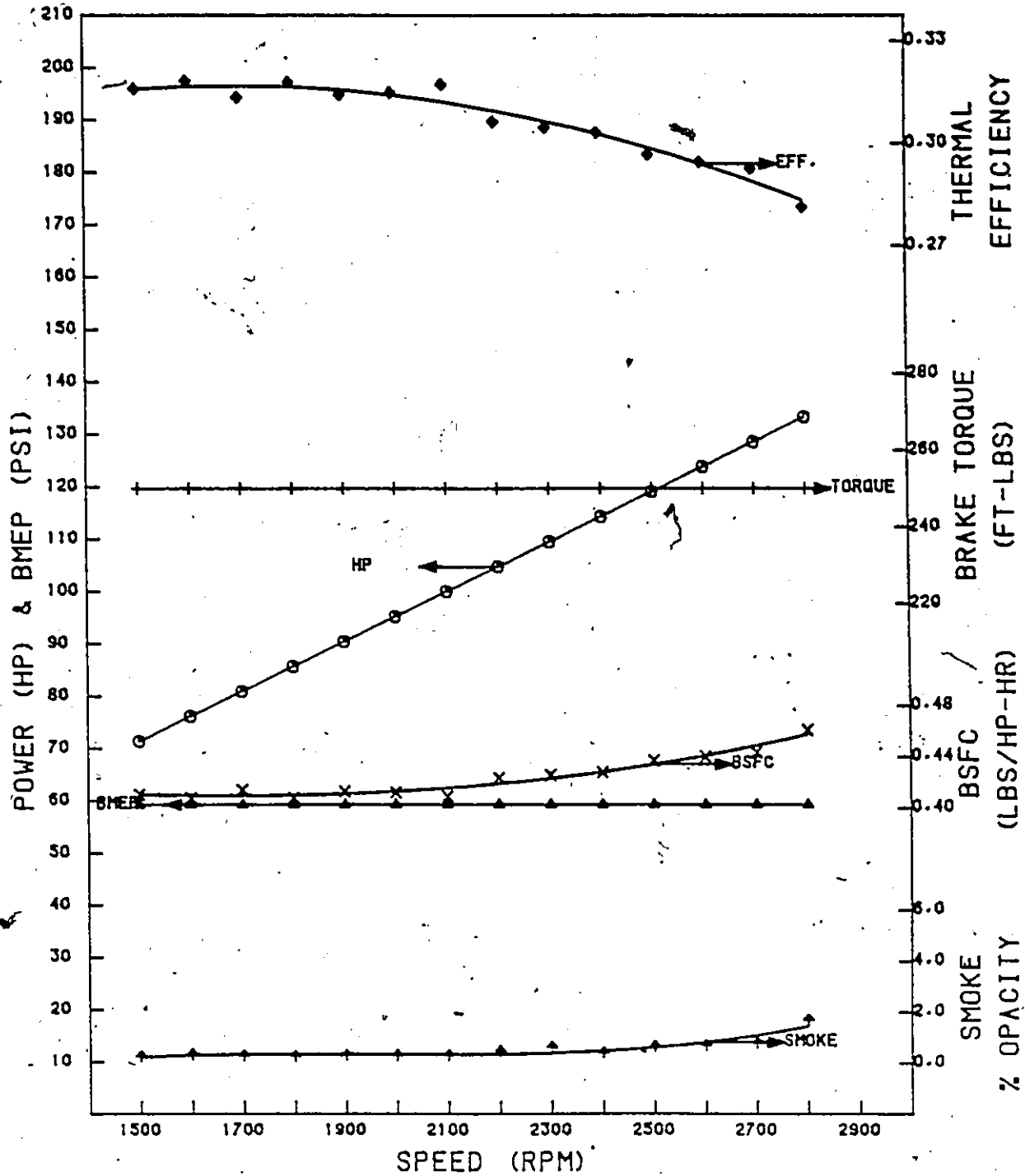


Fig. 4.5: Engine Brake Performance Characteristics.
6V53T Engine, Part Load (Brake Torque =
250 Ft.lbs.) Fuel 1 (3GP30, reference).

ENGINE BRAKE PERFORMANCE CHARACTERISTICS

TORQUE = 250

FUEL = #2 DIESEL

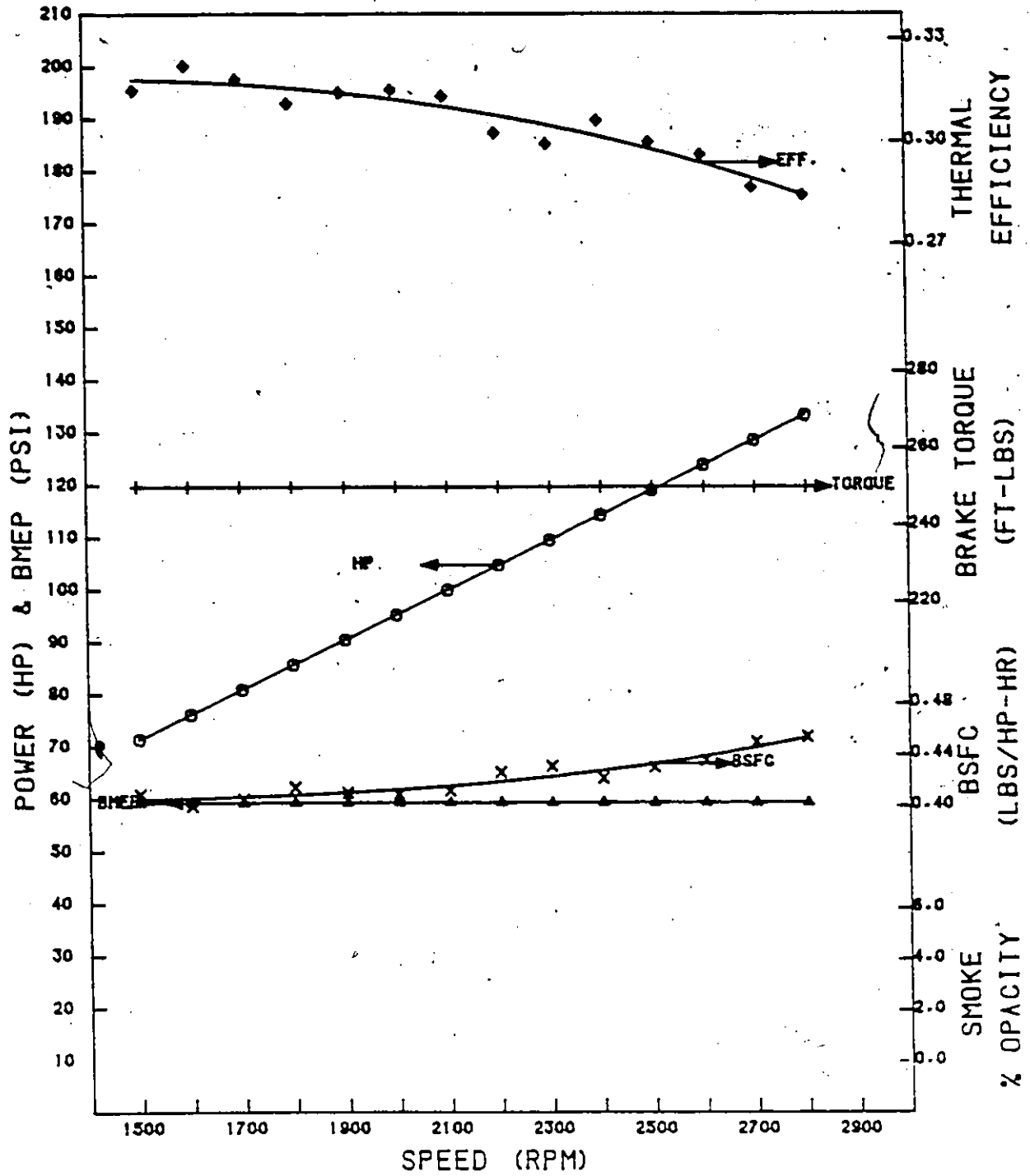


Fig. 4.6: Engine Brake Performance Characteristics.
6V53T Engine, Part Load (Brake Torque =
250 Ft.lbs.) Fuel 2 (#2-D).

ENGINE BRAKE PERFORMANCE CHARACTERISTICS

TORQUE = 250 FUEL = SHELL (BEST CASE)

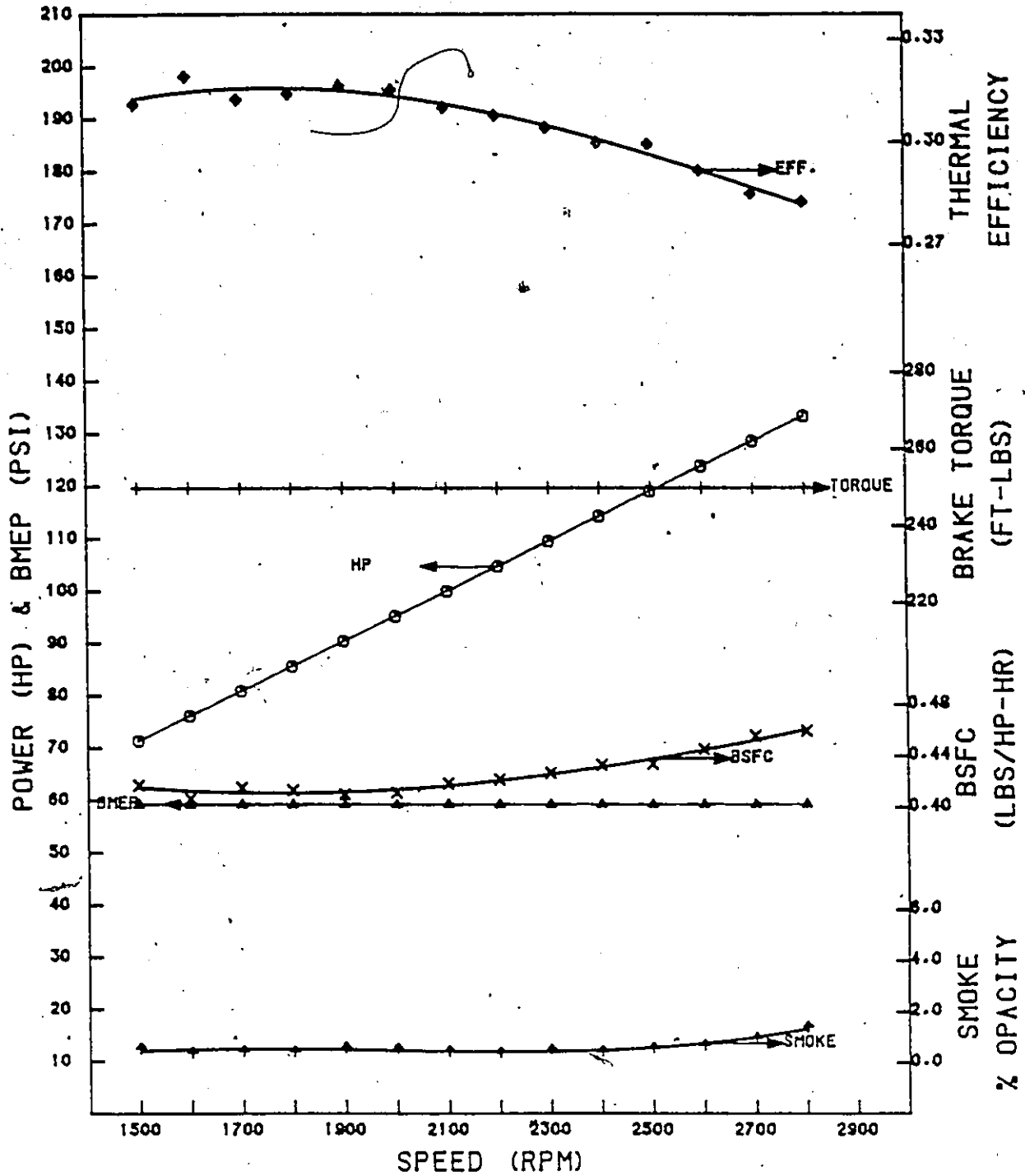


Fig. 4.7: Engine Brake Performance Characteristics. 6V53T Engine, Part Load (Brake Torque = 250 Ft.lbs.) Fuel 3 (Shell, 1990).

ENGINE BRAKE PERFORMANCE CHARACTERISTICS

TORQUE = 250. FUEL = 1990 (WORST CASE)

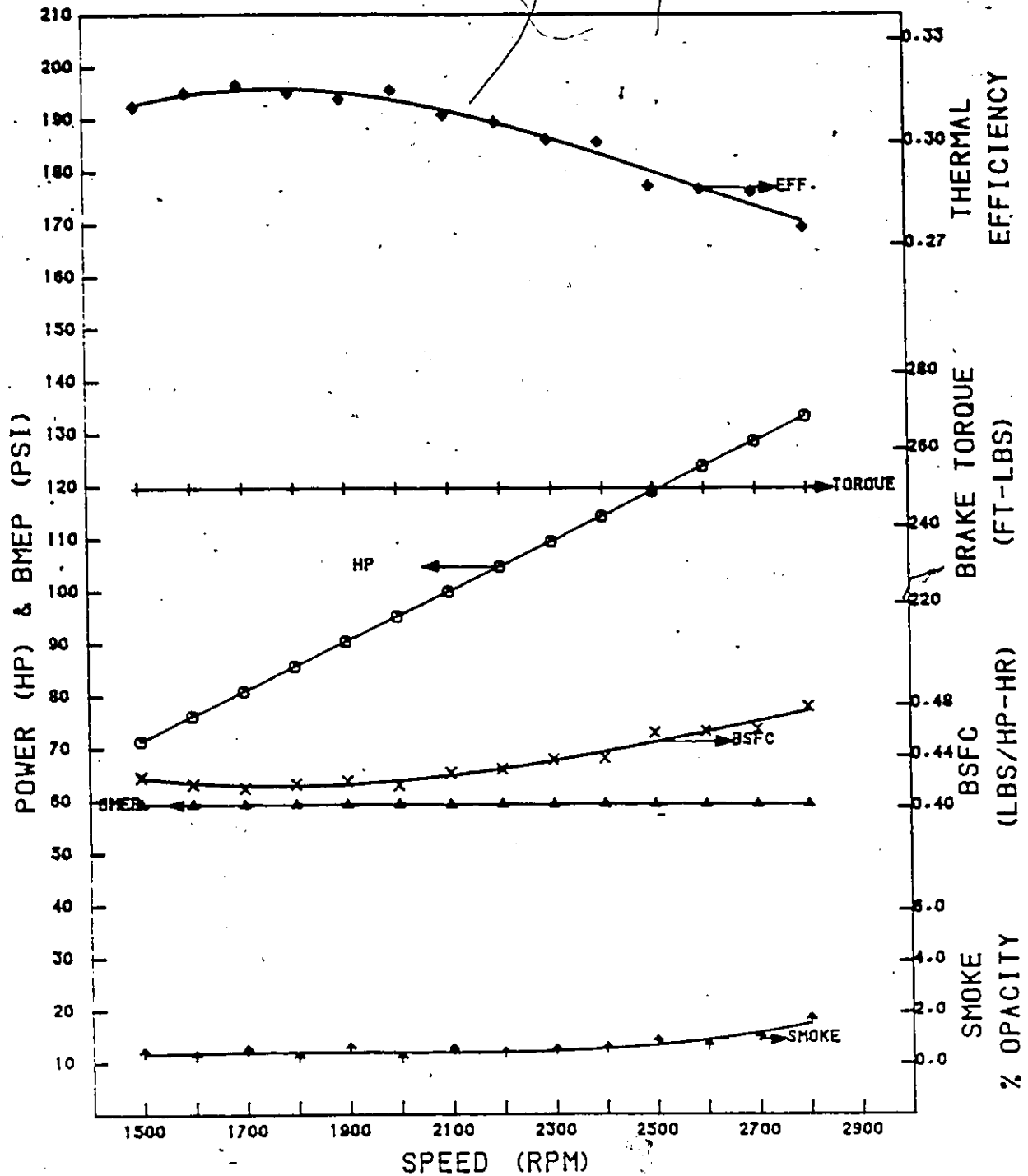


Fig. 4.8: Engine Brake Performance Characteristics. 6V53T Engine, Part Load (Brake Torque = 250 Ft.lbs.) Fuel 4 (1990).

ENGINE INDICATED PERFORMANCE CHARACTERISTICS

TORQUE = MAX

FUEL = REFERENCE

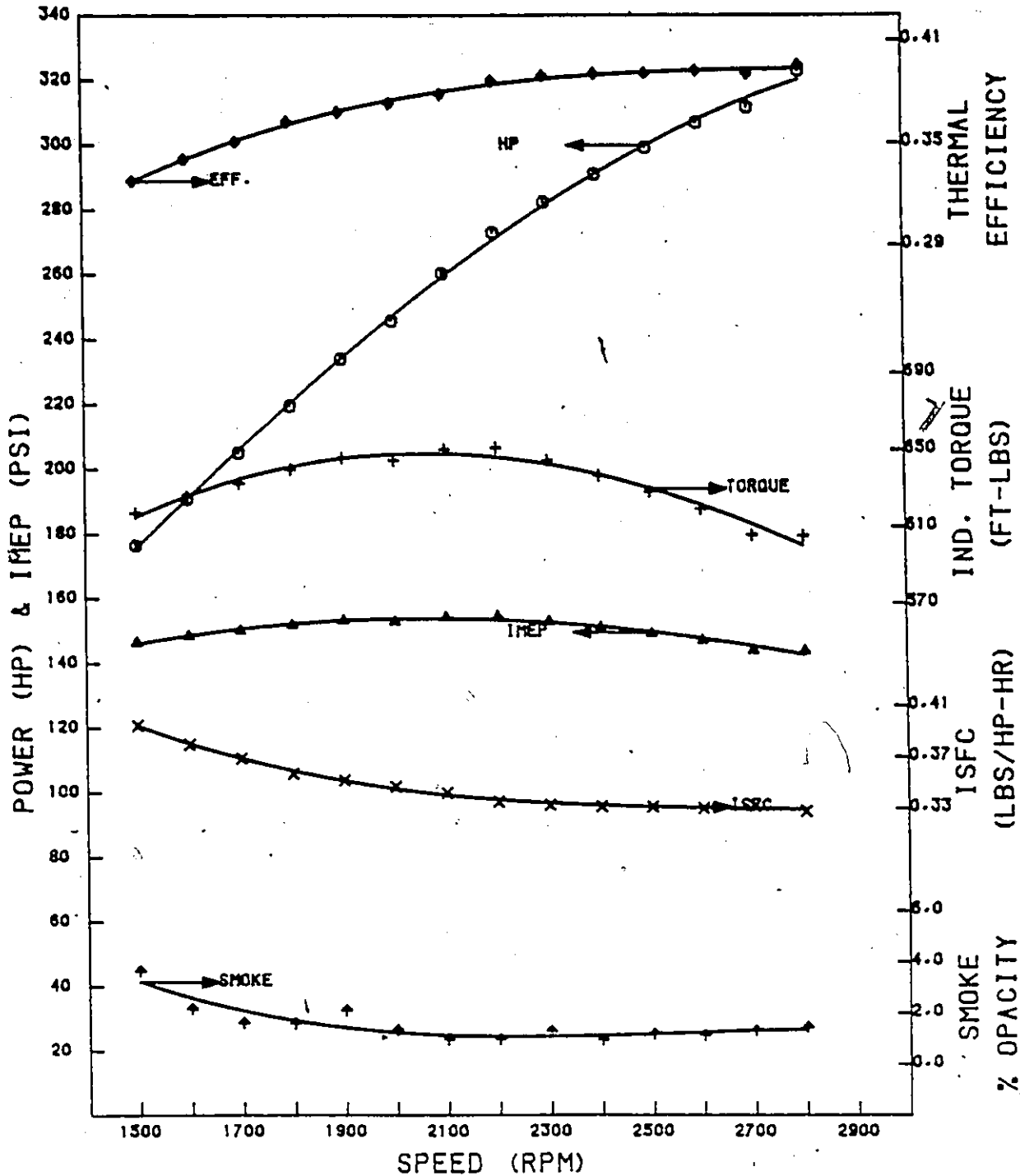


Fig. 4.9: Engine Indicated Performance Characteristics.
6V53T Engine, Full Rack, Fuel 1 (3GP30, reference).

ENGINE INDICATED PERFORMANCE CHARACTERISTICS

TORQUE = MAX

FUEL = #2 DIESEL

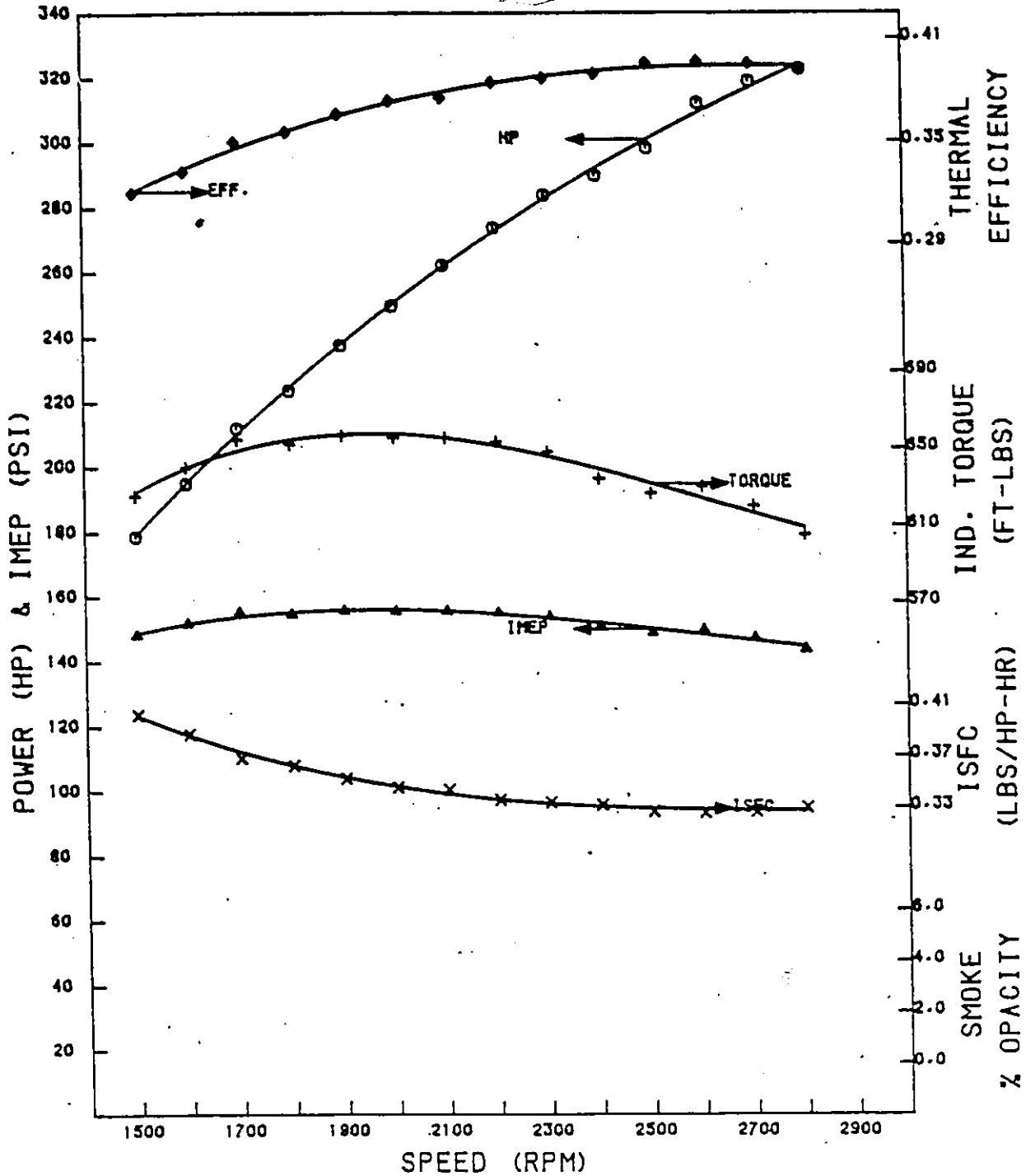


Fig. 4.10: Engine Indicated Performance Characteristics.
6V53T Engine, Full Rack, Fuel 2 (#2-D).

ENGINE INDICATED PERFORMANCE CHARACTERISTICS

TORQUE = MAX

FUEL = SHELL (1990)

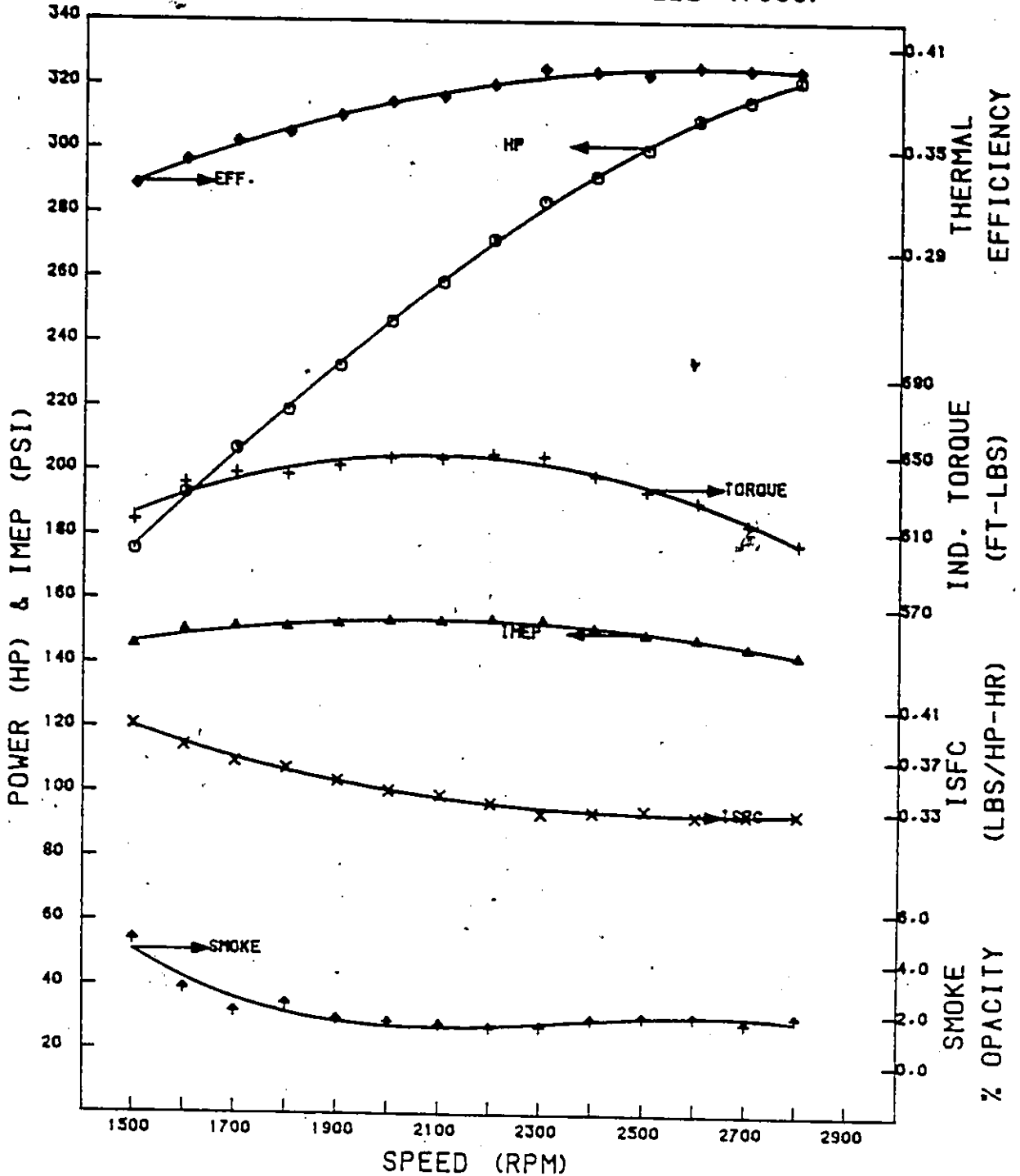


Fig. 4.11: Engine Indicated Performance Characteristics. 6V53T Engine, Full Rack, Fuel 3 (Shell, 1990).

ENGINE INDICATED PERFORMANCE CHARACTERISTICS

TORQUE = MAX FUEL = 1990 (WORST CASE)

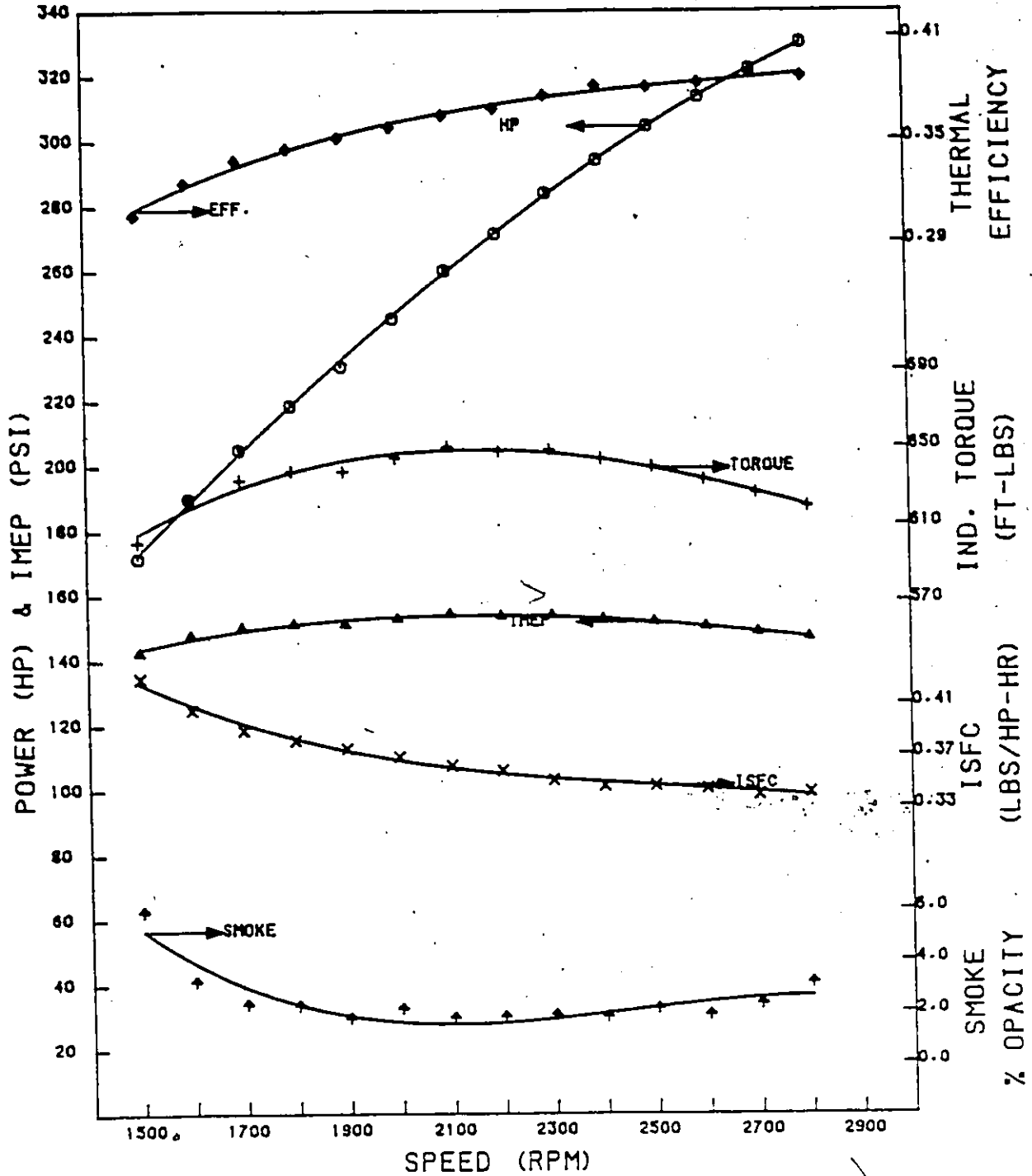


Fig. 4.12: Engine Indicated Performance Characteristics. 6V53T Engine, Full Rack, Fuel 4 (1990).

ENGINE INDICATED PERFORMANCE CHARACTERISTICS

TORQUE = 250

FUEL = REFERENCE

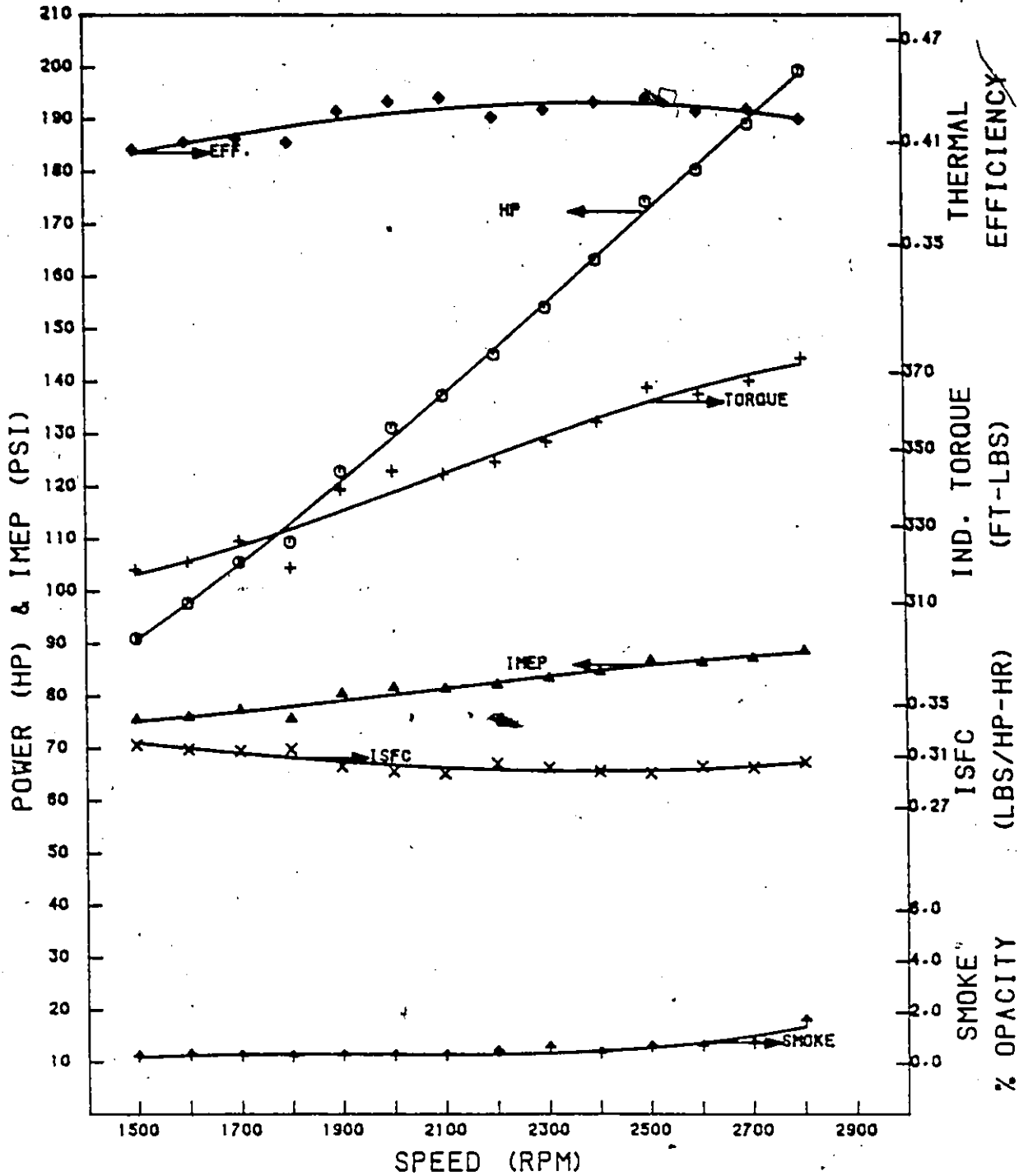


Fig. 4.13: Engine Indicated Performance Characteristics.
6V53T Engine, Part Load (Brake Torque = 250
Ft.lbs.) Fuel 1 (3GP30, reference).

ENGINE INDICATED PERFORMANCE CHARACTERISTICS

TORQUE = 250

FUEL = #2 DIESEL

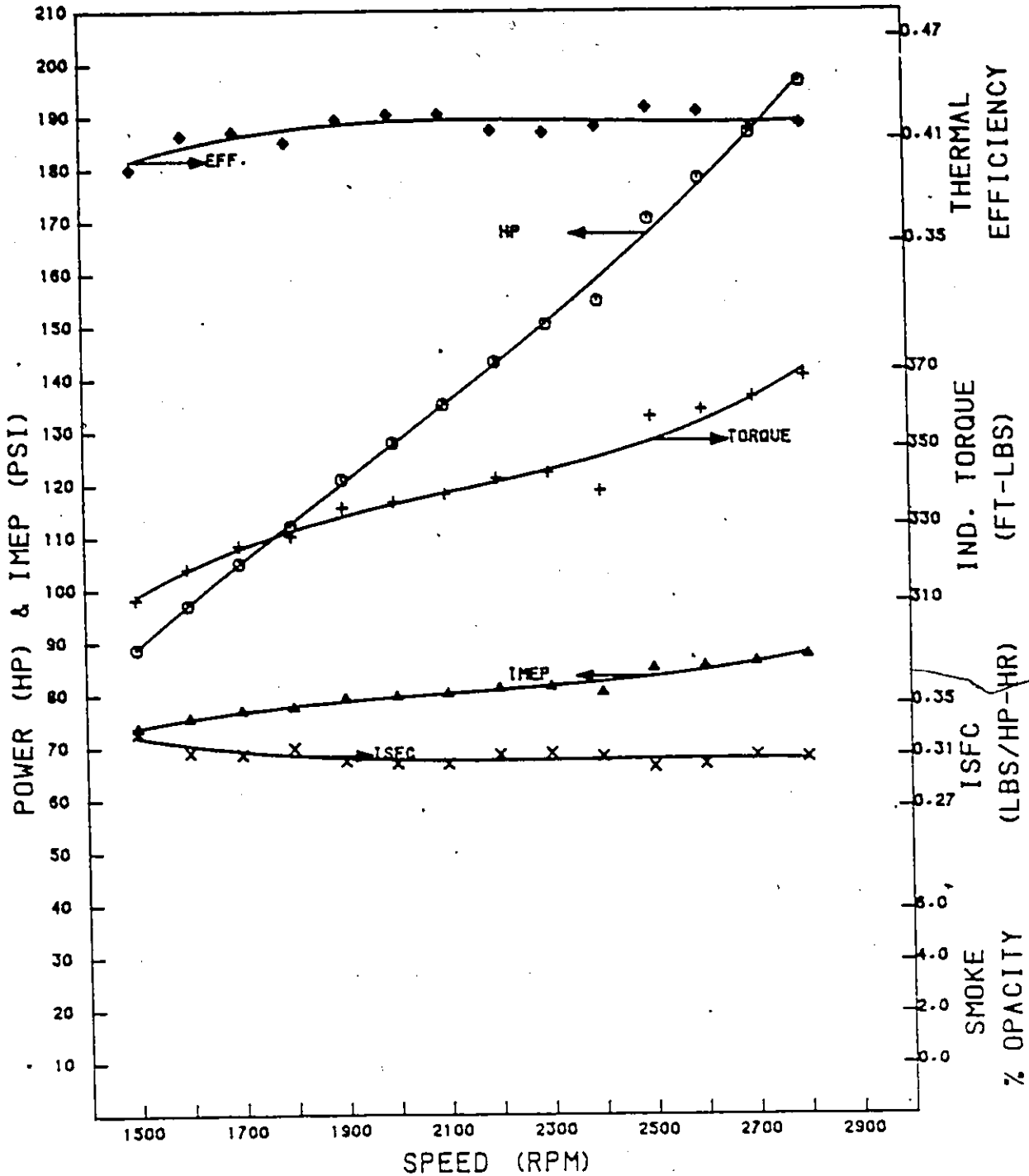


Fig. 4.14: Engine Indicated Performance Characteristics. 6V53T Engine, Part Load (Brake Torque = 250 Ft.lbs.) Fuel 2 (#2-D).

ENGINE INDICATED PERFORMANCE CHARACTERISTICS

TORQUE = 250

FUEL = SHELL (1990)

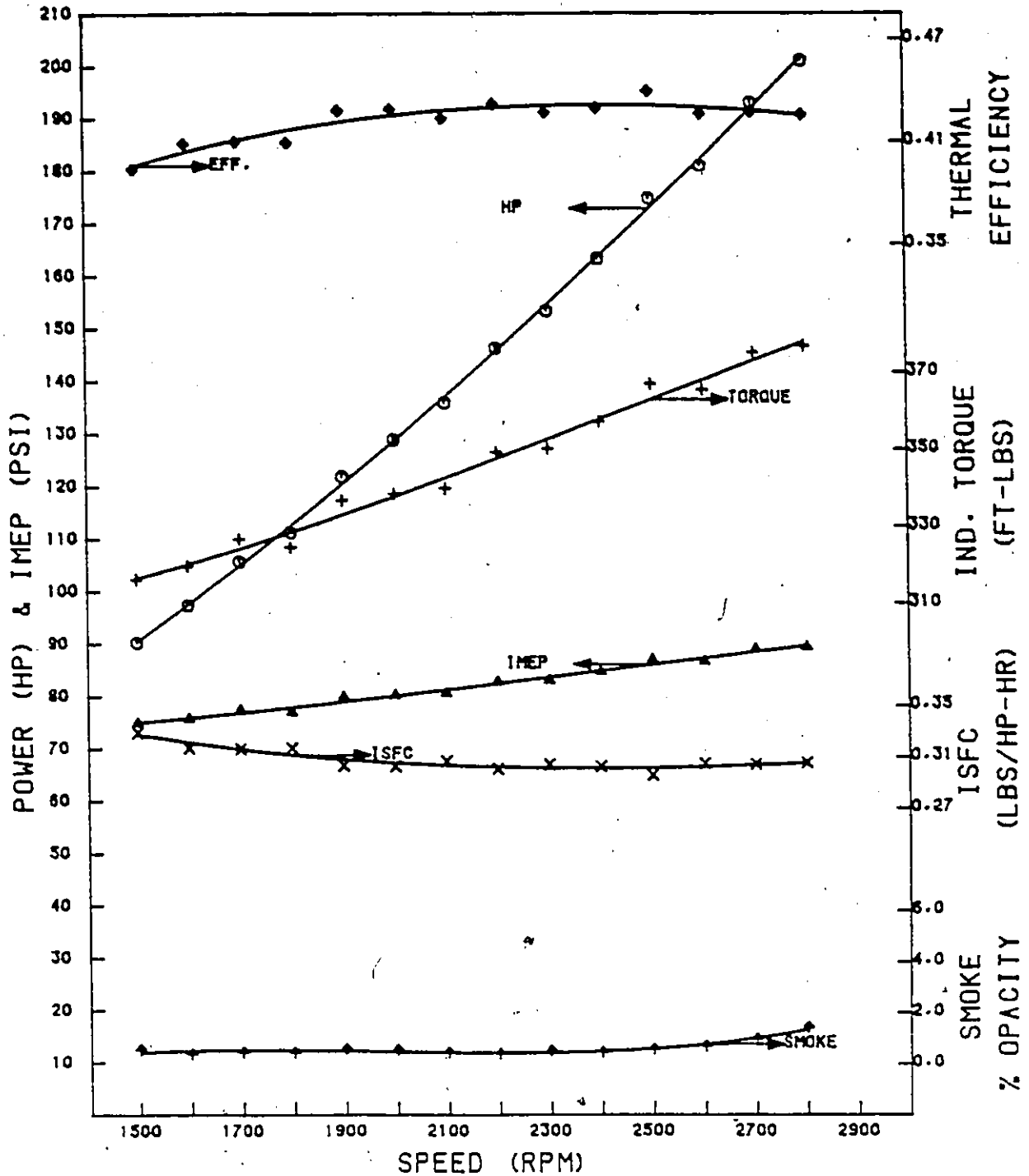


Fig. 4.15: Engine Indicated Performance Characteristics. 6V53T Engine, Part Load (Brake Torque = 250 Ft.lbs.) Fuel 3 (Shell, 1990).

ENGINE INDICATED PERFORMANCE CHARACTERISTICS

TORQUE = 250 FUEL = 1990 (WORST CASE)

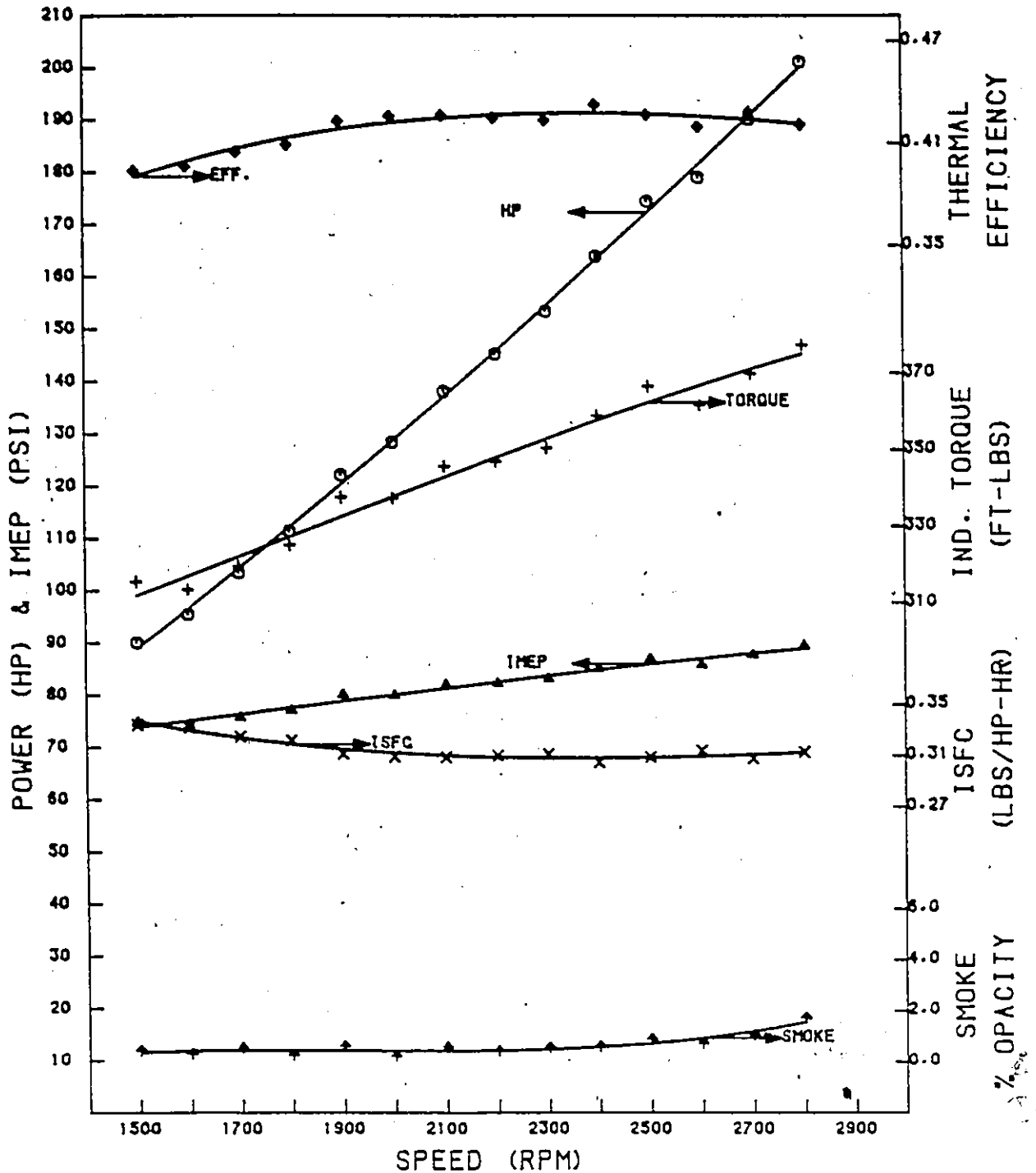


Fig. 4.16: Engine Indicated Performance Characteristics. 6V53T Engine, Part Load (Brake Torque = 250 Ft.lbs.) Fuel 4 (1990).

PRESSURE RATE VS CRANK ANGLE SPAN
FUEL 1: 3GP30

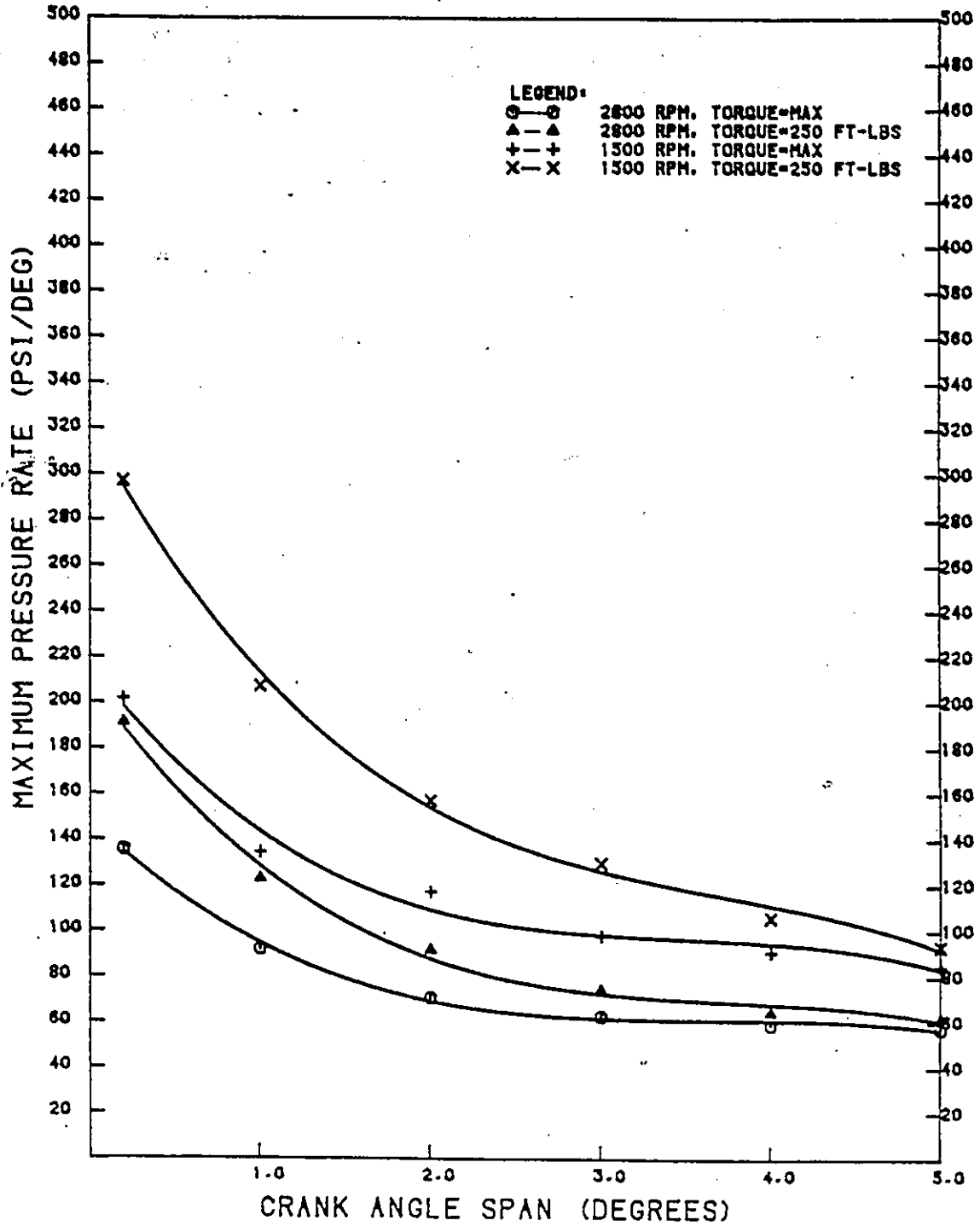


Fig. 4.17: Effect of Crank Angle Span on the Calculation of Maximum Pressure Rates.

ENGINE COMBUSTION CHARACTERISTICS DATA

TORQUE = MAX FUEL = REFERENCE

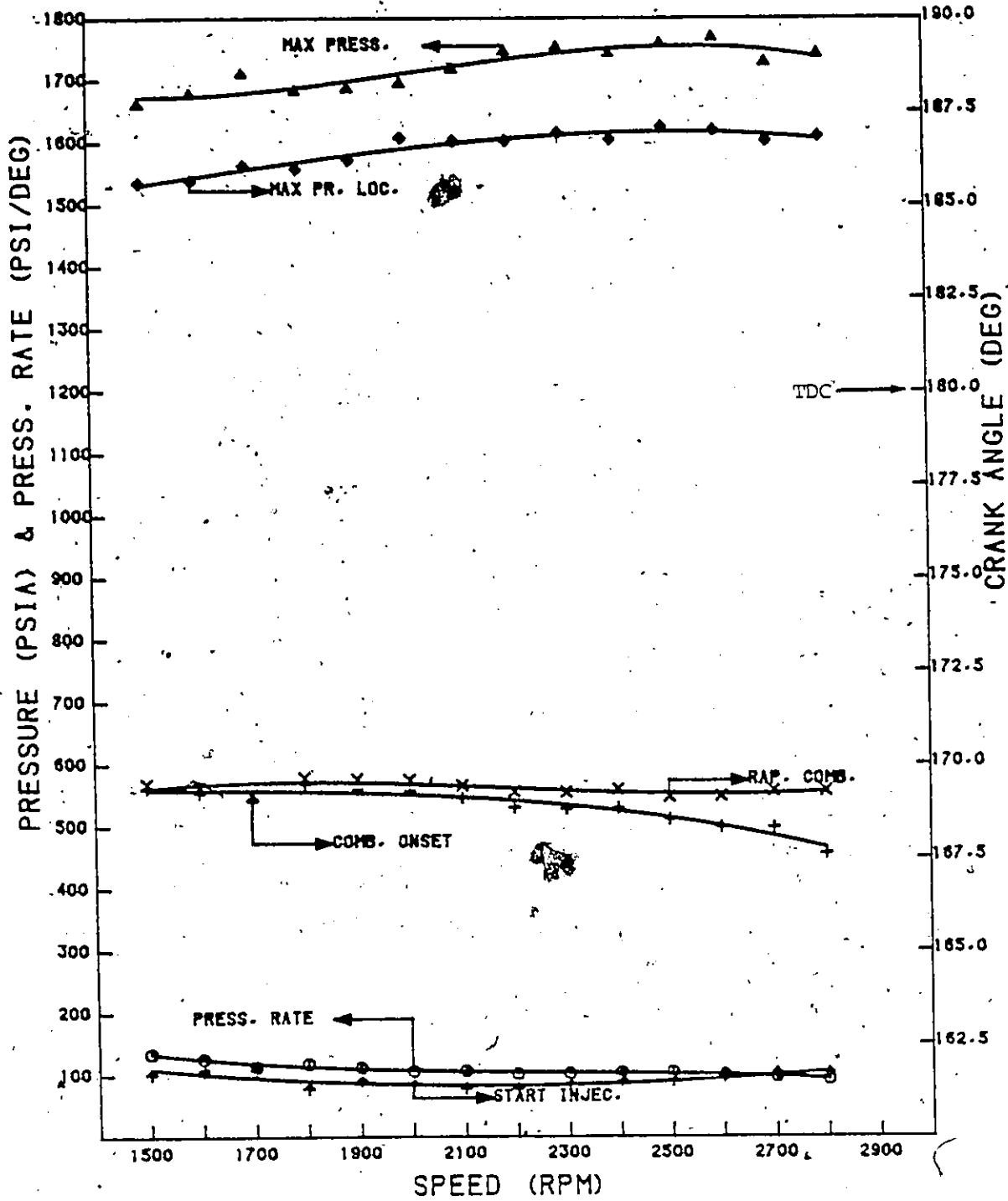


Fig. 4.18: Engine Combustion Characteristic Curves.
6V53T Engine, Full Rack, Fuel 1 (3GP30,
reference).

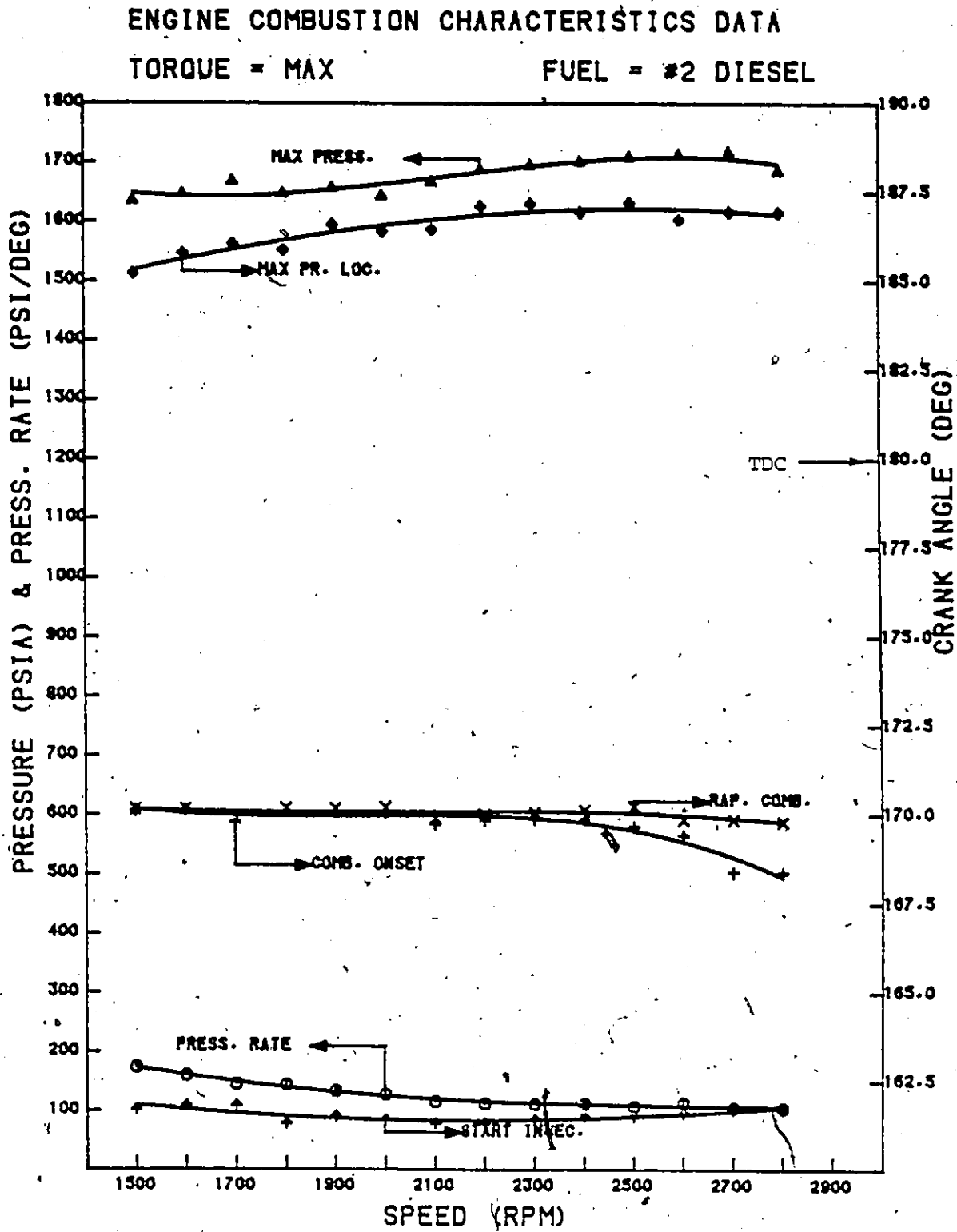


Fig. 4.19: Engine Combustion Characteristic Curves.
6V53T Engine, Full Rack, Fuel 2 (#2-D).

ENGINE COMBUSTION CHARACTERISTICS DATA

TORQUE = MAX FUEL = SHELL (BEST CASE)

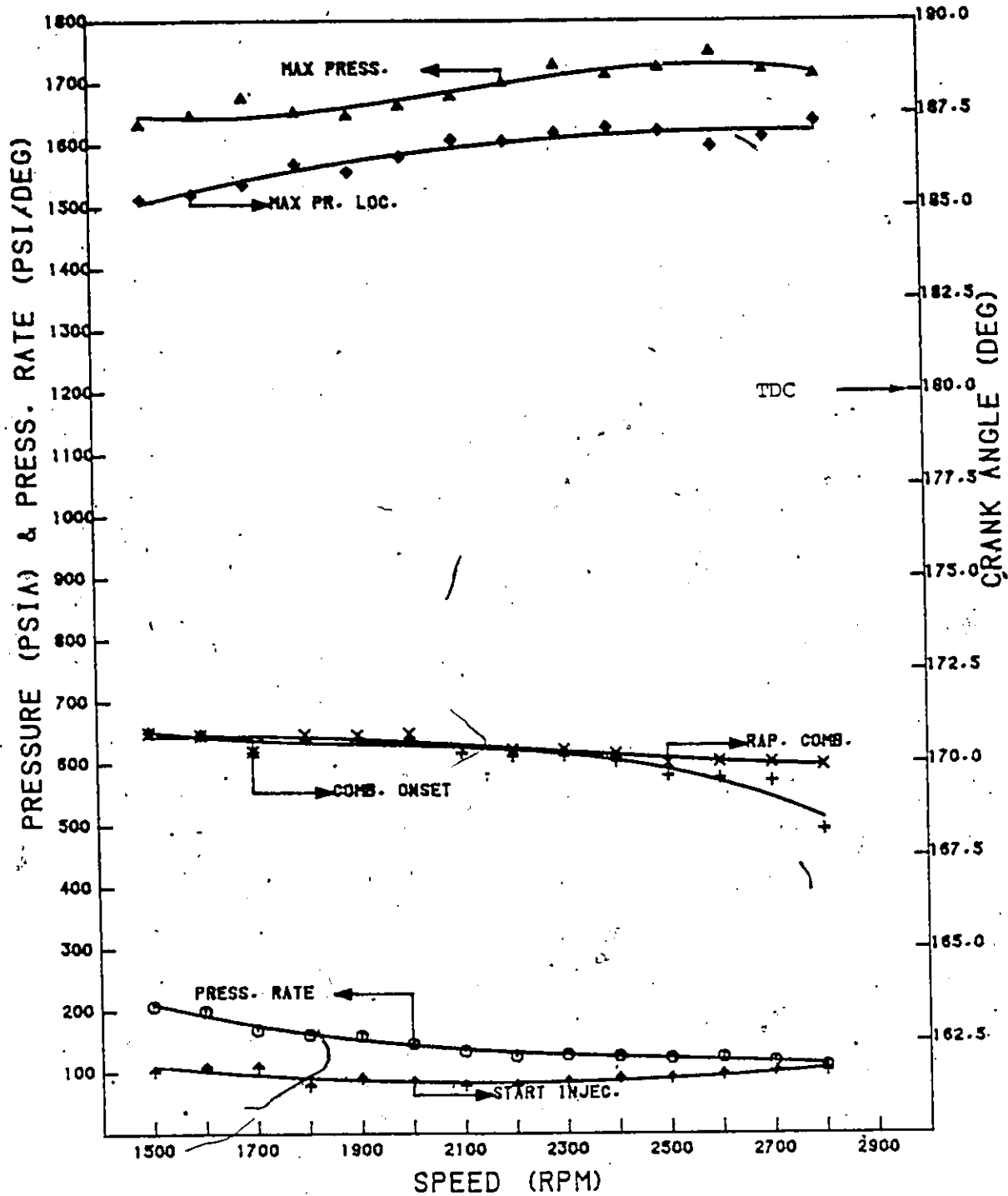


Fig. 4.20: Engine Combustion Characteristic Curves.
6V53T Engine, Full Rack, Fuel 3 (Shell, 1990).

ENGINE COMBUSTION CHARACTERISTICS DATA

TORQUE = MAX FUEL = 1990 (WORST CASE)

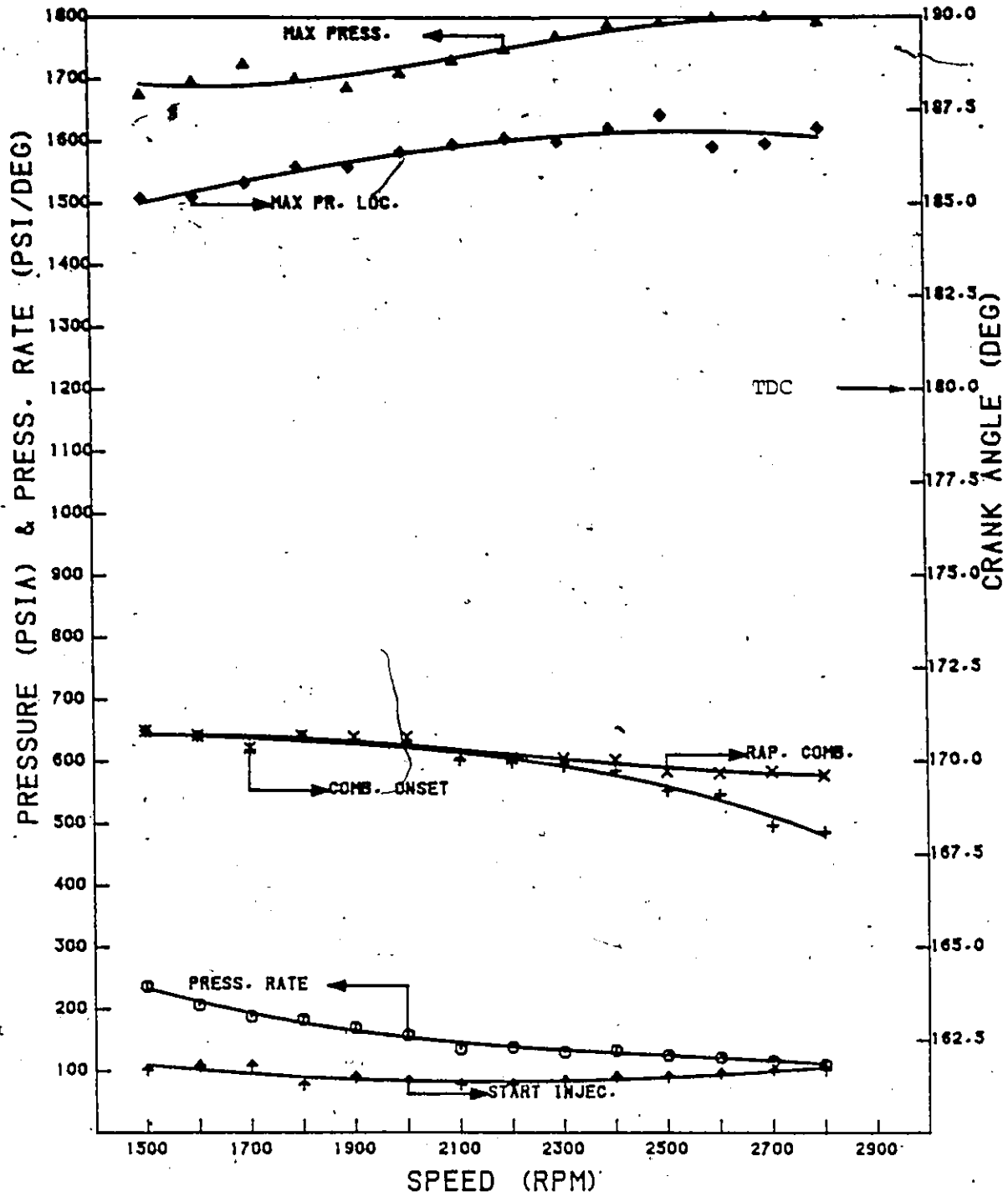


Fig. 4.21: Engine Combustion Characteristic Curves.
6V53T Engine, Full Rack, Fuel 4 (1990).

ENGINE COMBUSTION CHARACTERISTICS DATA
TORQUE = 250 FUEL = REFERENCE

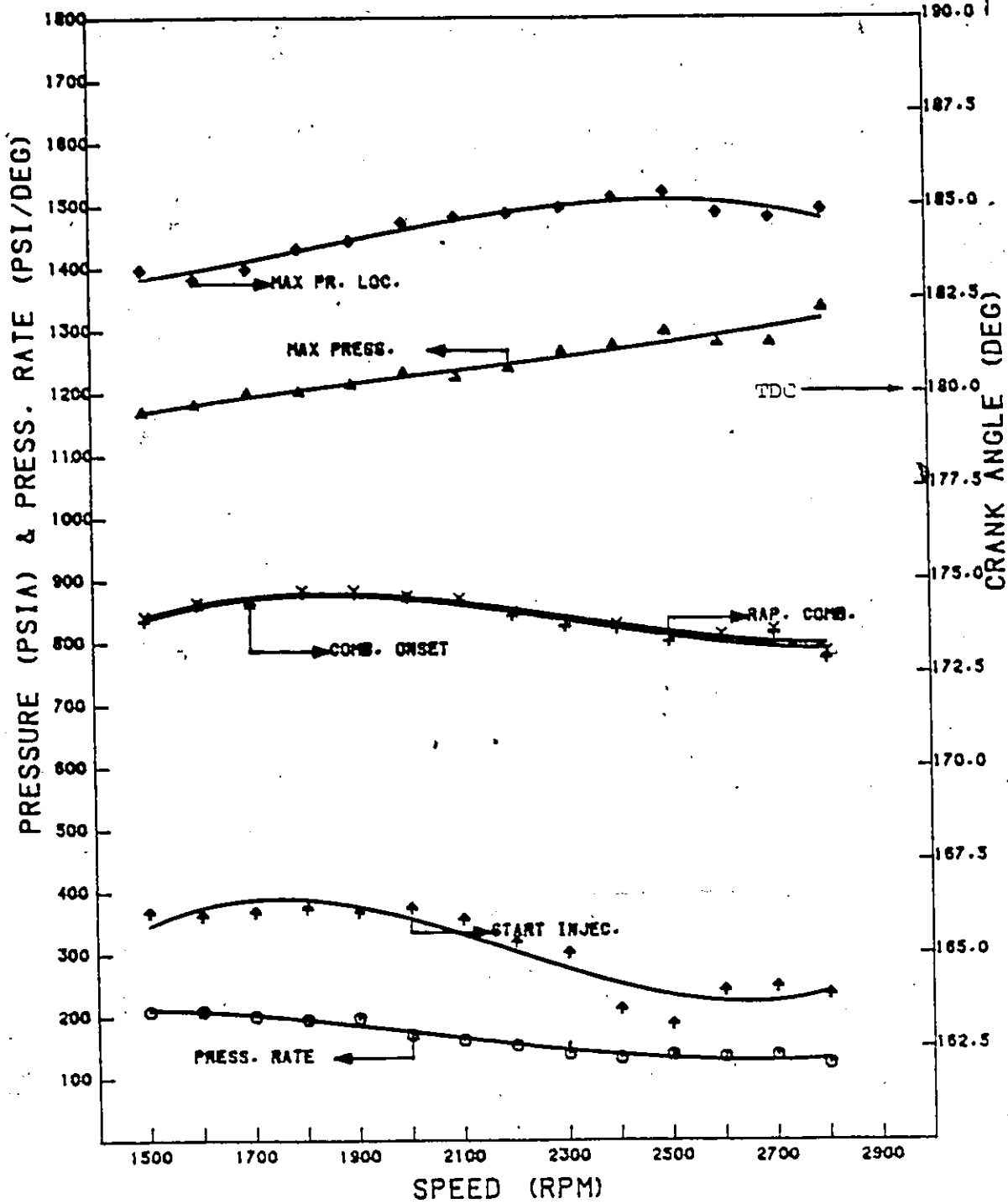


Fig. 4.22: Engine Combustion Characteristic Curves.,
6V53T Engine, Part Load (Brake Torque =
250 Ft.lbs.) Fuel 1 (3GP30, reference)

ENGINE COMBUSTION CHARACTERISTICS DATA
TORQUE = 250 FUEL = #2 DIESEL

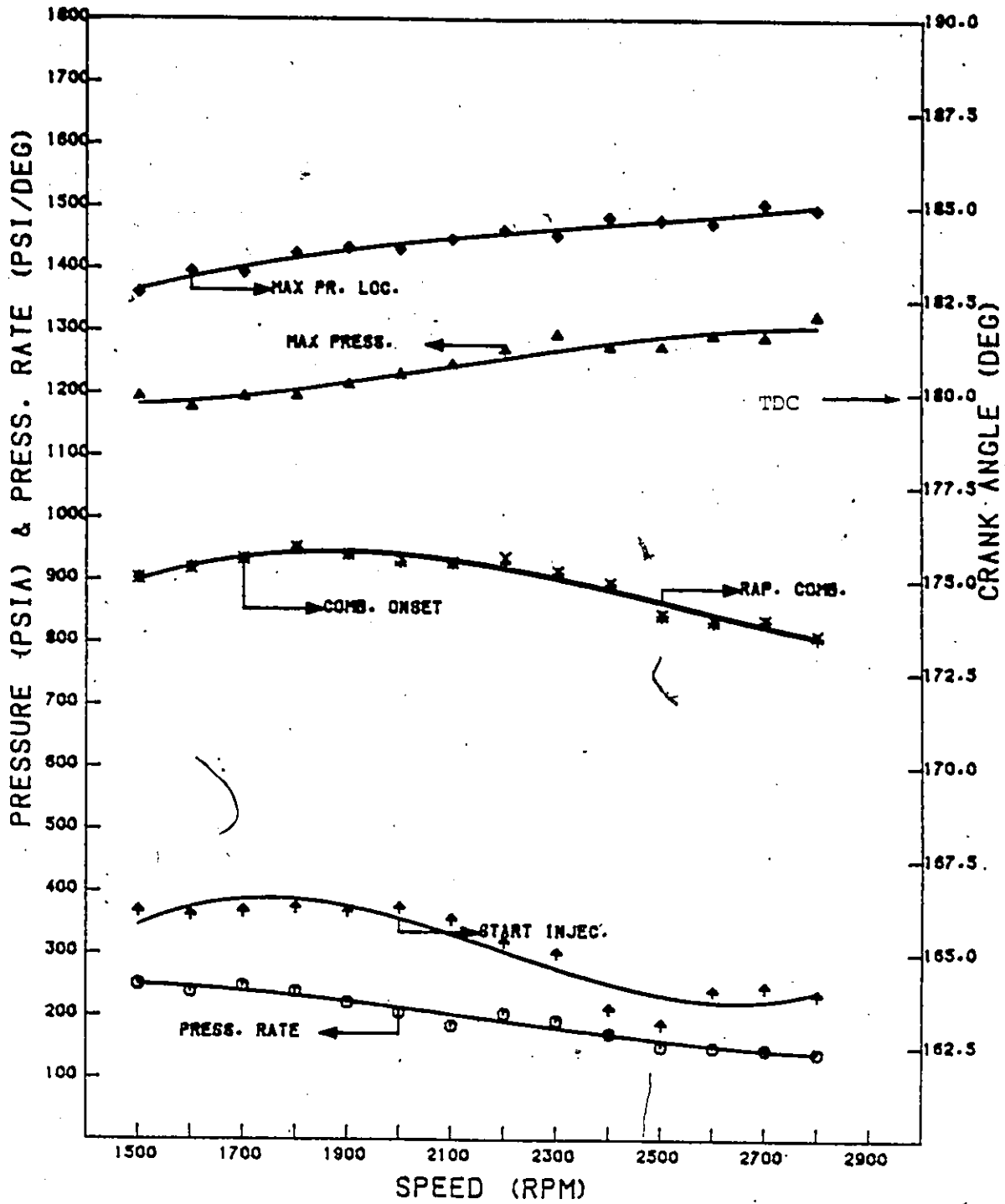


Fig. 4.23: Engine Combustion Characteristic Curves. 6V53T Engine, Part Load (Brake Torque = 250 Ft.lbs.) Fuel 2 (#2-D).

ENGINE COMBUSTION CHARACTERISTICS DATA

TORQUE = 250 FUEL = SHELL (BEST CASE)

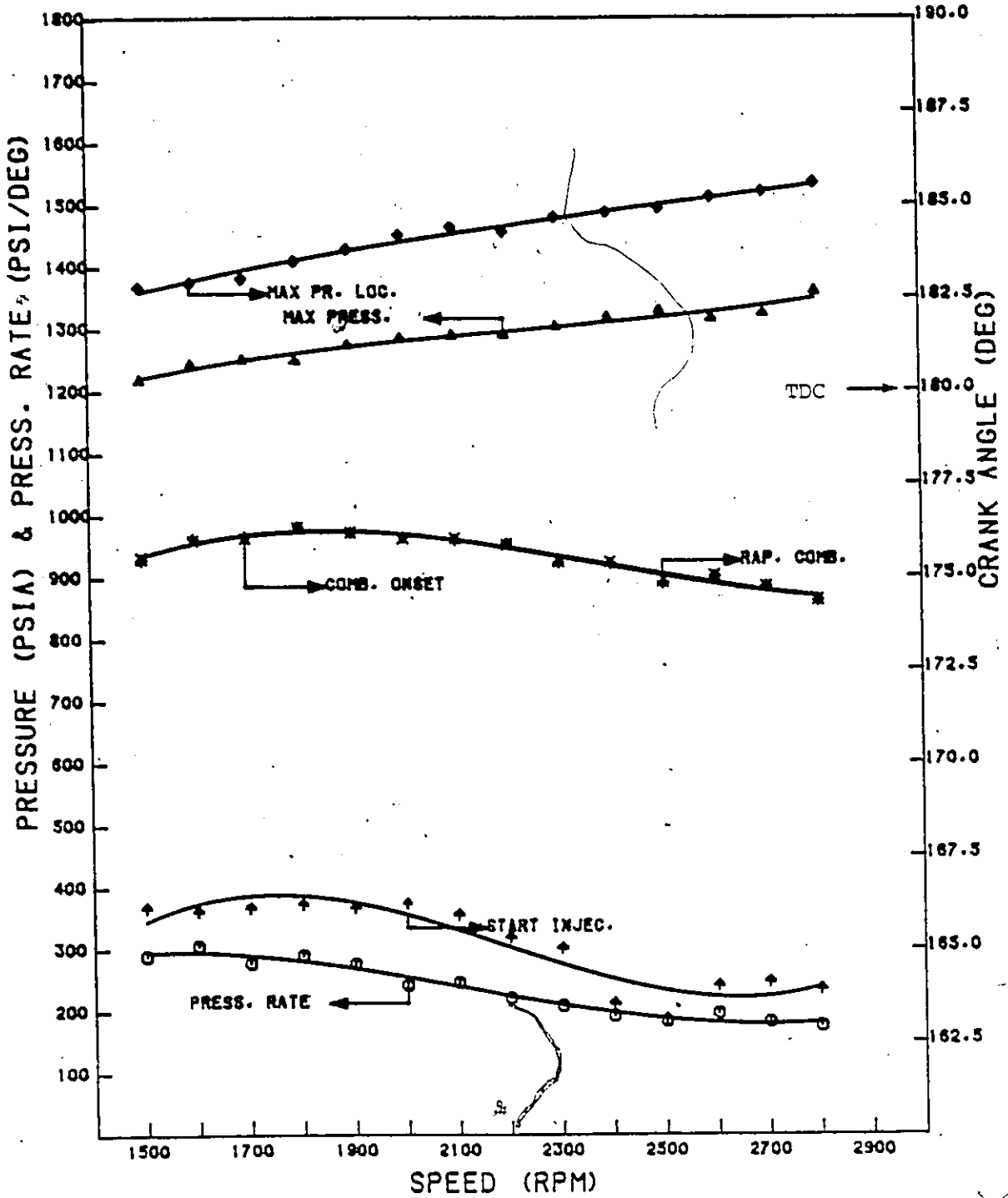


Fig. 4.24: Engine Combustion Characteristic Curves.
6V53T Engine, Part Load (Brake Torque = 250 Ft.lbs.) Fuel 3 (Shell, 1990).

ENGINE COMBUSTION CHARACTERISTICS DATA
TORQUE = 250 FUEL = 1990 (WORST CASE)

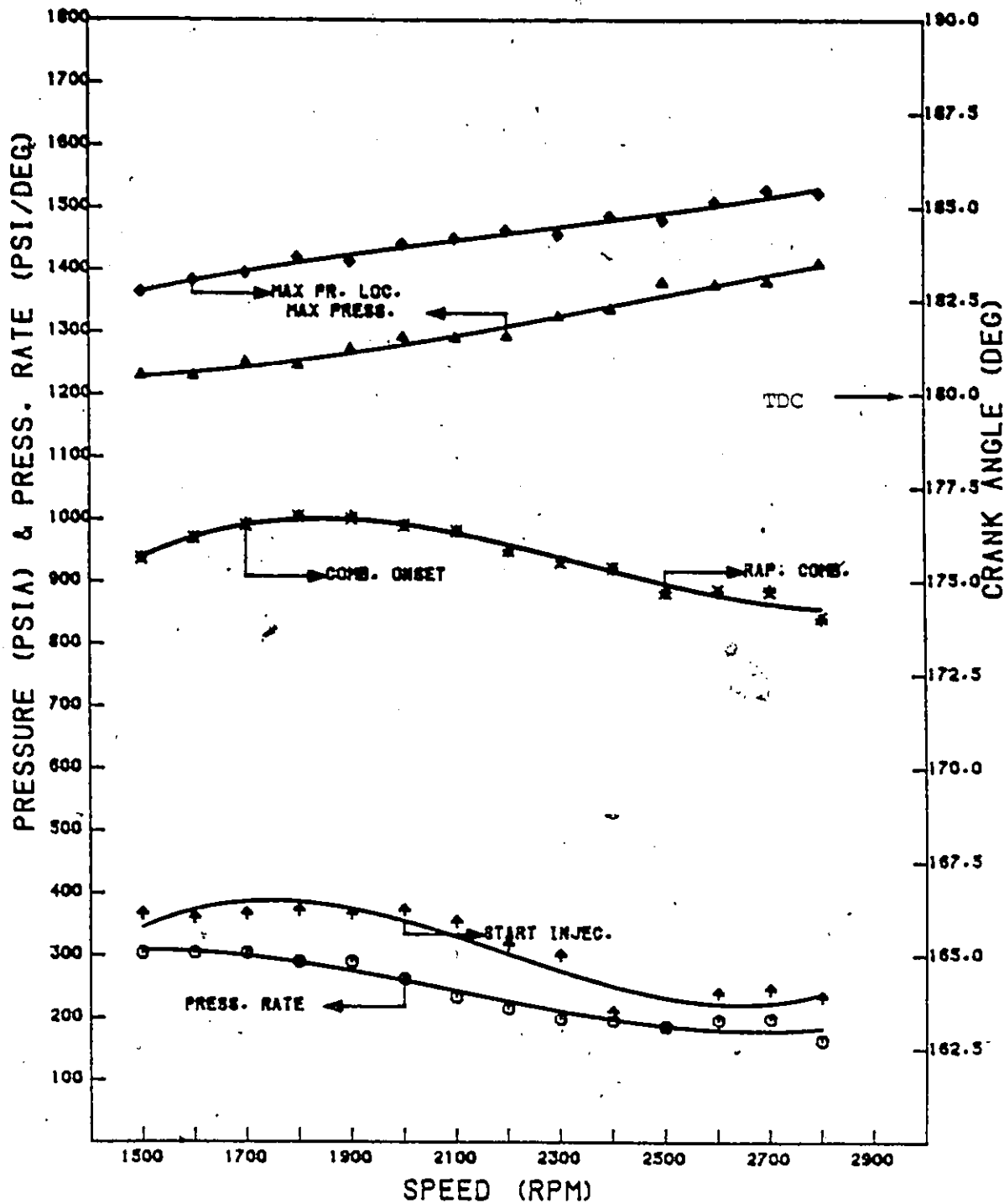


Fig. 4.25: Engine Combustion Characteristic Curves.
6V53T Engine, Part Load (Brake Torque = 250 Ft.lbs.) Fuel 4 (1990).

IGNITION AND COMBUSTION DELAYS VS RPM
TORQUE = MAX FUEL = REFERENCE

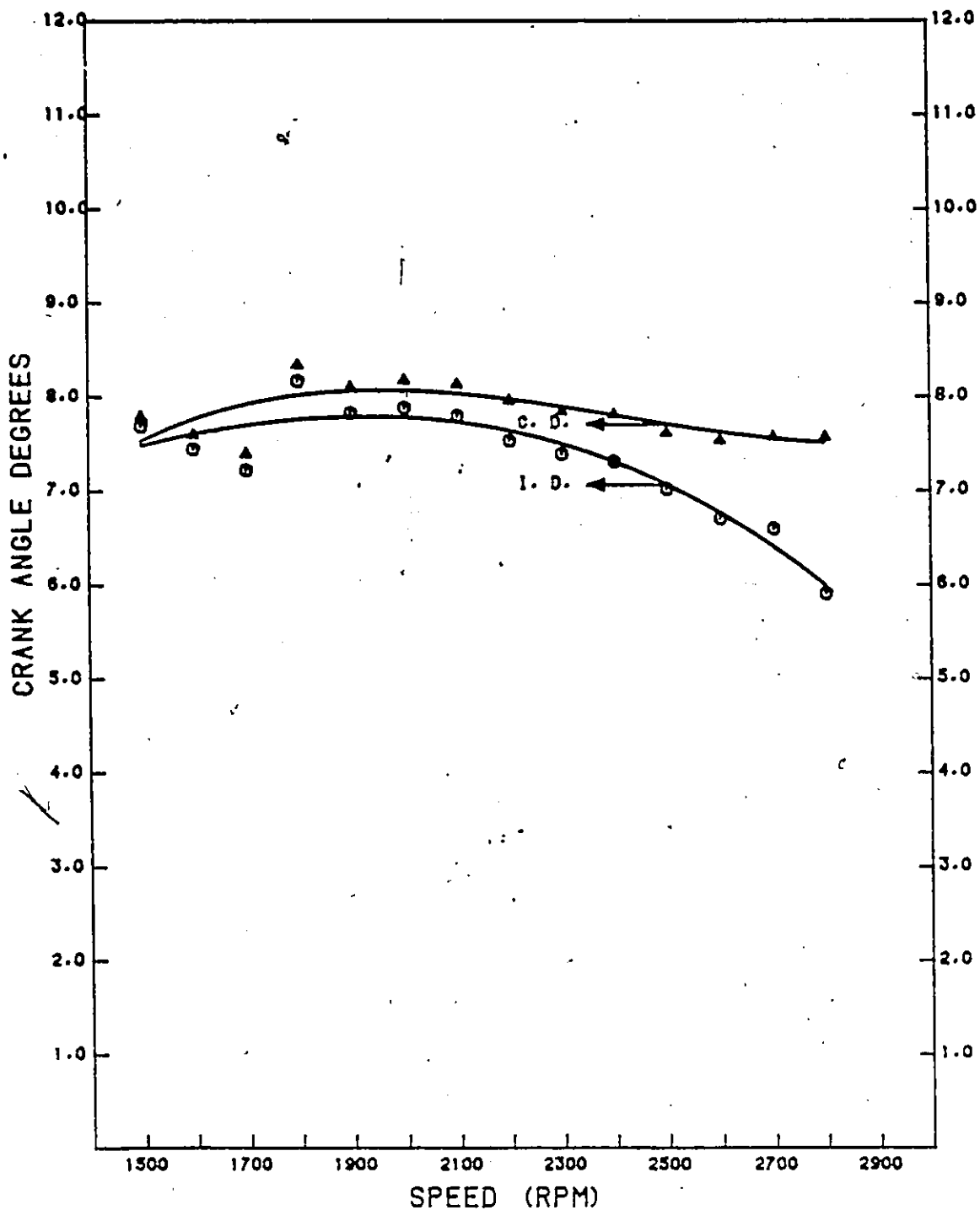


Fig. 4.26: Ignition and Combustion Delays,
6V53E Engine, Fuel 1 (3GP30),
Full Load.

IGNITION AND COMBUSTION DELAYS VS RPM
TORQUE = MAX FUEL = #2 DIESEL

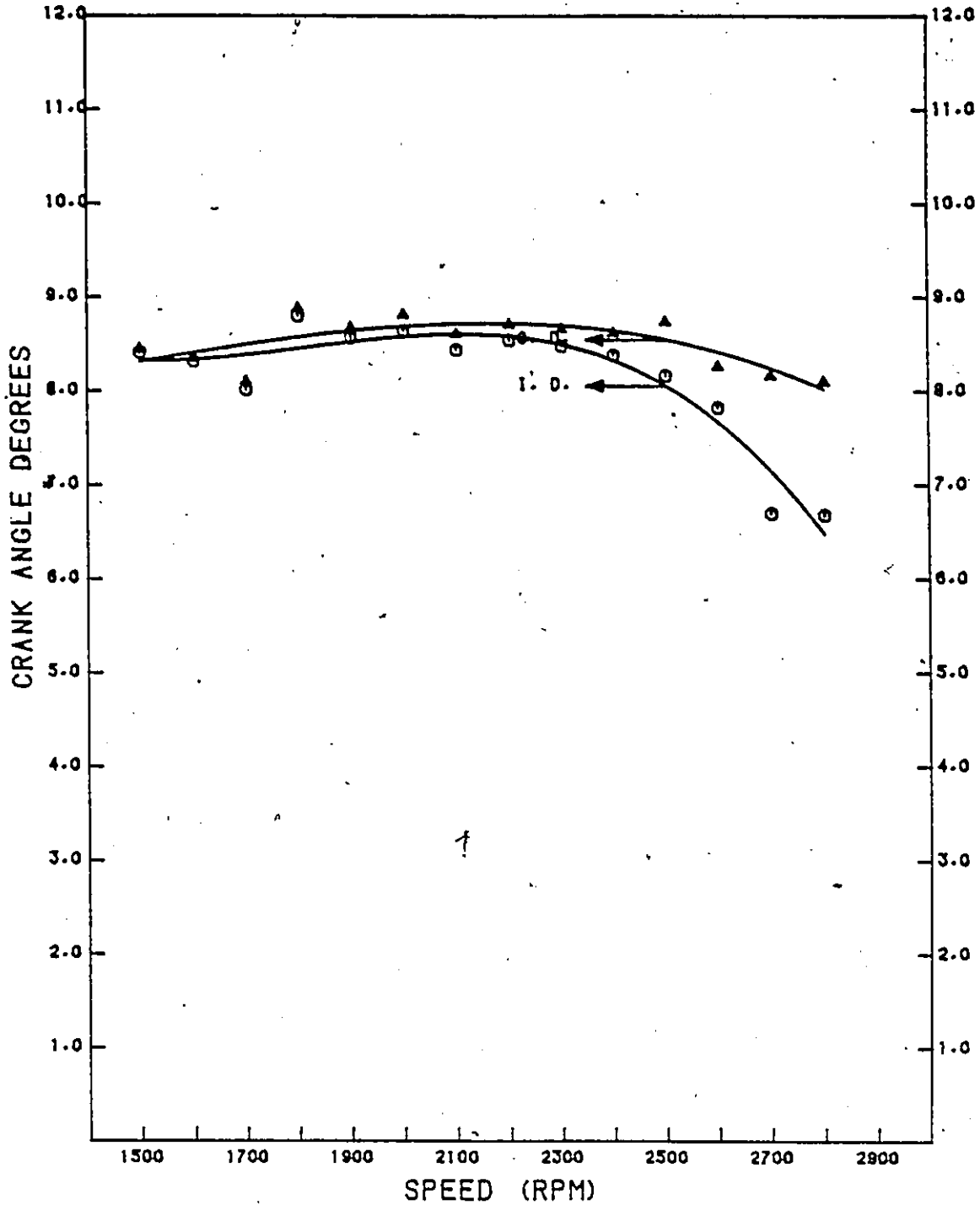


Fig. 4.27: Ignition and Combustion Delays,
6V53T Engine, Fuel 2 (#2-D).
Full Load.

IGNITION AND COMBUSTION DELAYS VS RPM
TORQUE = MAX FUEL = SHELL (1990)

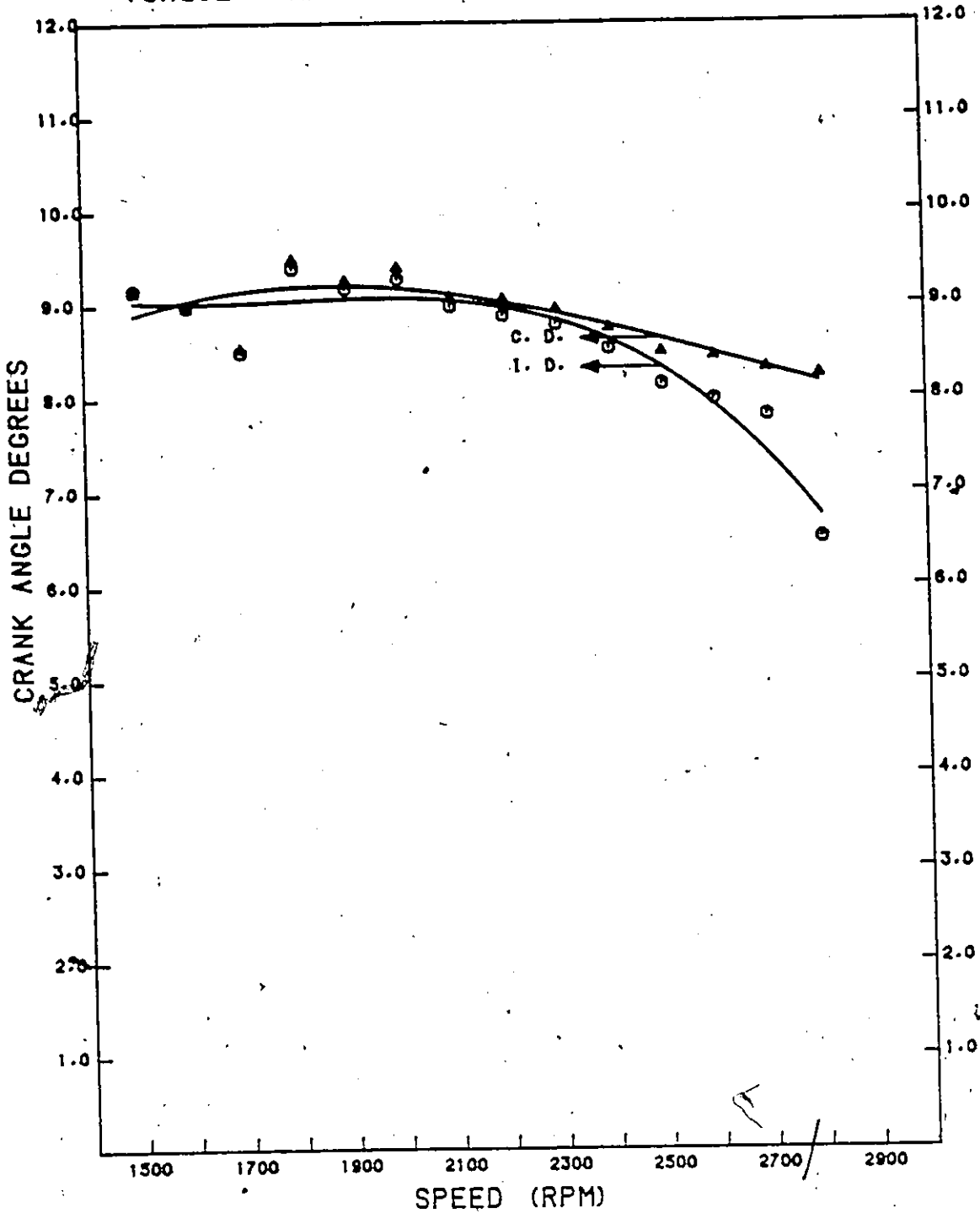


Fig. 4.28: Ignition and Combustion Delays,
6V53T Engine, Fuel 3 (Shell, 1990).
Full Load.

IGNITION AND COMBUSTION DELAYS VS RPM
TORQUE = MAX FUEL = 1990 (WORST CASE)

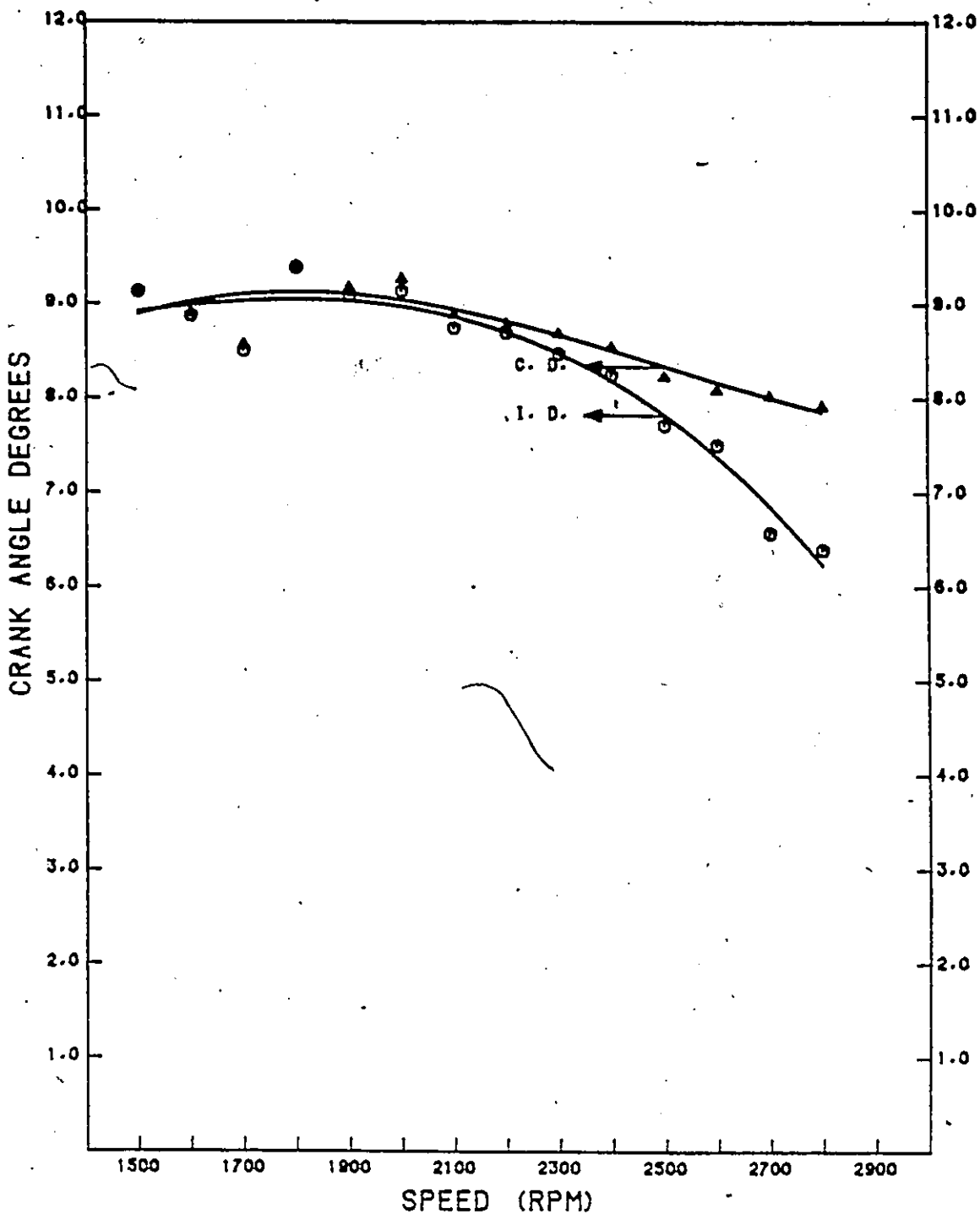


Fig. 4.29: Ignition and Combustion Delays,
6V53T Engine, Fuel 4 (1990).
Full Load.

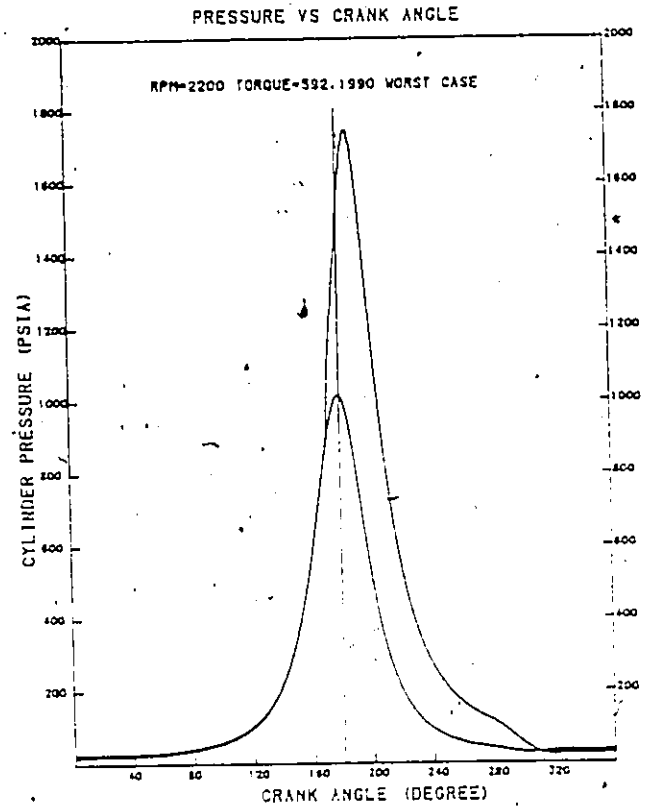
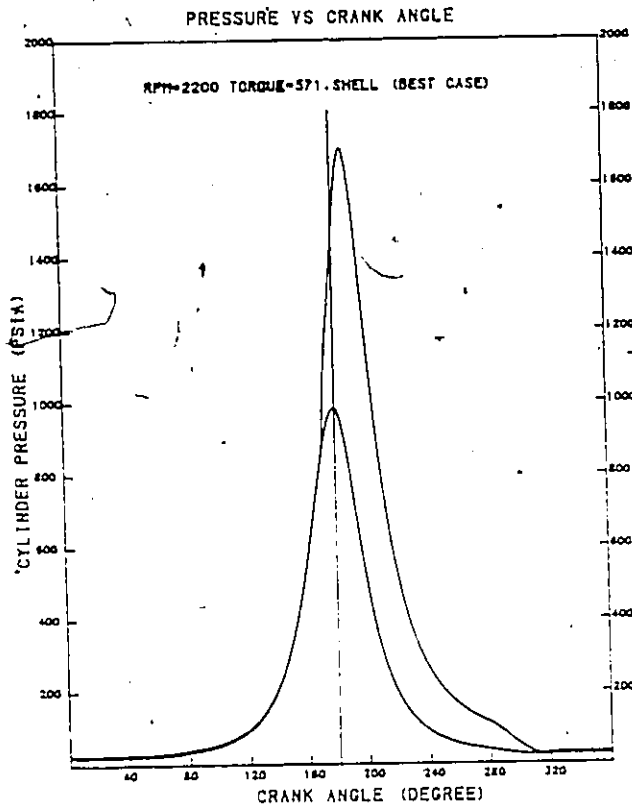
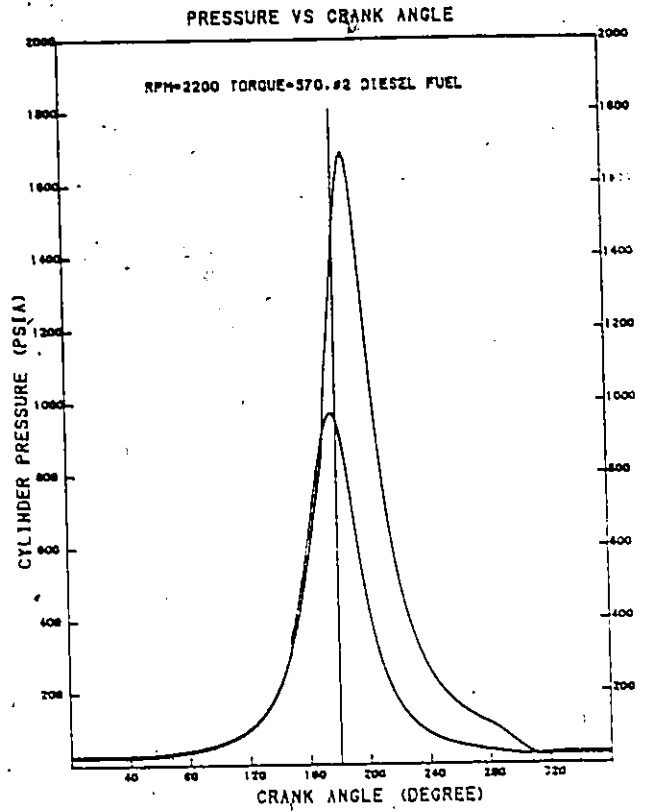
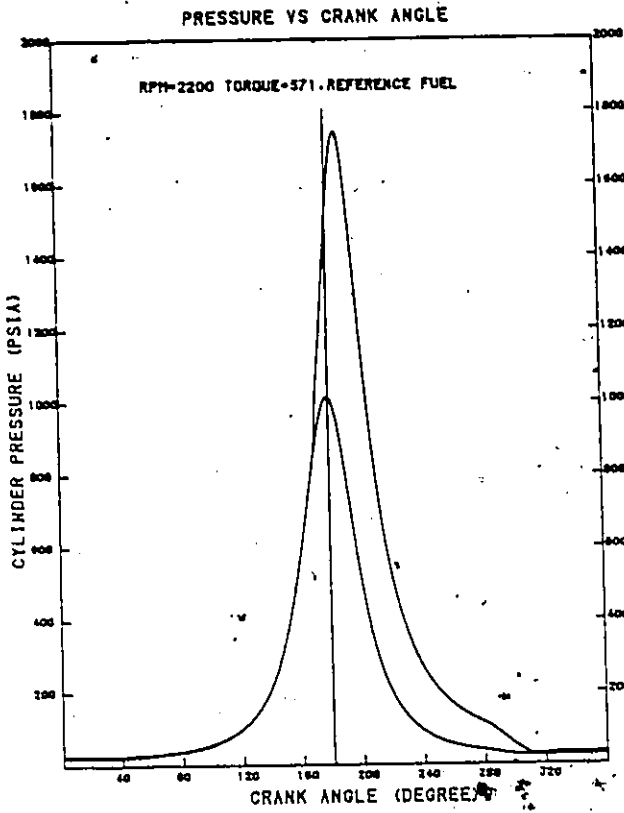


Fig. 4.30: Typical Average P-CA Curves (Motored and Fired).
6V53T Engine, Full Load, 2200 RPM.

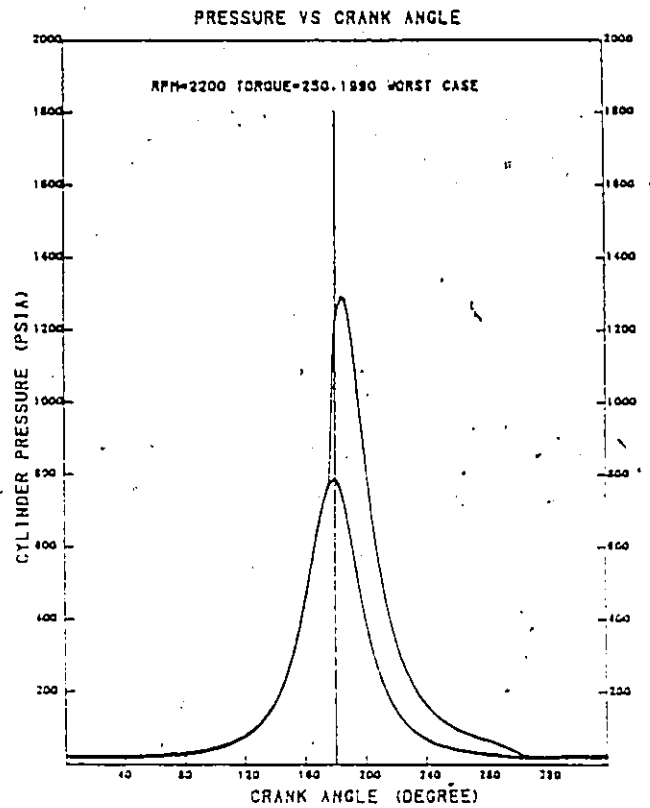
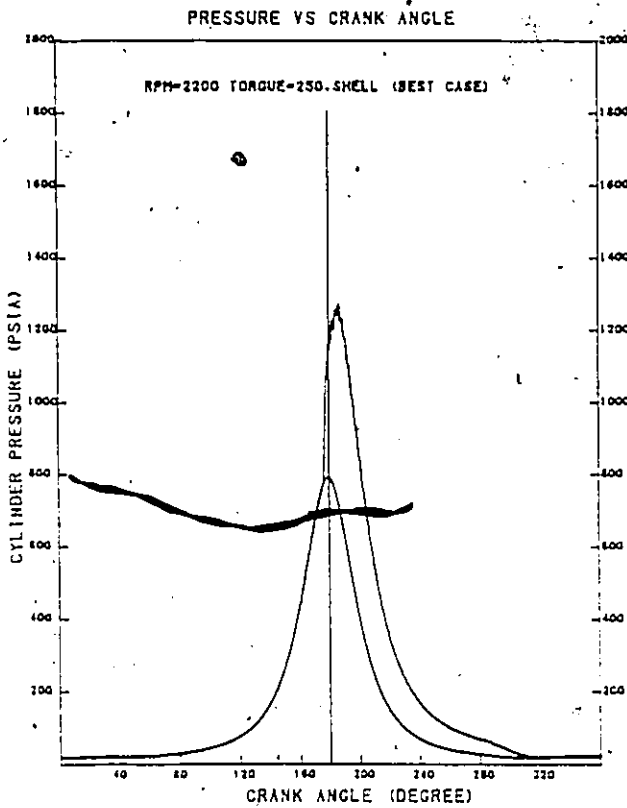
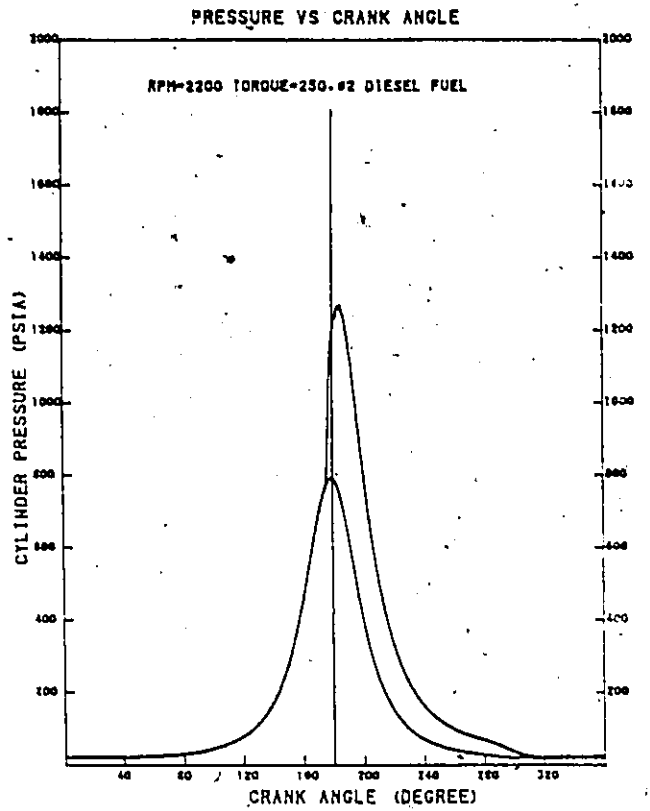
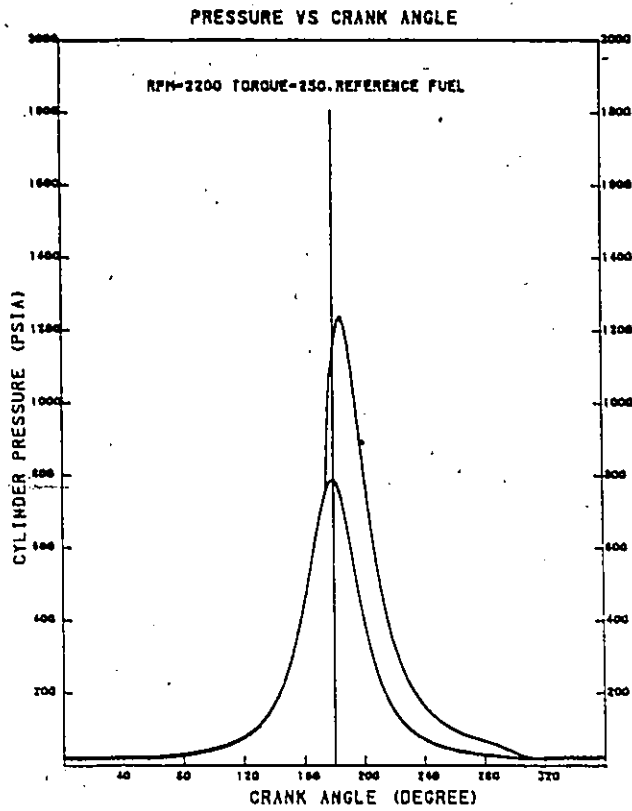


Fig. 4.31: Typical Average P-CA Curves (Motored and Fired).
6V53T Engine, Part Load, (Brake Torque=250 Ft.lbs),

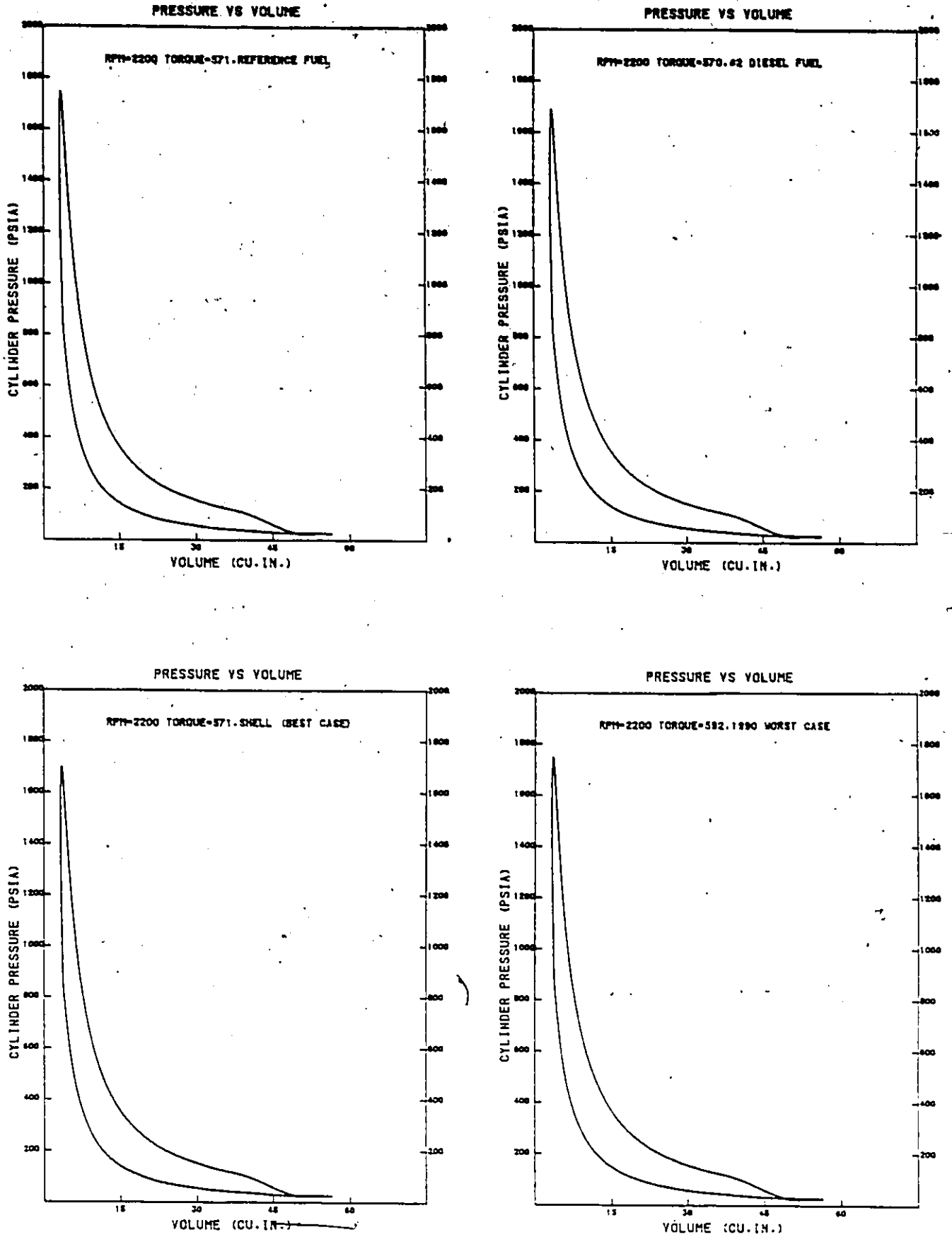


Fig. 4.32: Typical Average P-V Diagram. 6V53T Engine, Full Load, 2200 RPM.

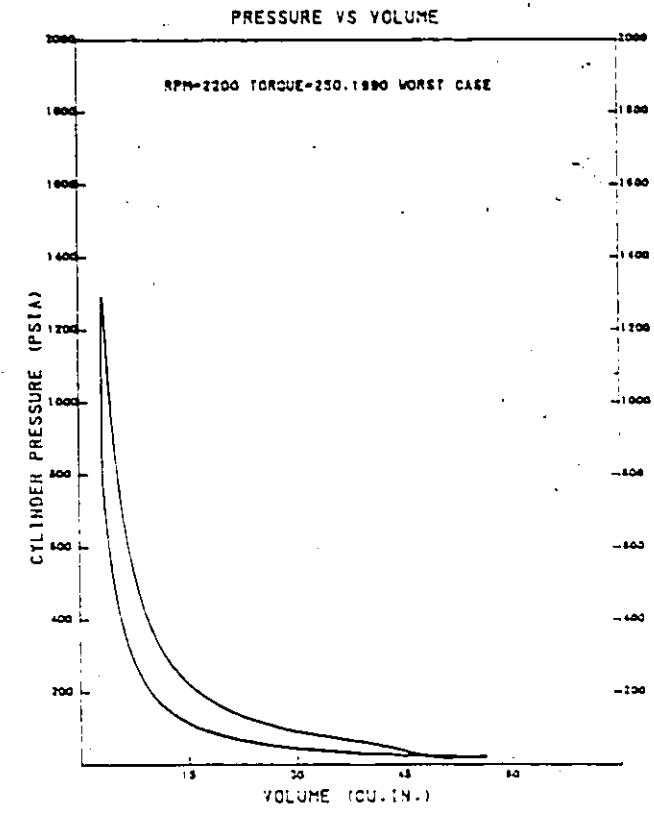
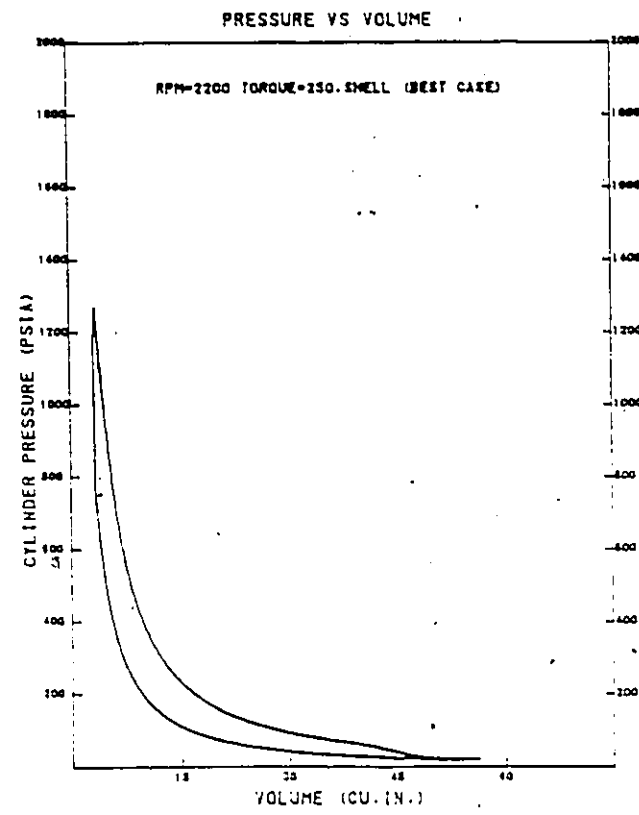
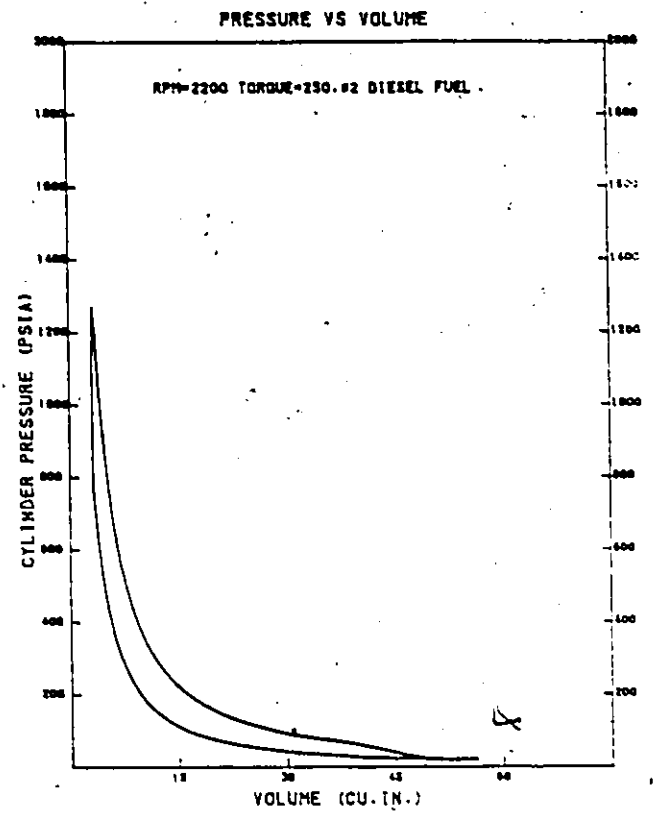
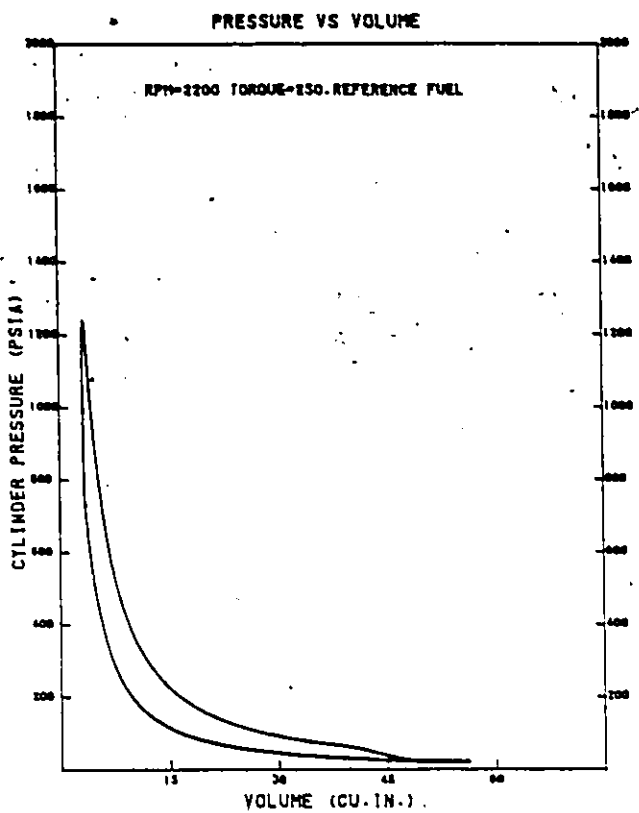


Fig. 4.33: Typical Average P-V Diagram. 6V53T Engine.
Part Load (Brake Torque = 250 Ft.lbs.),
2200 RPM

CHAPTER 5

ENGINE-FUEL CHARACTERISTIC PERFORMANCE COMPARISONS

Both the standard maximum torque characteristics as well as part load characteristics (brake torque of 250 ft.lb. held constant over the RPM test range) are presented in multi-fuel comparison plots in this chapter.

Each of the curve sets allows a subtly different view or comparison of the engine-fuel performance. In the first case, maximum torque is a fixed rack (full) setting and gives the maximum output of the engine on each of the fuels tested. The second family of curves are at variable rack settings selected so as to produce a fixed brake torque or power output from the engine. Thus, they assess the ability of each particular fuel to perform a fixed amount of work.

As was mentioned elsewhere, any brake torque could be selected from the engine-fuel data bank for the part load setting. Throughout this study a brake torque of 250 ft.lbs. was selected as being representative of the mid operating (power) setting for the engine.

The order of presentation set out in Chapter 4 will be followed: Section 5.1 gives the Brake Characteristic Performance Comparisons; Section 5.2 the Indicated Characteristic Performance Comparisons; Section 5.3 the Combustion Parameter Characteristic Comparisons and Section 5.4 presents Pressure Curve Comparisons.

For comparison of these test fuels, it was found that the precision of the results was an important factor. With computer control on the engine giving control updates every one-quarter second, RPM and torque measurements are expected to be with ± 3 RPM and ± 2 ft.lb. respectively. This represents a maximum possible measurement error of $\pm 0.55\%$ (0.51%) on BHP at 1500 (2800) RPM. However, three sets of brake data are measured during the test period which lasts about six minutes. The average of the brake data were used to calculate the brake parameters, thus, errors are expected to be considerably lower.

For IHP and related parameters, engine speed (± 3 RPM); recorded cylinder pressure (± 2 psi from the transducer signal) and the integral of P-dV combined to give the error band assuming TDC is accurately located. It is, however, not the reading of the cylinder pressure signal but rather the signal generating equipment that gives rise to the maximum possible error in recorded pressure. Here the transducer/amplifier linearity is specified to be within 1% which can result in pressure errors greater than ± 2 psi for most of the pressure curve. Further, the integrated effect

would be very difficult to determine, if at all possible. Again however, an average of 32 P-CA curves are used for the indicated power calculations and errors due to linearity can be expected to be minimal.

Concerning the numerical integration, a number of experiments were conducted involving both the lab computer and the University mainframe including single and double precision numerical evaluations, single-shot and averaged pressure curve evaluations and repeat engine-fuel (3GP30) tests.

It was found that variations of calculated IHP due to single or double precision, mainframe or HP computer, single shot or averaged pressure curves were typically within $\frac{1}{2}\%$. As a final check, a repeat engine - 3GP30 full test was run. Variation in the calculated IHP was only 0.6%. Thus, the error band for IHP and related parameters is taken to be, in the worst case, very similar to the BHP error band of just over $\frac{1}{2}\%$.

Thus, it is the opinion of the author, that the brake and indicated performance data presented here are of a very high degree of precision. However, in making fuel-to-fuel comparisons, no differentiation should be made between curves which fall within the projected error bands. It should also be noted that for combustion related parameters, a statistical analysis and standard deviation are presented directly.

Finally, the reader should note that fuel 2 (#2-D, commercially available) was used for calibration of the test cell/data acquisition/software systems. More importantly, the fuel was purchased, as required, from a local supplier. Thus, fuel variability can be expected (indeed, this is visible in the results) and further, average #2-D fuel properties were used for the calculations, eg. fuel density and heating value. The No. 2-D characteristic curves are presented for three reasons: (i) to provide a typical data set for engine behaviour on commercially available fuel; (ii) to show the variability experienced with commercially available fuels, and (iii) the results provide some interesting insight at specific operating points. Again, however, any detailed comparisons between the #2-D and the other three 'controlled' fuels should not be made.

5.1 BRAKE CHARACTERISTIC PERFORMANCE COMPARISONS

For all comparison curves, the plotting option for a 'smooth' curve was chosen, on a full axis scale, to show the general characteristic trends (plot set (a)). In addition, a second plot set (b), which uses an expanded axis and the 'continuous' curve fit passing through the points, is presented. This latter set allows detailed comparisons to be made and subtle engine/fuel trends to be identified.

5.1.1 MAXIMUM TORQUE TESTS

Figures 5.1 - 5.6 plot the brake characteristic parameter comparisons for the fuels tested: namely, BHP, torque, fuel consumption, BSFC, thermal efficiency and smoke number.

Brake power for the first three fuels (Fuels 1, 2 and 3) are virtually the same and within the experimental error band. However, Fuel 4 (1990) shows a consistent torque increase (about 20 ft.lbs. on the average) resulting in a BHP maximum output increase of from 1% (1500 RPM) to 4.5% (2800 RPM). Since fuel injection is a volume metered quantity, this power increase is attributable to the higher fuel density and hence mass of fuel injected as can be clearly seen in Fig. 5.3. However, the increase in power is not directly proportional to the mass increase since this fuel also shows the highest BSFC (Fig. 5.4) and, after incorporating heat values, marginally lower brake thermal efficiency (Fig. 5.5). The thermal efficiency and higher smoke numbers (Fig. 5.6) of the off-specification 1990 fuel suggest a higher degree of incomplete combustion (likely the high end components), especially at lower RPM.

In all respects, Fuel 3 (Shell, 1990) shows brake characteristics very similar to the reference fuel and shows less variability than commercially available No. 2-D.*

5.1.2 CONSTANT TORQUE (PART LOAD) TESTS

The constant torque tests (fuel consumption, BSFC and thermal efficiency; Figs. 5.7, 5.8 and 5.9 respectively) show characteristics very similar to the full load tests. Again, for a given engine brake power setting, Fuels 1, 2 and 3 are virtually indistinguishable. However, Fuel 4 does require a slightly higher mass flow rate of fuel (Fig. 5.7) to produce the output energy demands and results in a higher BSFC compared to all other fuels (Fig. 5.8). However, brake thermal efficiencies of all the fuels (Fig. 5.9) are very close with Fuel 4 tending to be slightly lower at the higher engine speeds.

* Note: The reader should note that the No. 2-D tests were conducted with two commercial supplies of fuel, the changeover occurring about the 2200-2300 RPM range. This is clear from the plots, especially fuel consumption. It is especially interesting to note that the lower RPM tests (1500-2200) were conducted with a moderately high density fuel (about half way between Fuels 1 and 4) and, as will be shown later, resulted in moderately rough combustion as per the P-CA data measurements.

5.2 INDICATED CHARACTERISTIC PERFORMANCE COMPARISON

Indicated horsepower and ISFC characteristics are shown in Figures 5.10 and 5.11 for the maximum torque tests (full power) while Figures 5.12 and 5.13 give the results of the part load tests (constant brake torque).

At full load, all fuels produce very similar IHP's over the speed range of the engine. The only exception being Fuel 4, and then only at higher RPM's (2400-2800), where slightly higher IHP's occur. Likewise, at a given power output (Fig. 5.12), all IHP's are very close and within the experimental/calculation error range. It thus follows, for both test cases, that Fuel 4 will show moderately higher ISFC (Figs. 5.11 and 5.13) and correspondingly lower indicated thermal efficiency (not plotted) relative to the other three fuels which show virtually the same results.

Full load IHP was expected to show Fuel 4 producing a higher IHP for the full RPM range in line with the BHP results. Due to this, a number of numerical experiments were run using both lab and mainframe computers as well as an experimental retest (3GP30 fuel), as described at the beginning of the chapter. The results of all the experiments confirmed the accuracy of IHP calculations. In short, this apparent discrepancy remains unexplained. Fuel 4 resulted in rough combustion giving rise to substantial pressure waves (see Section 5.4). A fixed digitizing rate of five points per crank angle degree (1800/revolution) was used for all fuels at all RPM's. For Fuel 4, a higher digitizing rate may be required to completely characterize the pressure curve. However, should this be true, then the part load calculated IHP (Fig. 5.12) should be lower for Fuel 4 than the others, which it isn't. This phenomena is further exemplified by the comparison of the mechanical efficiency curves. Figure 5.14 shows the mechanical efficiency of Fuel 4 at full load about two percentage points higher than the other fuels while at part load (Fig. 5.15), mechanical efficiencies of all fuels are virtually the same. In Chapter 6, engine mapping will help clarify this phenomena and show that it is related essentially to the maximum torque curve only.

Thus, based on both brake and indicated characteristic performance comparison (at both full and part load), no major discernable differences are evident. The high BSFC (IFSC) of Fuel 4 is principally a result of high fuel density and hence would not represent significant changes in operator costs. Further, the high BHP performance available with Fuel 4 would be both discernable and desirable to an operator.

5.3 COMBUSTION PARAMETER CHARACTERISTIC COMPARISON

The 'onset of combustion' and 'onset of rapid combustion' parameters together with the corresponding ignition and combustion delay periods are primarily diagnostic and provide considerable insight into the 'ignition and burn' character of a fuel.

On the other hand, peak pressures and in particular maximum pressure rates, while they do provide significant diagnostic information, are the principal parameters relating to engine mechanical stressing. As such, they provide information on engine durability and fuel suitability.

5.3.1 MAXIMUM TORQUE TESTS

The onset of combustion is compared in 5.16 (relative ignition delay can be read from the curves) while Fig. 5.17 plots the ignition delay ($^{\circ}\text{CA}$) for each of the fuels tested. Fuels 1, 2 and 3 show fairly consistent trends (Fig. 5.16a) with respect to onset of combustion or ignition delay, Fuel 3 being 1.2-1.4 $^{\circ}\text{CA}$ later than Fuel 1 with Fuel 2 (No. 2-D) falling about half way between Fuels 1 and 3, but approaching Fuel 3 (longer I.D.'s) at the higher engine speeds. (Note again the changeover in the No. 2-D fuel supply at 2100-2200 RPM). However, Fuel 4 follows Fuel 3 very closely at low RPM's but has a pronounced roll-off with increasing engine speed and exhibits shorter ignition delays at higher RPM's than the No. 2-D.

Further insight can be gained from Table 5.1 which lists the numerical values of the combustion events (eg. onset of combustion) together with the standard deviation of each value as determined from the statistical analysis of thirty-two single-shot pressure curves. The standard deviations provide considerable insight. Large standard deviations, especially on the 'onset of combustion', indicate large cycle-to-cycle variation. In this regard, Fuels 3 and 4 show the greatest cycle-to-cycle variability, the extreme being reached by Fuel 4 at 2800 RPM. On the other hand, the statistical data shows a remarkable cycle-to-cycle repeatability at the low-to-mid speed ranges of the engine.

In general, all fuels show a slight roll-off in both ignition delay and onset of combustion with increasing engine speed (measured in $^{\circ}\text{CA}$). Further, the detailed inflections of the curves are remarkably similar for all fuels, the earlier onset of combustion (relative to the general trend) at 1700 RPM being a good example. It should be noted that such an inflection can be traced through the other measured events (eg. the higher cylinder pressure at 1700 RPM, etc.) as well as both brake and indicated parameters (see brake torque curve, Fig. 5.2b).

TABLE 5.1

NUMERICAL VALUES AND STATISTICAL RESULTS *
COMBUSTION PARAMETER DATA (FULL LOAD)

CONDITION AND COMBUSTION PARAMETER	FUEL 1		FUEL 2		FUEL 3		FUEL 4	
	Value	Std. Dev.	Value	Std. Dev.	Value	Std. Dev.	Value	Std. Dev.
<u>RPM = 1500 Torque = Maximum</u>								
Peak pressure in psia	1666.4	13.78	1643.9	15.60	1640.9	19.65	1683.5	21.79
Peak pressure loc. in °CA	185.6	0.34	185.2	0.42	185.2	0.44	185.1	0.60
Maximum pressure rate in psi/°CA	134.6	8.79	173.7	12.35	207.6	20.45	236.7	23.08
Maximum pressure rate loc. in °CA	170.4	.36	171.3	0.36	171.8	0.39	171.7	0.22
Onset of combustion in °CA	169.4	0.0	170.1	0.15	170.9	0.22	170.8	0.23
Onset of rapid combustion in °CA	169.5	0.0	170.4	0.13	170.9	0.10	170.8	0.23
<u>RPM = 2200 Torque = Maximum</u>								
Peak pressure in psia	1751.5	22.06	1692.9	18.71	1706.4	19.27	1752.2	27.91
Peak pressure loc. in °CA	186.7	0.44	187.1	0.36	186.8	0.54	186.7	0.81
Maximum pressure rate in psi/°CA	101.0	6.57	111.6	8.68	125.6	10.52	138.4	10.51
Maximum pressure rate loc. in °CA	169.6	0.17	170.9	1.14	171.2	0.27	170.7	0.14
Onset of combustion in °CA	168.8	0.24	169.8	0.17	170.2	0.19	170.0	0.14
Onset of rapid combustion in °CA	169.0	0.0	170.0	0.13	170.4	0.13	170.1	0.19
<u>RPM = 2800 Torque = Maximum</u>								
Peak pressure in psia	1744.1	29.46	1692.8	26.24	1715.2	27.29	1794.4	20.15
Peak pressure loc. in °CA	186.8	0.57	186.9	0.55	187.3	0.31	187.0	0.33
Maximum pressure rate in psi/°CA	92.1	7.77	104.7	10.31	109.7	11.98	109.8	11.19
Maximum pressure rate loc. in °CA	169.5	0.15	170.1	0.17	170.3	.24	169.9	.18
Onset of combustion on °CA	167.6	1.60	168.4	2.26	168.2	2.23	168.0	2.71
Onset of rapid combustion in °CA	169.3	0.15	169.8	0.14	169.9	0.15	169.6	0.11

Note: TDC = 180°CA

* From ...

The correlation between subtle inflections in the onset of combustion (approximately 0.4°CA early at 1700 RPM) and what is actually produced by the engine (brake torque or power) is quite intriguing and reinforces the reliability and accuracy of the data. It is particularly interesting to observe that the previously unexplained drop in brake torque and power for the No. 2-D fuel at 2400-2600 RPM (see Fig. 5.1b and 5.2b) can now be explained and is a direct result of long ignition delays or late onset of combustion of the No.2-D at these speeds evident in Fig. 5.16(b).

Onset of rapid combustion (Fig. 5.18) and combustion delay (Fig. 5.19) exhibit very similar trends and relative behavior (fuel-to-fuel) as do onset of combustion and ignition delay with one subtle but important exception, that being the roll-off with RPM is now almost non-existent. Thus, onset of rapid combustion appears quite independent of engine speed. The following table summarizes:

TABLE 5.2

RPM	ONSET OF RAPID COMBUSTION VS. ENGINE SPEED			
	FUEL (1)	FUEL (2)	FUEL (3)	FUEL (4)
1500	169.49	170.15	170.84	170.82
1600	169.40	170.15	170.77	170.70
1700	169.20	169.90	170.33	170.37
1800	169.64	170.18	170.78	170.71
1900	169.61	170.18	170.76	170.67
2000	169.58	170.21	170.79	170.67
2100	169.44	169.91	170.38	170.19
2200	169.26	170.01	170.36	170.09
2300	169.25	170.06	170.34	170.09
2400	169.31	170.12	170.24	170.04
2500	169.12	170.24	169.98	169.73
2600	169.14	169.86	170.04	169.69
2700	169.28	169.86	170.01	169.72
2800	169.27	169.80	169.94	169.62
AVE.	169.36	170.05	170.40	170.22
STD.DEV.	0.17	0.15	0.34	0.43

Thus, combustion delay becomes quite independent of engine speed making it a considerably more attractive (and tractable) parameter to study and work with (including engine modeling) than ignition delay.

It should also be noted, at this time, that the combustion development period ($^{\circ}\text{CA}$) increases with engine speed (0.0-0.2 $^{\circ}\text{CA}$ at 1500 RPM increasing to 1.4-1.8 $^{\circ}\text{CA}$ at 2800 RPM) and shows a similar behavior for all fuels. This parameter will be discussed later.

The maximum cylinder pressure curves vs. engine speed (Fig. 5.20) show classical trends. At full load, Fuel 4 produced the highest cylinder pressures followed by Fuels 1, 3 and 2 respectively. The lower peak cylinder pressures associated with the No. 2-D, relative to the reference 3GP30 fuel, were not expected but does correlate nicely with the relatively longer combustion or ignition delays observed. The maximum cylinder pressure produced by Fuel 4 was only about 30 psi higher (1.7%) than that produced by the reference fuel but about 80 psi higher than that produced by the No. 2-D.

In general, maximum cylinder pressures appear well behaved for all fuels (Fig. 5.20a) and none of the fuels produced pressures that would appear to be unacceptable to the engine from a design stress point of view.

On the other hand, the maximum pressure rate curves (Fig. 5.21, 1 $^{\circ}\text{CA}$ span) begin to reflect the severity of the off-specification fuel combustion and will be an important parameter in assessing fuel suitability and engine durability.

In general, low RPM (and part rack) settings produce the highest rates. This will be identified in engine mapping, Chapter 6. It is clear that both Fuels 3 and 4 give rise to pressure rates that are pushing the design limits of the engine.

5.3.2 CONSTANT TORQUE TESTS

As in the previous section, combustion parameter comparison plots (Fig. 5.22 - 5.25) and statistical data (Table 5.3) are presented for the part load engine setting.

Since these curves are generated at a constant power output from each fuel, caution should be exercised in interpreting ignition and combustion delay since rack setting, hence start of injection, can vary from fuel to fuel. A review of Fig. 5.7 suggests very similar rack settings for each fuel at each RPM, thus, the curves do provide a good indication

TABLE 5.3

NUMERICAL VALUES AND STATISTICAL RESULTS,
COMBUSTION PARAMETER DATA (PART LOAD)

CONDITION AND COMBUSTION PARAMETER	FUEL 1		FUEL 2		FUEL 3		FUEL 4	
	Value	Std. Dev.	Value	Std. Dev.	Value	Std. Dev.	Value	Std. Dev.
RPM = 1500 Torque = 250 ft.lbs.								
Peak pressure in psia	1175.4	13.74	1186.7	21.00	1228.0	21.01	1248.6	23.65
Peak pressure loc. in °CA	183.3	0.46	182.7	0.35	182.8	0.61	182.7	0.55
Maximum pressure rate in psi/°CA	207.3	20.67	248.9	16.91	288.8	19.96	303.2	30.48
Maximum pressure rate loc. in °CA	174.8	0.15	176.1	0.31	176.3	0.09	176.7	0.28
Onset of combustion in °CA	173.9	0.23	175.0	0.20	175.5	0.0	175.6	0.13
Onset of rapid combustion in °CA	174.0	0.25	175.0	0.19	175.5	0.0	175.6	0.0
RPM = 2200 Torque 250 ft.lbs.								
Peak pressure in psia	1246.3	15.43	1286.0	19.40	1312.1	22.86	1313.0	20.37
Peak pressure loc. in °CA	184.8	0.60	184.4	0.79	184.1	.76	184.4	0.66
Maximum pressure rate in psi/°CA	152.5	13.36	202.2	23.36	220.5	29.67	215.5	29.07
Maximum pressure rate loc. in °CA	174.9	0.27	176.8	0.43	176.8	0.43	177.1	0.50
Onset of combustion in °CA	174.0	0.49	175.5	0.13	175.9	0.15	175.8	0.20
Onset of rapid combustion in °CA	174.1	0.20	175.6	0.23	176.0	0.11	175.8	0.23
RPM = 2800 Torque = 250 ft.lbs.								
Peak pressure in psia	1342.2	10.86	1333.3	13.08	1367.6	14.26	1416.5	13.82
Peak pressure loc. in °CA	184.9	0.79	184.9	0.33	185.6	0.78	185.4	0.27
Maximum pressure rate in psi/°CA	122.9	9.63	140.1	18.47	175.1	23.16	163.9	19.76
Maximum pressure rate loc. in °CA	173.5	0.19	174.0	.35	175.1	0.28	174.7	0.26
Onset of combustion in °CA	172.9	0.19	173.5	0.13	174.3	0.23	174.1	0.23
Onset of rapid combustion in °CA	173.0	0.18	173.5	0.09	174.3	0.18	174.1	0.24

Note: TIC = 180°C

* See reference 36

of the delay periods. In general, relative delay appears more pronounced at part load (Fig's. 5.22 and 5.23) and results in very similar onset of combustion and onset of rapid combustion crank angle positions. Thus, short combustion development periods, especially for the off-specification fuels, are associated with part-load operation.

It should also be noted that the crank angle positions remain better ordered (i.e. no major crossing of the curves) at the part load setting. The No. 2-D now consistently follows the reference fuel and, in general, Fuel 4 exhibits the longest delay periods with minor crossings with Fuel 3 at the higher RPM ranges.

Maximum cylinder pressures at part load (Fig. 5.24) are not of any numerical significance. However, it should be noted that the ordering of the curves is again more logical with the reference and No. 2-D fuels grouping and exhibiting lower values than the off-specification fuels.

As expected, maximum pressure rates (Fig. 5.25) show a substantial increase at the part load setting reaching values in the order of 300 psi/°CA (using a 1°CA span). Indeed, instantaneous pressure rates (based on a 0.2°CA span), at these settings, can reach 500 psi/°CA for the off-specification fuels as shown in Fig. 5.26. Such rates suggest diesel knock and, as a minimum, substantial pressure waves can be expected as will be viewed in the following section.

5.4 PRESSURE CURVE COMPARISONS

Pressure curves will be presented in the order of increasing maximum pressure rate severity as evident from Figures 5.21 and 5.25, viz:

1. 2800 RPM, FULL LOAD: LOW PRESSURE RATES:
Fuel 1: 92 psi/°CA
Fuel 2: 105 psi/°CA
Fuel 3: 110 psi/°CA
Fuel 4: 110 psi/°CA
(Figures 5.27 and 5.28)

2. 2800 RPM, PART LOAD: MODERATE PRESSURE RATES:
Fuel 1: 123 psi/°CA
Fuel 2: 140 psi/°CA
Fuel 3: 175 psi/°CA
Fuel 4: 164 psi/°CA
(Figures 5.29 and 5.30)

3. 1500 RPM, FULL LOAD: HIGH PRESSURE RATES:
Fuel 1: 135 psi/°CA
Fuel 2: 174 psi/°CA
Fuel 3: 208 psi/°CA
Fuel 4: 237 psi/°CA
(Figures 5.31 and 5.32)
4. 1500 RPM, PART LOAD: VERY HIGH PRESSURE RATES:
Fuel 1: 207 psi/°CA
Fuel 2: 249 psi/°CA
Fuel 3: 289 psi/°CA
Fuel 4: 303 psi/°CA
(Figures 5.33 and 5.34)

It should be noted that all the statistical values*(eg. maximum pressures, pressure rates, etc.) are based on the average of thirty-two single-shot P-CA curves. For all comparison studies (Figures 5.27 - 5.34), single-shot P-CA curves are presented. As such, the statistical data will not correspond directly with the curve.

The comparison figures show first the complete P-CA curve (fired and motored) for each fuel followed by an expanded axis plot which focuses on the injection-combustion-peak pressure region of the curve (i.e. $\pm 20^\circ$ about TDC).

Evaluating the single-shot P-CA curves can be difficult for two reasons: first, the interpretation of pressure fluctuations can be misleading and second, it must be realized that any discrete single-shot may not represent the normal engine-fuel behaviour. Further, interpretation must objectively account for the digitizing rate.

Three distinct characteristics of the P-CA curves can be identified and defined.

1. "Normal" Combustion: During the main combustion period (from onset to peak pressure) normal combustion can be moderately smooth (Fig. 5.28, a and b) to fairly rough (Fig. 5.30, a and b). These pressure undulations are characterized by: random shape and frequency, relatively small fluctuations, no sharp peaks and result in smooth expansion curves. They are considered to be a direct and expected result of the heterogeneous combustion of a diesel engine. Further, due to their random nature, the average curve will be quite smooth (see Chapter 4 curves).

* See reference 36

2. "Pressure Waves": Pressure waves are a direct result of high pressure rates and/or diesel knock. They are gas vibrations within the combustion zone and as such are independent of the fuel and will show a cyclic, sinusoidal type motion which will continue during expansion. If the digitizing rate is adequate, the undulations will show smooth tips and the highest frequency at TDC. Typical gas vibrations are shown in Figure 5.32 (b,c,d) and larger amplitude vibrations in Figure 5.34 (b,d).

Gas vibration frequency at 1500 RPM, from any of the figures mentioned, is about seven cycles per 10° period over TDC ($\pm 5^\circ$ TDC) reducing to about six cycles/ 10° C.A. on expansion. Thus, at a digitizing rate of five points/C.A. degree, the pressure wave is characterized by only 7-8 points. This is barely sufficient but adequate as can be seen from the plots.

3. "Knock": Knock is uncontrolled detonation of excessive amounts of prepared fuel and will result in extreme pressure rates provided the transducer and digitizing rates are fast enough to follow the pressure rise. It will always occur at the beginning of combustion during the 'classical' rapid pressure rise region of the P-CA curve (i.e. always well before TDC).

In these tests, it is now recognized that the digitizing rate was not adequate to properly characterize knock. However, sharp points on the pressure rise curve (eg. first two points in Fig. 5.32, c and d) can be suspected of knock being as they are clearly not gas vibrations.

Thus a general overview of the P-CA plots can now be taken. At 2800 RPM, full load (Figs. 5.27, 5.28) combustion is judged to be normal, slightly rougher for Fuels 3 and 4 but nothing that would suggest engine durability/operability problems. The same holds for the part load, 2800 RPM setting (Figs. 5.29, 5.30).

However, at 1500 RPM, full load (Figs. 5.31, 5.32) the combustion character changes. Fuels 2, 3 and 4 all show moderate pressure waves. Further, fuels 3 and 4 can be suspected of knock and, as noted earlier, produce average maximum pressure rates in excess of normal design limits. This observation is furthered at the 1500 RPM, part load setting where substantial pressure waves result (Figs. 5.33, 5.34). Interestingly, Fuel 3 does not result in a pressure wave characteristic that would be expected from other evidence (eg. excessive average maximum pressure rate, etc.). Two possible explanations are offered: (a) the single shot P-CA curve captured is not representative (supporting evidence: even the average P-CA curve at this point shows substantial pressure waves) and/or (b) the curve is characterized by knock which could not be captured at the digitizing rate used (supporting evidence: the high frequency, sharp pointed undulations in the curve just before TDC suggest possible knock).

In summary, combustion evidence suggests that Fuels 3 and 4 may not be engine compatible and could possibly result in premature engine component failure. Further, a direct correlation between maximum pressure rates measured and severity of combustion is evident.

Two last observations are of interest, the No. 2-D (Fuel 2) shows quite severe combustion at 1500 RPM and resembles the off-specification fuels while at 2800 RPM similarity with the reference (Fuel 1) is more notable. As pointed out earlier, the 1500 RPM and 2800 RPM tests were performed with two different supplies of commercial grade No. 2-D. Clearly, the variability in the commercial products is evident, the first supply (1500 RPM tests) being a fairly low grade fuel. Secondly, it is interesting to note the cylinder pressure drop (relative to the motored curves), due to fuel vaporization, visible on many of the curves presented (eg. Fig. 5.34,d).

5.5 CLOSURE

The characteristic performance (both brake and indicated) at full and partload settings of the engine did not reveal any evidence that would cause concern over using the off-specification fuels in the 6V53T engine. However, combustion analysis and P-CA readings do give rise to concerns over fuel compatibility and engine life or durability. Some experimental evidence does exist to substantiate this although, in the opinion of the author, it is likewise not completely conclusive.

Fuels were tested in the order of their suspected combustion severity. Following the initial system calibration runs (#2-D, Fuel 2, approximately 100 hours), engine-fuel tests were conducted on Fuel 1, 3 and 4 respectively. A complete test requires approximately forty hours of engine operation.

Nearing the end of the Fuel 4 tests, coolant was found in the oil pan and the problem was traced to a crack in the cylinder head gasket (Fig. 5.35) on cylinder number two, right bank which, in turn, precipitated a burn out of the coolant o-ring. Figure 5.36 shows the head and block of the failed right cylinder bank. For comparison, the left bank is shown in Fig. 5.37. It should be noted that the pressure transducer is fitted to cylinder No. 1 on the left bank (visible in Fig. 5.37, head photograph on left at 6.00 o'clock).

A loose head bolt was found at the failure location. The loosening of the bolt and gasket failure could have been promoted by the head vibrations which would result from the substantial pressure waves known to be produced by Fuel 4. However, as stated, no firm conclusion of this fact could be drawn.

Throughout the Chapter, the combustion development period was seen to increase with increasing engine speed and to decrease with decreasing load. Further, the maximum pressure rate was found to exhibit an inverse relationship. Thus a correlation between the combustion development period and maximum pressure rates (or severity of combustion) was examined.

Figure 5.38 plots maximum instantaneous pressure rate (0.2°CA span) vs. the combustion development period (°CA). Each data point on the plot is the average value of thirty-two measurements (i.e. from the statistical data) and represent both full load and part load measurements taken over the complete operating speed range of the engine for all fuels tested.

Clearly a direct correlation exists and is particularly interesting in that it is directly applicable to all fuels tested and at all engine speeds and loads.

Finally, examining Figures 5.17 and 5.22 suggest that a direct correlation between fuel cetane number and ignition delay does not exist at full load (Fig. 5.17) but could exist at part load (Fig. 5.22). Considering the nature of the fuel cetane test procedure, one would expect a correlation to exist only if the physical conditions (injection, turbulence, etc.) of the engine under test and the ASTM-CFR engine were similar.

6V53T TWO STROKE ENGINE

BRAKE HORSE POWER VS RPM

TORQUE = MAX

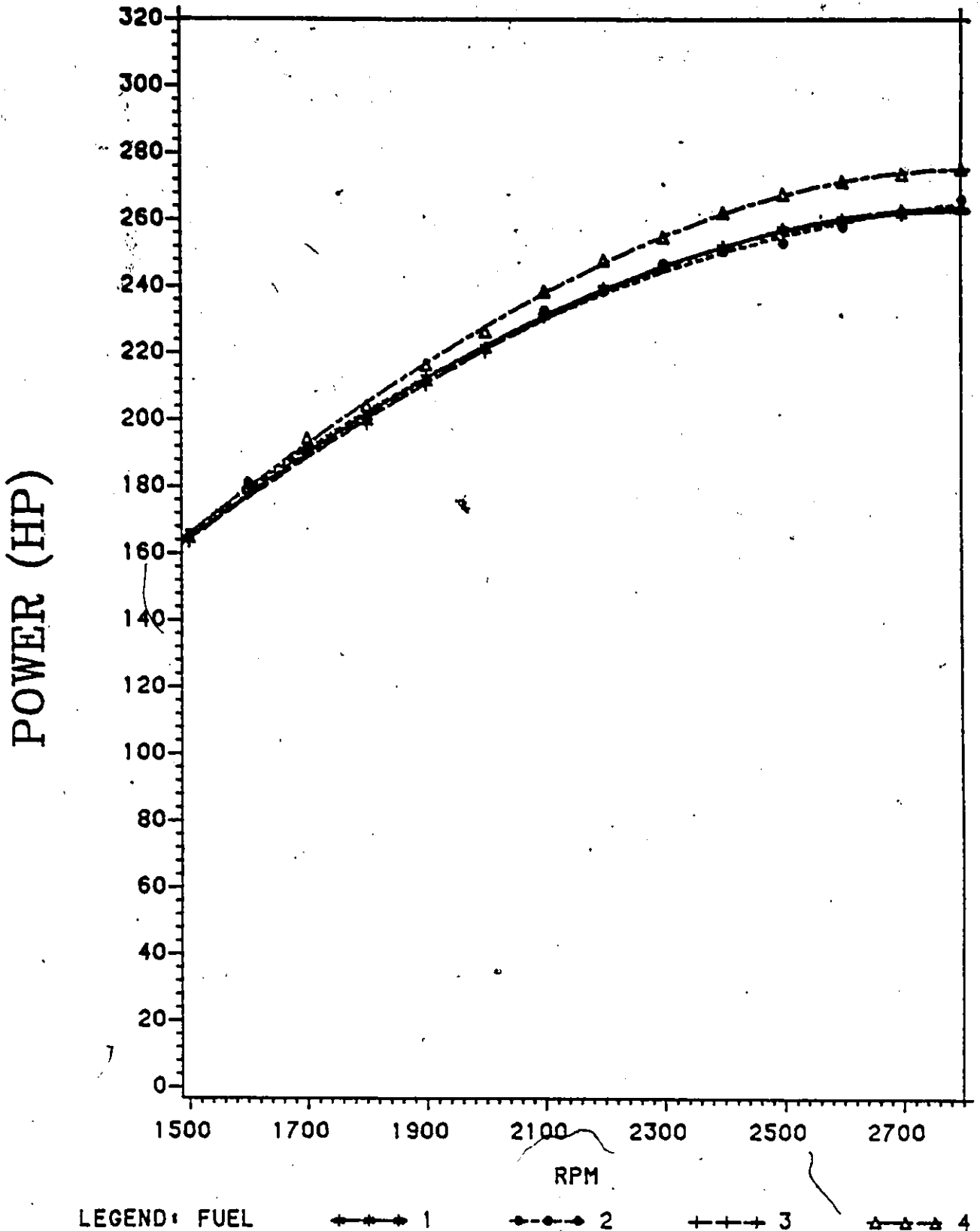
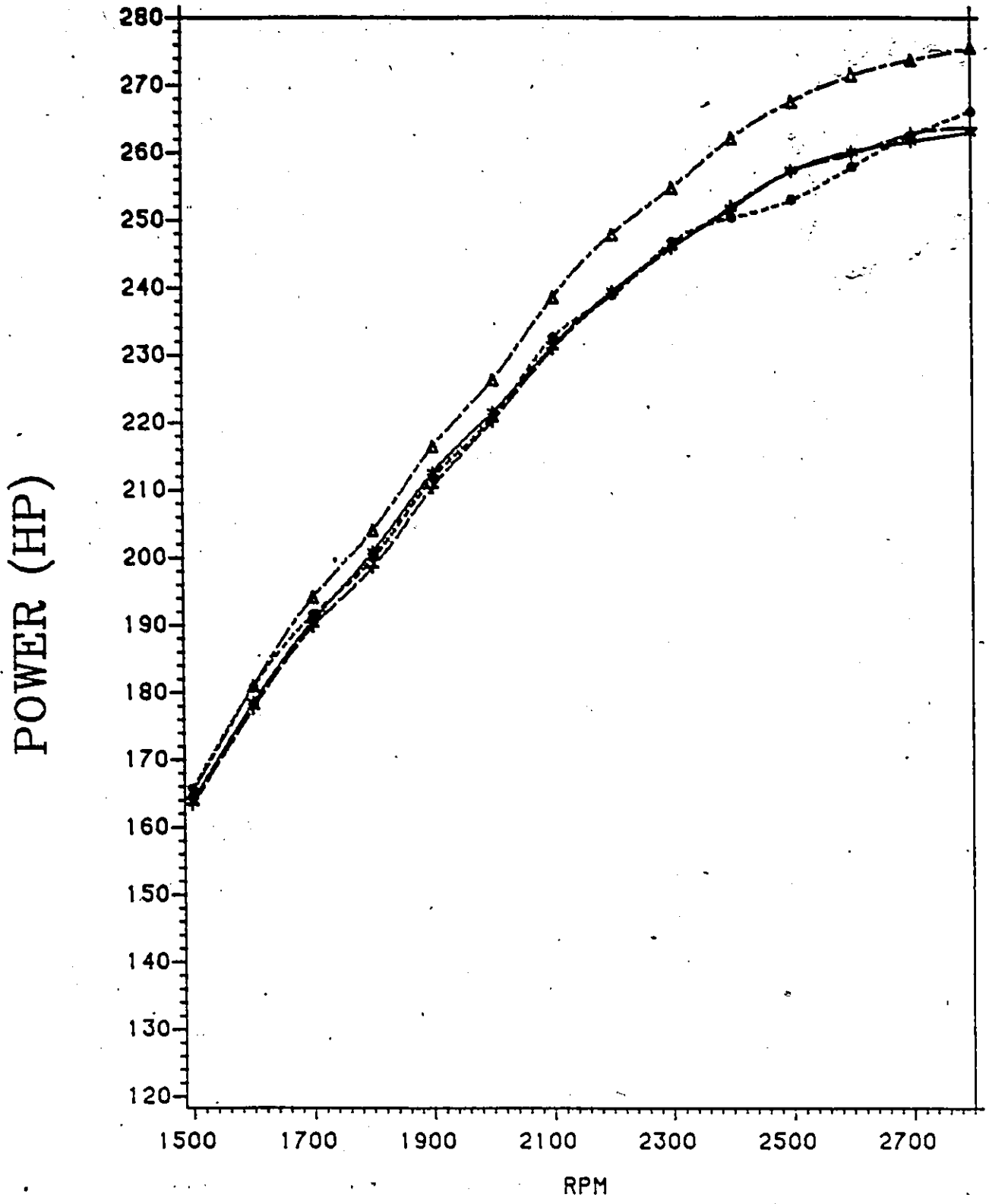


Fig. 5.1(a): Brake Horsepower Comparison at Full Load. Full Scale Characteristic Trends.

6V53T TWO STROKE ENGINE

BRAKE HORSE POWER VS RPM
TORQUE = MAX



LEGEND: FUEL +--+ 1 -●-●- 2 +--+ 3 ▲-▲-▲ 4

Fig. 5.1(b): Brake Horsepower Comparison at Full Load.
Expanded Axis Detailed Comparison.

6V53T TWO-STROKE ENGINE

BRAKE TORQUE VS RPM
TORQUE - MAX

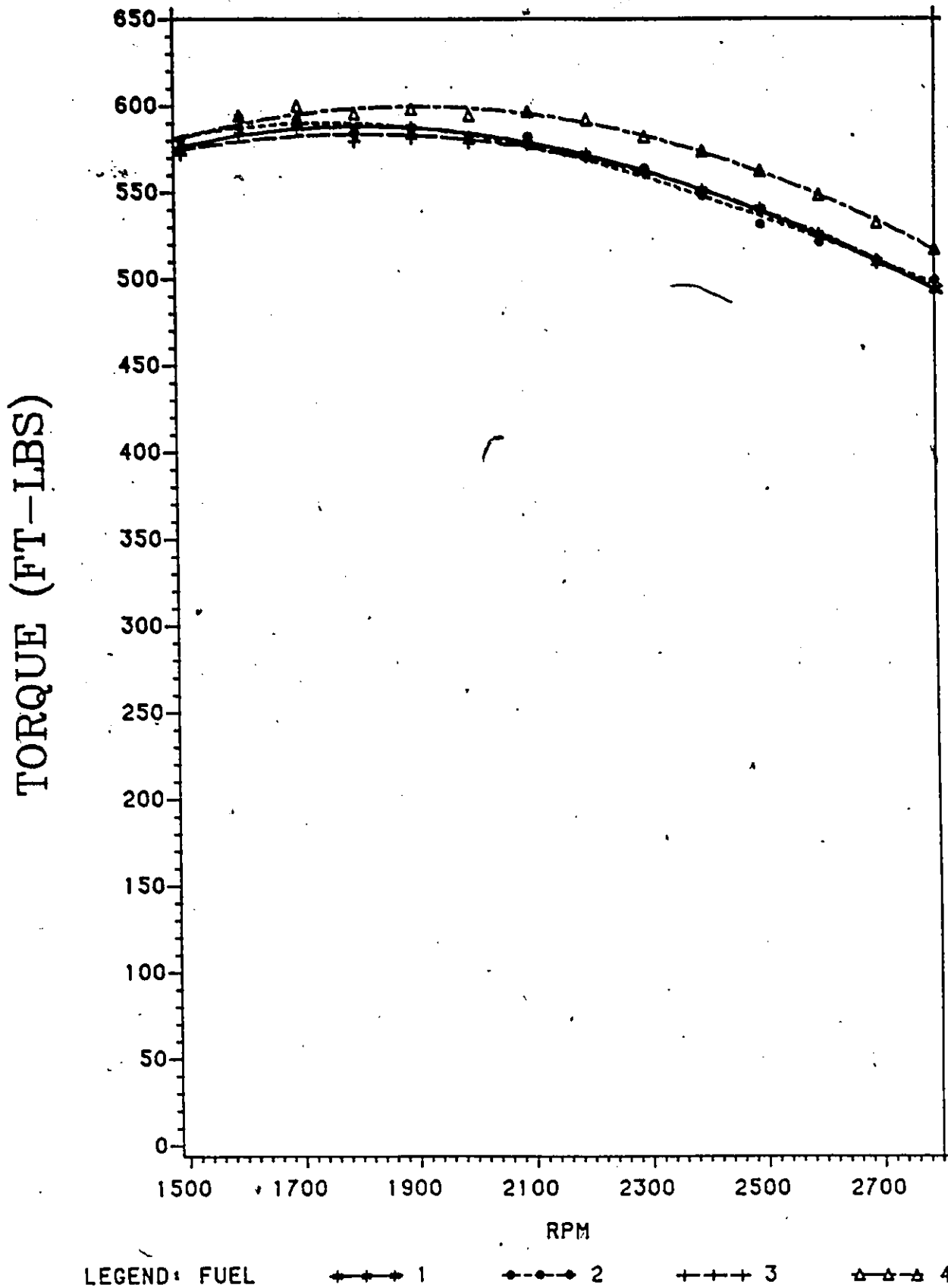


Fig. 5.2(a): Brake Torque Comparison at Full Load.
Full Scale Characteristic Trends.

6V53T TWO STROKE ENGINE

BRAKE TORQUE VS RPM
TORQUE - MAX

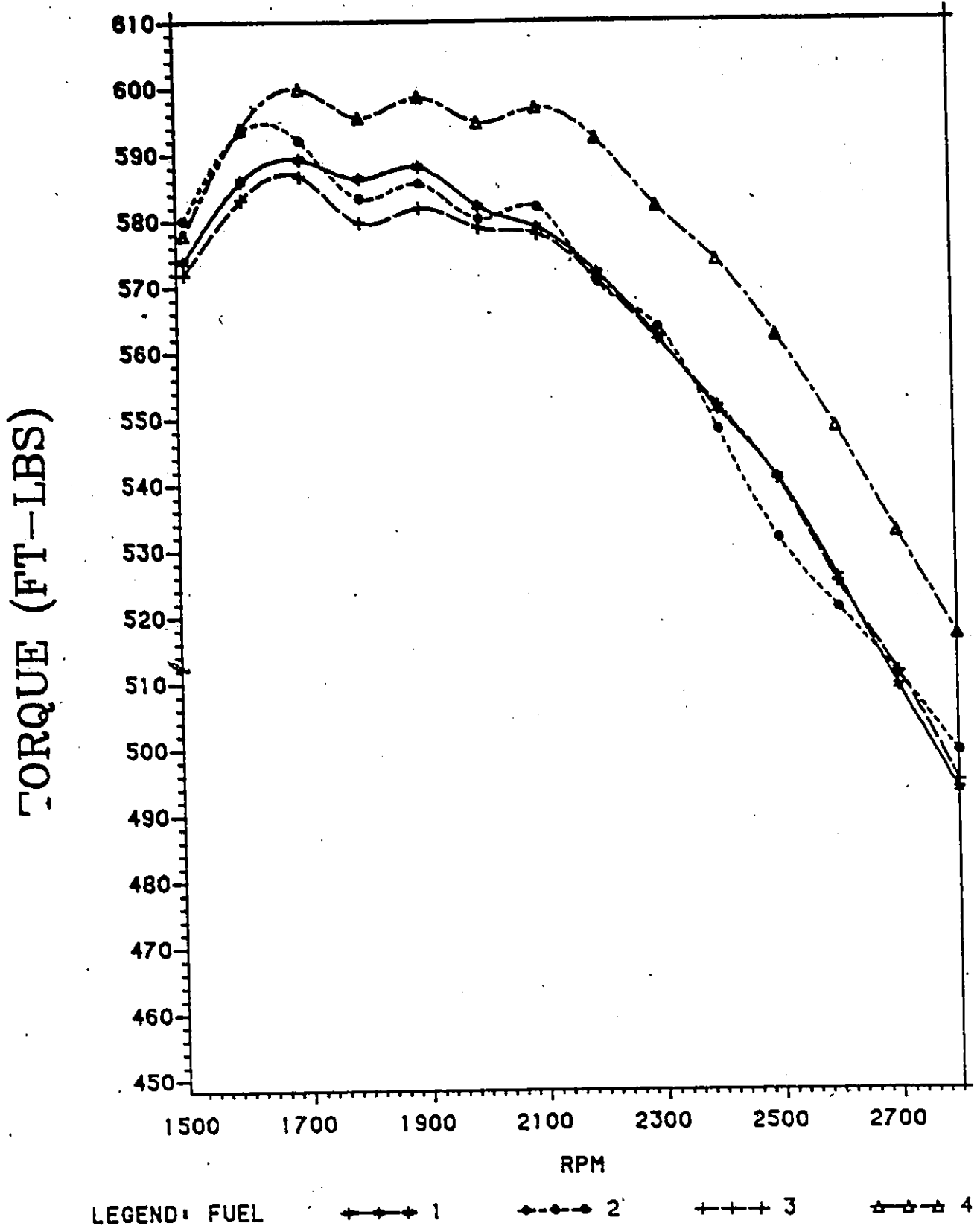
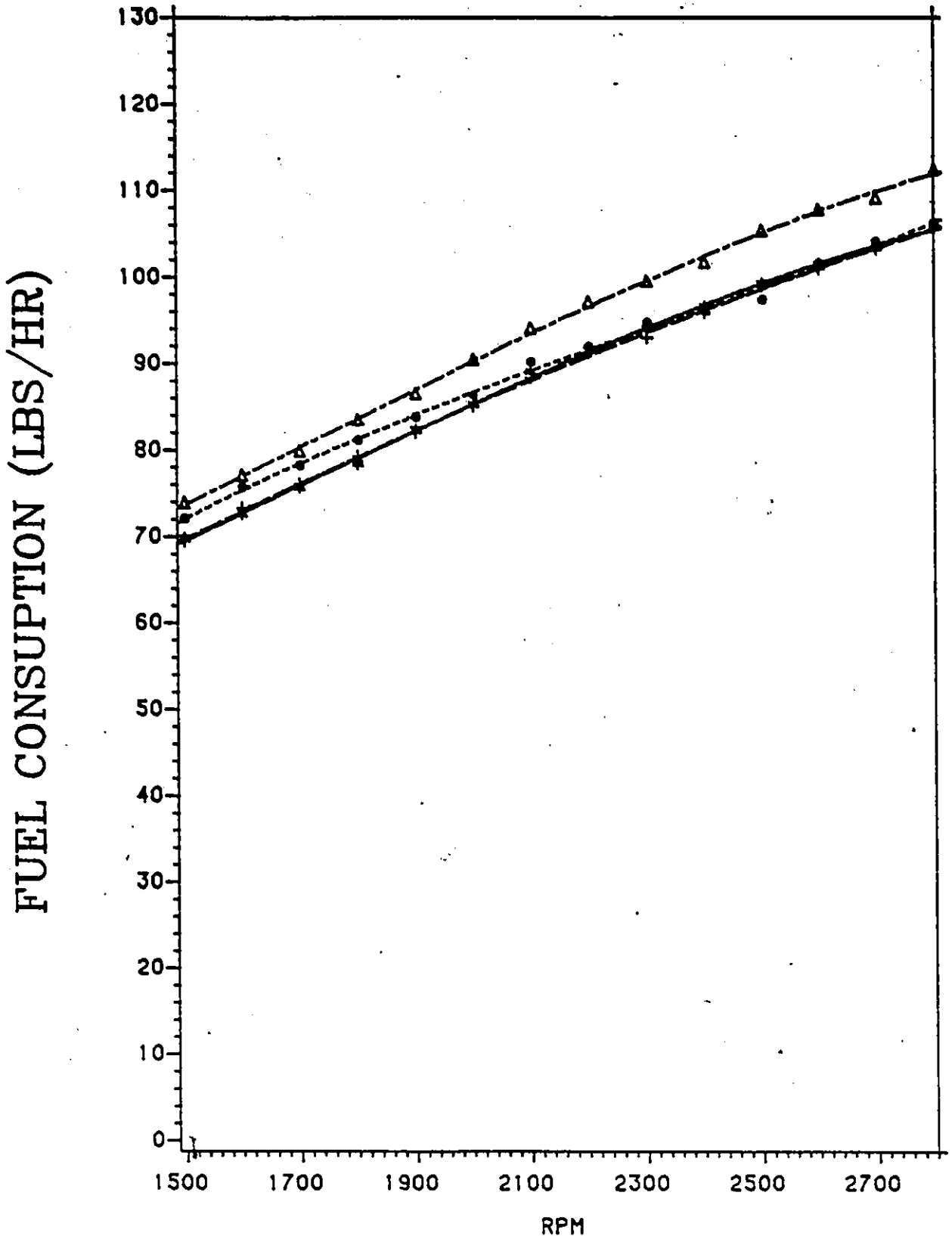


Fig. 5.2(b): Brake Torque Comparison at Full Load.
Expanded Axis Detailed Comparison.

6V53T TWO STROKE ENGINE

FUEL CONSUMPTION VS RPM
TORQUE = MAX



LEGEND: FUEL ◆◆◆ 1 ●●● 2 + + + 3 △△△ 4

Fig. 5.3(a): Fuel Consumption Comparison at Full Load. Full Scale Characteristic Trends.

6V53T TWO STROKE ENGINE

FUEL CONSUMPTION VS RPM
TORQUE = MAX

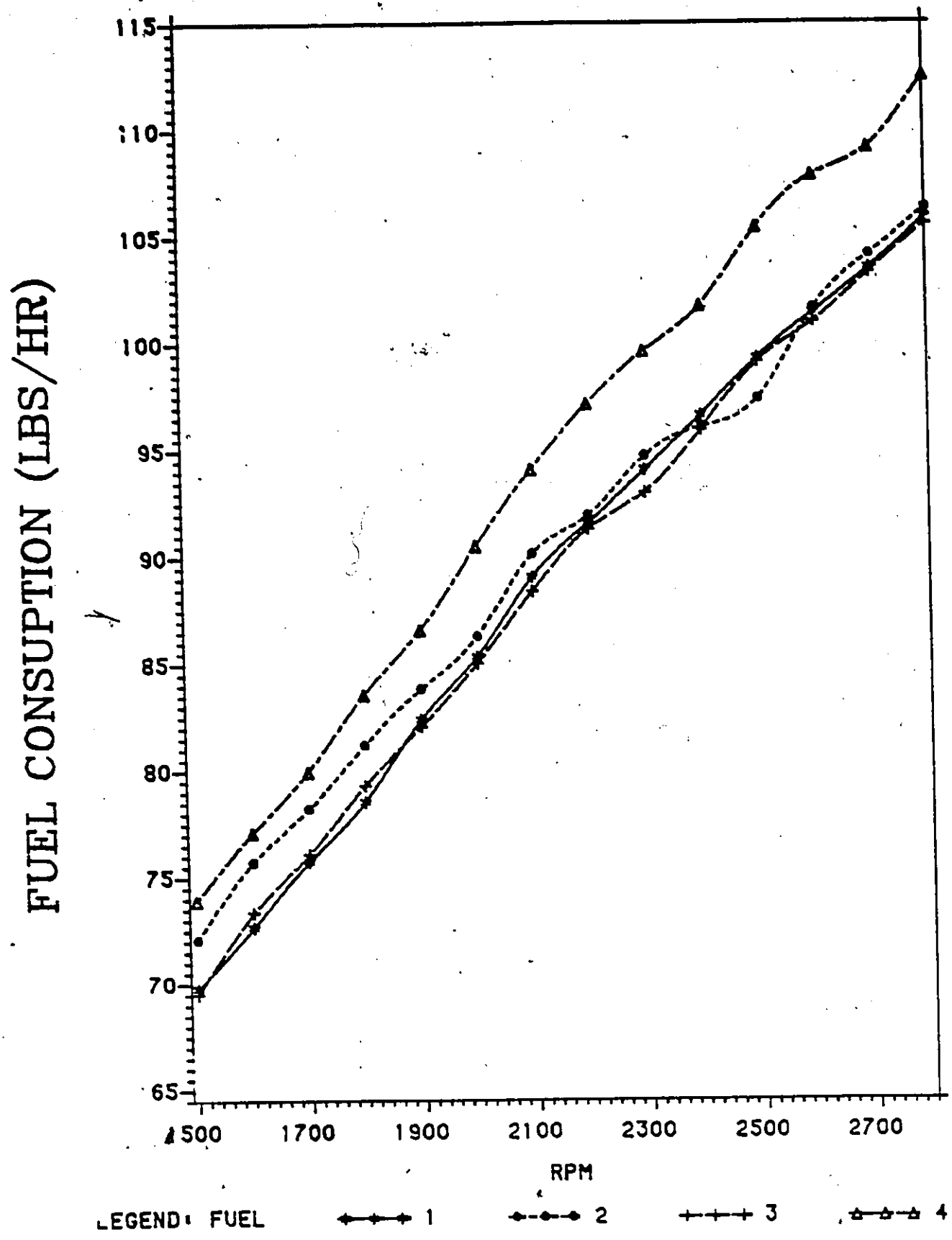


Fig. 5.3(b): Fuel Consumption Comparison at Full Load. Expanded Axis Detailed Comparison.

6V53T TWO STROKE ENGINE

BRAKE SPECIFIC FUEL CONSUMPTION VS RPM
TORQUE = MAX

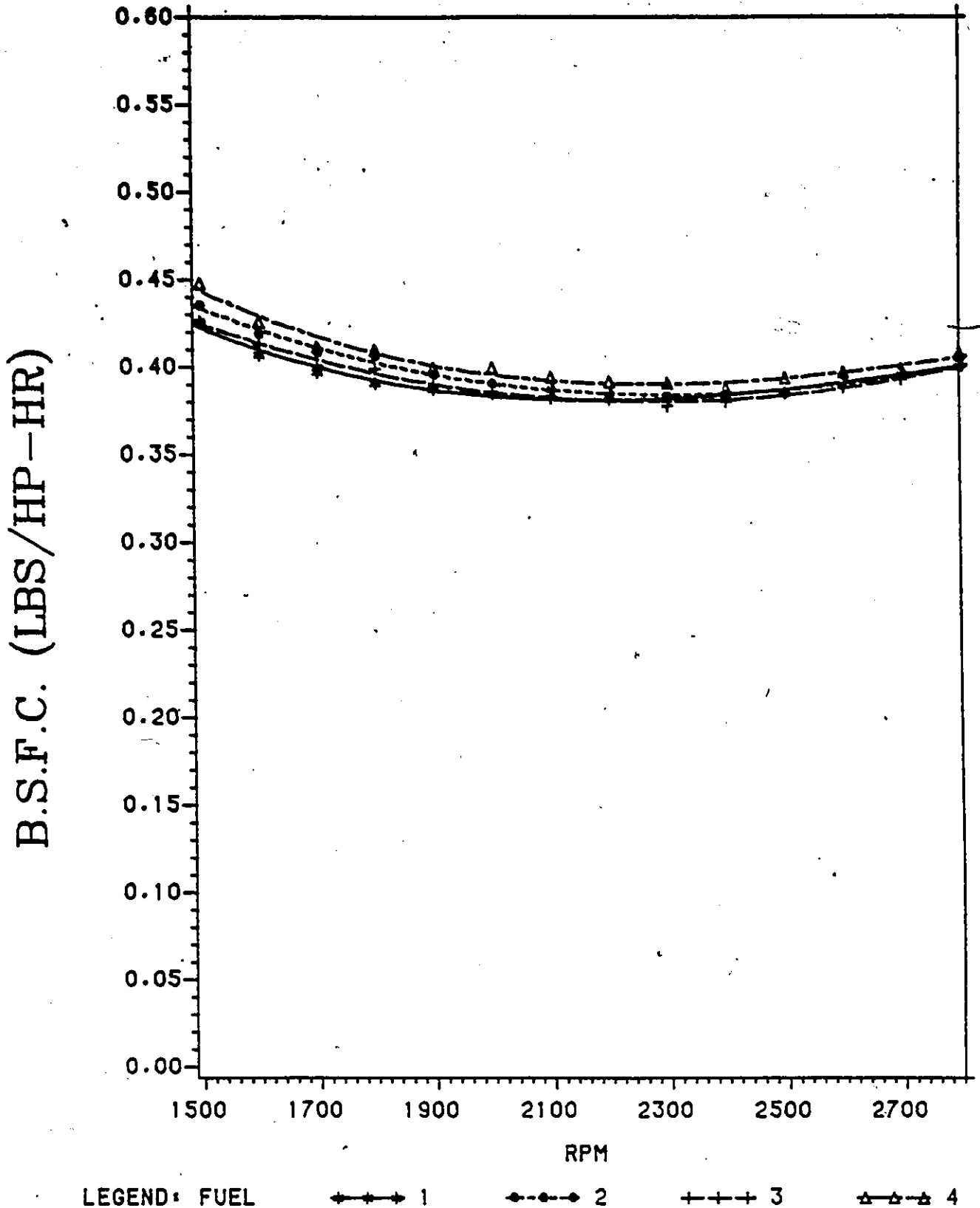


Fig. 5.4(a): Brake Specific Fuel Consumption Comparison at Full Load.
Full Scale Characteristic Trends.

6V53T TWO STROKE ENGINE

BRAKE SPECIFIC FUEL CONSUMPTION VS RPM
TORQUE - MAX

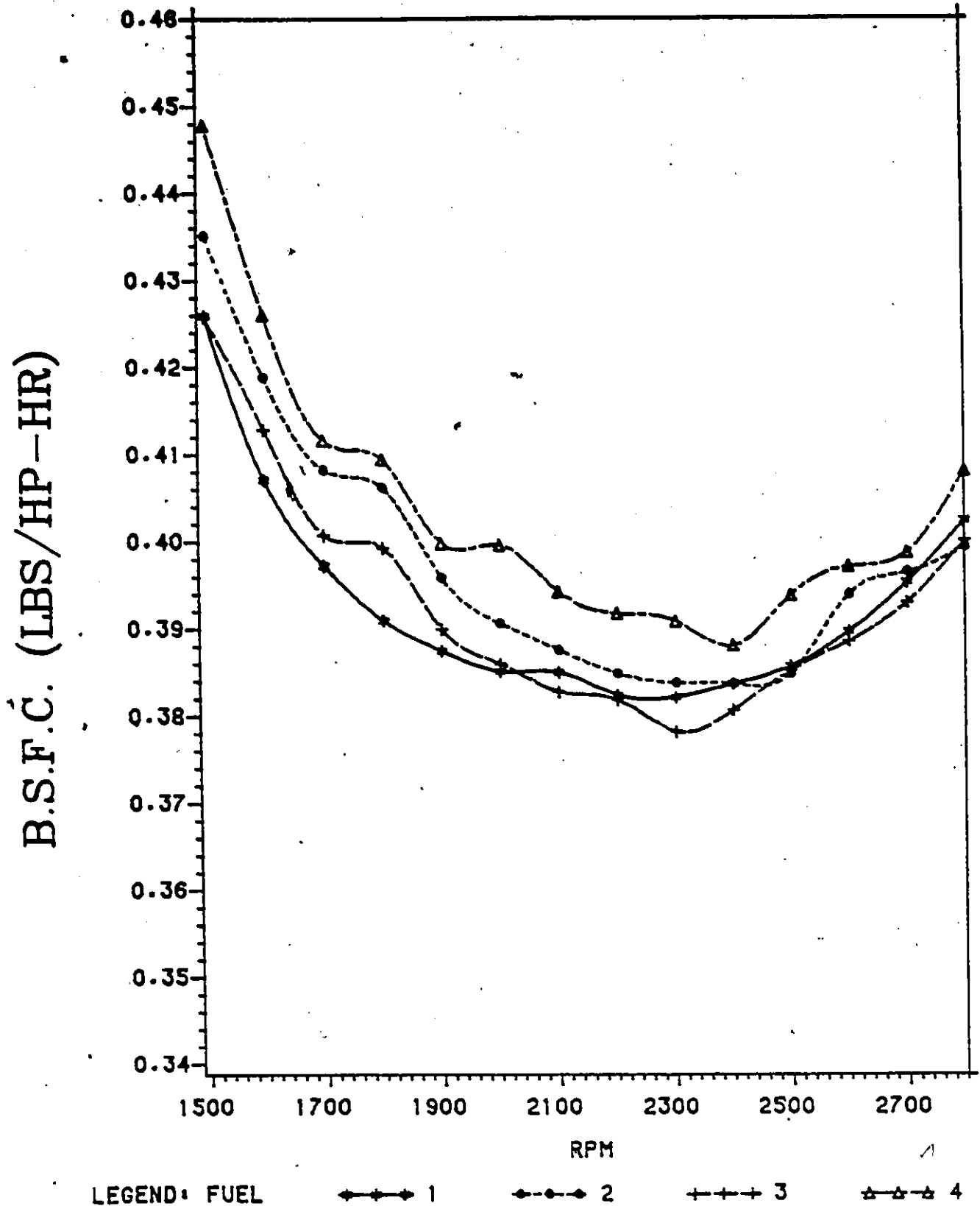


Fig. 5.4(b): Brake Specific Fuel Consumption Comparison at Full Load. Expanded Axis Detailed Comparison.

6V53T TWO STROKE ENGINE

BRAKE THERMAL EFFICIENCY VS RPM
TORQUE = MAX

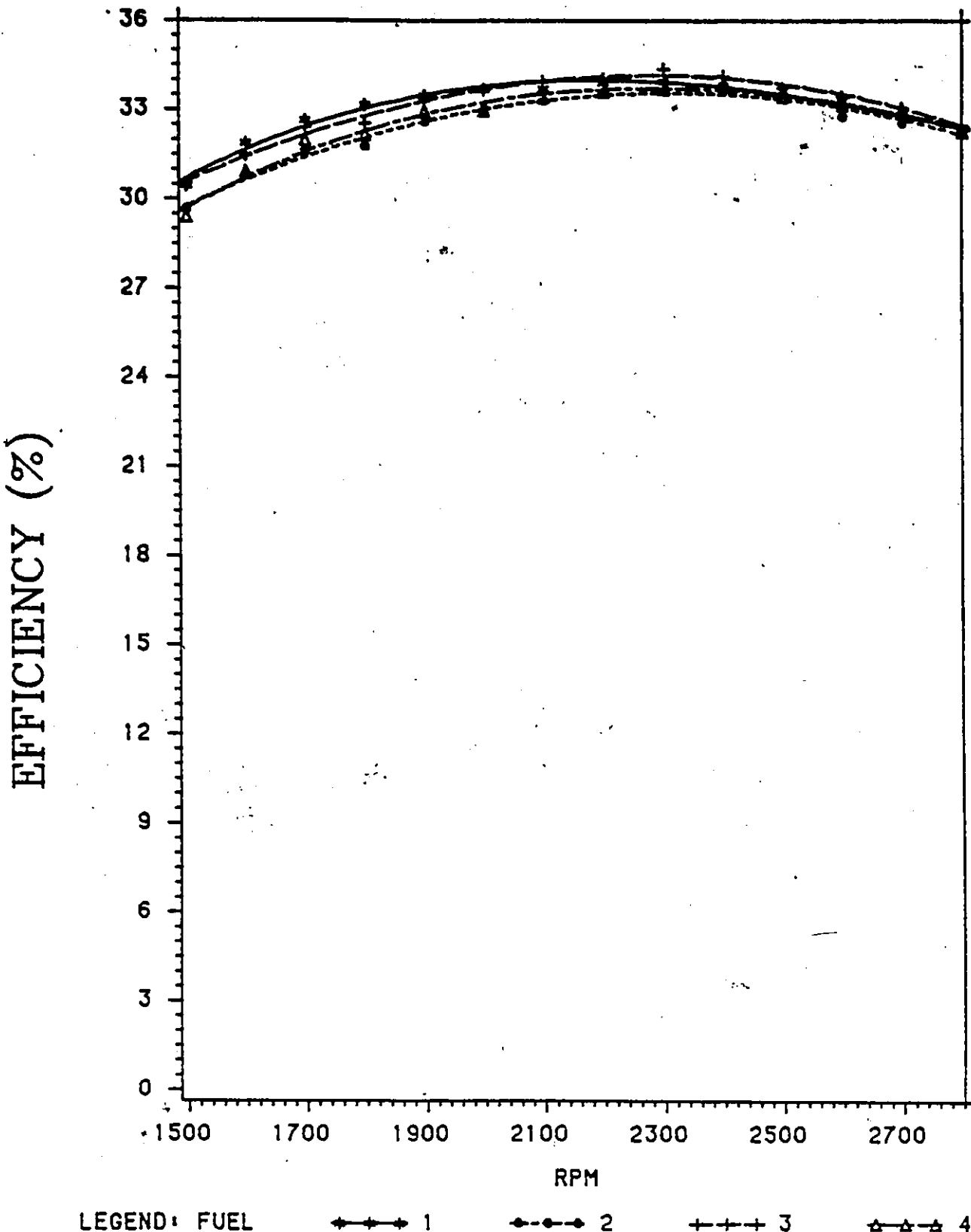


Fig. 5.5(a): Brake Thermal Efficiency Comparison at Full Load.
Full Scale Characteristic Trends.

6V53T TWO STROKE ENGINE

BRAKE THERMAL EFFICIENCY VS RPM

TORQUE = MAX

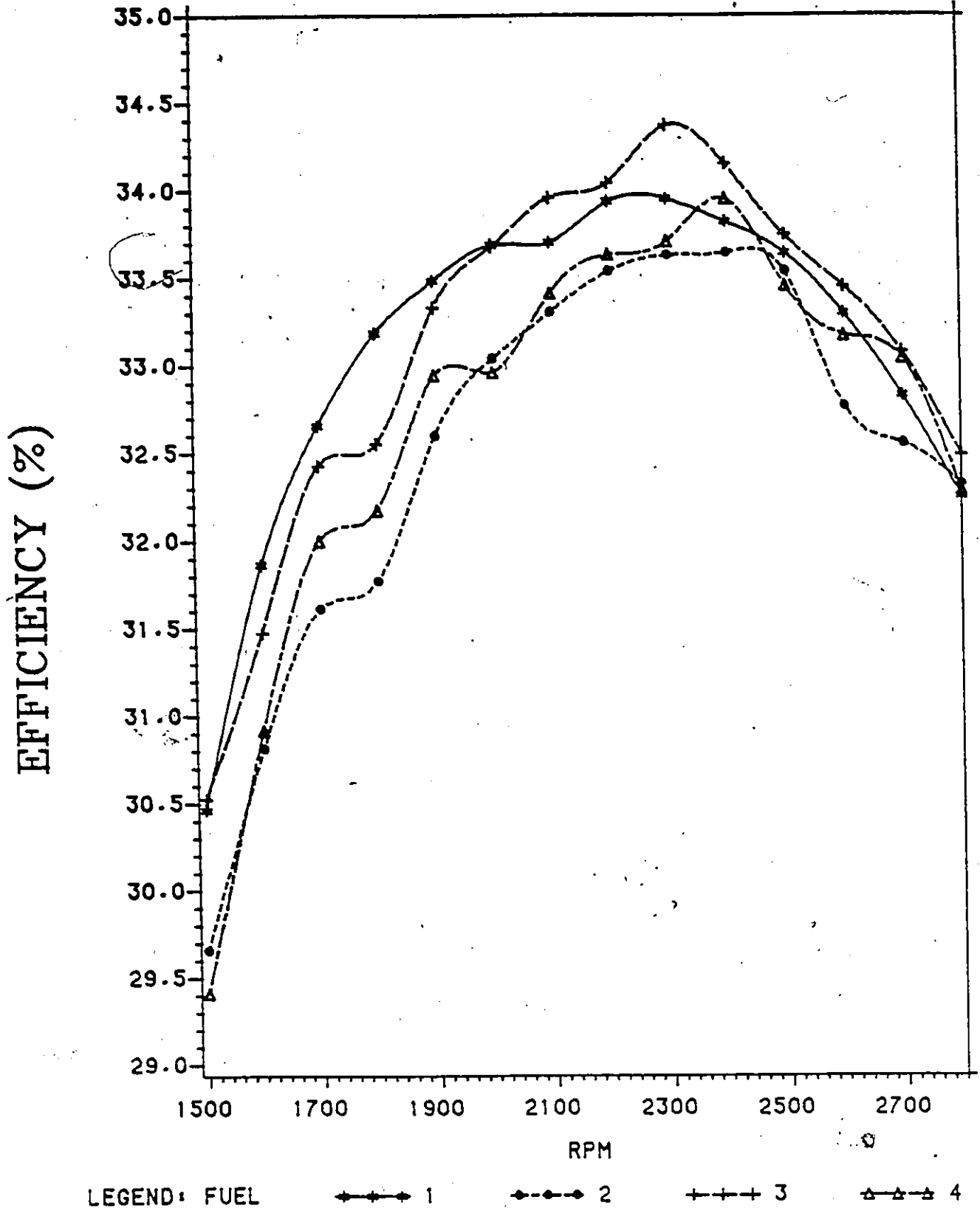


Fig. 5.5(b) Brake Thermal Efficiency Comparison at Full Load. Expanded Axis Detailed Comparison.

6V53T TWO STROKE ENGINE

SMOKE VS RPM
TORQUE - MAX

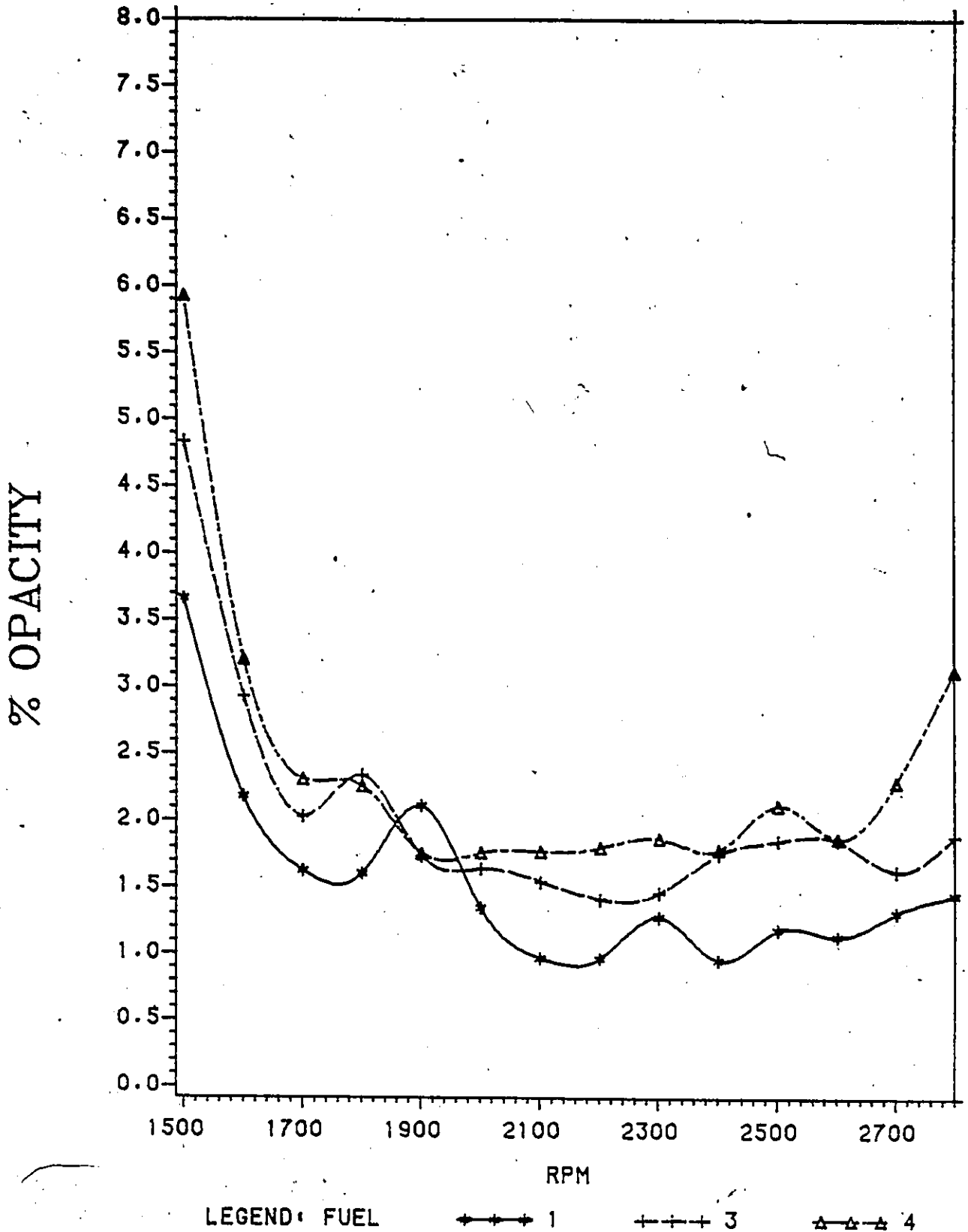


Fig. 5.6: Smoke Number Comparison at Full Load.

6V53T TWO STROKE ENGINE

FUEL CONSUMPTION VS RPM

TORQUE = 250 FT-LBS

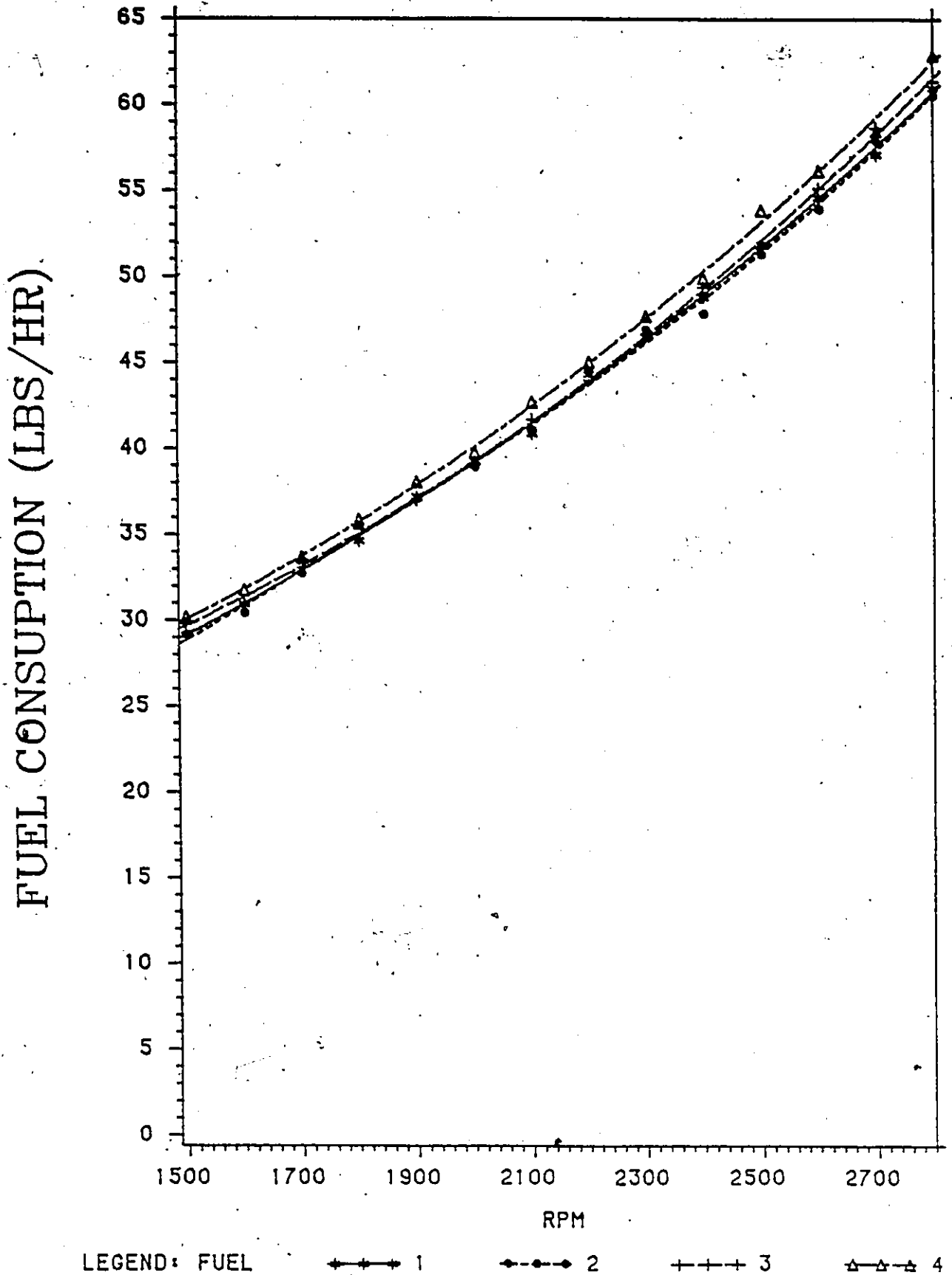


Fig. 5.7(a): Fuel Consumption Comparison at Part Load (Constant Torque). Full Scale Characteristic Trends.

6V53T TWO STROKE ENGINE

FUEL CONSUMPTION VS RPM

TORQUE = 250 FT-LBS

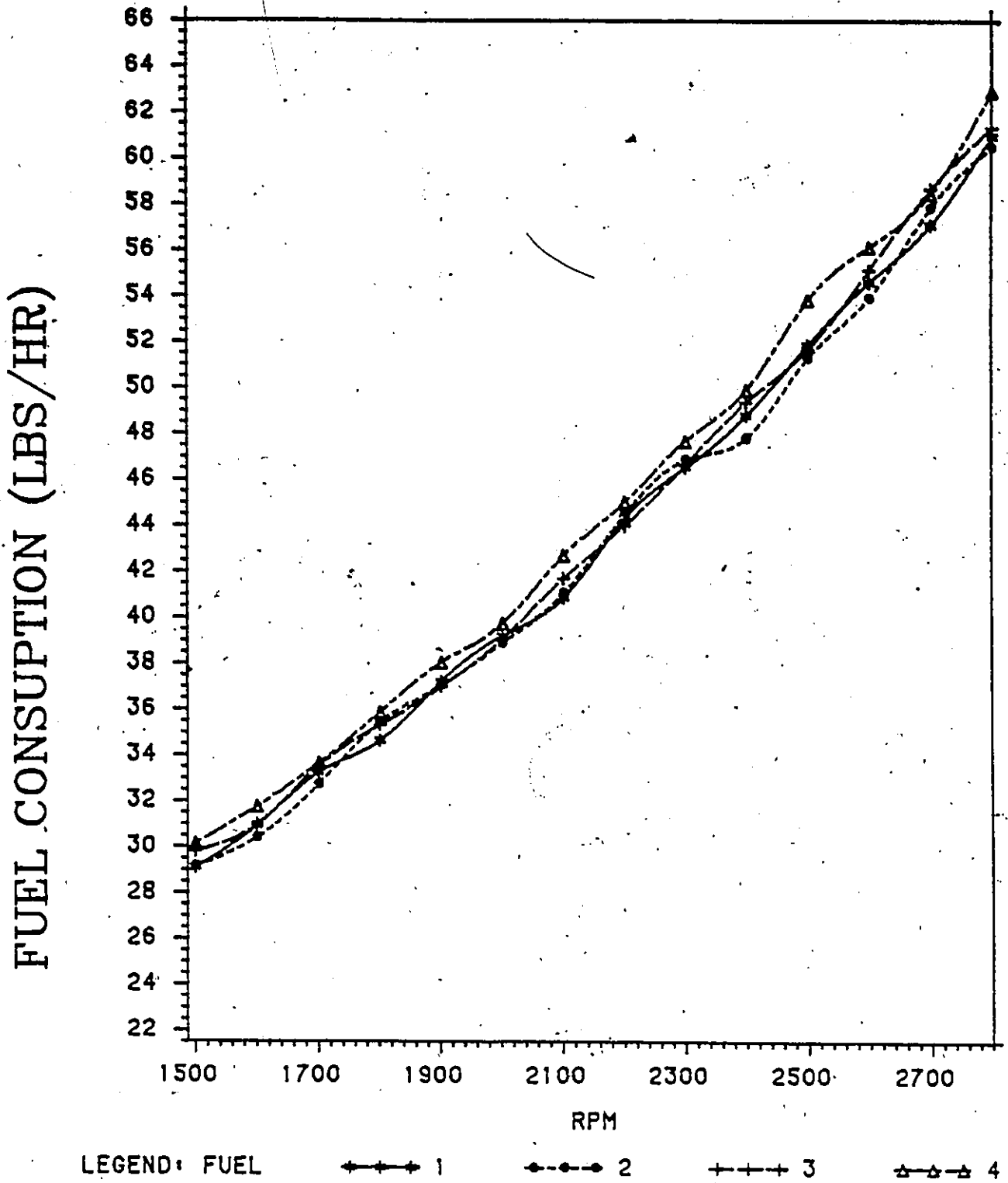


Fig. 5.7(b): Fuel Consumption Comparison at Part Load
(Constant Torque).
Expanded Axis Detailed Comparison.

6V53T TWO STROKE ENGINE

BRAKE SPECIFIC FUEL CONSUMPTION VS RPM

TORQUE = 250 FT-LBS

B.S.F.C. (LBS/HP-HR)

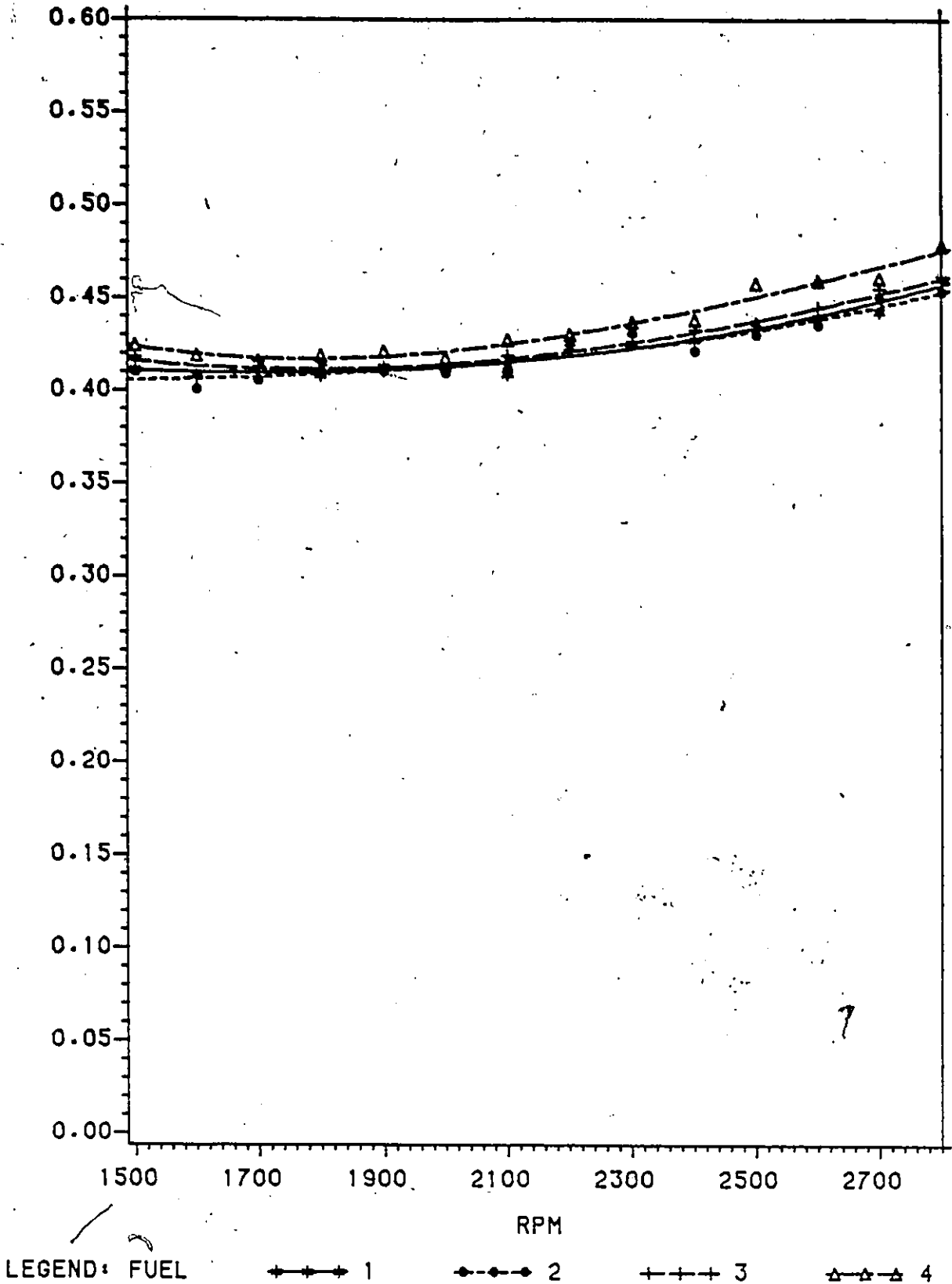


Fig. 5.8(a): Brake Specific Fuel Consumption Comparison at Part Load (Constant Torque). Full Scale Characteristic Trends.

6V53T TWO STROKE ENGINE

BRAKE SPECIFIC FUEL CONSUMPTION VS RPM
TORQUE = 250 FT-LBS

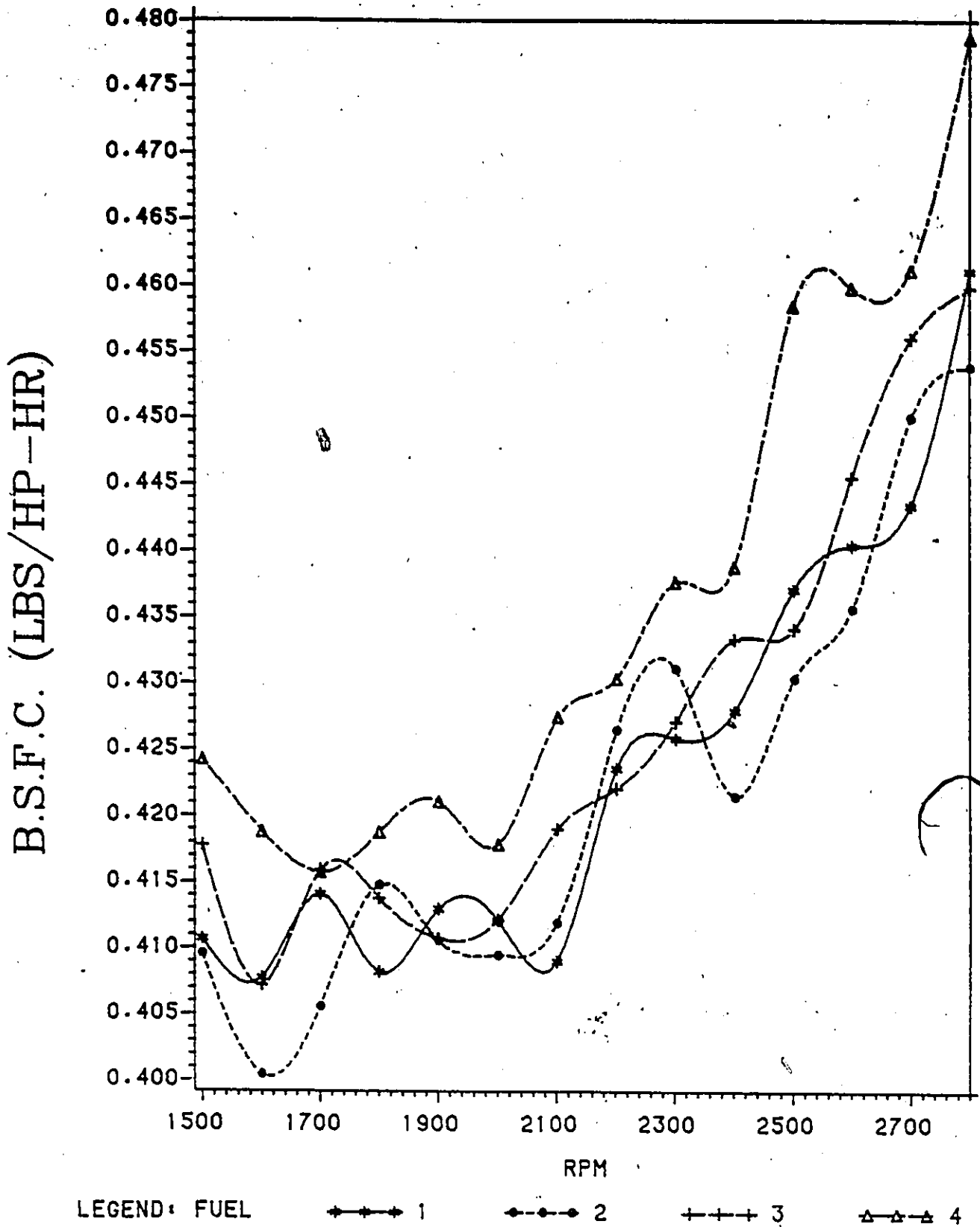


Fig. 5.8(b): Brake Specific Fuel Consumption Comparison at Part Load (Constant Torque). Expanded Axis Detailed Comparison.

6V53T TWO STROKE ENGINE

BRAKE THERMAL EFFICIENCY VS RPM
TORQUE = 250 FT-LBS

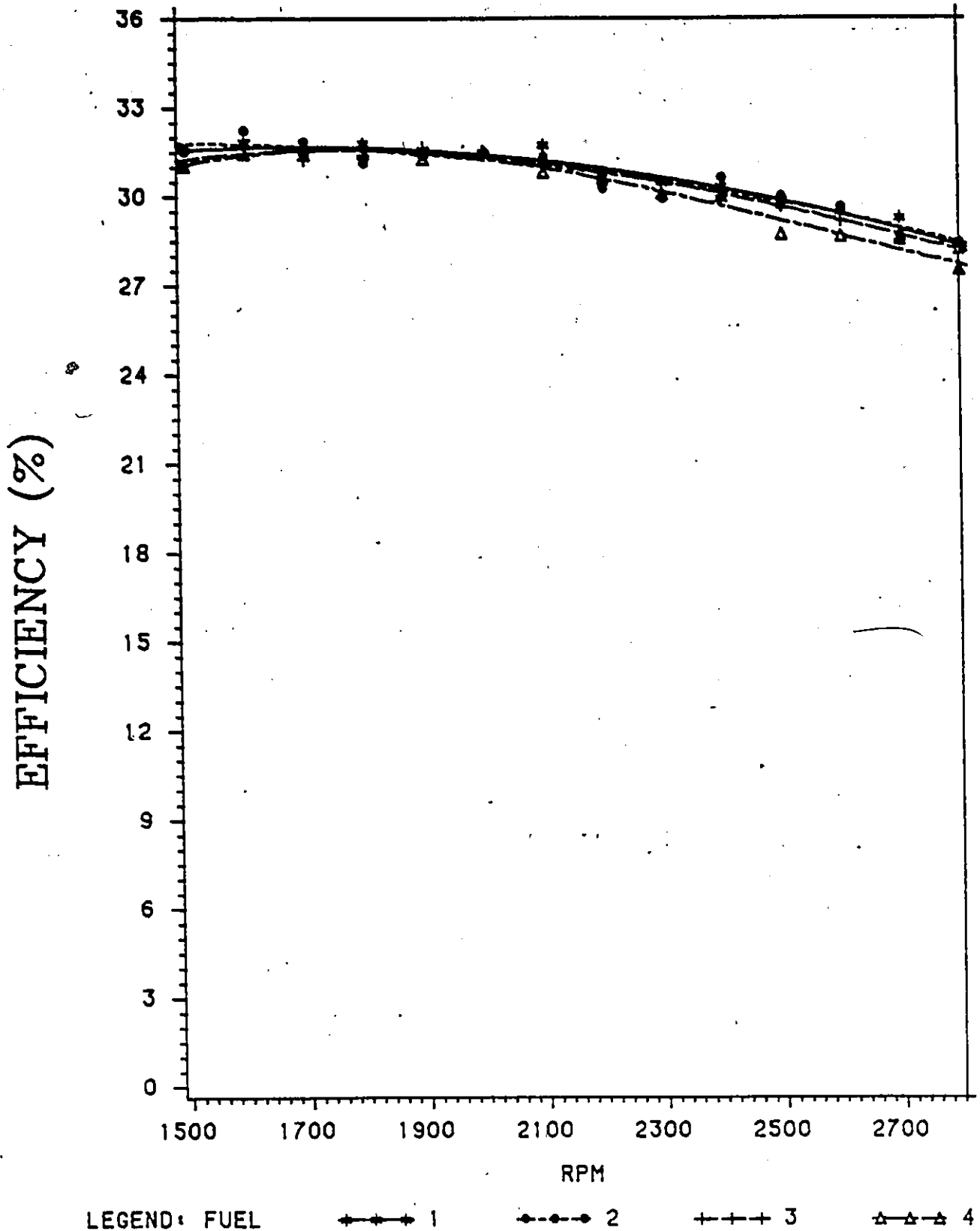


Fig. 5.9(a): Brake Thermal Efficiency Comparison at Part Load (Constant Torque). Full Scale Characteristic Trends.

6V53T TWO STROKE ENGINE

BRAKE THERMAL EFFICIENCY VS RPM
TORQUE = 250 FT-LBS

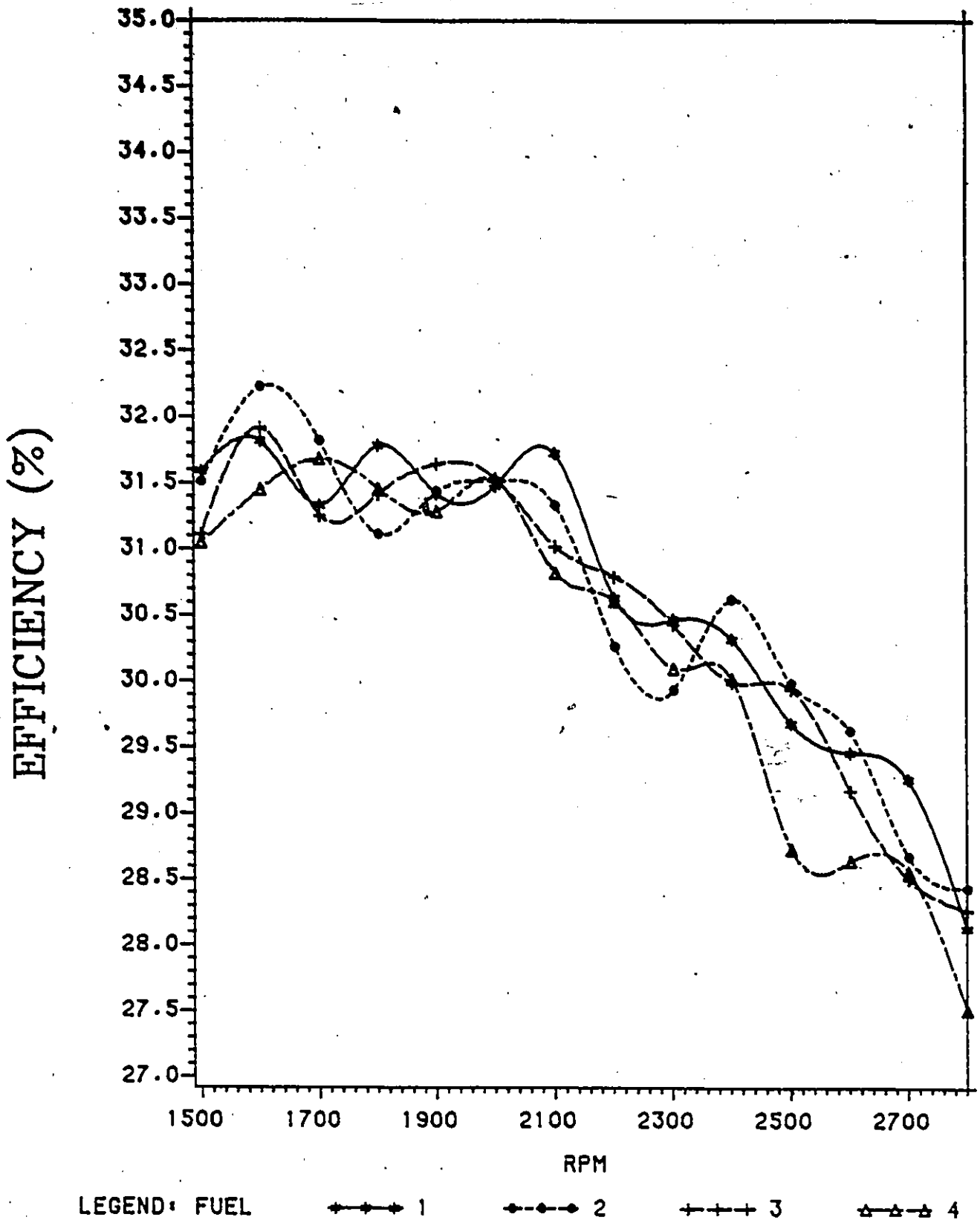


Fig. 5.9(b): Brake Thermal Efficiency Comparison at Part Load (Constant Torque). Expanded Axis Detailed Comparison.

6V53T TWO STROKE ENGINE

INDICATED HORSE POWER VS RPM
TORQUE - MAX

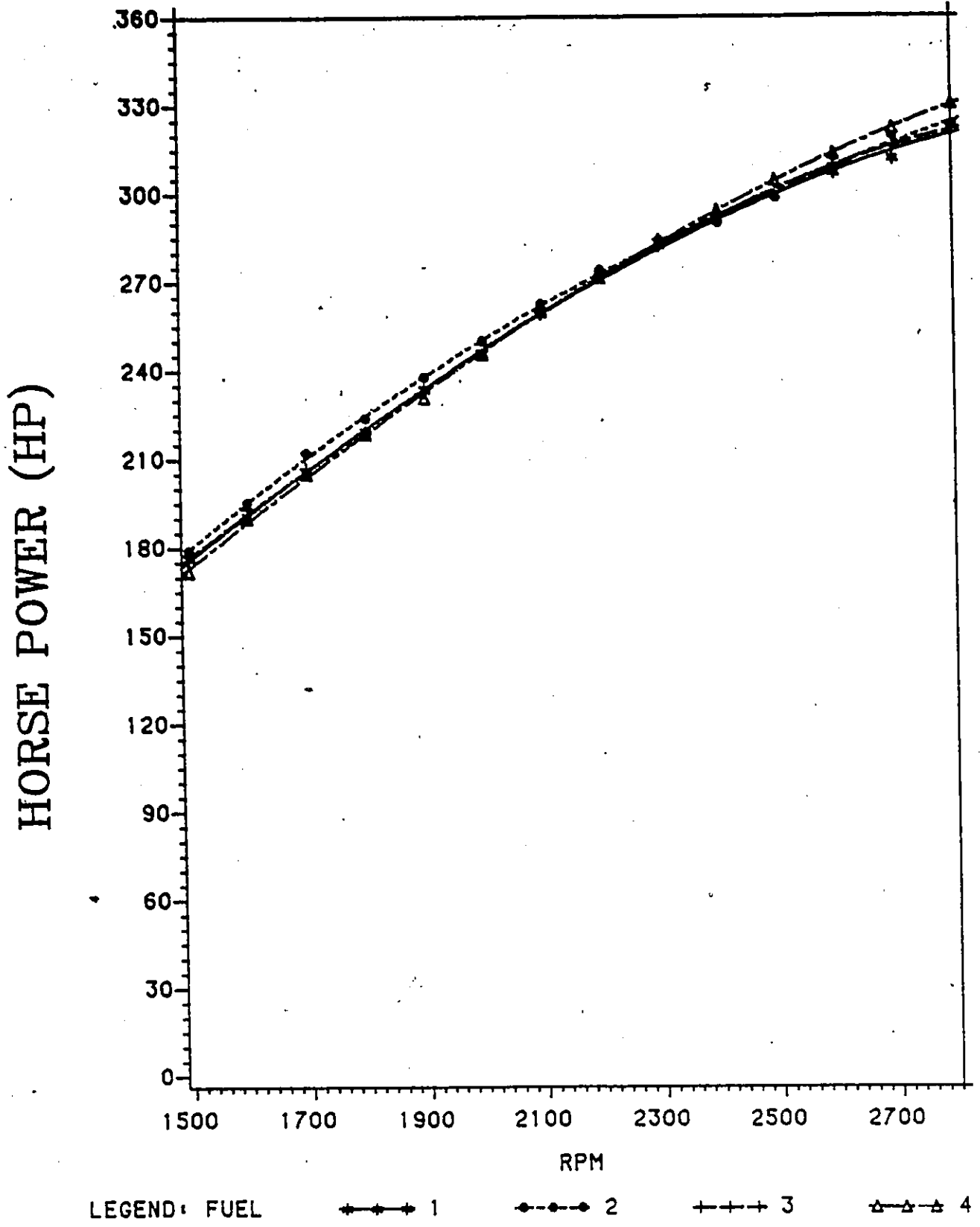


Fig. 5.10(a): Indicated Horsepower Comparison at Full Load.
Full Scale Characteristic Trends.

6V53T TWO STROKE ENGINE

INDICATED HORSE POWER VS RPM
TORQUE - MAX

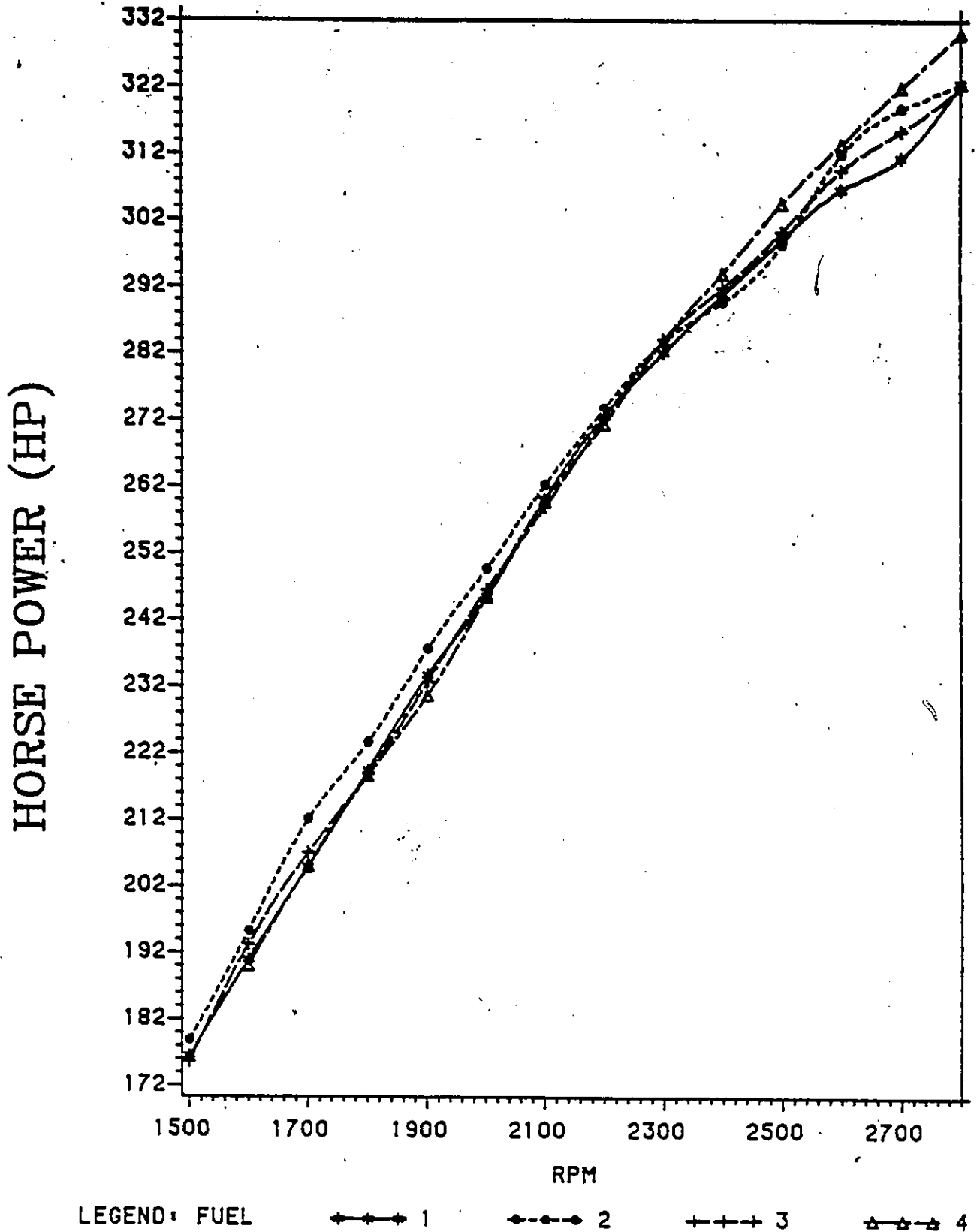


Fig. 5.10(b): Indicated Horsepower Comparison at Full Load.
Expanded Axis Detailed Comparison.

6V53T TWO STROKE ENGINE

INDICATED SPECIFIC FUEL CONSUMPTION VS RPM
TORQUE = MAX

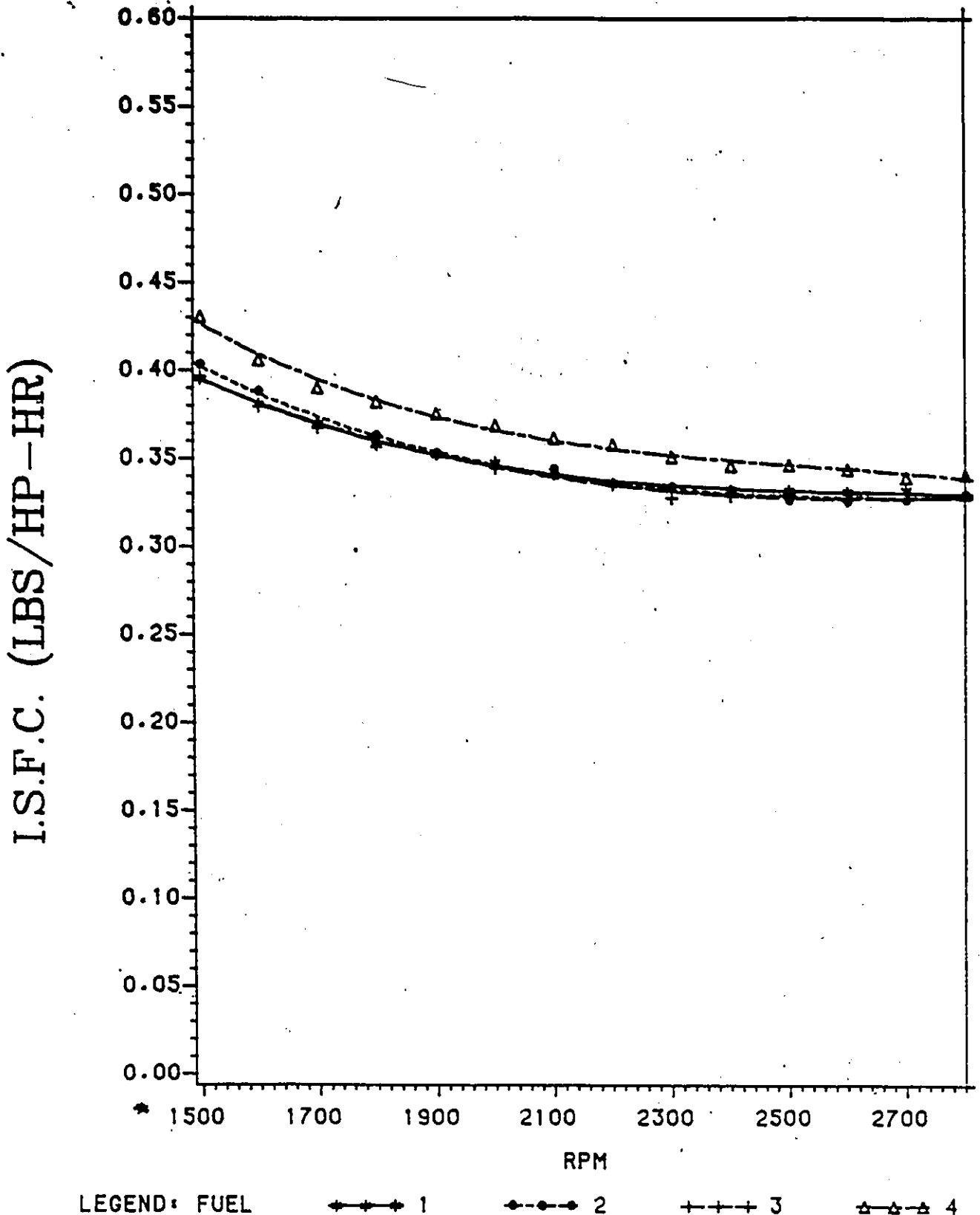


Fig. 5.11(a): Indicated Specific Fuel Consumption Comparison at Full Load. Full Scale Characteristic Trends.

6V53T TWO STROKE ENGINE

INDICATED SPECIFIC FUEL CONSUMPTION VS RPM
TORQUE = MAX

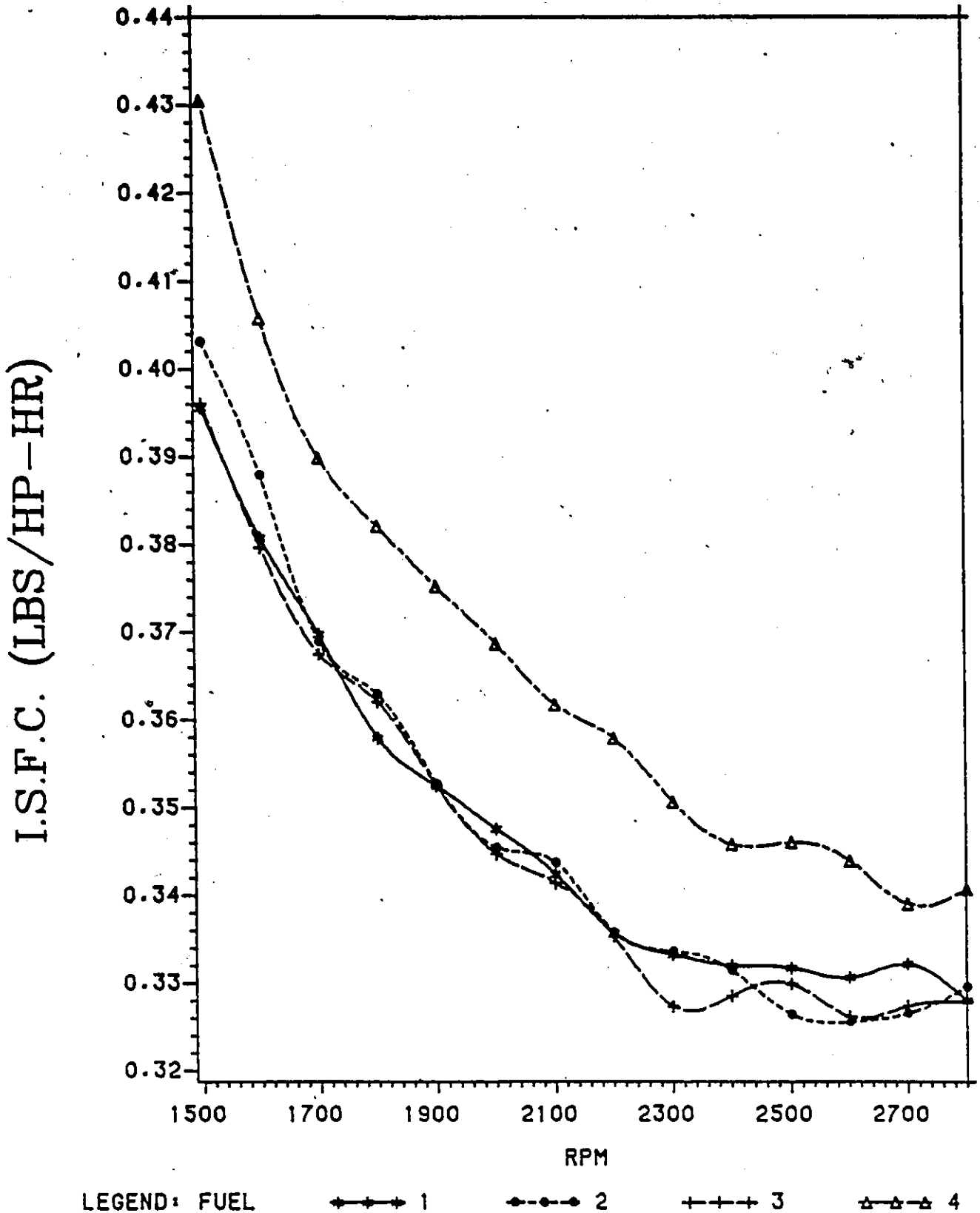


Fig. 5.11(b): Indicated Specific Fuel Consumption Comparison at Full Load.
Expanded Axis Detailed Comparison.

6V53T TWO STROKE ENGINE

INDICATED HORSE POWER VS RPM

TORQUE = 250 FT-LBS

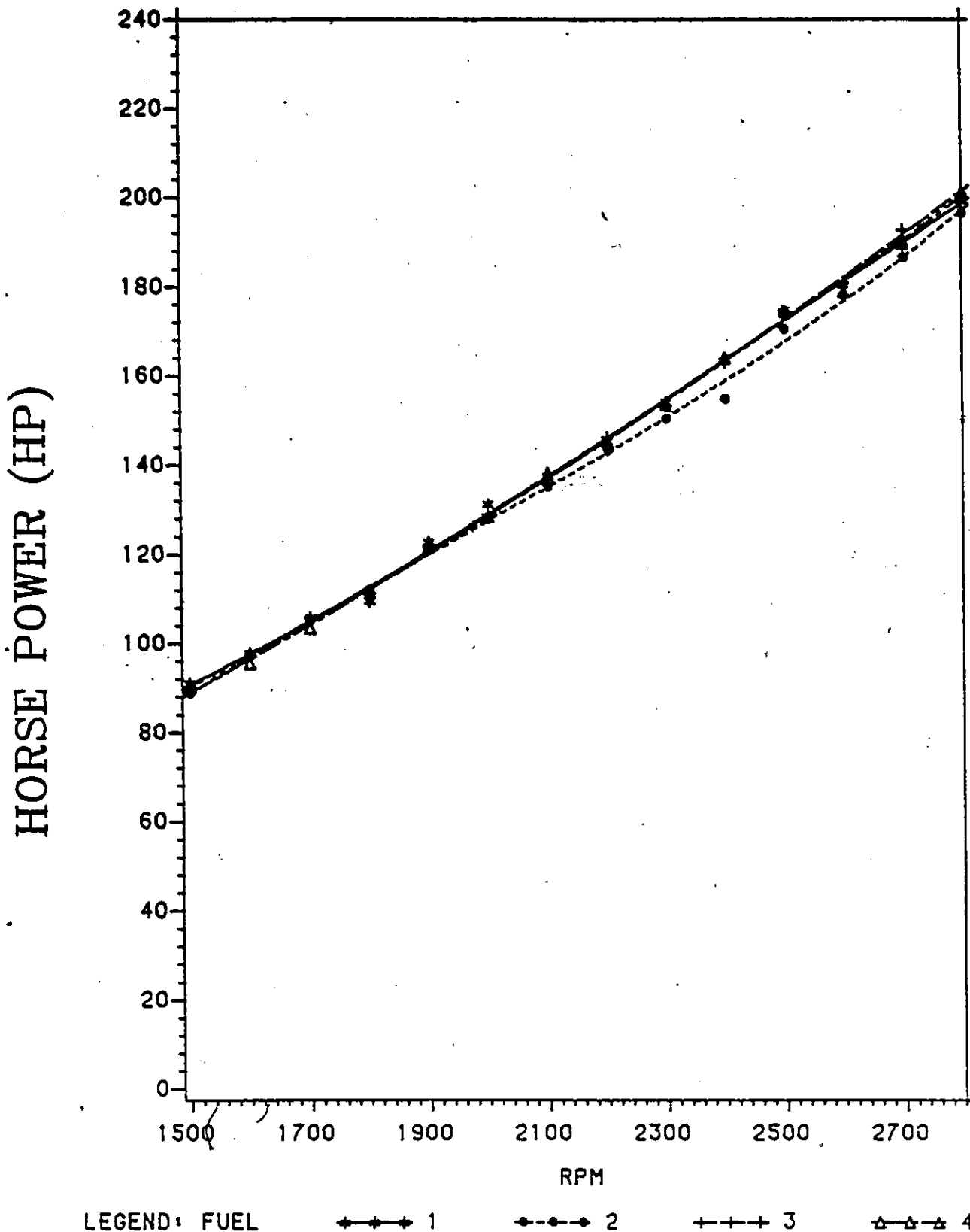


Fig. 5.12(a): Indicated Horsepower Comparison at Part Load (Constant Brake Torque). Full Scale Characteristic Trends.

-6V53T TWO STROKE ENGINE

INDICATED HORSE POWER VS RPM

TORQUE = 250 FT-LBS

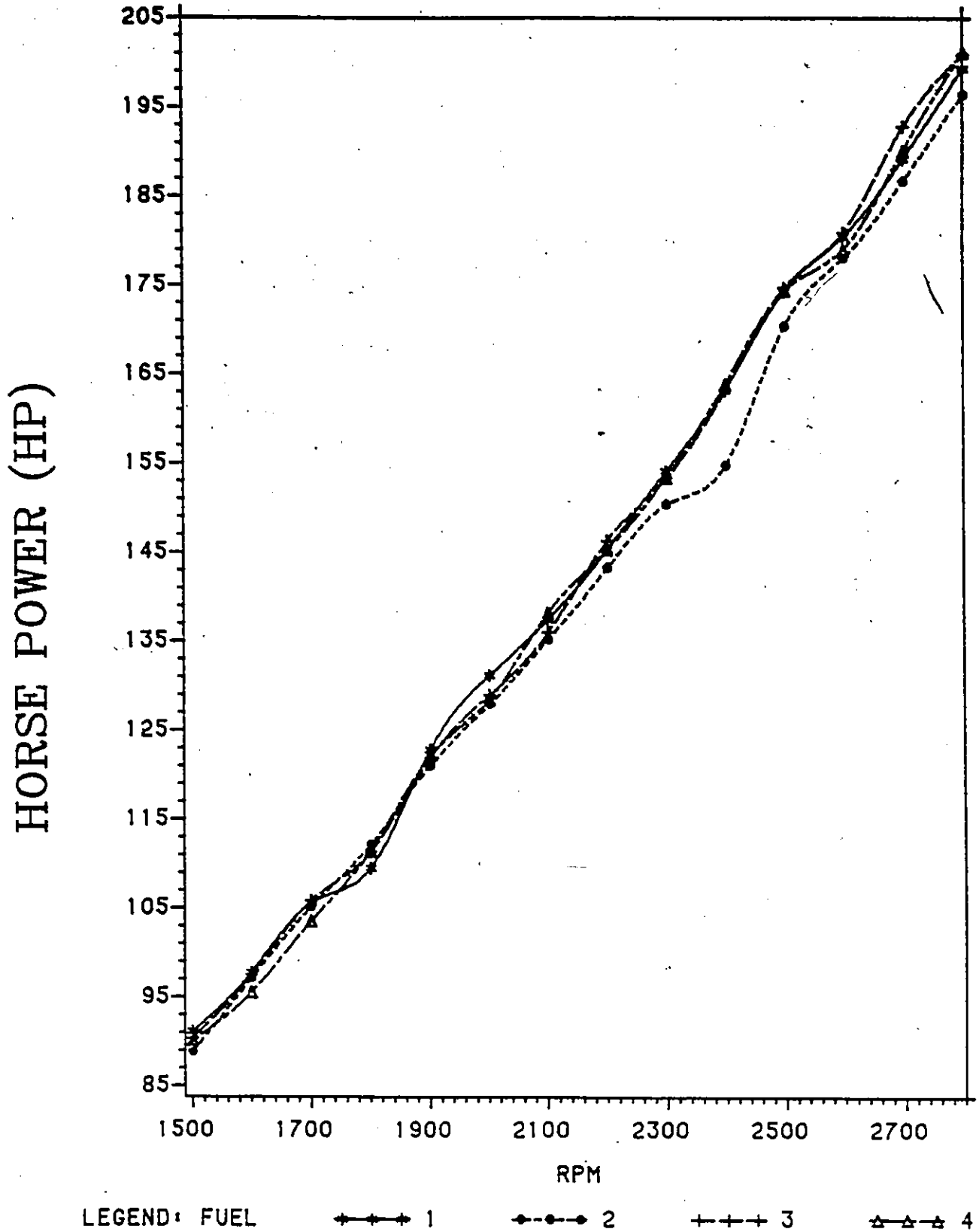


Fig. 5.12(b): Indicated Horsepower Comparison at Part Load (Constant Brake Torque). Expanded Axis Detailed Comparison.

6V53T TWO STROKE ENGINE

INDICATED SPECIFIC FUEL CONSUMPTION VS RPM

TORQUE = 250 FT-LBS

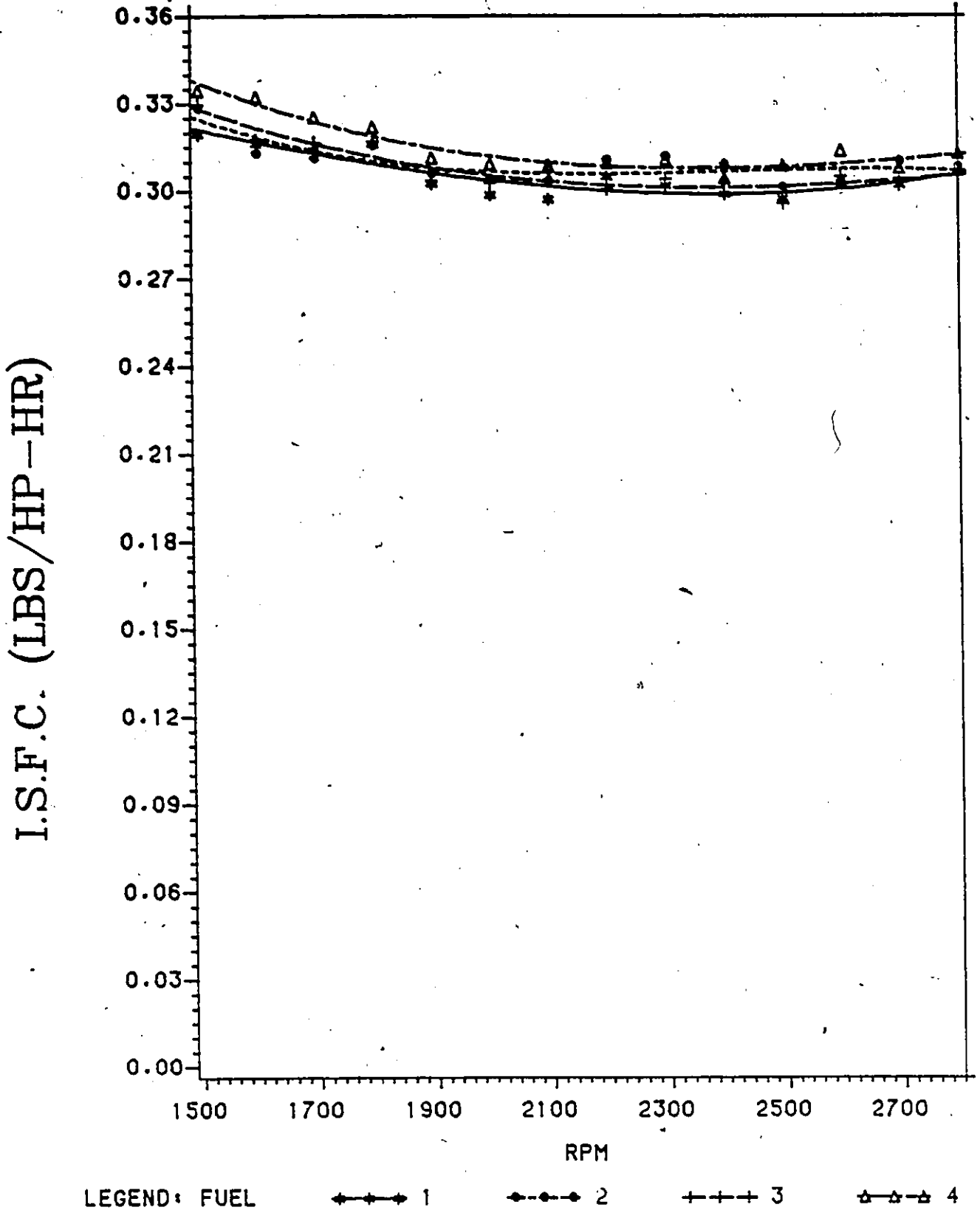


Fig. 5.13(a): Indicated Specific Fuel Consumption Comparison at Part Load (Constant Brake Torque). Full Scale Characteristic Trends.

6V53T TWO STROKE ENGINE

INDICATED SPECIFIC FUEL CONSUMPTION VS RPM
TORQUE = 250 FT-LBS

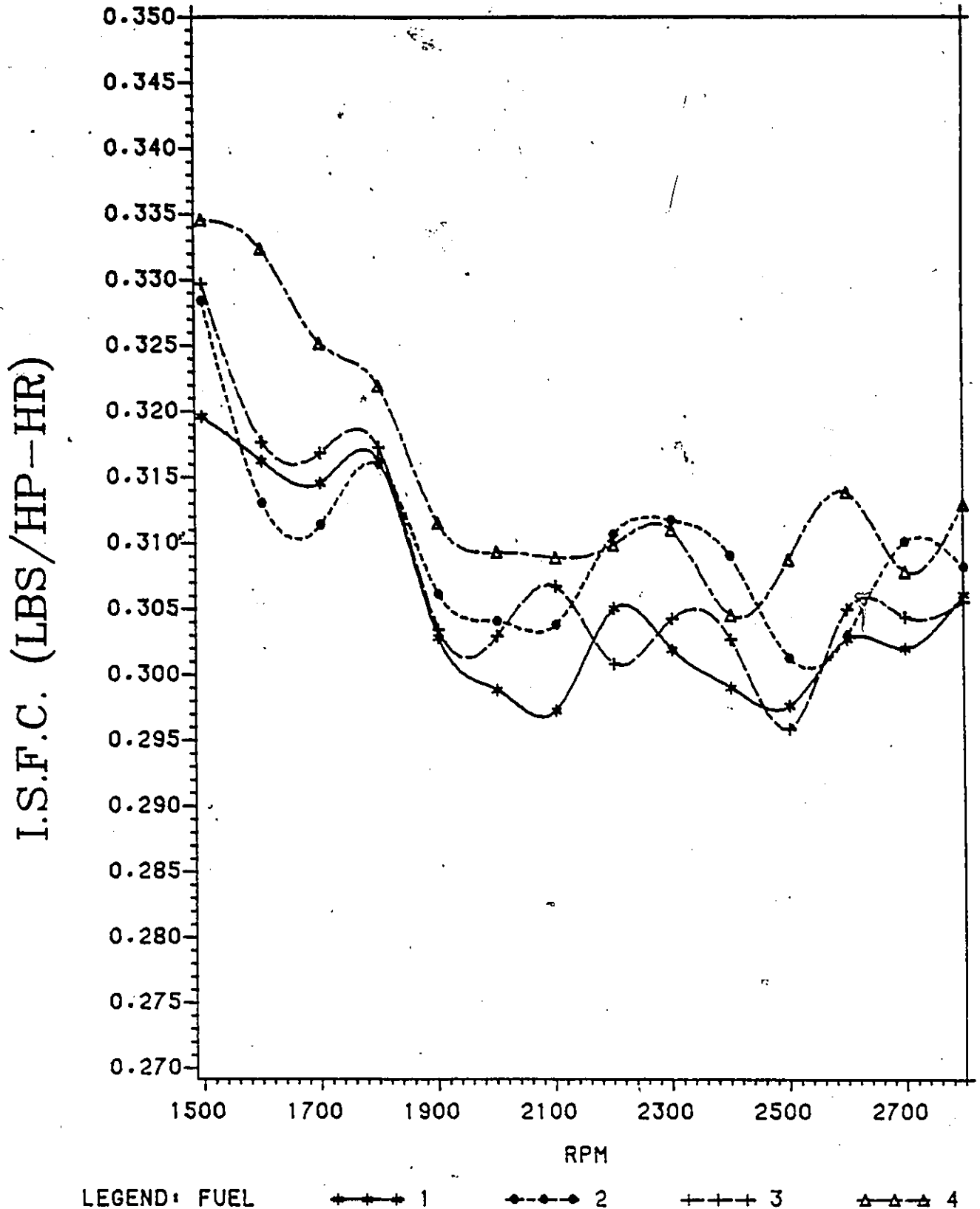


Fig. 5.13(b): Indicated Specific Fuel Consumption Comparison at Part Load (Constant Brake Torque). Expanded Axis Detailed Comparison.

- 117 -

6V53T TWO STROKE ENGINE

MECHANICAL EFFICIENCY VS RPM

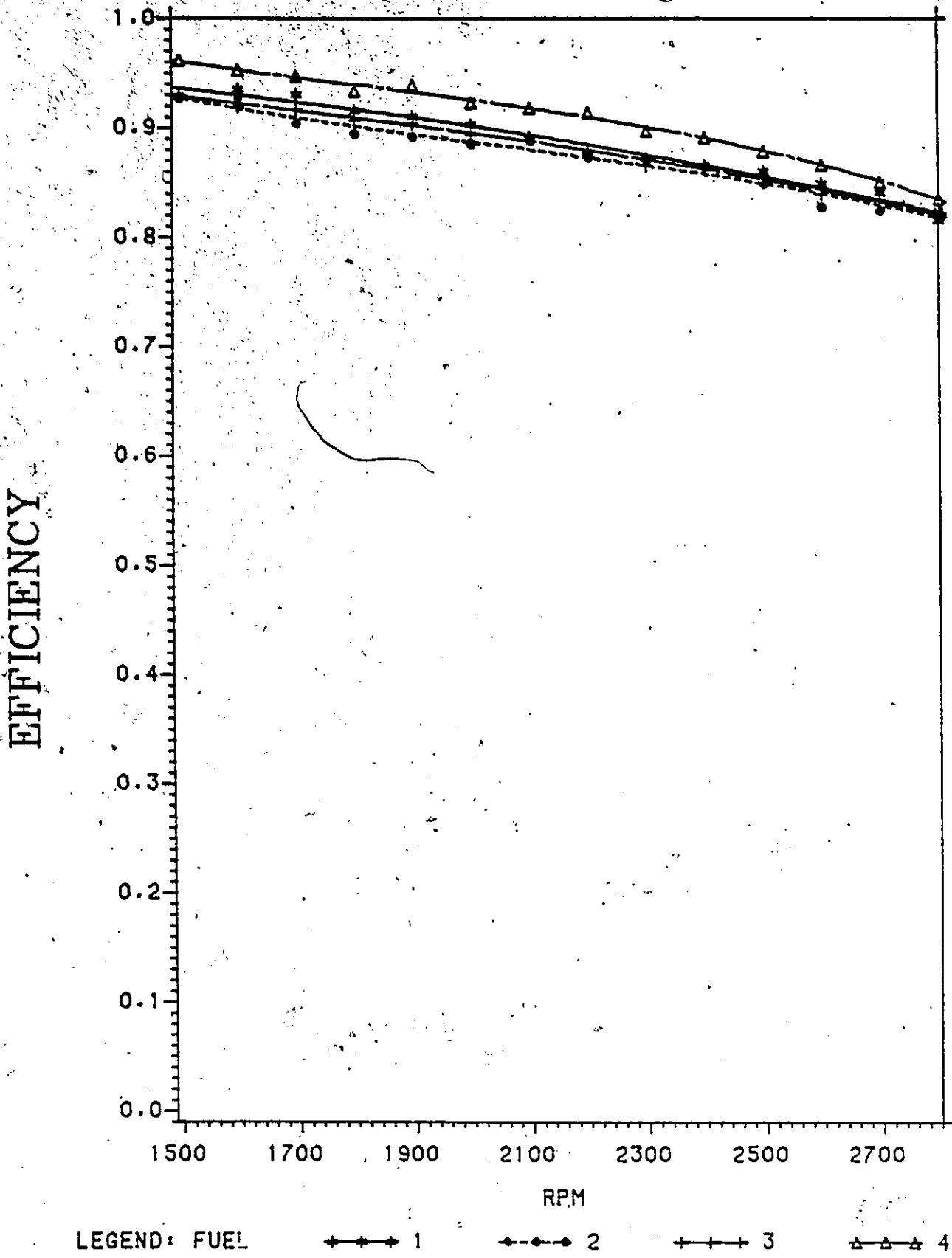


Fig. 5-14(a): Mechanical Efficiency Comparison at Full Load.
Full Scale Characteristic Trends.

6V53T TWO STROKE ENGINE

MECHANICAL EFFICIENCY VS RPM
TORQUE - MAX

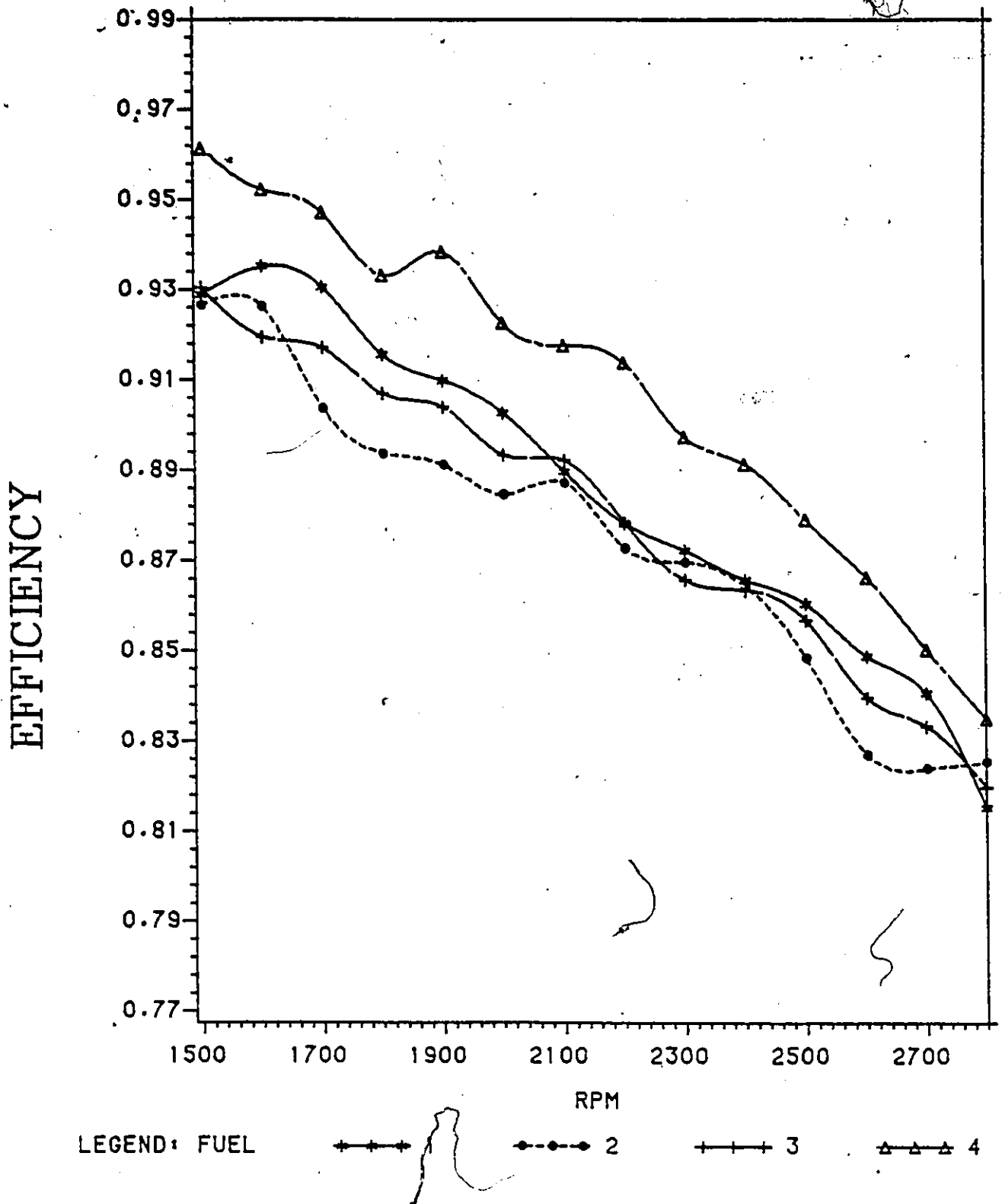


Fig. 5.14(b): Mechanical Efficiency Comparison at Full Load. Expanded Axis Detailed Comparison.

6V53T TWO STROKE ENGINE

MECHANICAL EFFICIENCY VS RPM
TORQUE = 250 FT-LBS

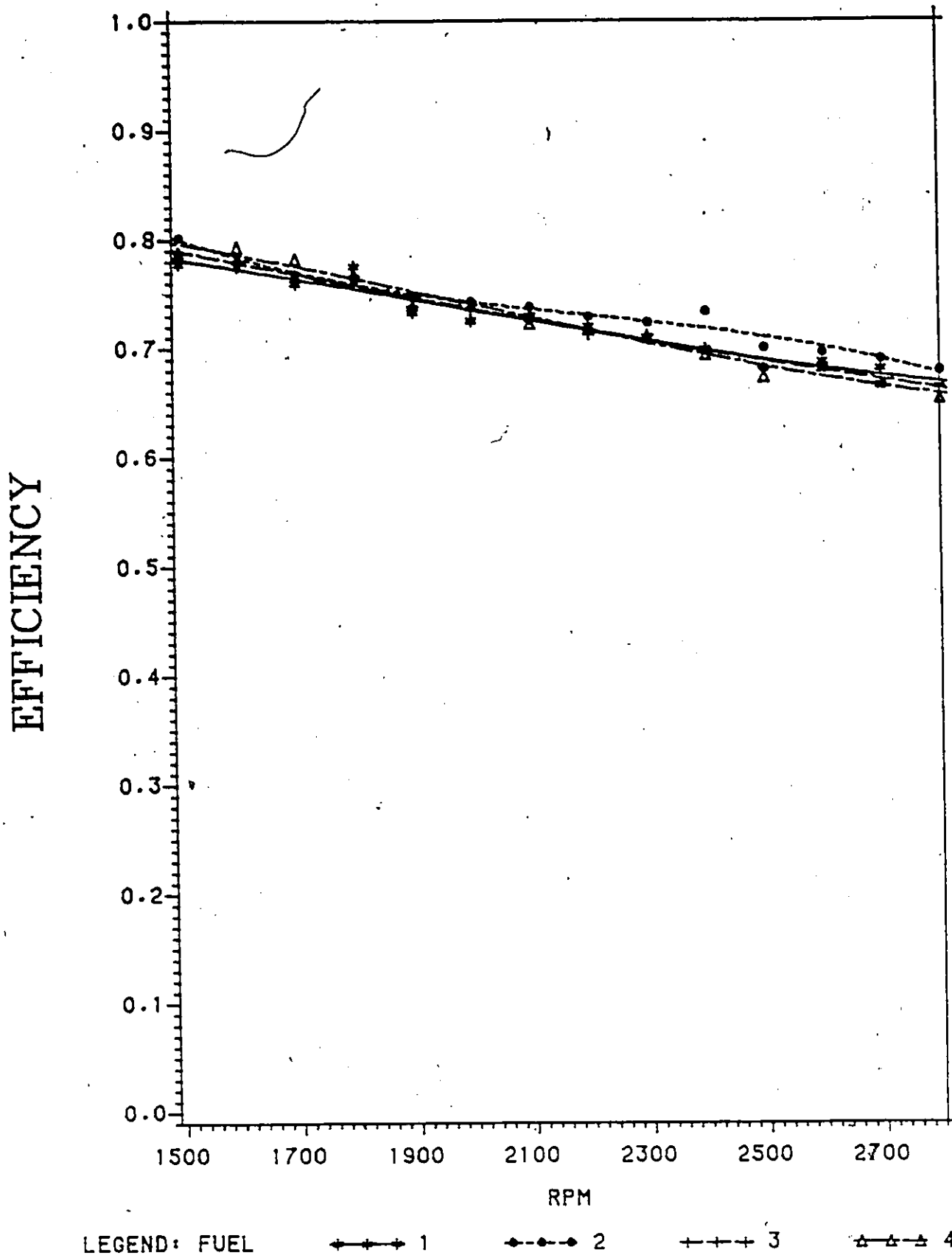


Fig. 5.15(a): Mechanical Efficiency Comparison at Part Load.
Full Scale Characteristic Trends.

6V53T TWO STROKE ENGINE

MECHANICAL EFFICIENCY VS RPM
TORQUE = 250 FT-LBS

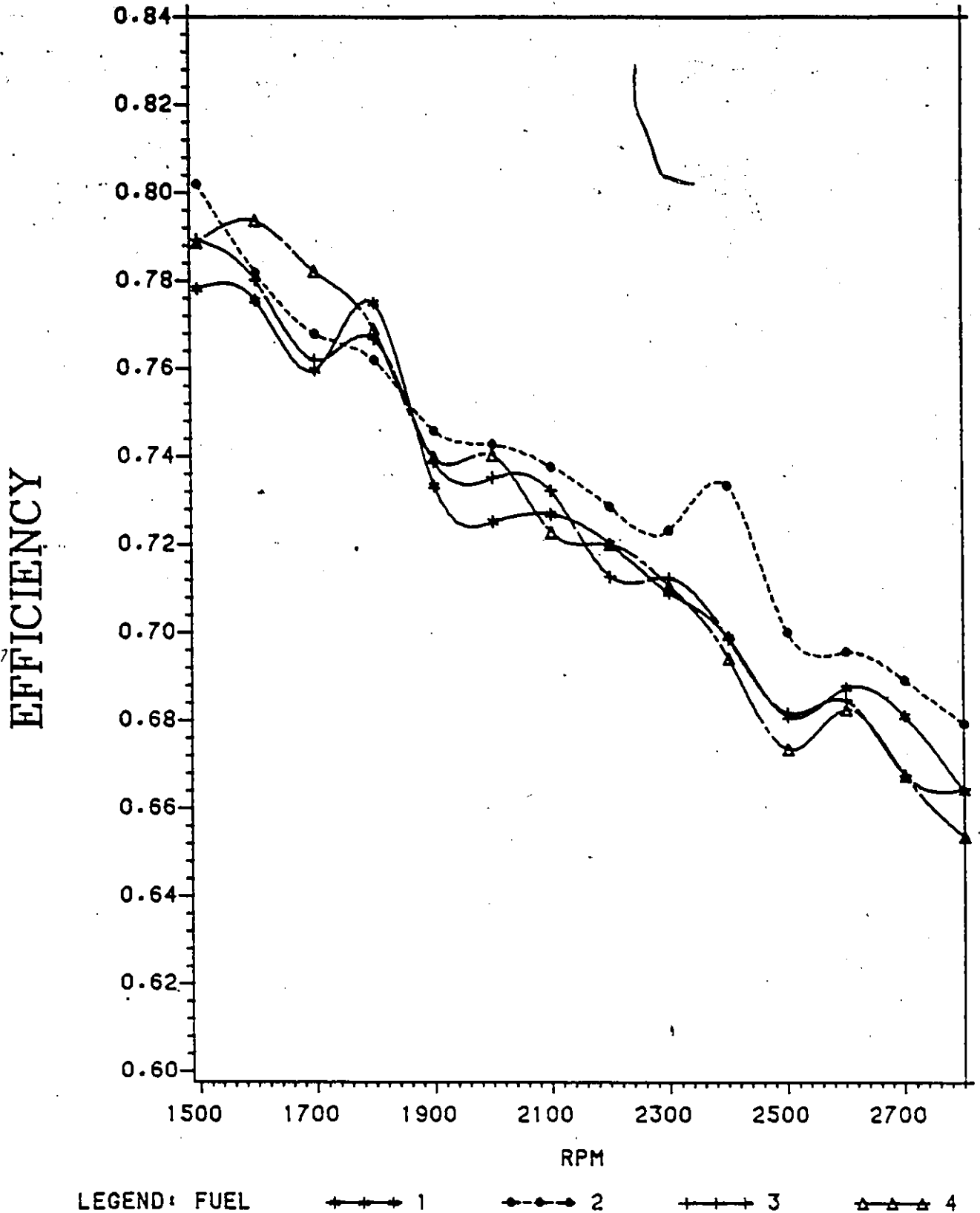


Fig. 5.15(b): Mechanical Efficiency Comparison at Part Load.
Expanded Axis Detailed Comparison.

6V53T TWO STROKE ENGINE

ONSET OF COMBUSTION VS RPM
TORQUE = MAX

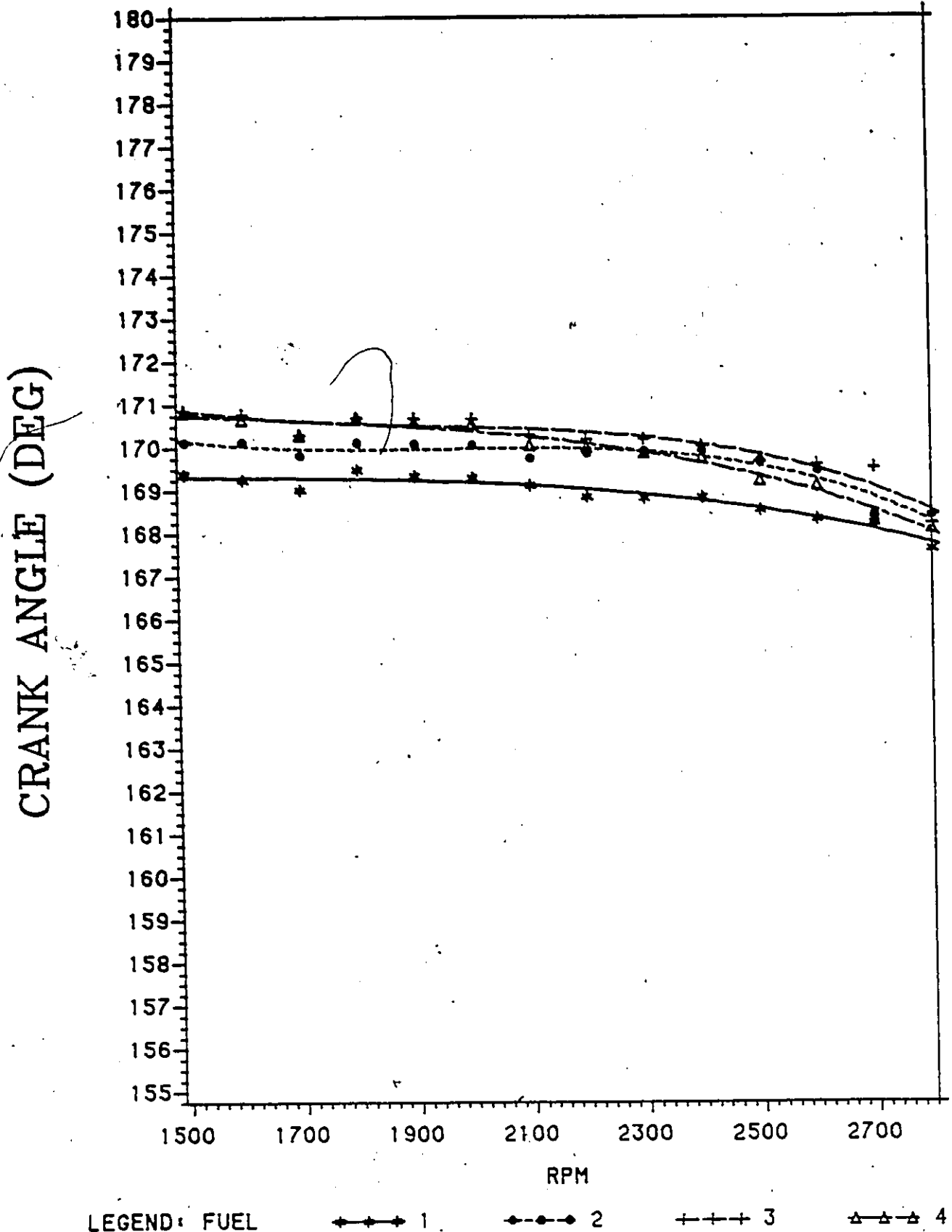


Fig. 5.16(a): Onset of Combustion Comparison Curves at Full Load.
Full Scale Characteristic Trends.

6V53T TWO STROKE ENGINE

ONSET OF COMBUSTION VS RPM
TORQUE = MAX

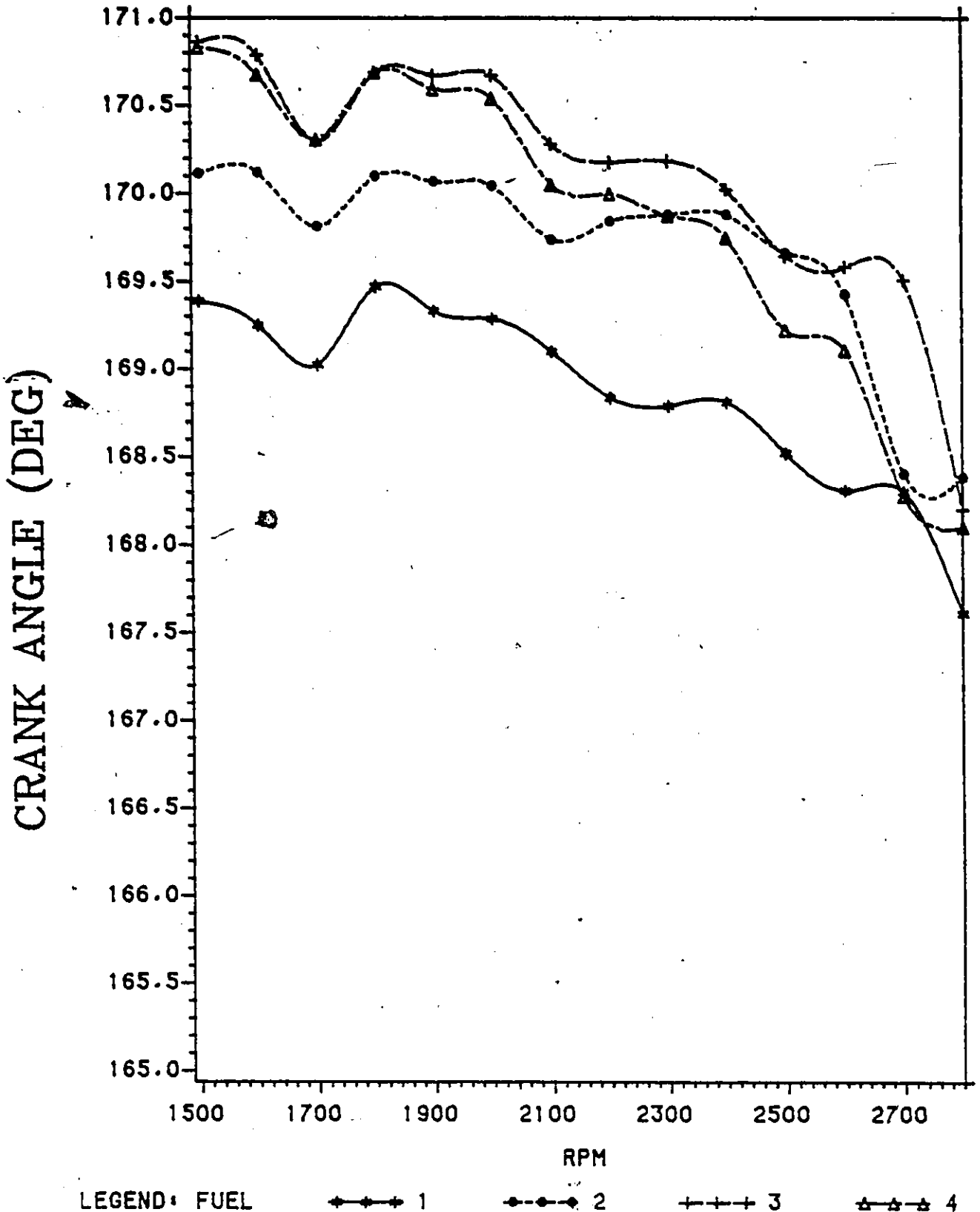


Fig. 5.16(b): Onset of Combustion Comparison Curves at Full Load.
Expanded Axis Detailed Comparison.

6V53T TWO STROKE ENGINE

IGNITION DELAY VS RPM
TORQUE - MAX

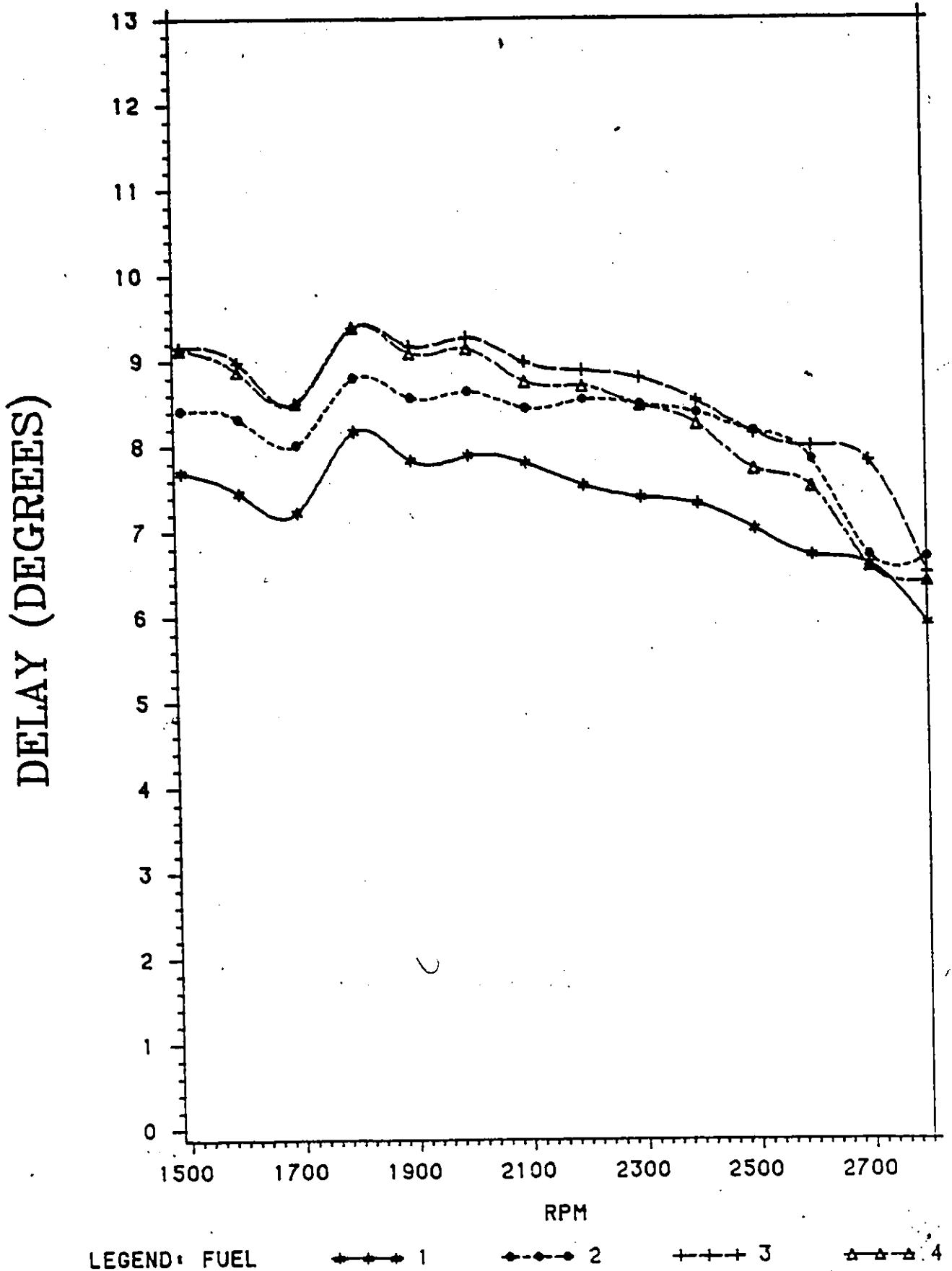


Fig. 5.17: Ignition Delay Comparison Curves at Full Load

6V53T TWO STROKE ENGINE

ONSET OF RAPID COMBUSTION VS RPM
TORQUE = MAX

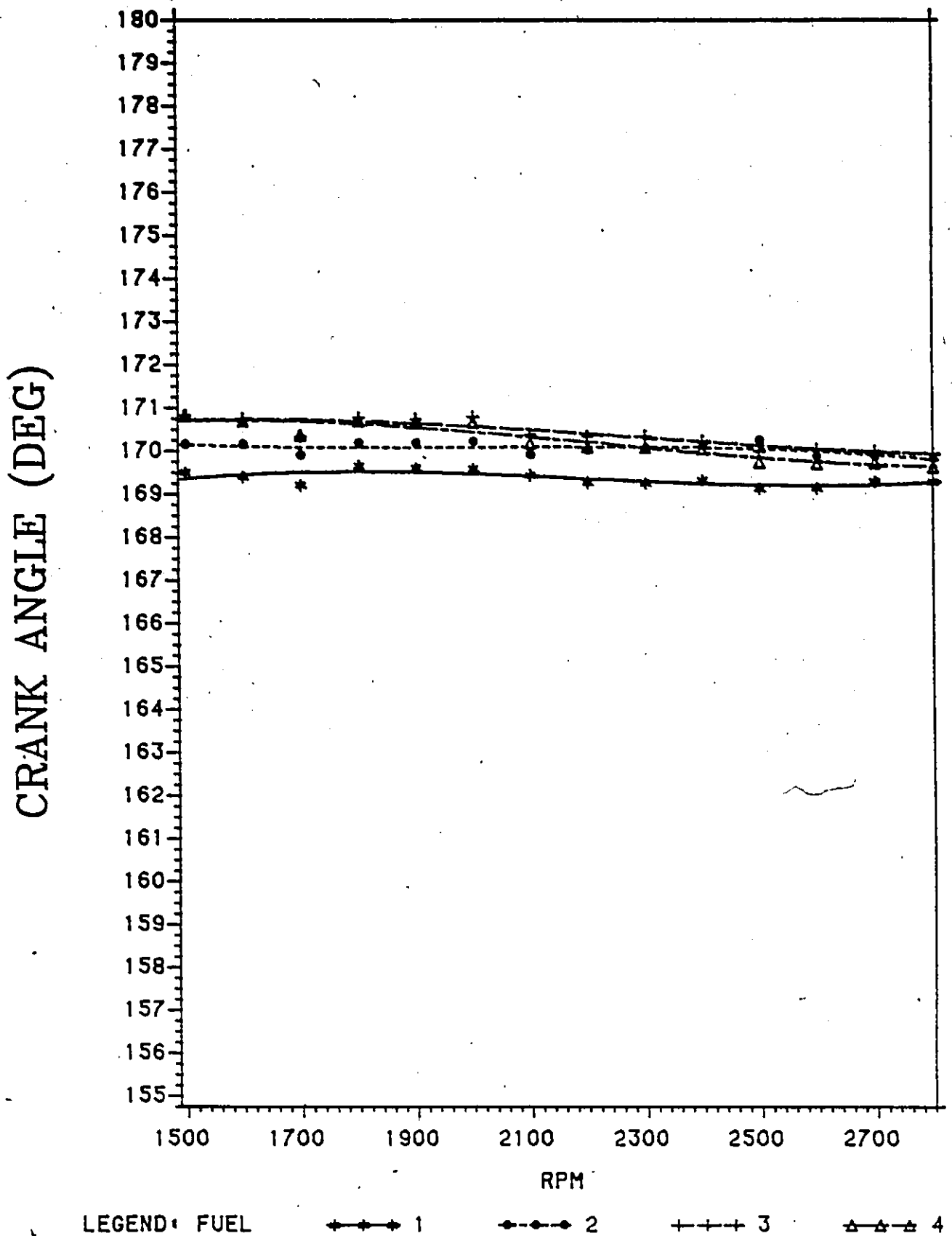


Fig. 5.18(a): Onset of Rapid Combustion Comparison Curves at Full Load.
Full Scale Characteristic Trends.

6V53T TWO STROKE ENGINE

ONSET OF RAPID COMBUSTION VS RPM
TORQUE = MAX

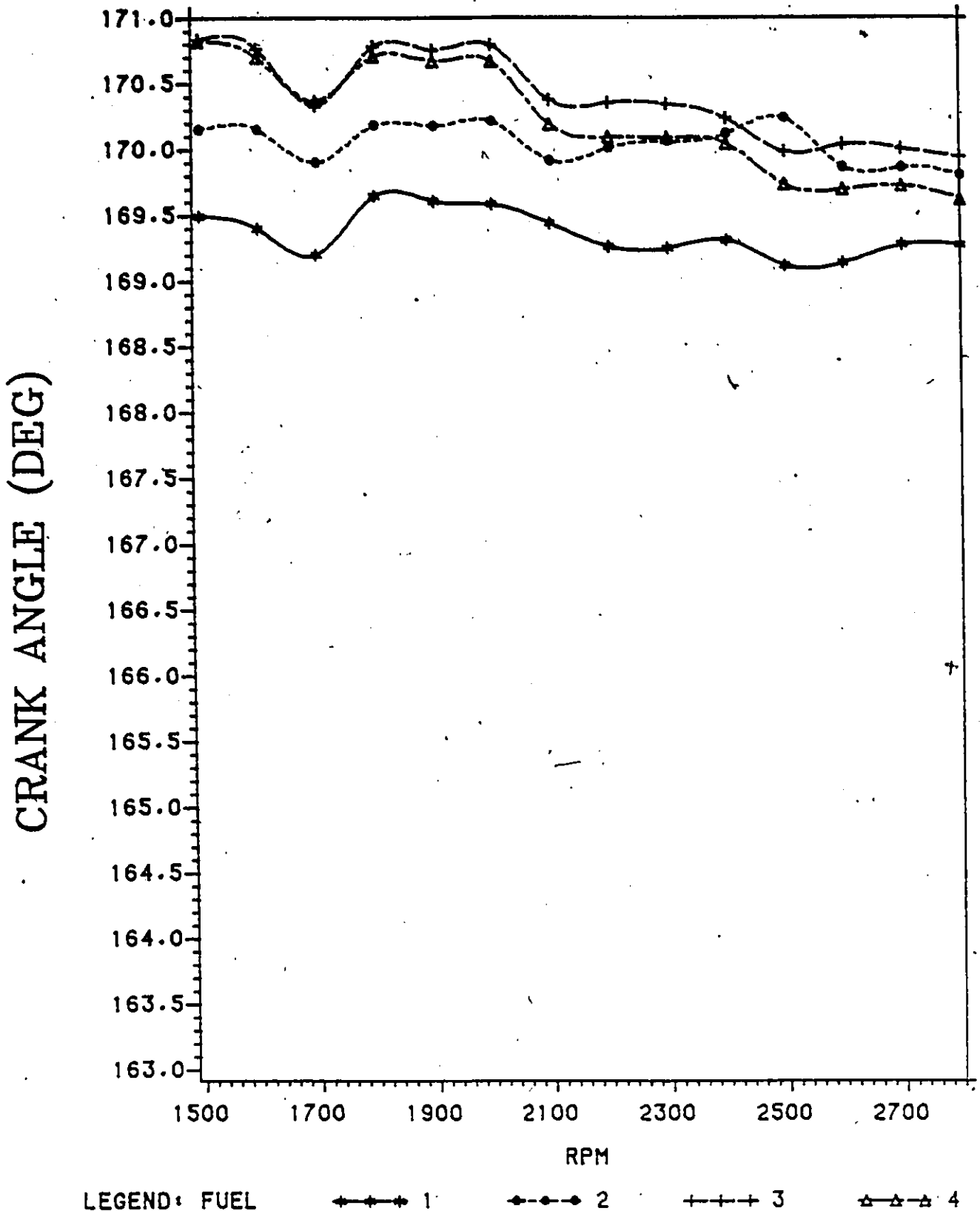


Fig. 5.18(b): Onset of Rapid Combustion Comparison Curves at Full Load. Expanded Axis Detailed Comparison.

6V53T TWO STROKE ENGINE

COMBUSTION DELAY VS RPM

TORQUE = MAX

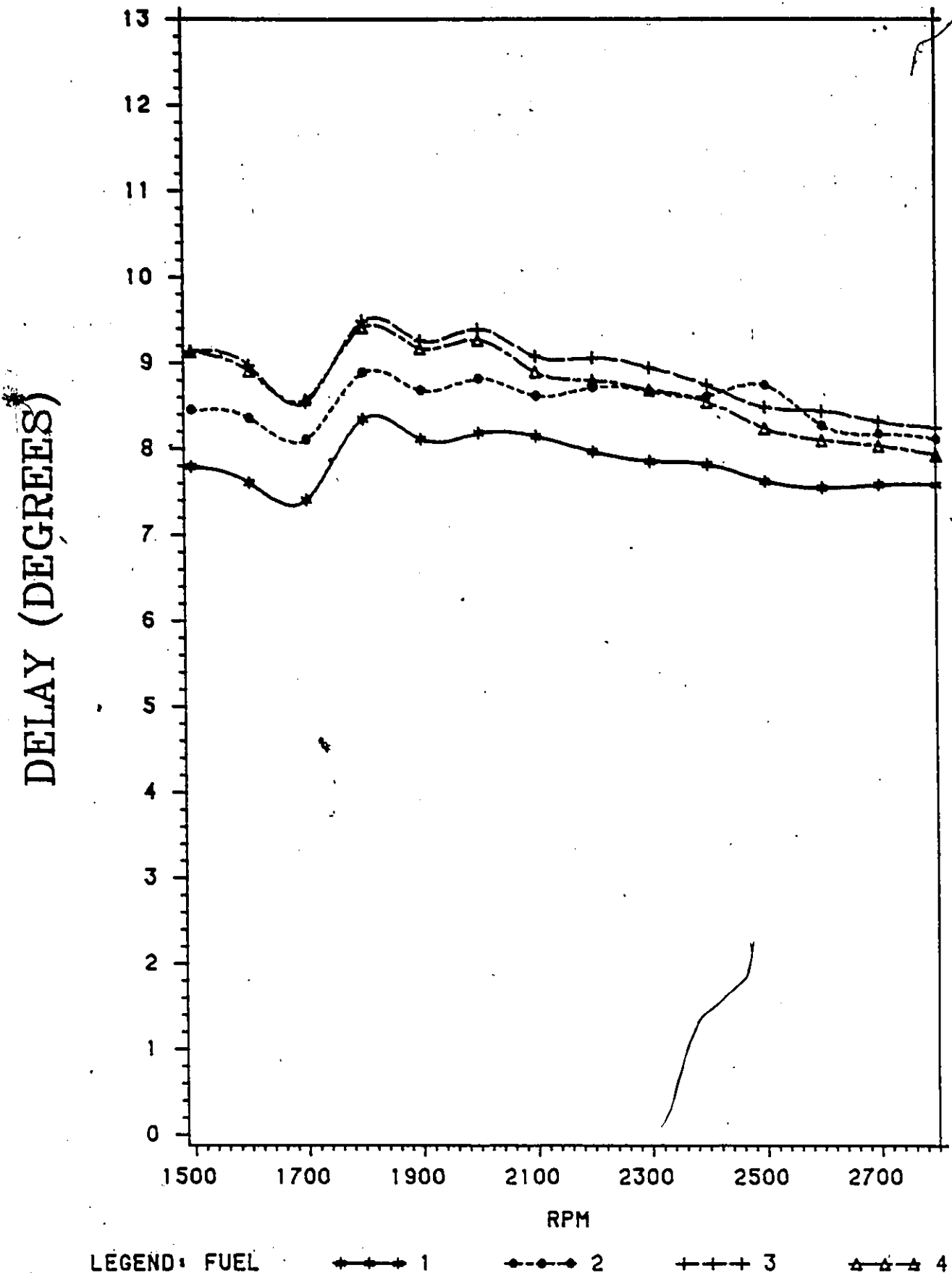


Fig. 5.19: Combustion Delay Comparison at Full Load

6V53T TWO STROKE ENGINE

MAXIMUM CYLINDER PRESSURE VS RPM

TORQUE = MAX

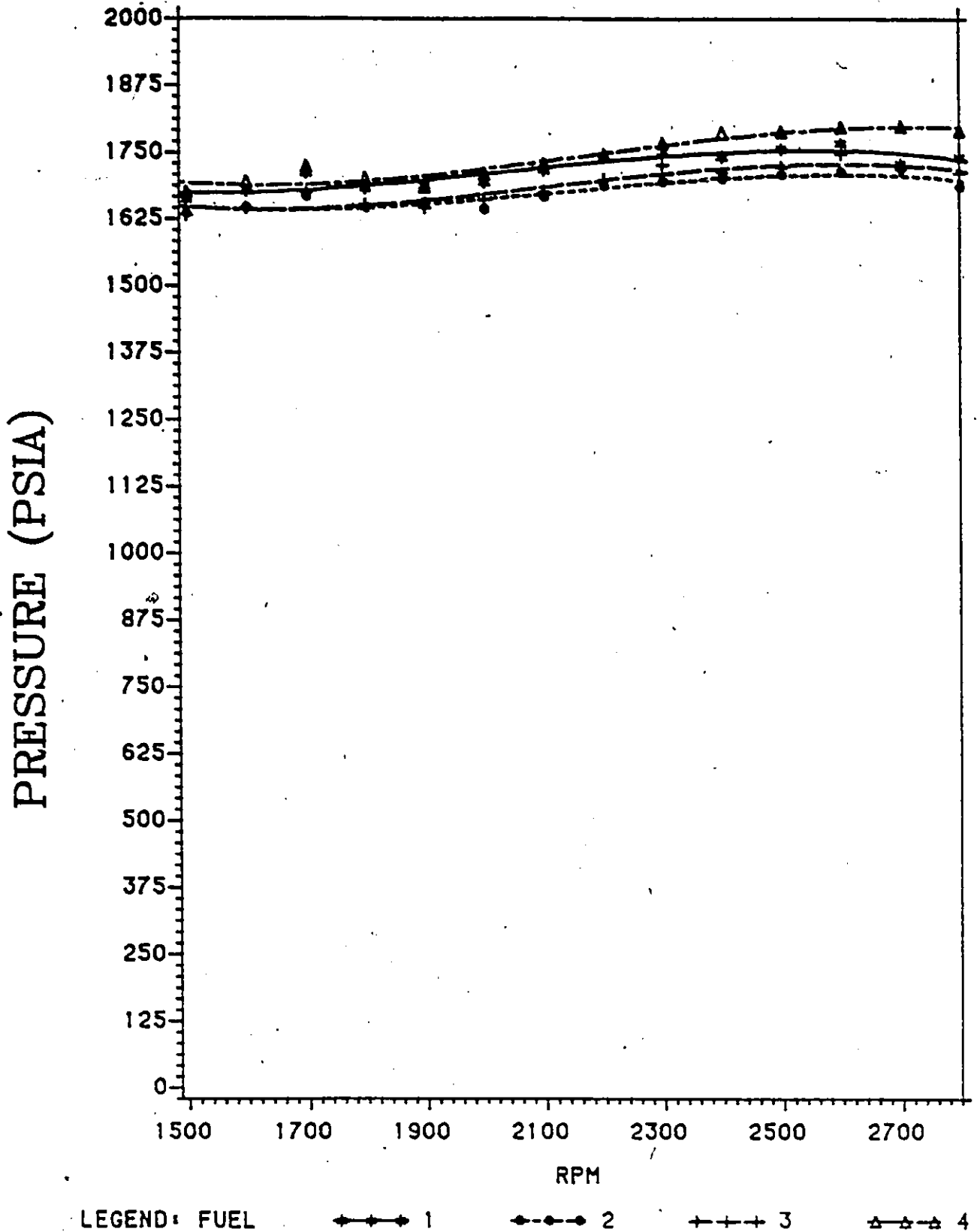


Fig. 5.20(a): Maximum Pressure Comparison Curves at Full Load. Full Scale Characteristic Trends.

6V53T TWO STROKE ENGINE

MAXIMUM CYLINDER PRESSURE VS RPM

TORQUE = MAX

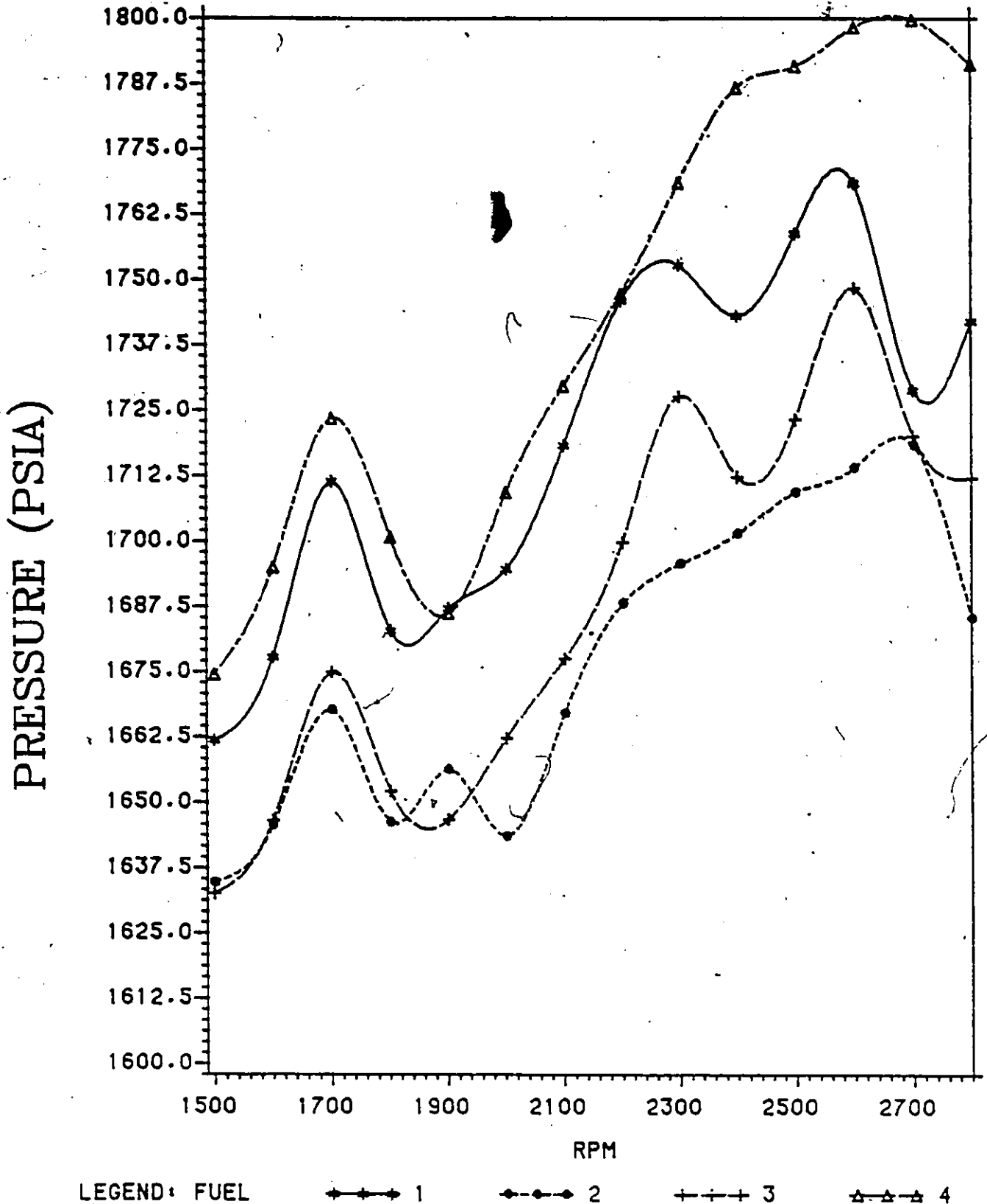


Fig. 5.20(b): Maximum Pressure Comparison Curves at Full Load. Expanded Axis Detailed Comparison.

6V53T TWO STROKE ENGINE

MAXIMUM PRESSURE RATE VS RPM

TORQUE = MAX

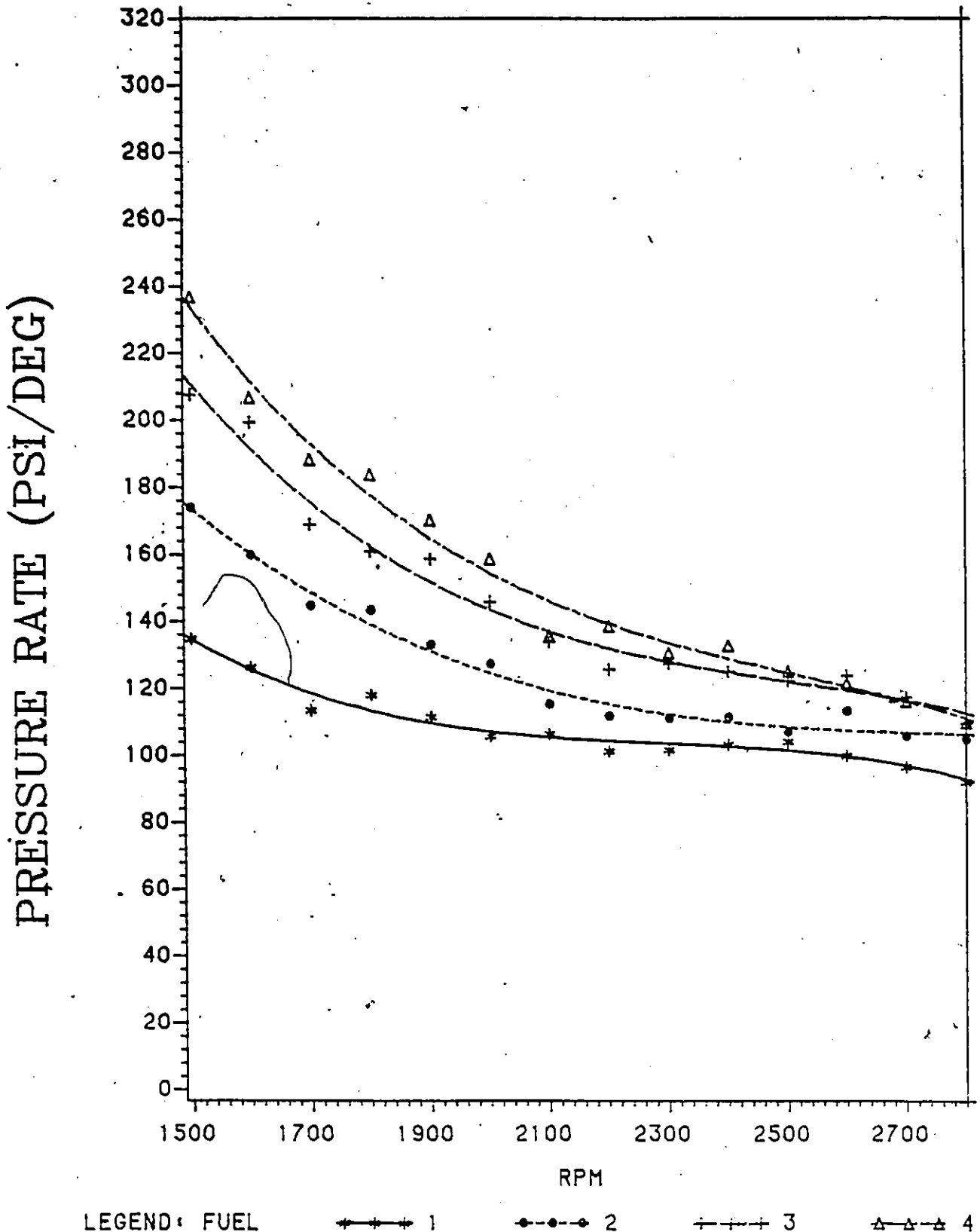
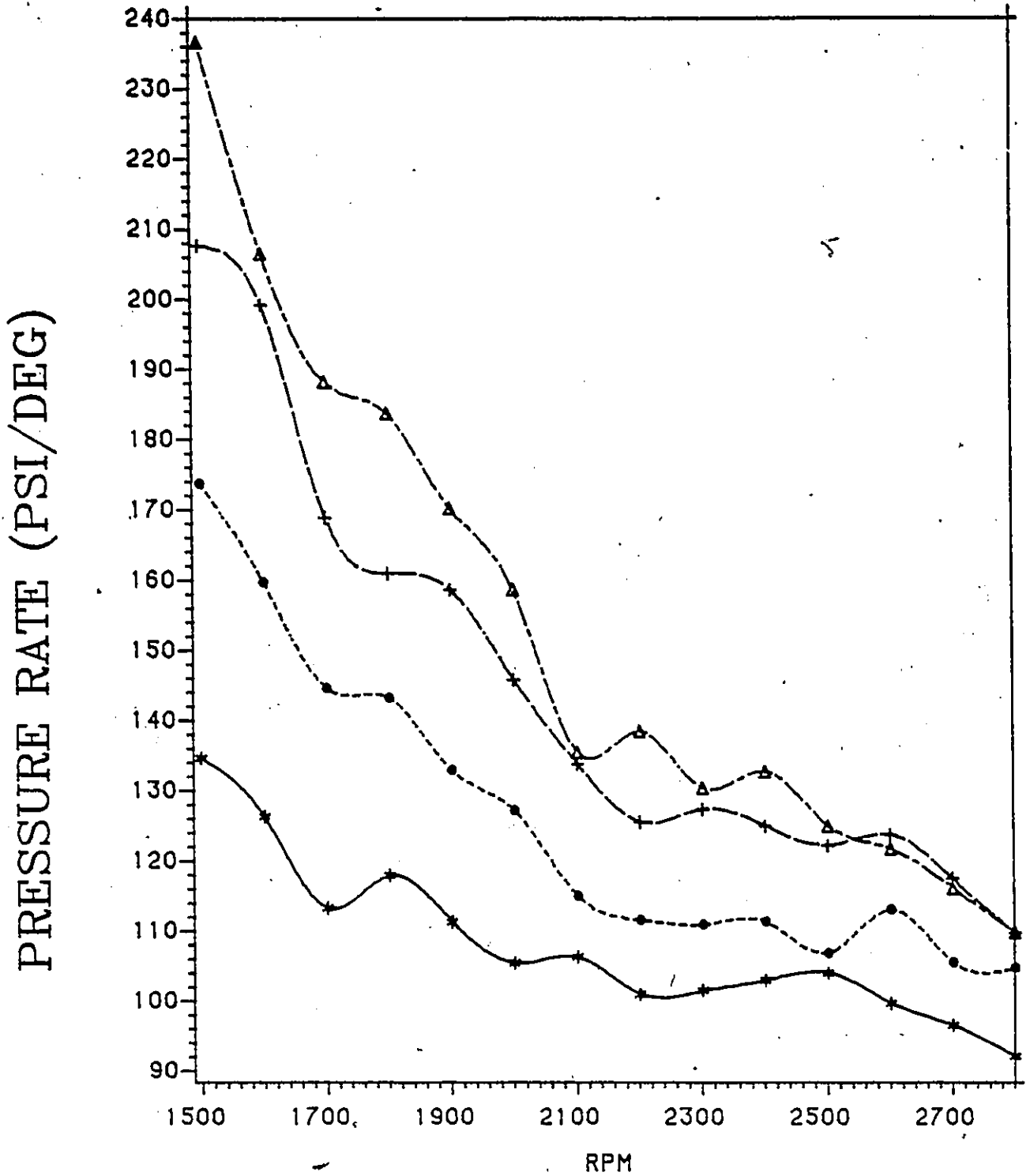


Fig. 5.21(a): Maximum Pressure Rate Comparison Curves at Full Load. Full Scale Characteristic Trends.

6V53T TWO STROKE ENGINE

MAXIMUM PRESSURE RATE VS RPM

TORQUE = MAX



LEGEND: FUEL +--+ 1 ●---● 2 ++++ 3 ▲---▲ 4

Fig. 5.21(b): Maximum Pressure Rate Comparison Curves at Full Load. Expanded Axis Detailed Comparison.

6V53T TWO STROKE ENGINE

ONSET OF COMBUSTION VS RPM

TORQUE = 250 FT-LBS

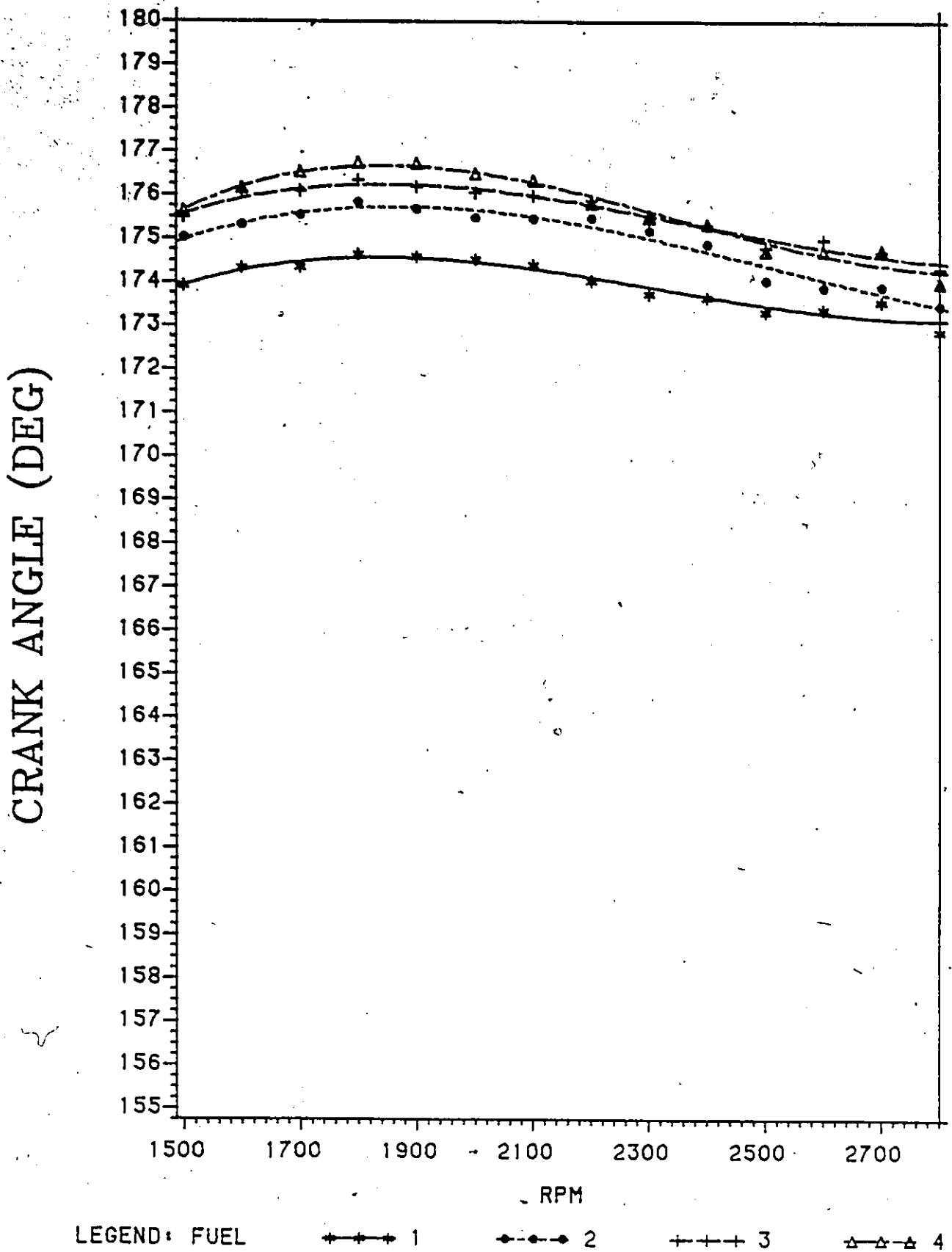


Fig. 5.22(a): Onset of Combustion Comparison Curves at Part Load. Full Scale Characteristic Trends.

6V53T TWO STROKE ENGINE

ONSET OF COMBUSTION VS RPM
TORQUE = 250 FT-LBS

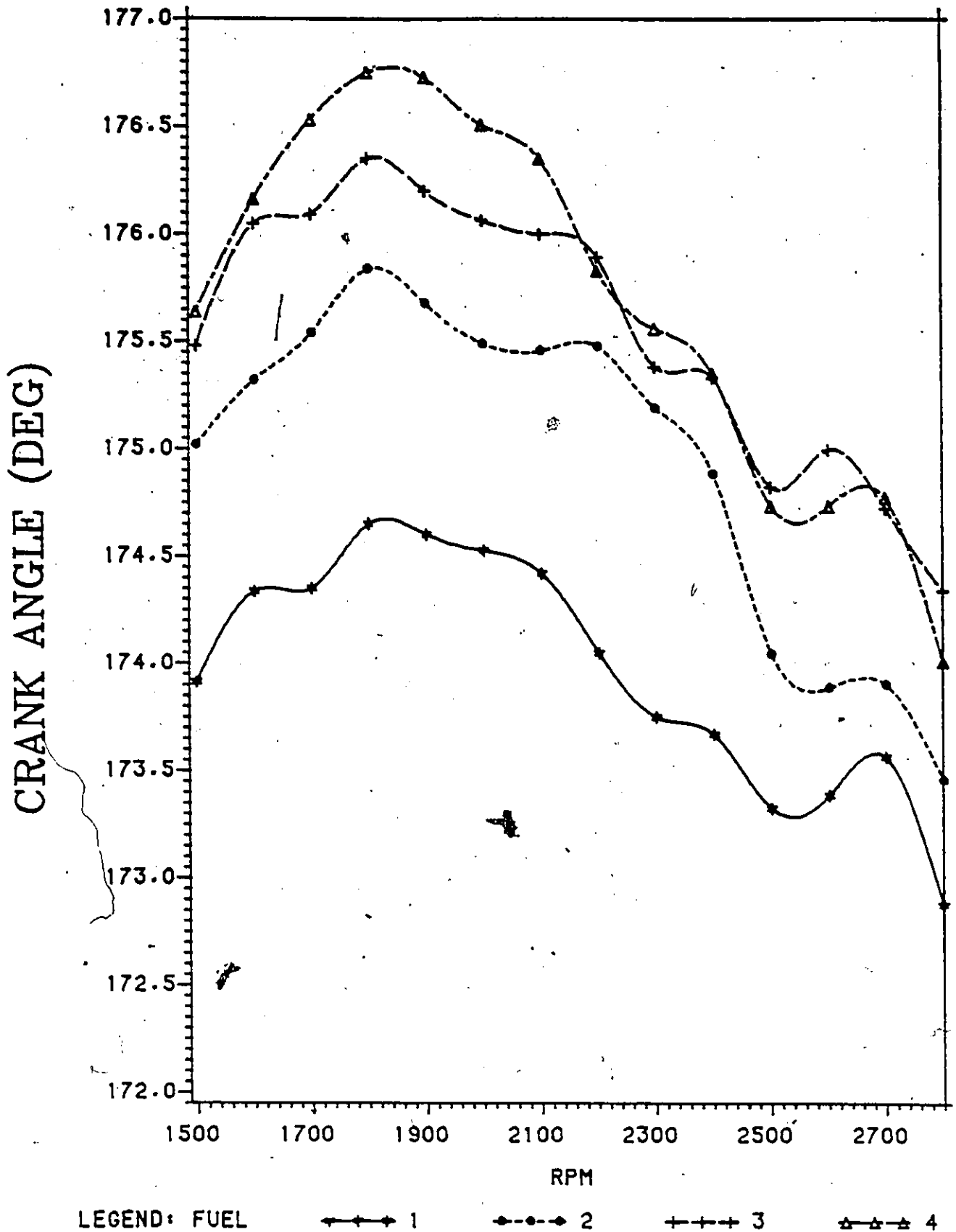


Fig. 5.22(b): Onset of Combustion Comparison Curves at Part Load. Expanded Axis Detailed Comparison.

6V53T TWO STROKE ENGINE

ONSET OF RAPID COMBUSTION VS RPM
TORQUE = 250 FT-LBS

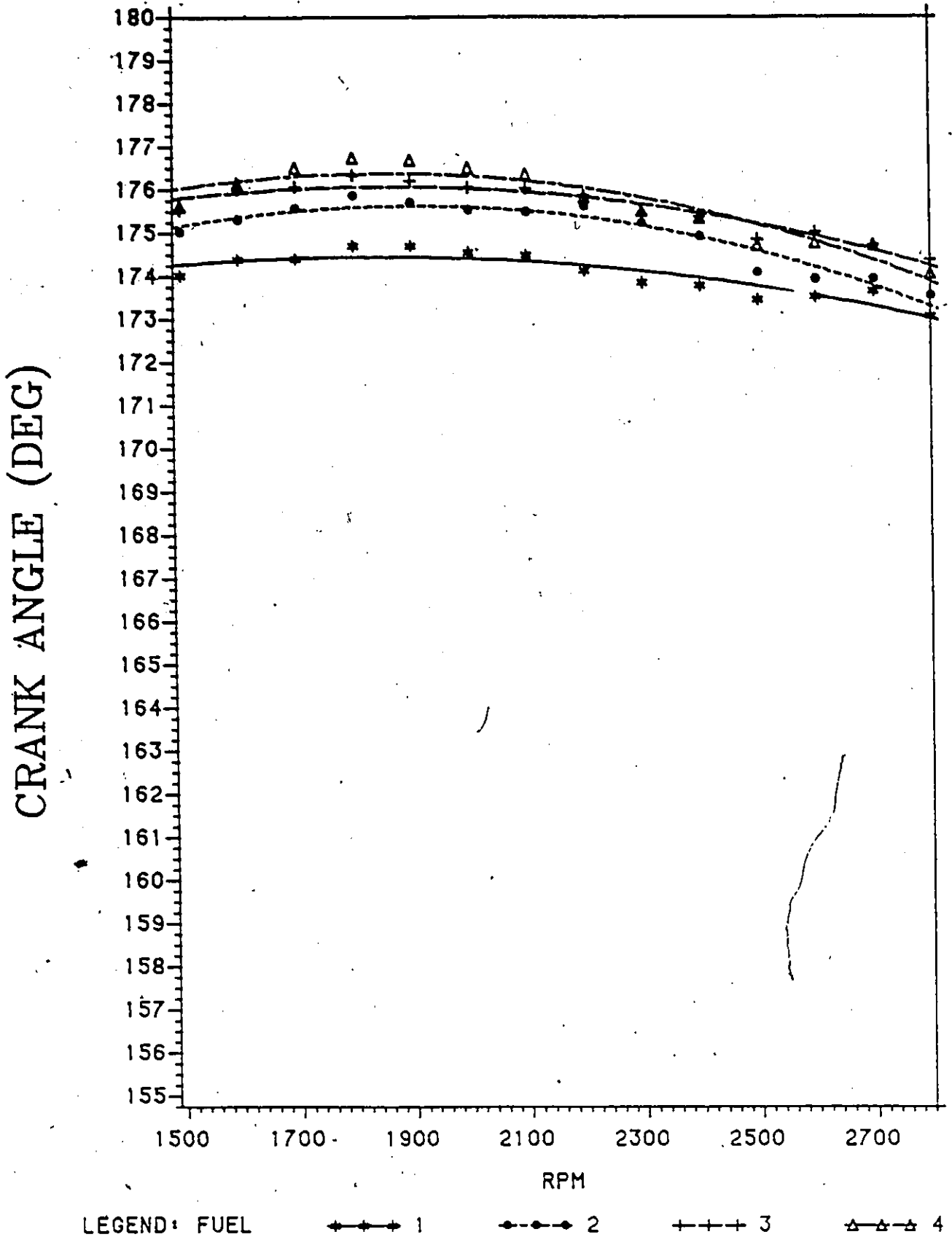


Fig. 5.23(a): Onset of Rapid Combustion Comparison Curves at Part Load.

6V53T TWO STROKE ENGINE

ONSET OF RAPID COMBUSTION VS RPM

TORQUE = 250 FT-LBS

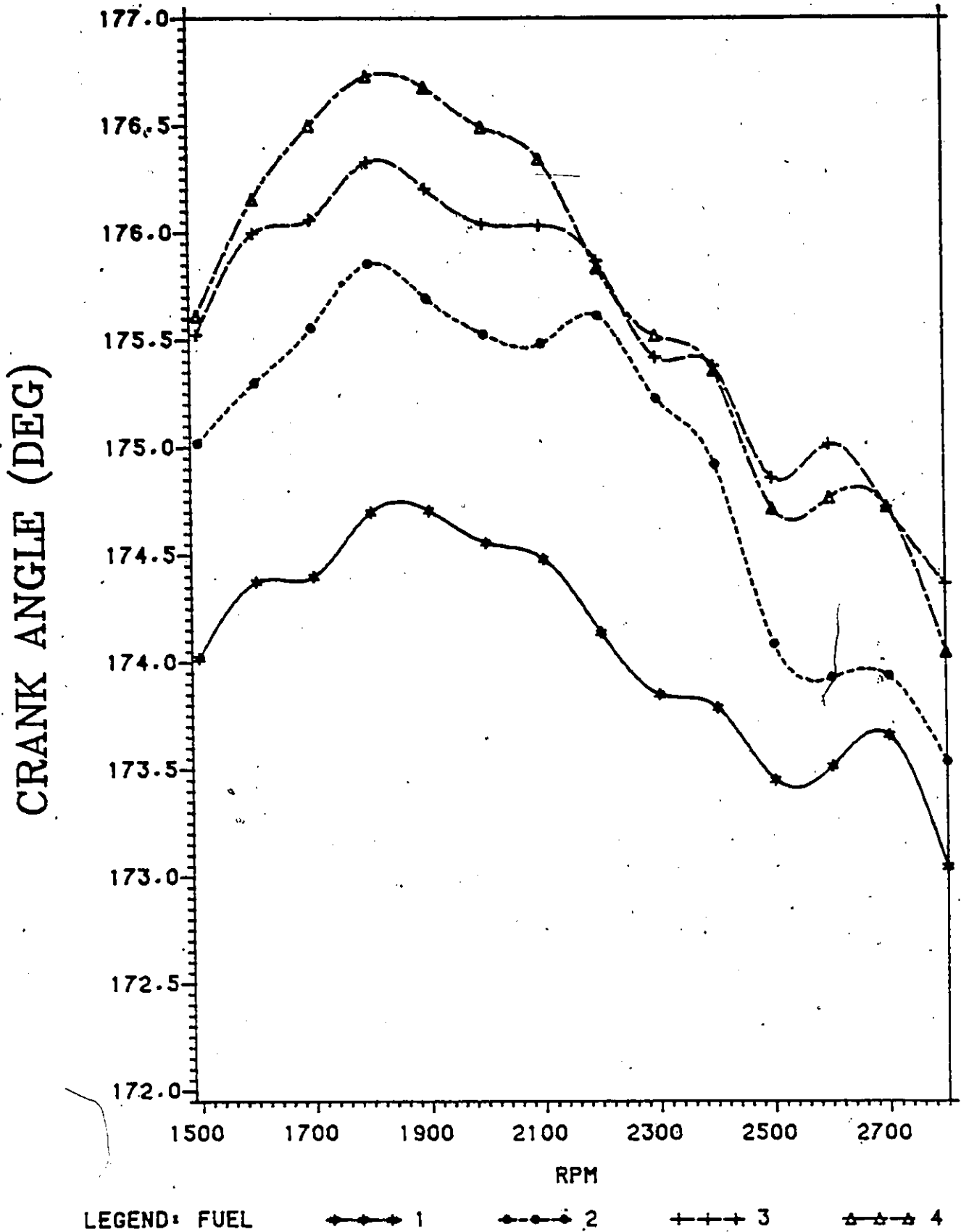


Fig. 5.23 (b): Onset of Rapid Combustion Comparison Curves at Part Load.

Expanded Axis Detailed Comparison.

6V53T TWO STROKE ENGINE

MAXIMUM CYLINDER PRESSURE VS RPM

TORQUE = 250 FT-LBS

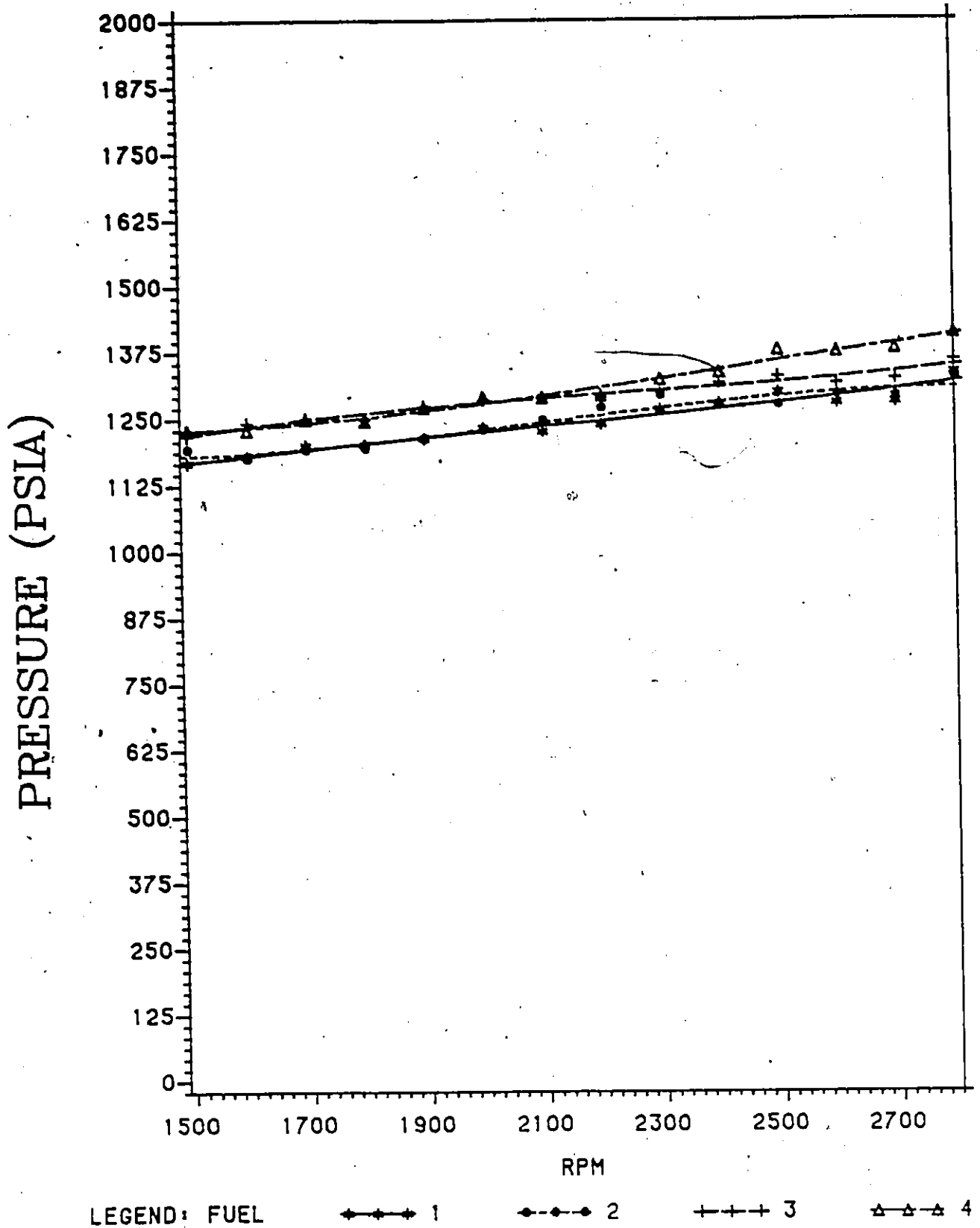


Fig. 5.24(a): Maximum Cylinder Pressure Comparison Curves at Part Load. Full Scale Characteristic Trends.

6V53T TWO STROKE ENGINE

MAXIMUM CYLINDER PRESSURE VS RPM

TORQUE = 250 FT-LBS

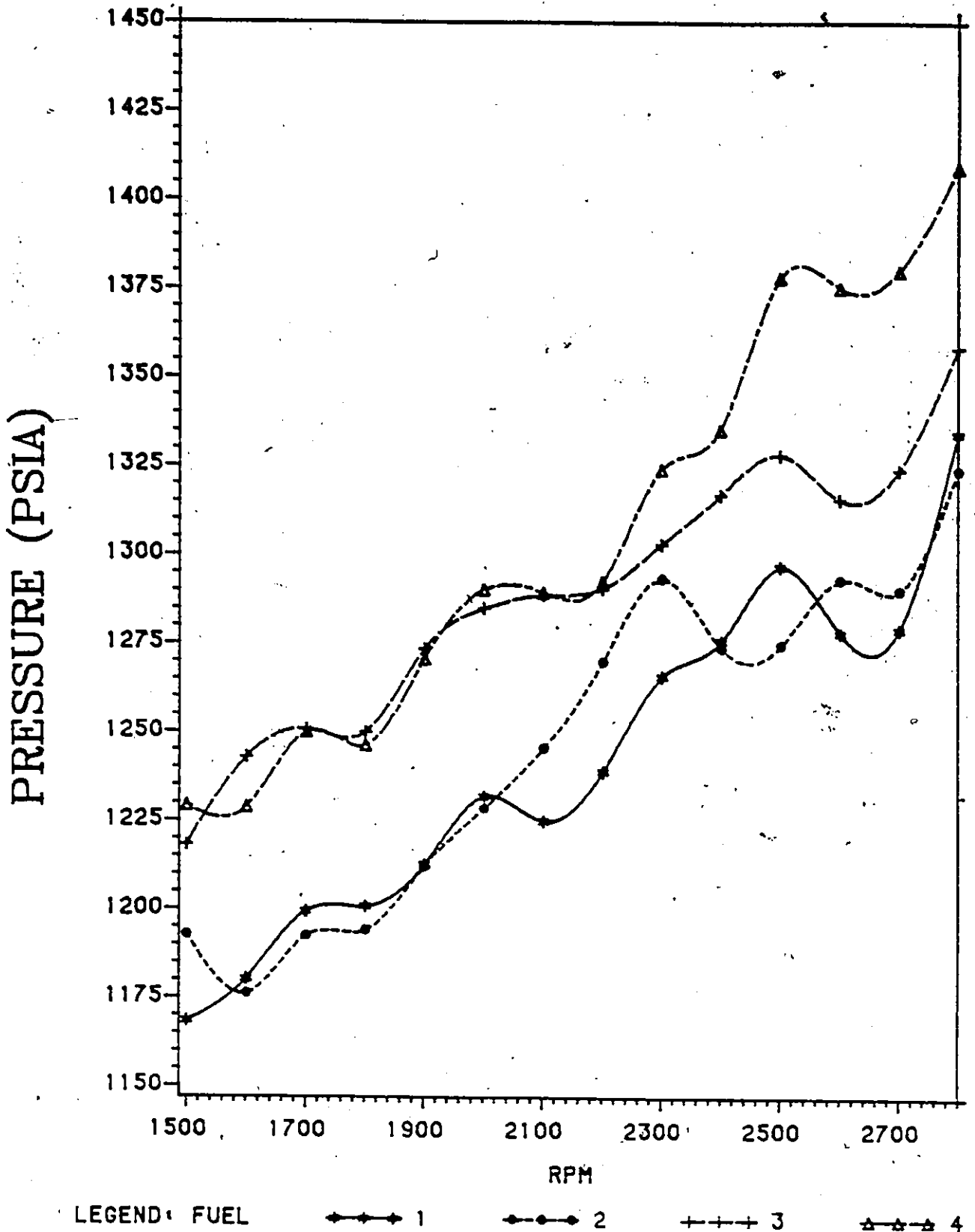


Fig. 5.24(b): Maximum Cylinder Pressure Comparison Curves at Part Load.

Expanded Axis Detailed Comparison.

6V53T TWO STROKE ENGINE

MAXIMUM PRESSURE RATE VS RPM

TORQUE = 250 FT-LBS

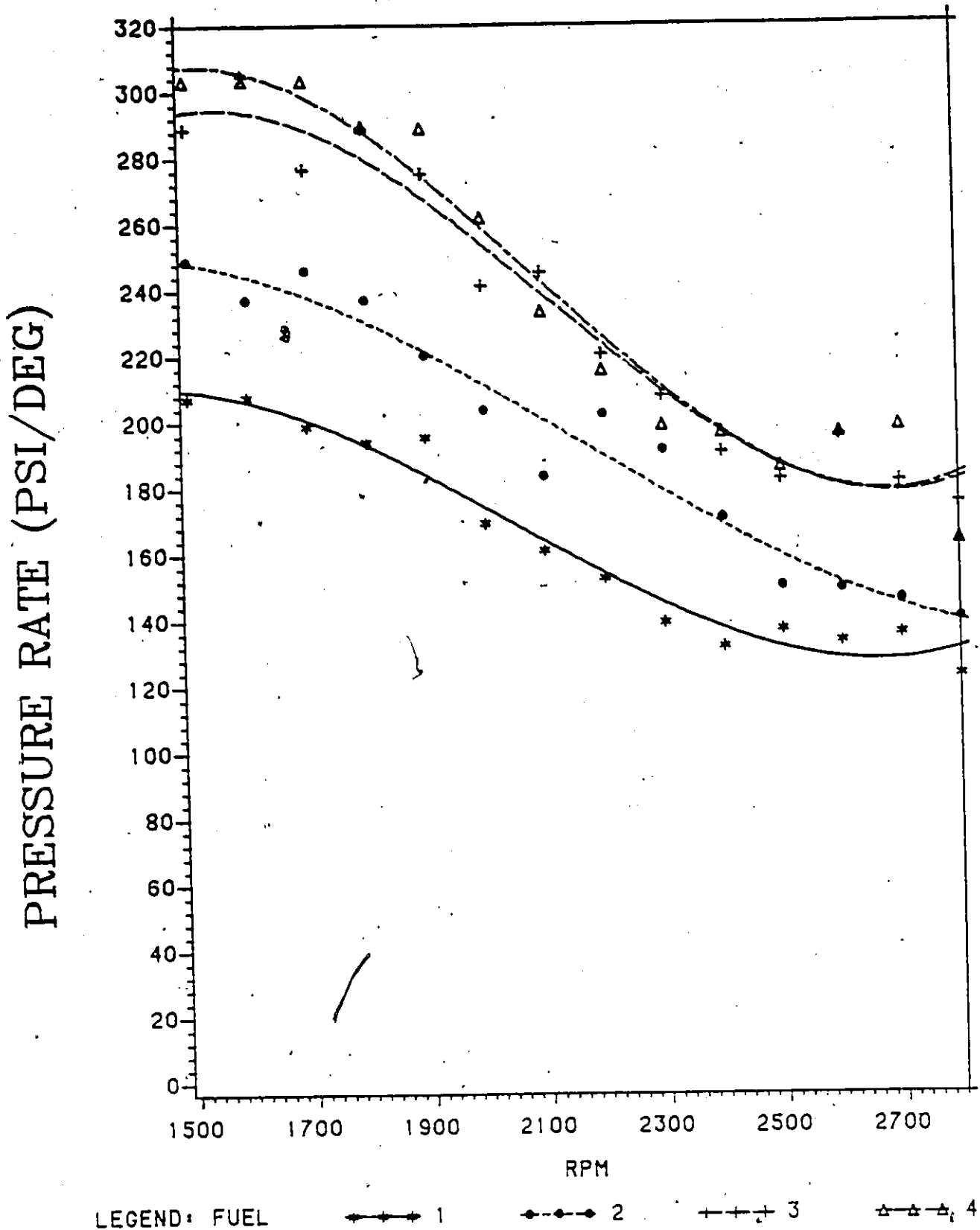


Fig. 5.25(a): Maximum Pressure Rate Comparison Curves at Part Load. Full Scale Characteristic Trends.

6V53T TWO STROKE ENGINE

MAXIMUM PRESSURE RATE VS RPM

TORQUE = 250 FT-LBS

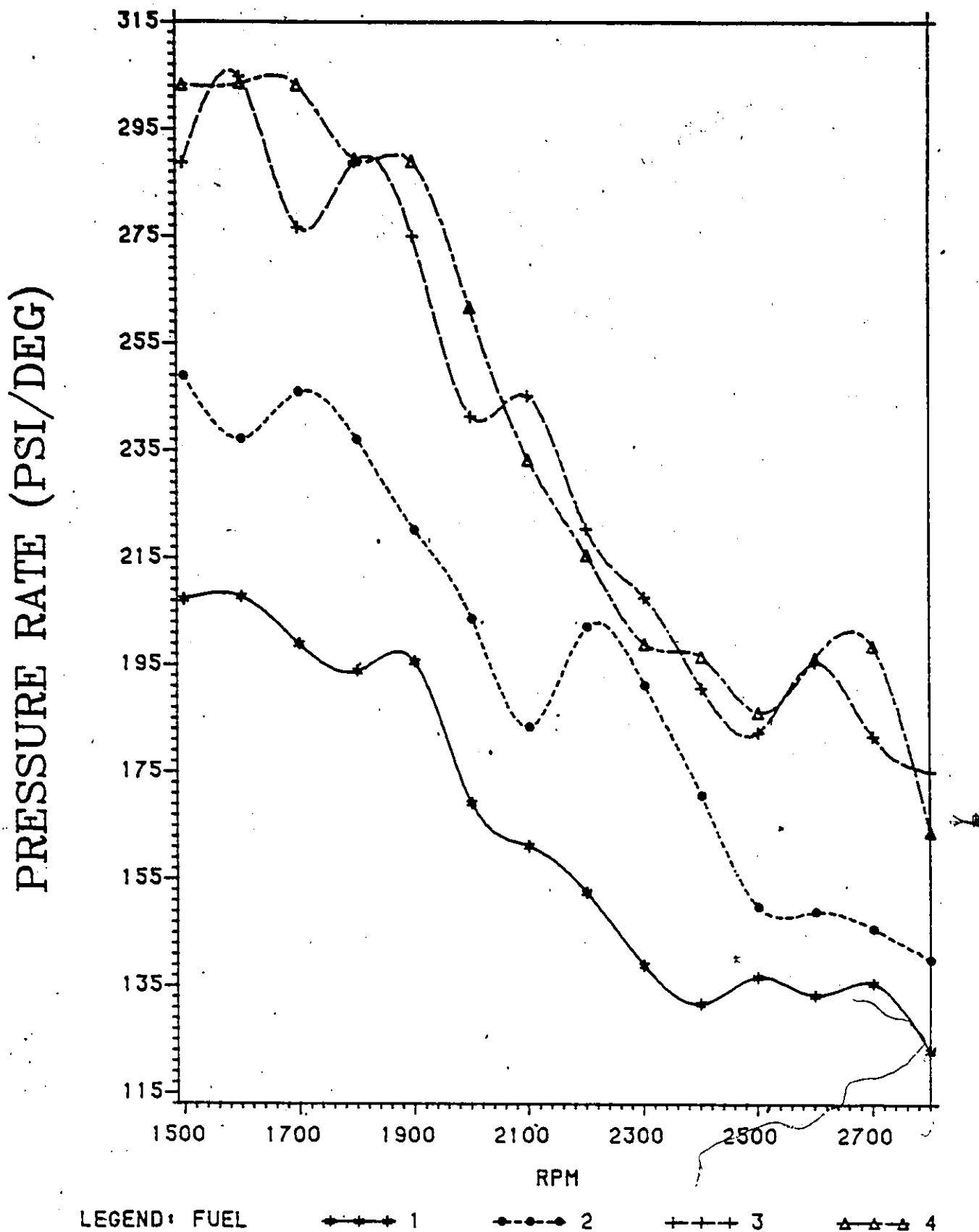


Fig. 5.25(b): Maximum Pressure Rate Comparison Curves at Part Load.

Expanded Axis Detailed Comparison.

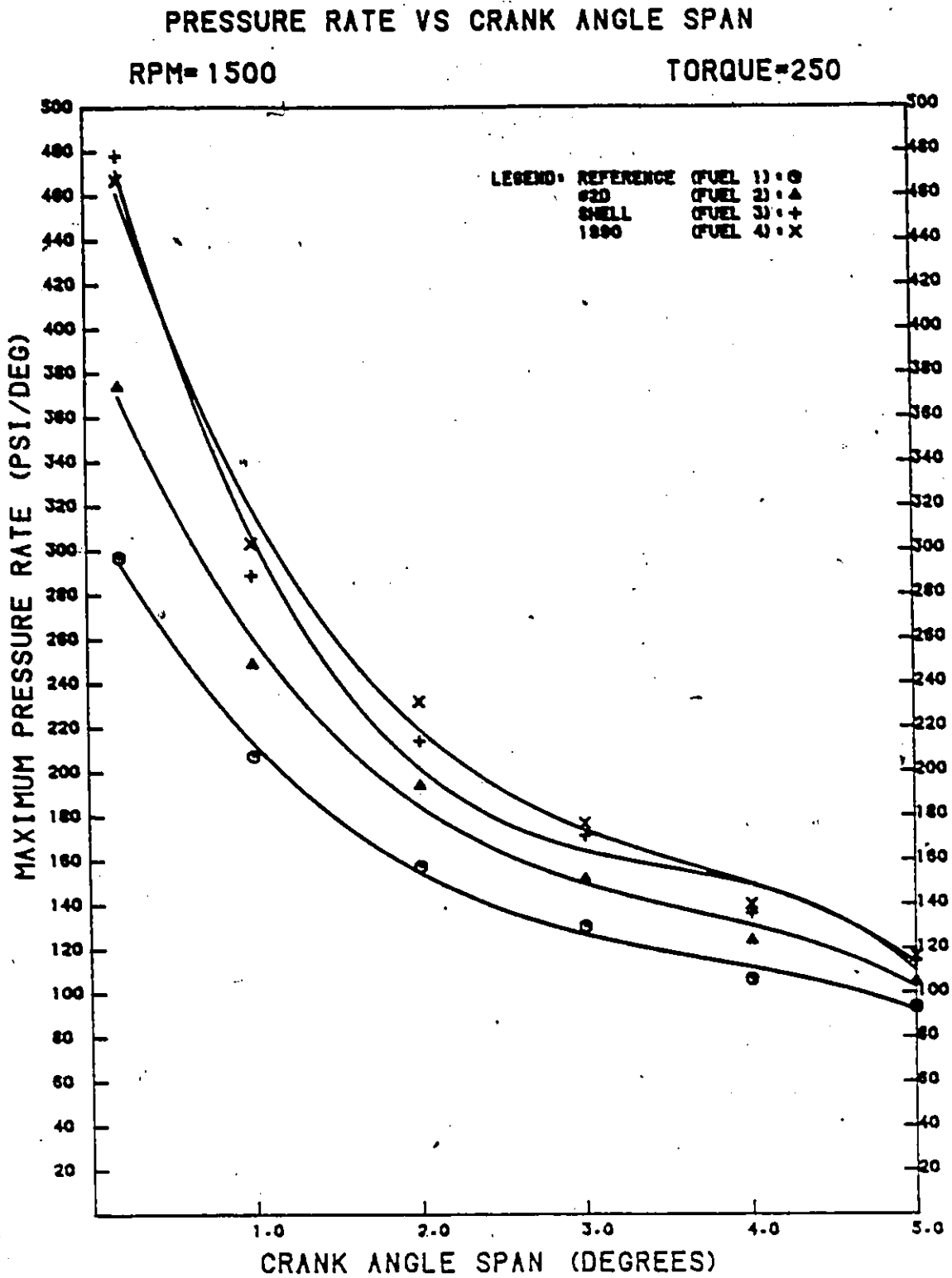
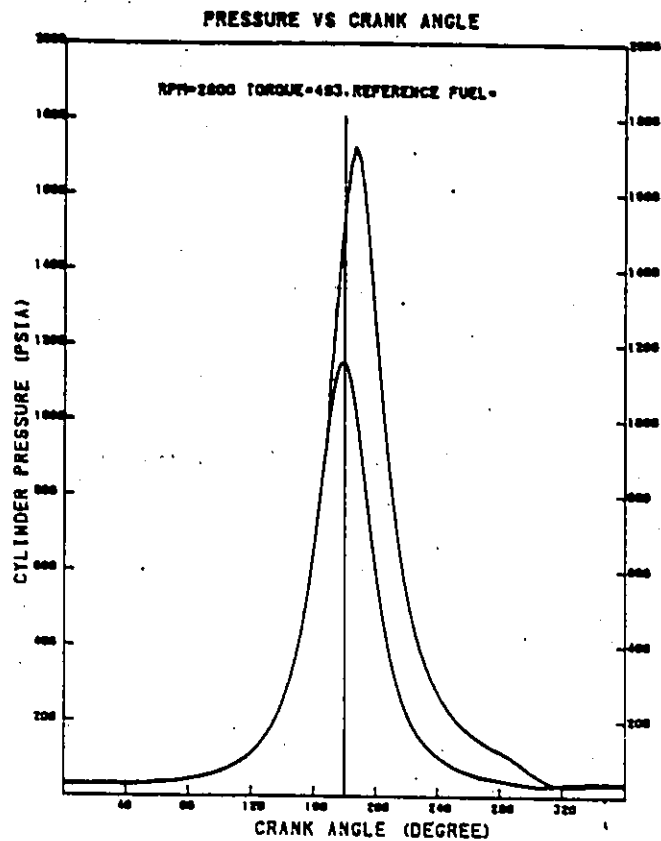
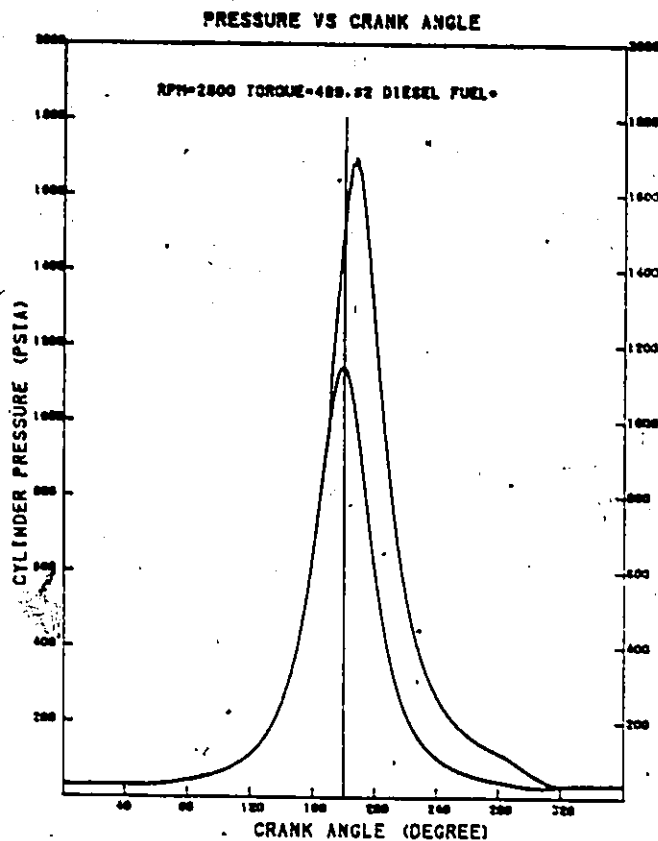


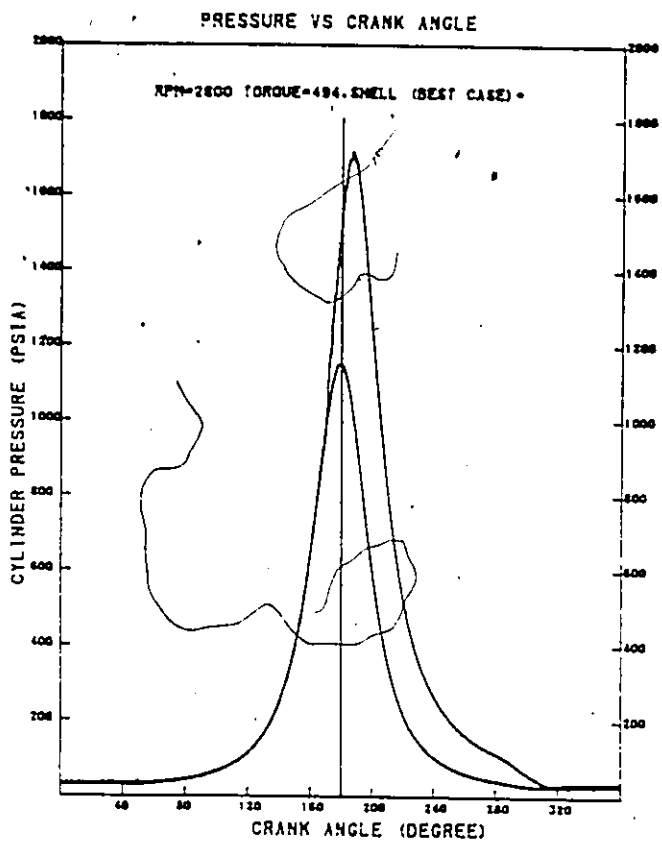
Fig. 5.26: Multi-Span Pressure Rate Comparison Plots.



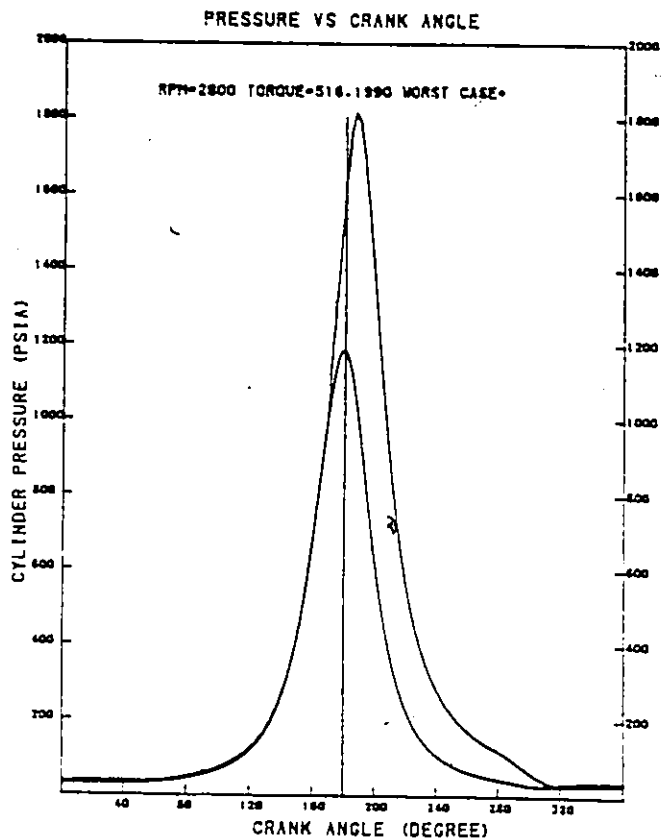
(a)



(b)



(c)



(d)

Fig. 5.27: Pressure Trace Comparison (2800 RPM, Full Load)

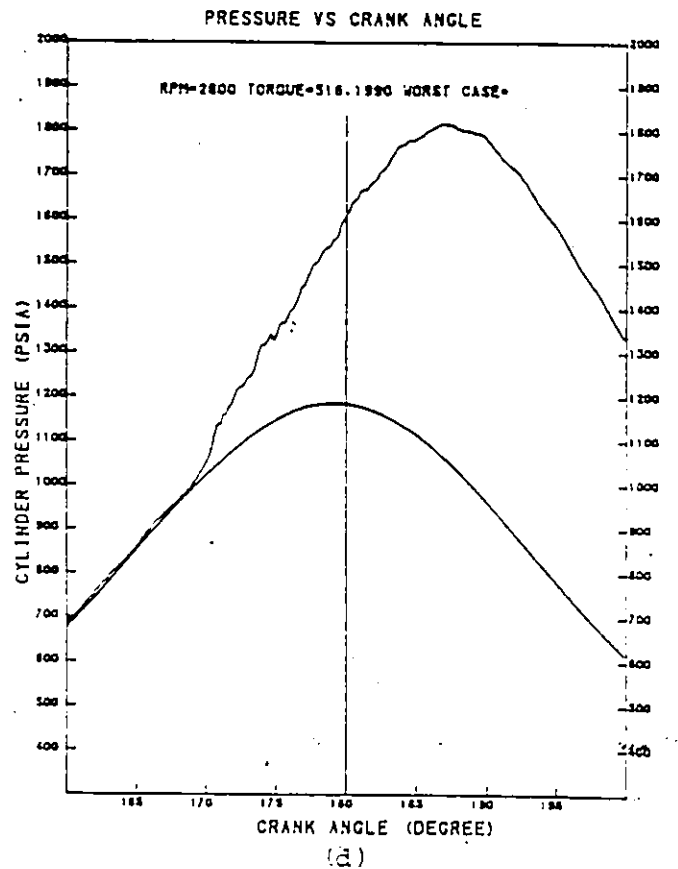
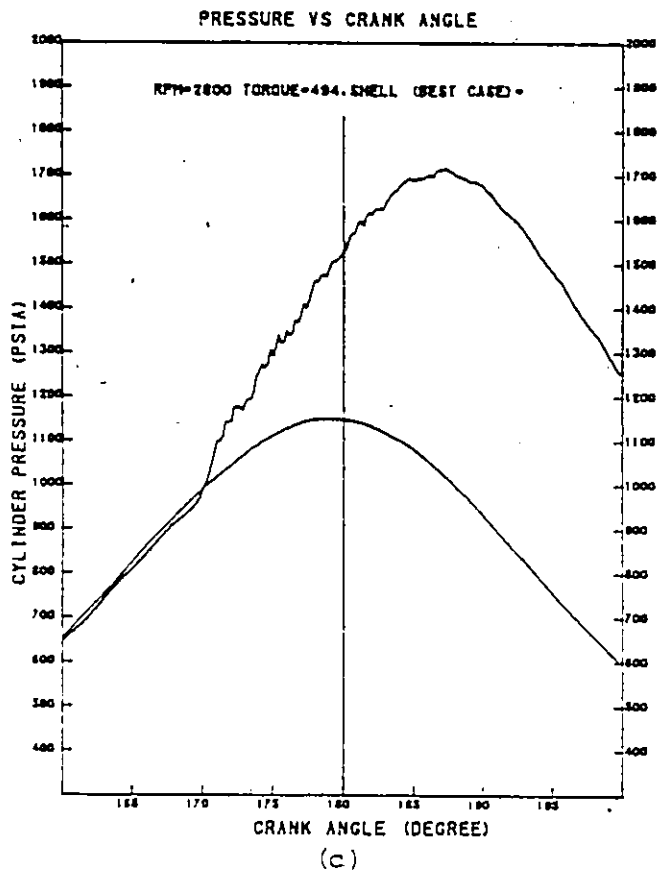
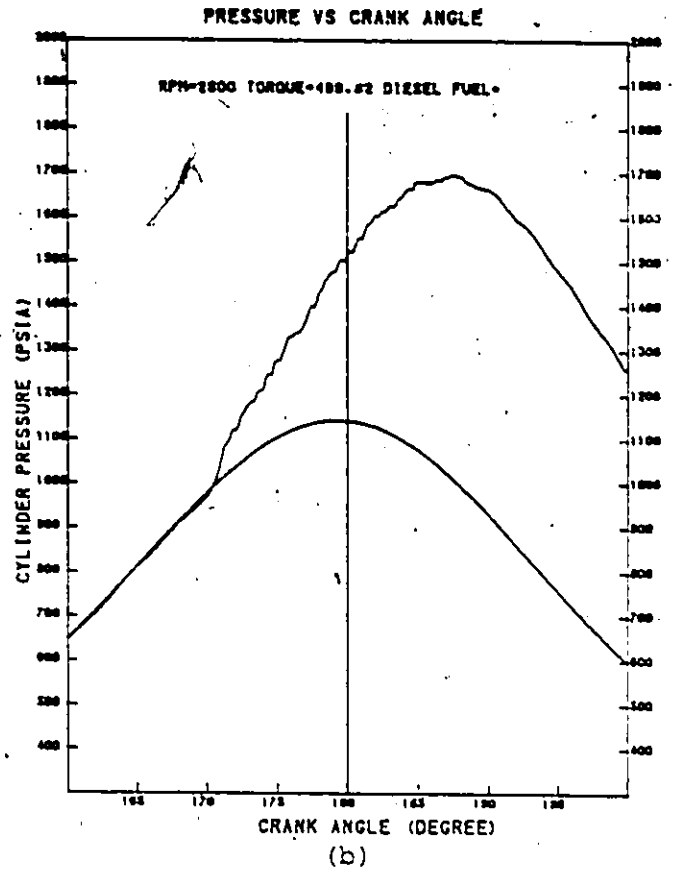
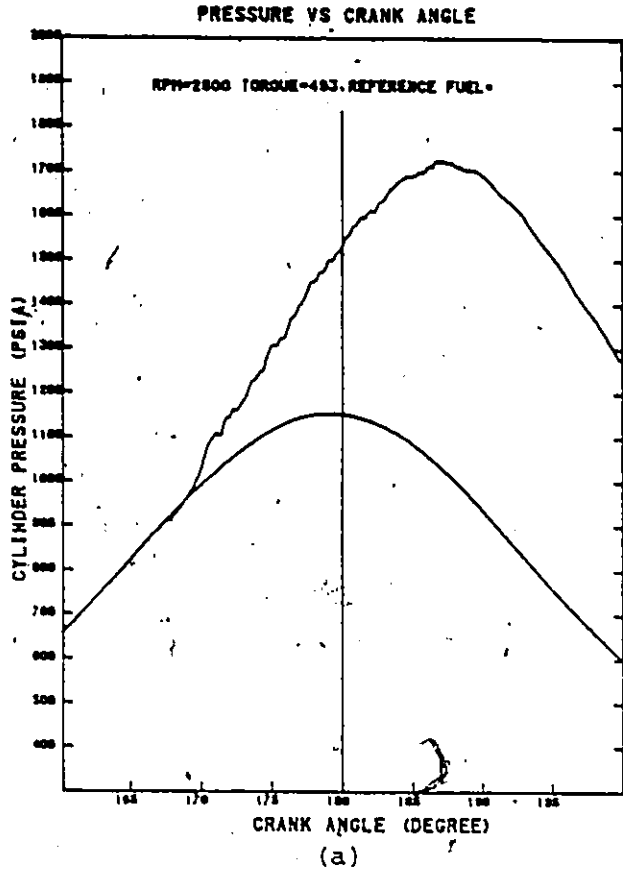
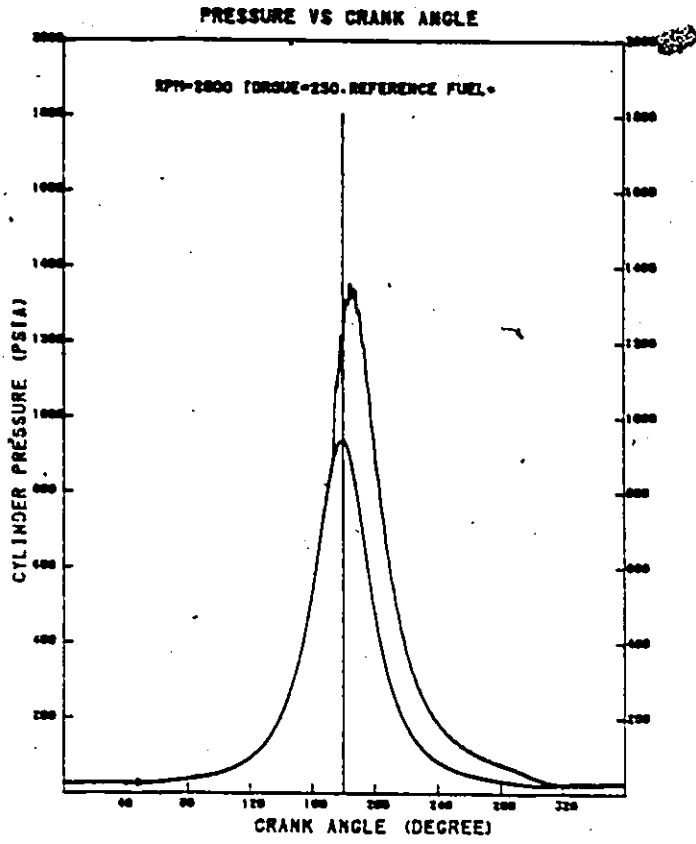
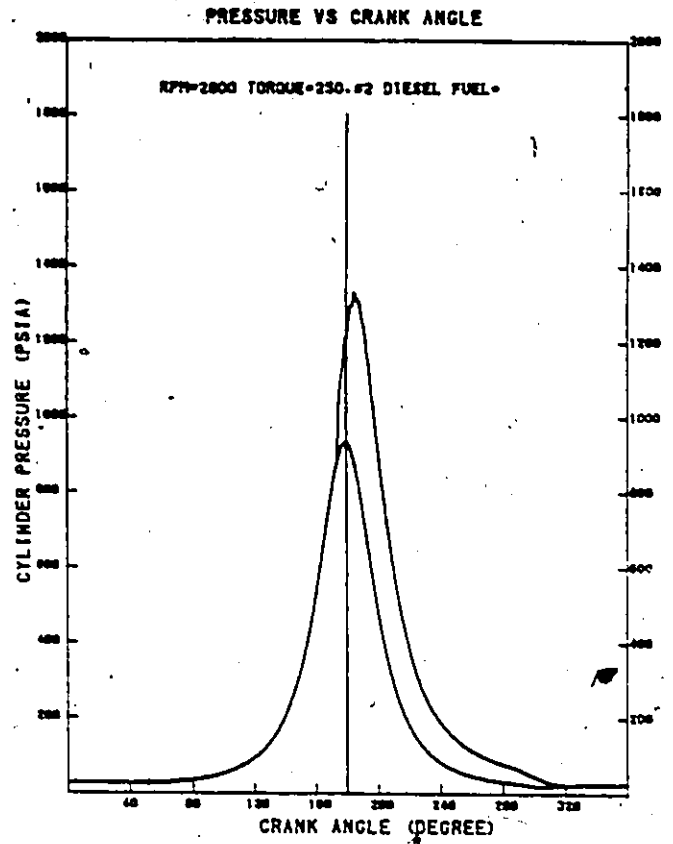


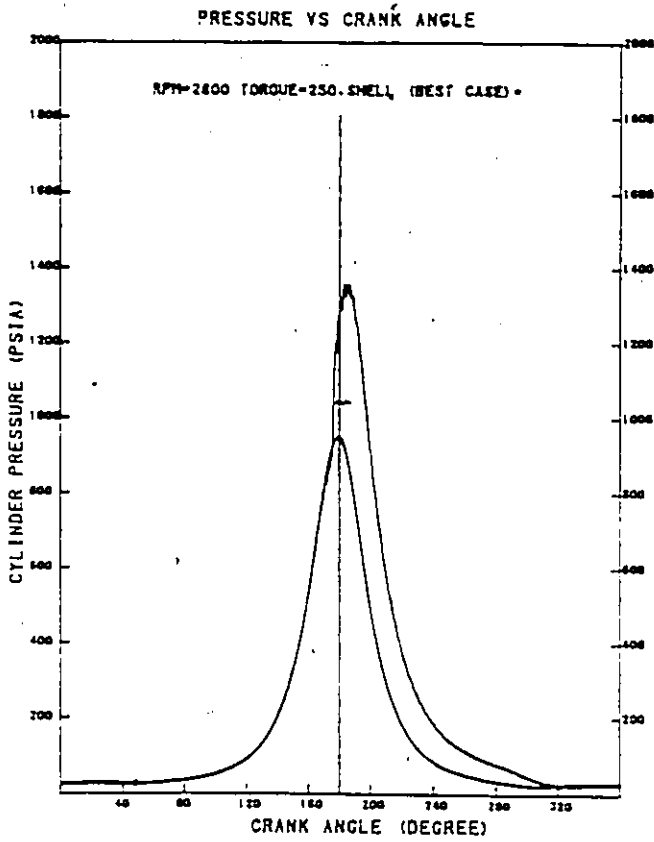
Fig. 5.28: Pressure Trace Comparison over TDC (2800 RPM, Full Load)



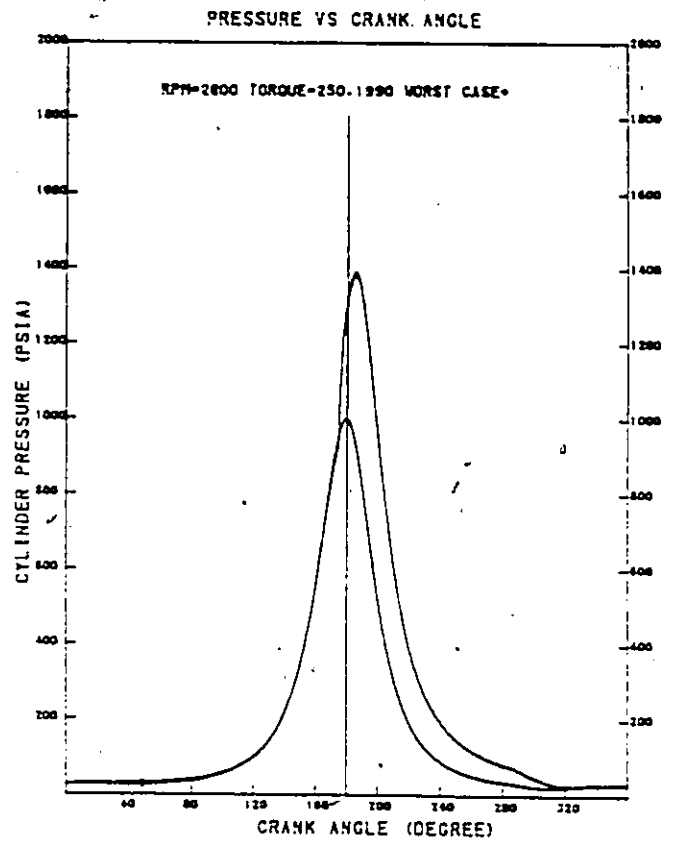
(a)



(b)



(c)



(d)

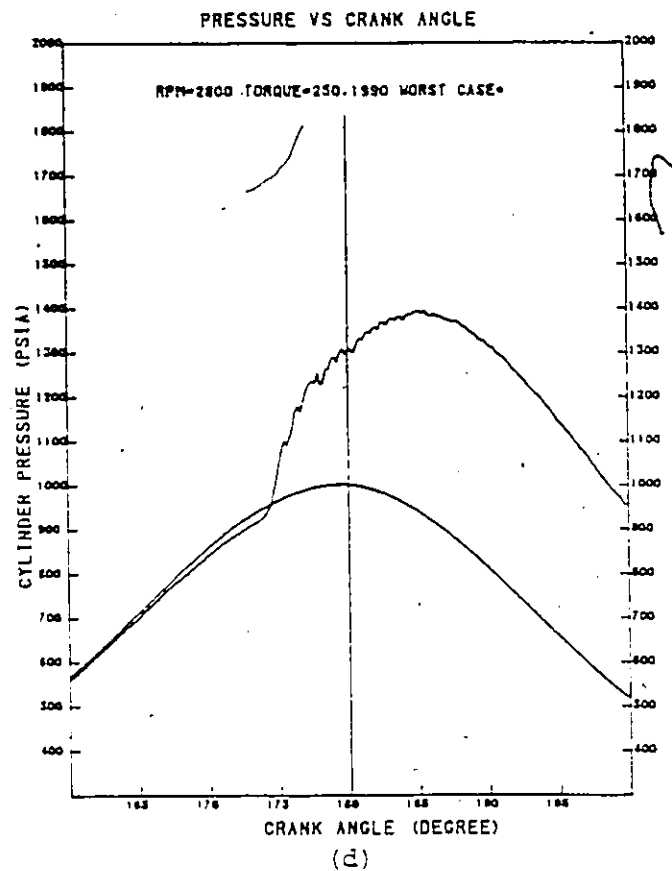
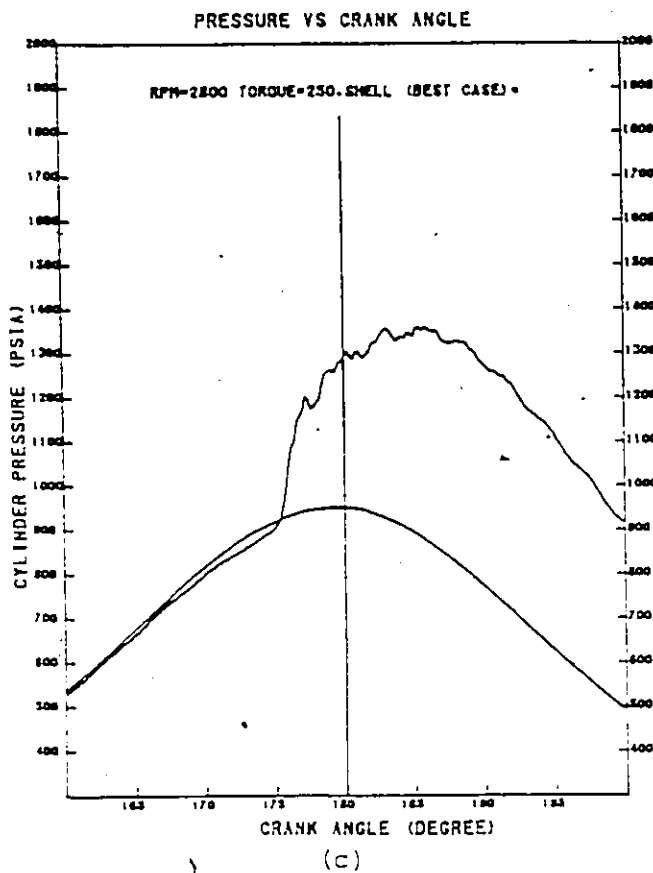
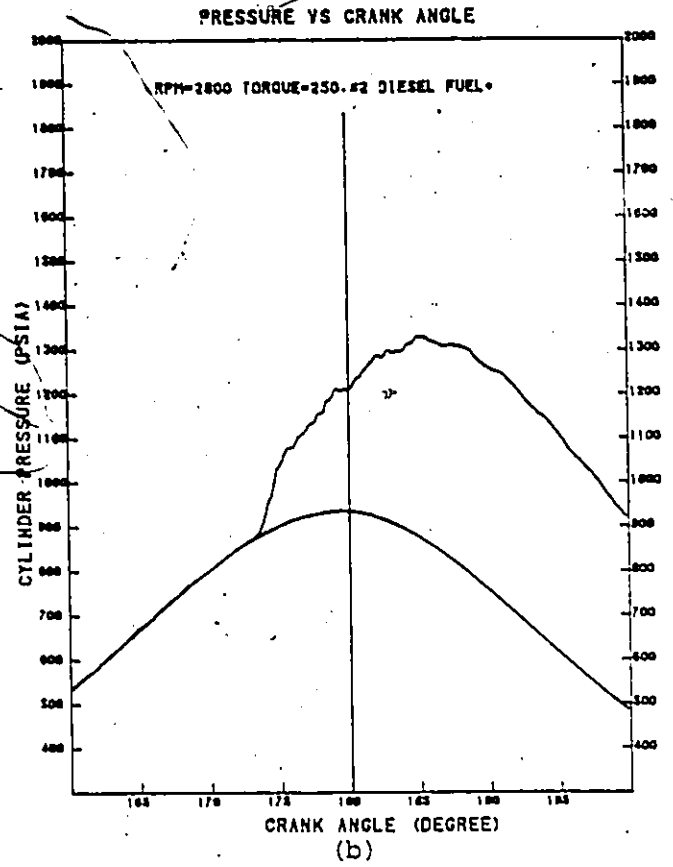
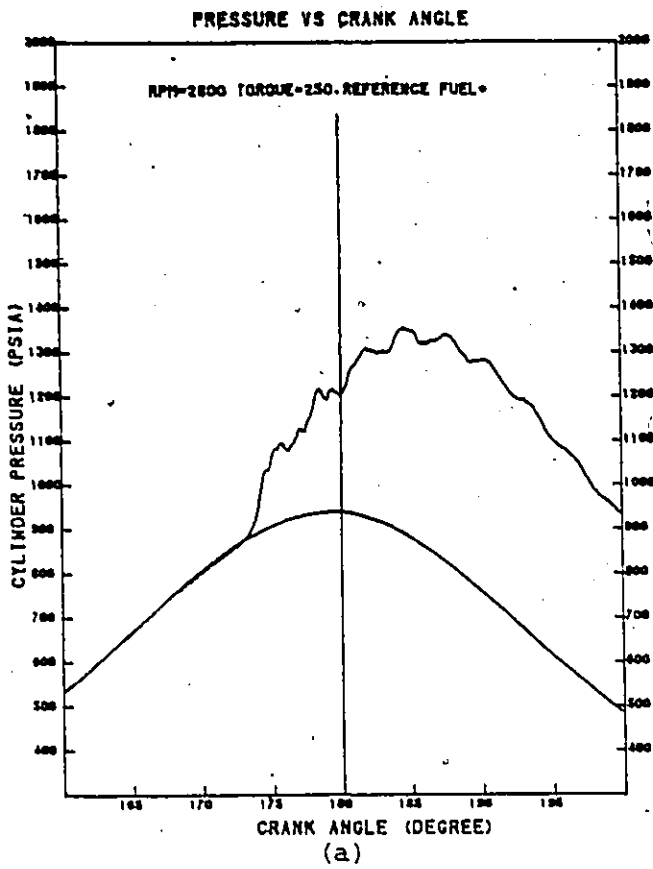


Fig. 5.30: Pressure Trace Comparison over TDC (2800 RPM, Part Load).

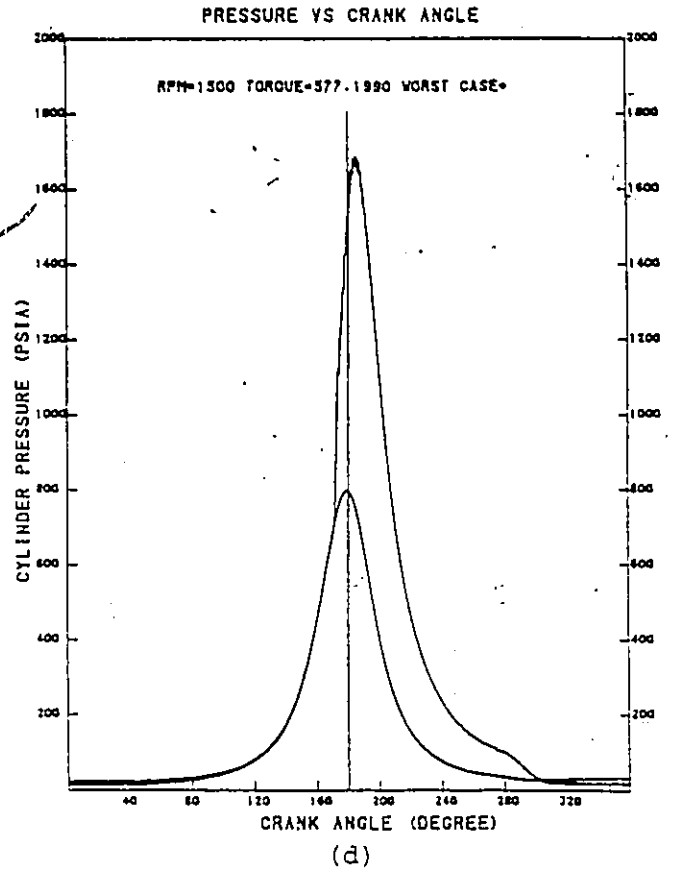
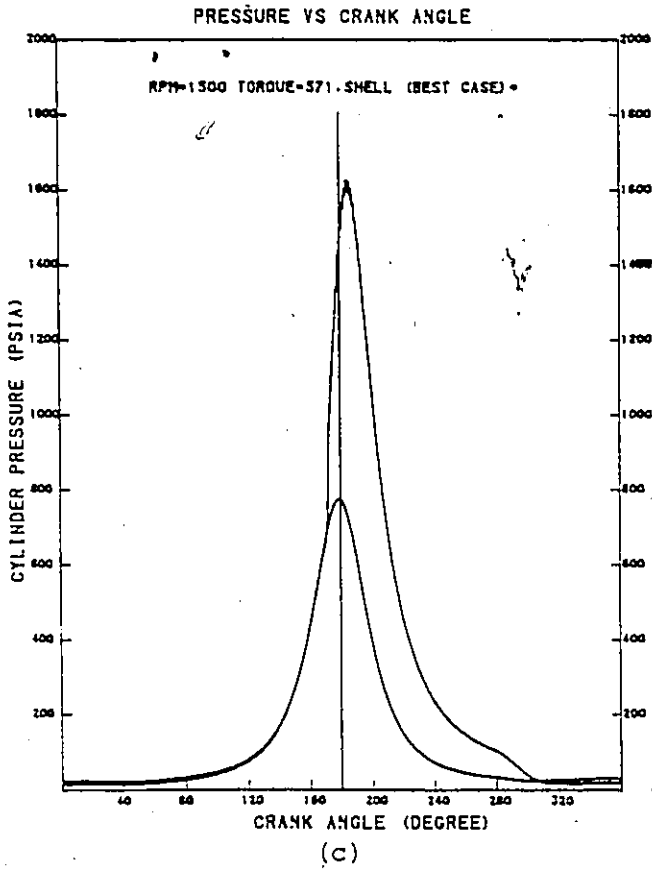
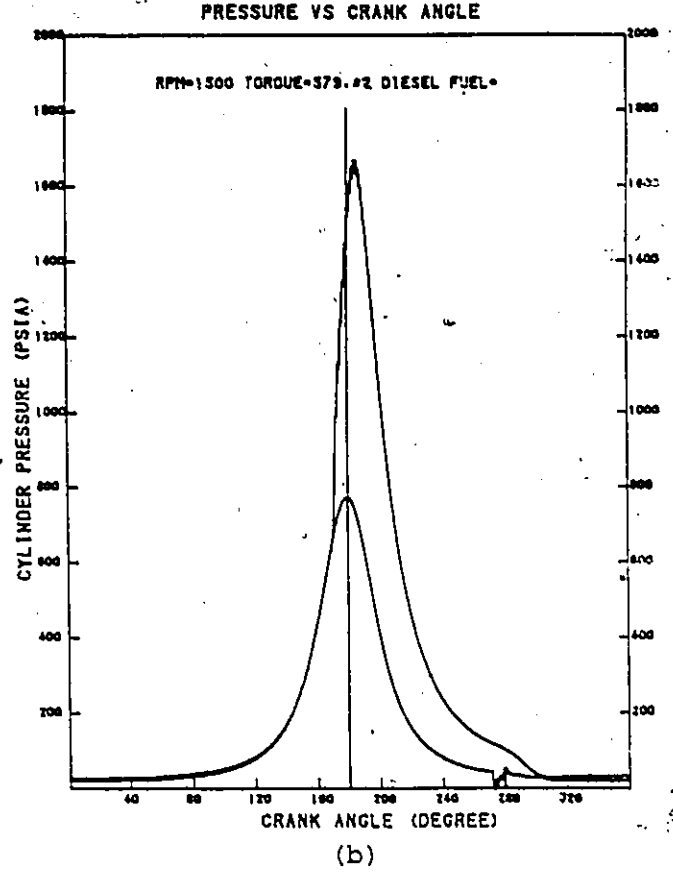
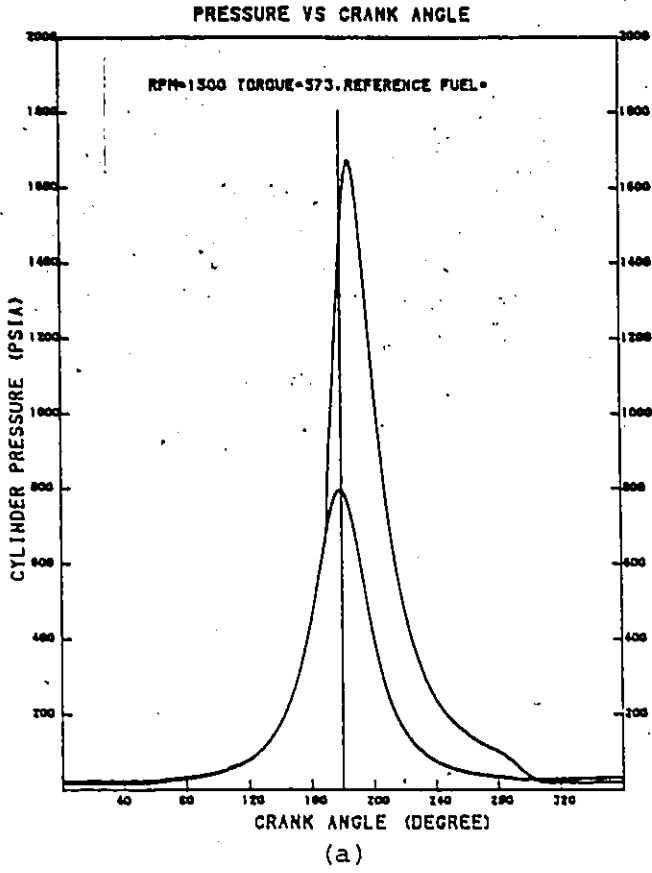


Fig. 5.31: Pressure Trace Comparison (1500 RPM, Full Load).

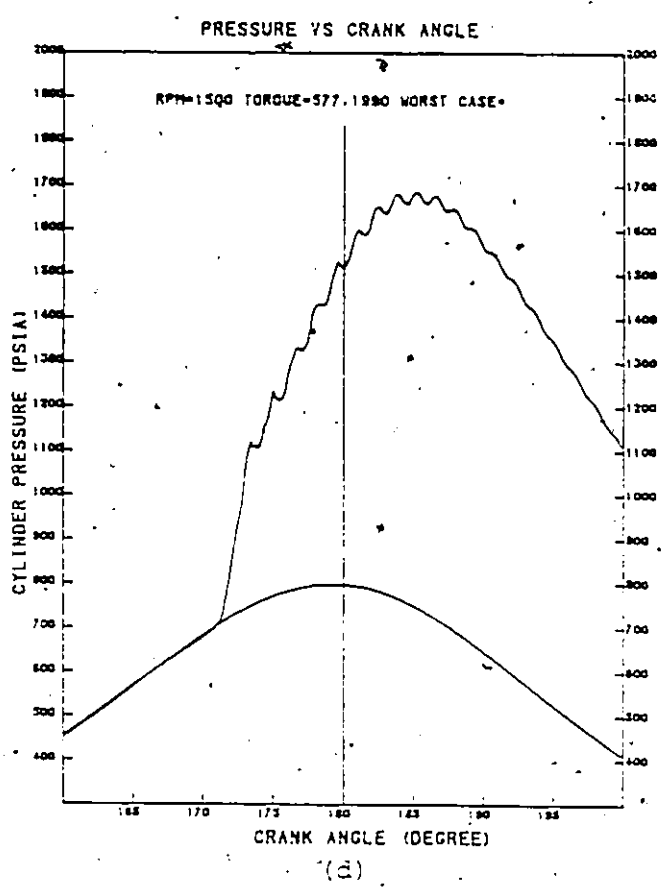
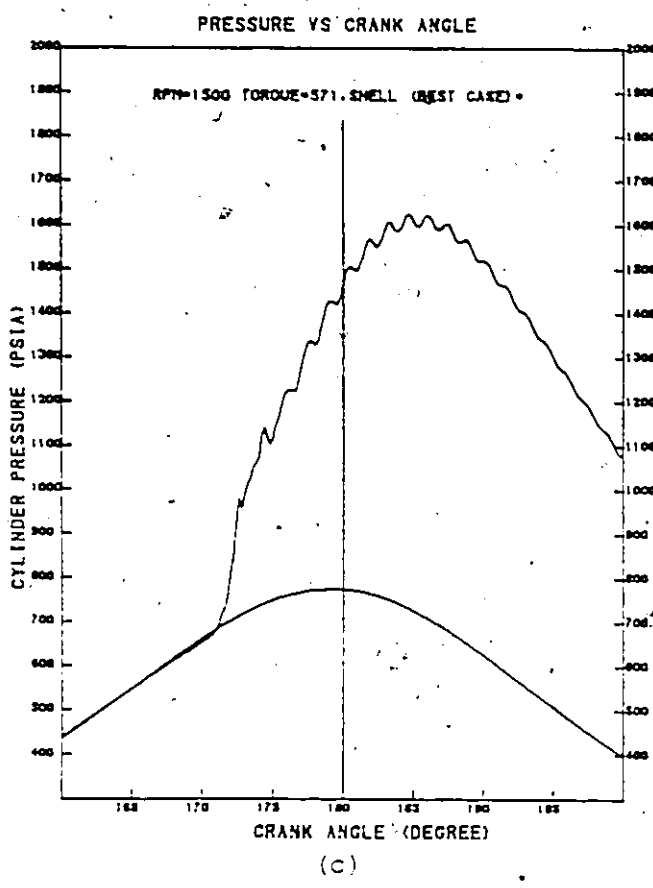
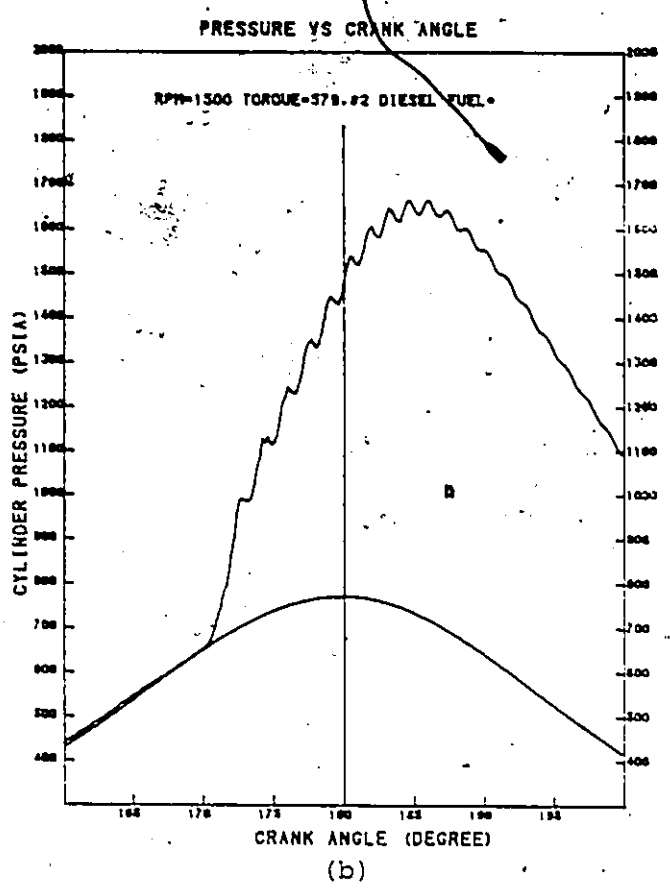
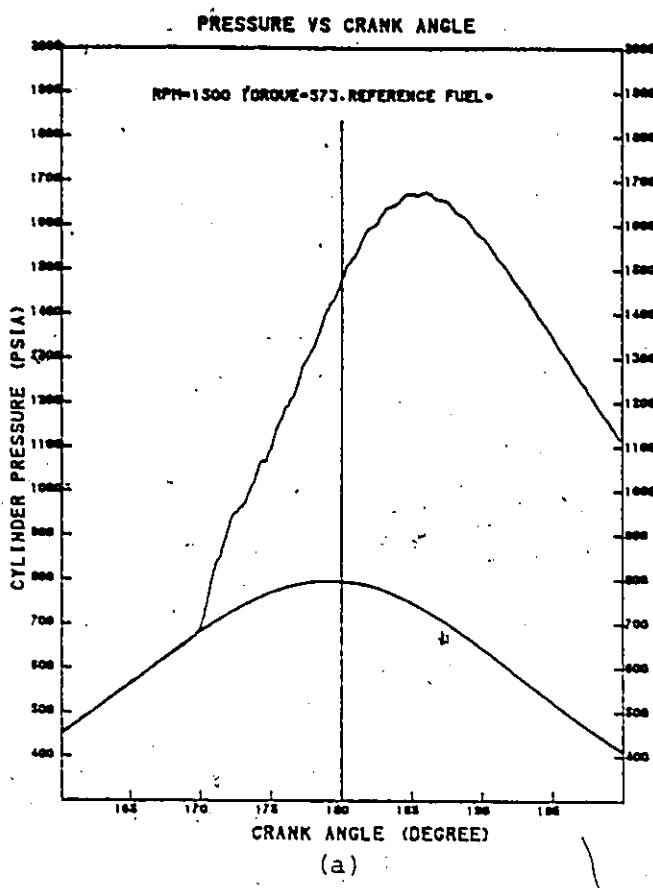
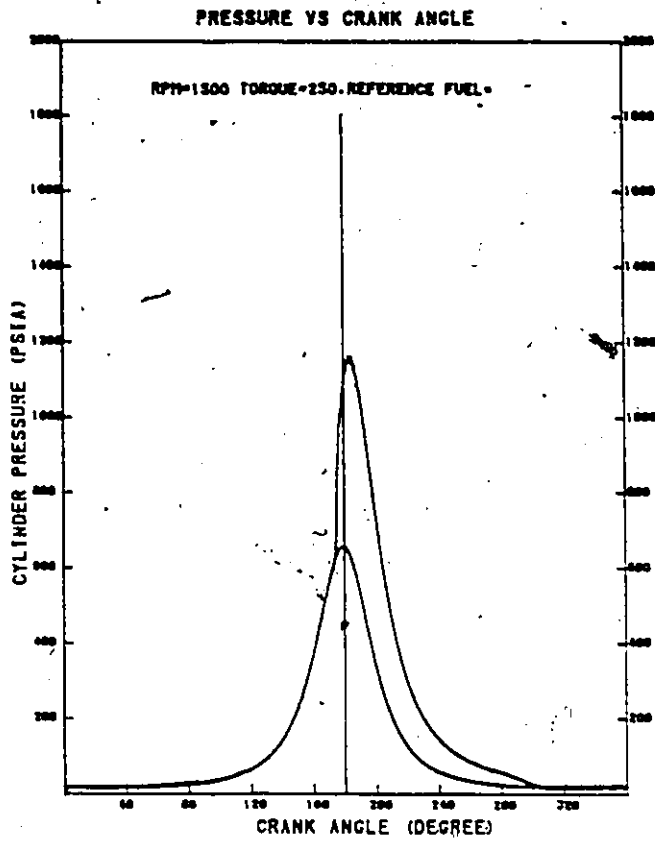
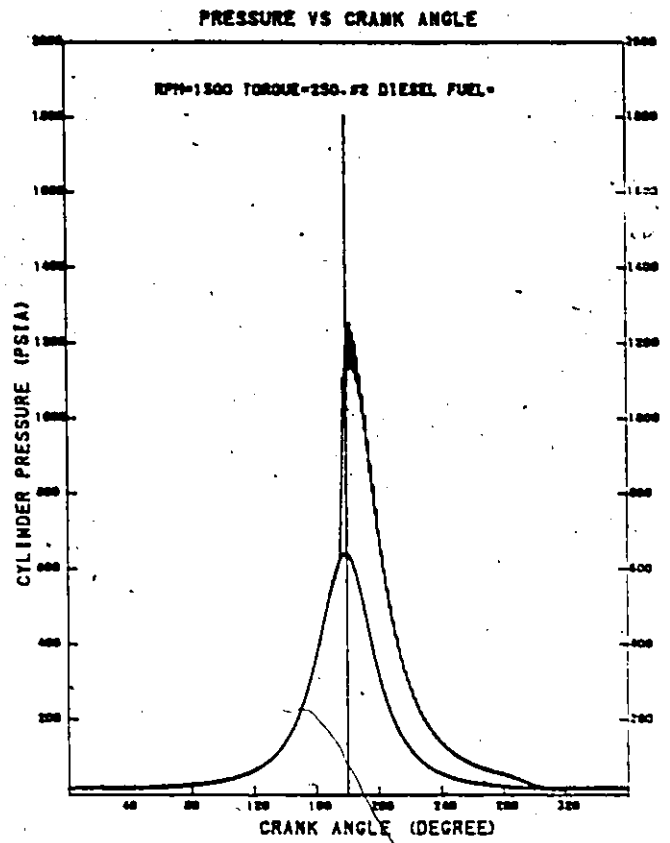


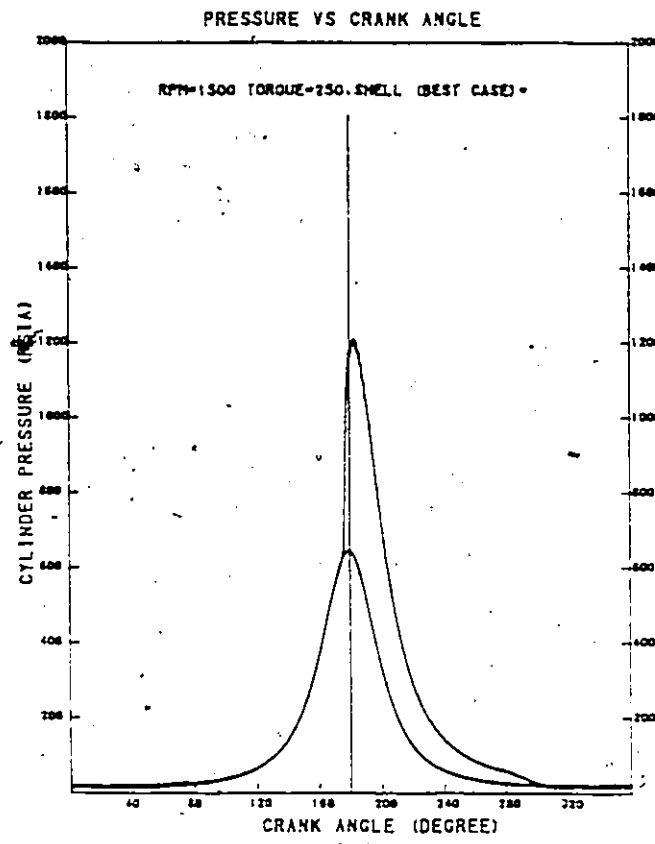
Fig. 5.32: Pressure Trace Comparison over TDC (1500 RPM, Full Load)



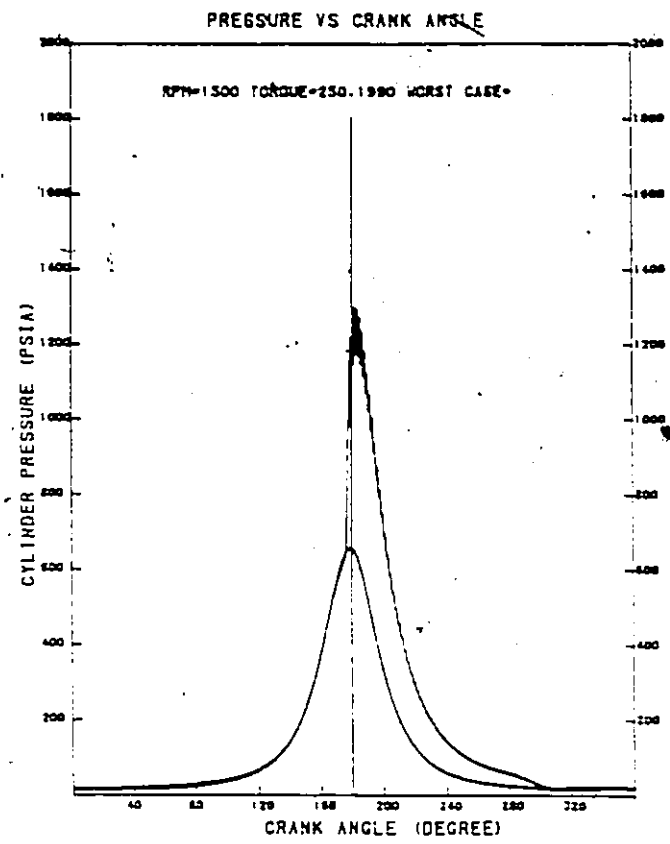
(a)



(b)



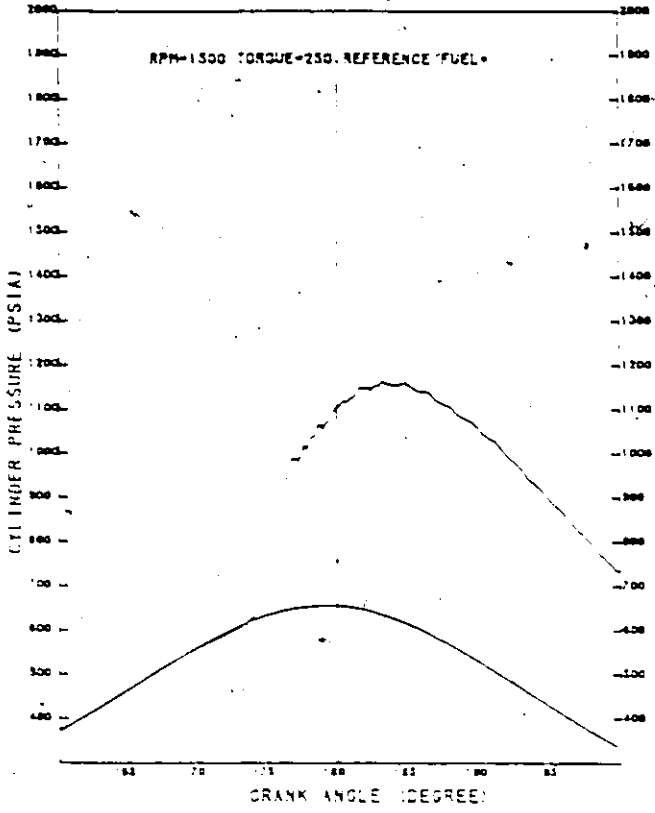
(c)



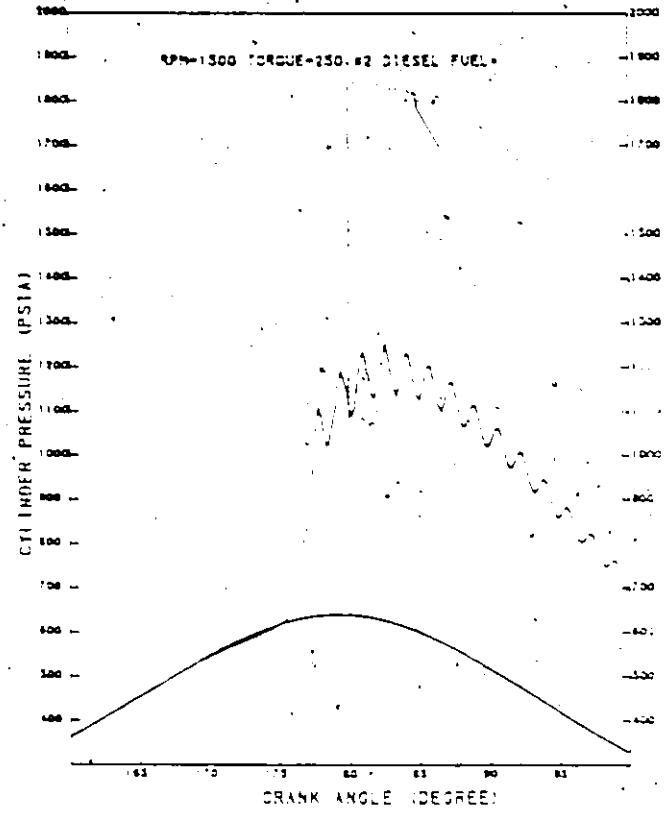
(d)

Fig. 5.33: Pressure Trace Comparison (1500 RPM, Part Load)

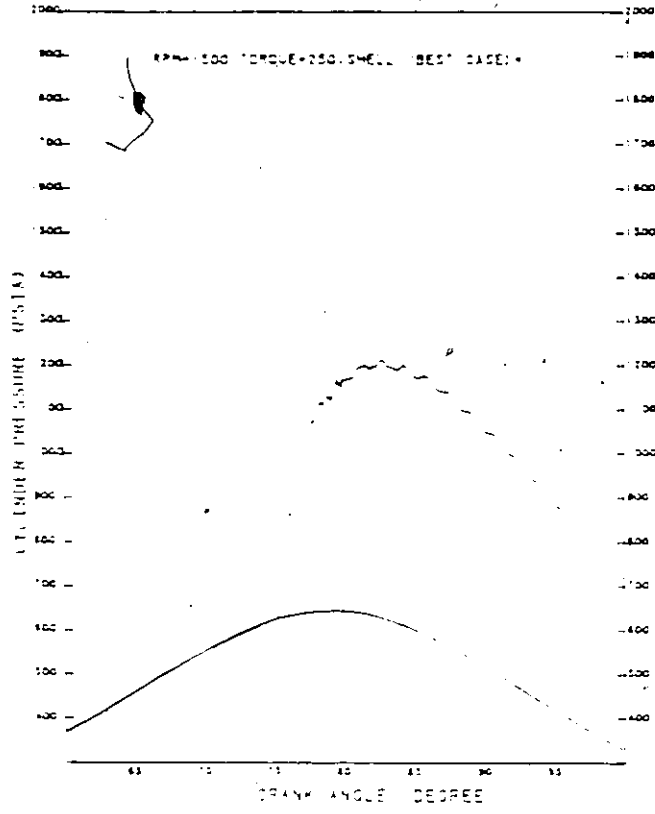
PRESSURE VS CRANK-ANGLE



PRESSURE VS CRANK ANGLE



PRESSURE VS CRANK ANGLE



PRESSURE VS CRANK ANGLE

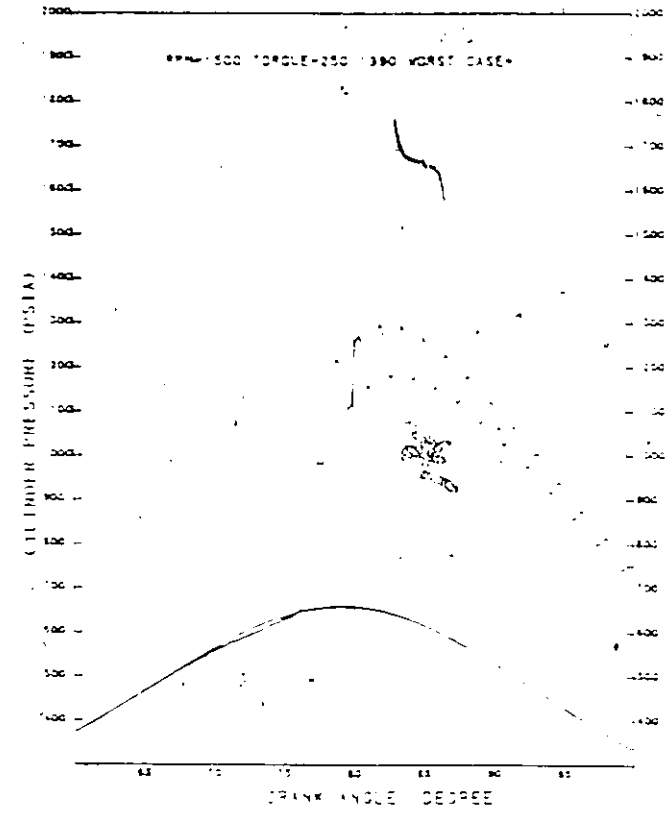


FIG. 1. CYLINDER PRESSURE (PSIA) vs. CRANK ANGLE (DEGREE) FOR 1500 RPM. DUMP LINE

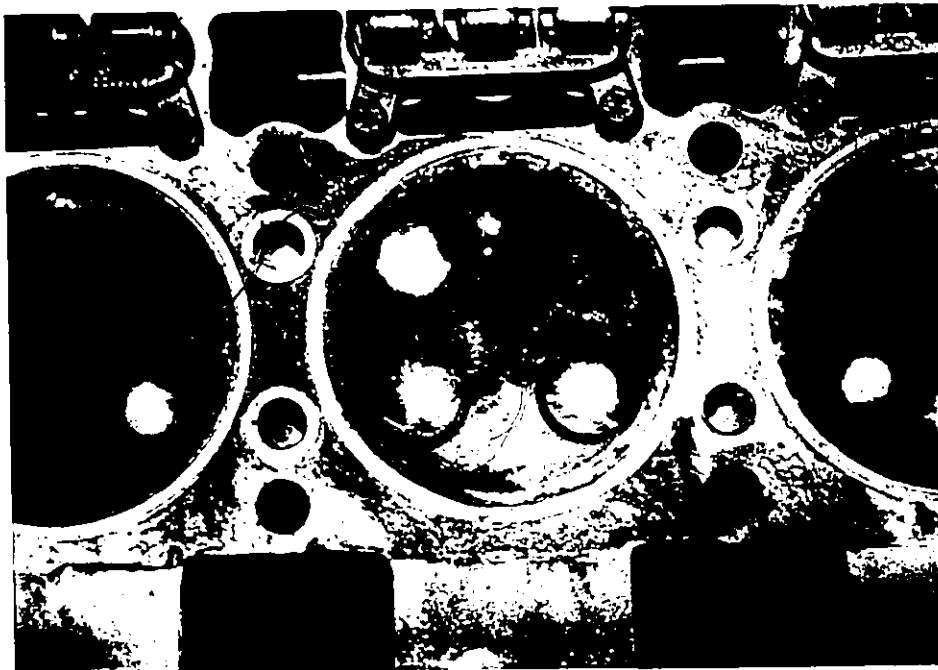
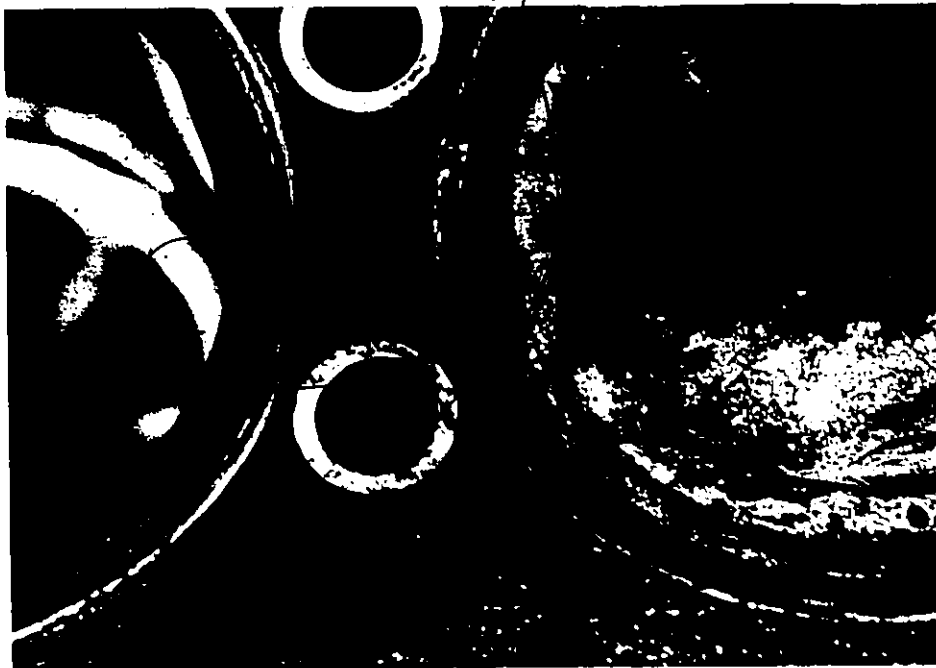


Fig. 5.35: Cracked Head Gasket.
Cylinder Number Two, Right Bank

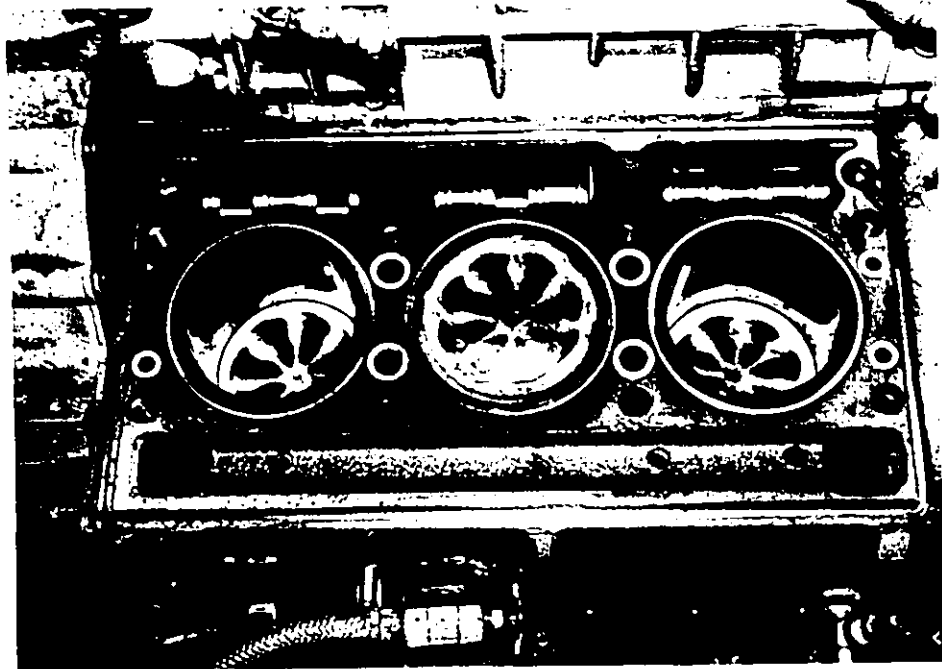
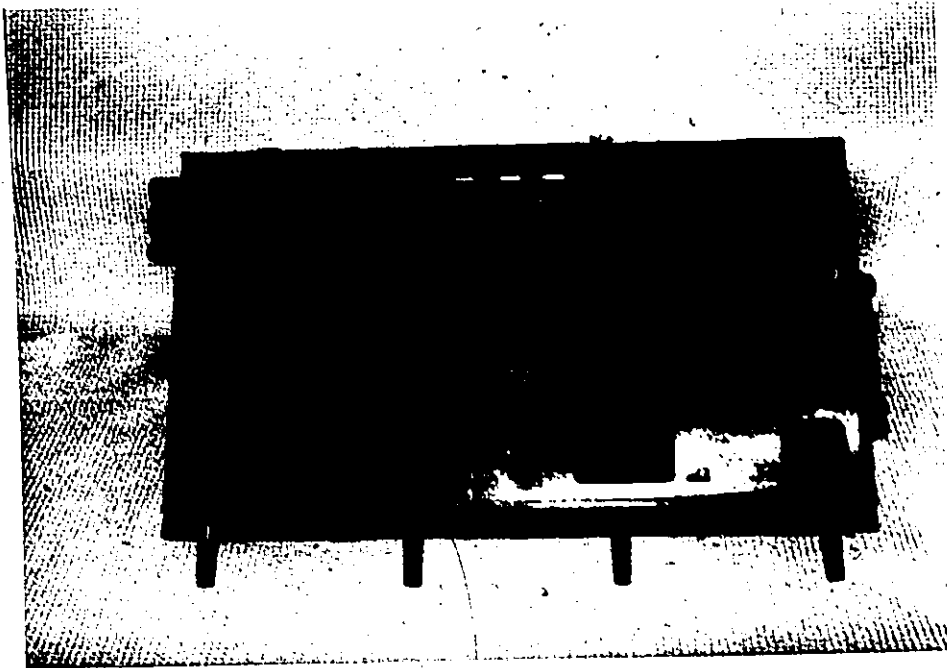


Fig. 5.36: View of the Head and Block,
Failed Right Cylinder Bank

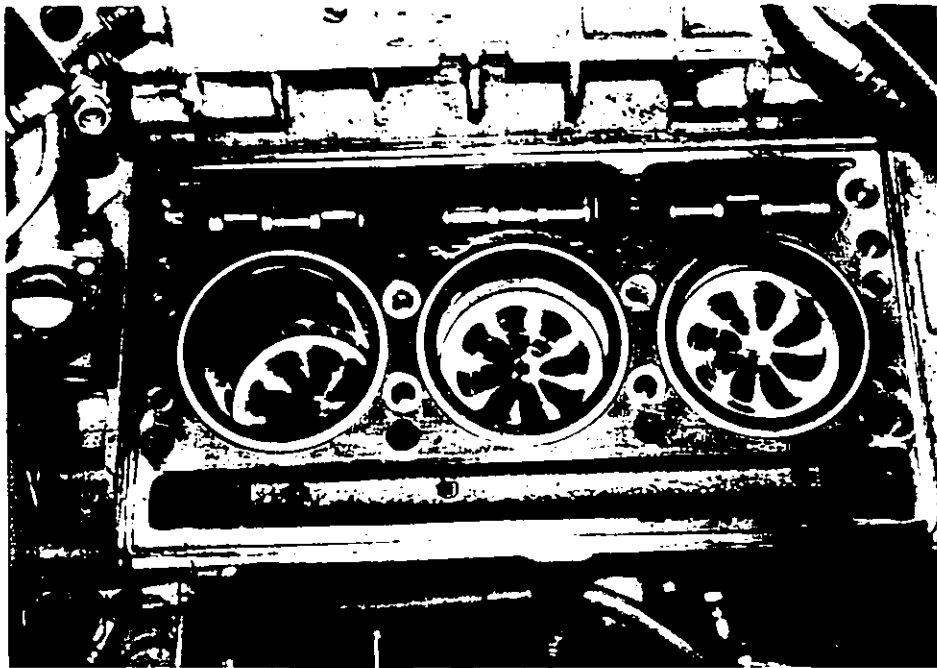
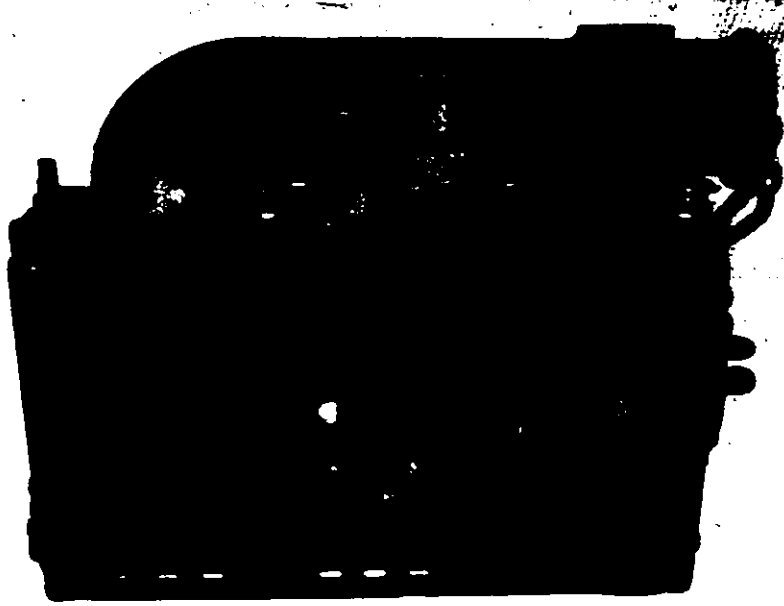


Fig. 5.37: View of the Head and Block,
Left Cylinder Bank (Unfailed)

6V53T TWO STROKE ENGINE

MAX PRESSURE RATE (0.2 DEG.) VS COMB. DEV. PER.
TORQUE = MAX

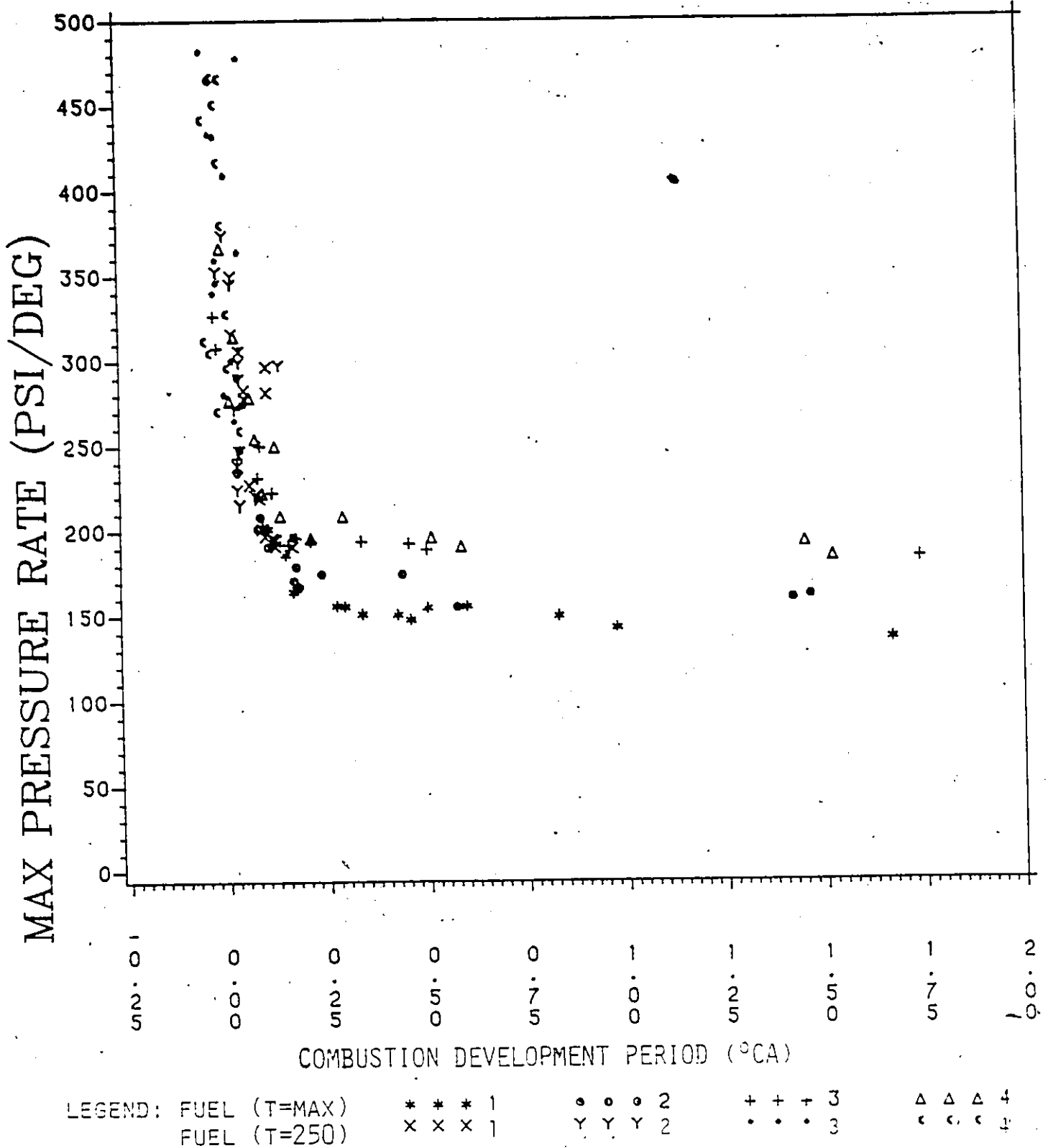


Fig. 5.33: Instantaneous Pressure Rate/Combustion Development Period Relationship.

CHAPTER 6

ENGINE PERFORMANCE MAPS

Engine performance and combustion parameter mapping is a new concept being used here for engine-fuel studies. The maps provide a perspective and an insight into engine-fuel behaviour not attainable from classical brake characteristic (maximum torque) testing. The maps provide, in a single plot, the behaviour pattern of any parameter over the complete speed/load operating range of the engine. Thus, engine-fuel trends become highly visible and extremum conditions (optimum or critical) can be located. One incidental advantage of mapping is the high visibility of a bad test point which appears as a nested ring of isoclines (i.e. location of a sensor malfunction, etc.).

For mapping purposes, an RPM-brake torque grid is used with approximately 154 test points plus the maximum torque curve. At each test point, approximately 64,000 data samples are taken (complete data set) or, for the maps, approximately 10,000,000 data samples per fuel tested. This data is reduced by the lab computer (HP 1000) and generates a map data matrix for each parameter (brake, indicated or combustion) of interest. This data matrix is then forwarded to the university mainframe.

The general mapping program* resident on the mainframe, expands the data matrix supplied to a 101 by 101 matrix, through interpolation, to increase map precision. From this 101x101 matrix, specified isocline values are searched and drawn and minimum/maximum values are located and printed.

However, if the surface being mapped is of low curvature, i.e. a plateau or 'flat' surface, the precision of the program creates a problem in that the plotted isoclines will follow very slight fluctuations in the data (eg. fluctuations within the experimental measurement error band, $\pm 1\%$ on BHP, etc.). This appears as distortions of the isocline curve. Thus, this fact must be considered in reading 'flat' maps, eg. BSFC, ISFC and thermal efficiency. To remedy this, the program should be modified to account for the level of data accuracy and smooth the isoclines accordingly.

On the other hand, where isoclines are drawn on steep gradient surfaces (eg. IHP, maximum pressure, etc.), this difficulty is no longer experienced. All parameters are mapped against the grid ordinates of brake torque (or BMEP) and engine speed (RPM).

* See reference 36

6.1 BRAKE PERFORMANCE MAPS

The only engine map commonly seen in engine research is that of BSFC, Fig. 6.1 plots these maps for the four fuels tested. From the maps, engine trends is similar on all four fuels: a very flat performance, especially about the optimum region, which is a very desirable engine characteristic. Further, all fuels show optimum points around 1800 RPM, 450 ft.lbs. torque. Fuels 1 and 2 show some variations in the RPM location of the optimum, however, it should be noted that the surface is so flat in this region that minor fluctuations in the data would result in the RPM shift. Numerically, Fuel 4 shows notably higher fuel consumption (pounds of fuel per unit energy output), however this is very much a consequence of fuel density.

This latter point is clarified in Fig. 6.2 which maps the brake thermal efficiencies. Here again, all fuels show very similar trending as well a numerically similar values. Fuels 3 and 4 give optimum efficiencies just slightly lower than Fuel 1 but equal to the No. 2-D (Fuel 2). Indeed, the similarity of thermal efficiency between all fuels is quite striking (larger variations from engine-to-engine for a fixed fuel can be expected). The major difference in the maps is the higher brake torque achieved with Fuel 4.

Finally, the fuel consumption (mass) maps are presented in Fig. 6.3. As can be expected, Fuel 4 shows the higher fuel consumption (mass) with the other three fuels showing nearly identical results. These maps do not provide much diagnostic value but do give directly the pounds of fuel consumed per hour at any engine operating point.

6.2 INDICATED ENGINE MAPS

Indicated parameter maps reflect what is occurring within the combustion space. As such they are judged to provide better insight into engine-fuel combustion behaviour than do brake parameter maps. The indicated parameters mapped and presented in this section are: indicated specific fuel consumption (Fig. 6.4); indicated horsepower (Fig. 6.5) and indicated mean effective pressure (Fig. 6.6).

Unlike BSFC, ISFC is not tempered by engine mechanical losses. Thus, the ISFC map takes on a different character due to a substantial shift in the optimum engine operating point. However, the character of all fuels remains very similar as can be expected. Further, the large, extremely 'flat' plateau region remains with an optimum in the 1500 RPM, 100-250 ft.lb. torque region. As before, the plateau is so flat that moderate shifts in the optimum RPM or torque are not a significant factor and reflect experimental accuracy only.

The IHP maps are very similar for all fuels. This was a very exciting result for the following two reasons:

- (a) The result confirms the accuracy of both the brake and indicated results presented for the complete engine operating range. The IHP isoclines are plotted on a BHP grid thus confirming that the engine mechanical efficiency does not change appreciably from fuel to fuel, which is to be expected.
- (b) The concern expressed earlier with respect to IHP numerical integration (for rough combustion fuels) is hereby dispensed with and the concern is limited to the maximum torque region of Fuel 4 only. An examination of the IHP isoclines show a steeper gradient (i.e. increasing mechanical efficiency) relative to the other fuels as they approach the maximum torque curve.

Mean effective pressure curves are a normalized parameter often used for engine-to-engine comparisons and provide a measure of engine stress levels. BMEP is an ordinate of all maps and IMEP is shown in Figure 6.6. The result is interesting in that, for all fuels, the maximum IMEP is virtually the same (highest for No. 2-D) and of very similar character.

6.3 COMBUSTION PARAMETER MAPS

Five combustion parameter maps are presented: onset of combustion (Fig. 6.7); onset of rapid combustion (Fig. 6.8); maximum cylinder pressure (Fig. 6.9); maximum pressure rates (Fig. 6.10) and maximum instantaneous pressure rates (Fig. 6.11).

As mentioned earlier, mapping of these parameters is new. There was early concern that these particular parameters would simply not be mappable in that a diesel engine is not a sufficiently precise instrument to allow mapping of, say, onset of combustion. However, the statistical studies on these parameters showed very high repeatability (small standard deviations) and indeed, all these parameters are highly mappable.

Considerable amounts of information are contained in these maps and it is only here that fuel to fuel variations and engine-fuel trends show substantial changes. The essential information to assess engine-fuel suitability and engine durability are contained in these maps.

Onset of combustion (Fig. 6.7) and onset of rapid combustion (Fig. 6.8) show similar general trends. Ignition delay increased from Fuel 1 through 4 in order and shows a consistent behavior over the operating range of the engine. The most notable exception is Fuel 4 at the higher speeds and somewhat more pronounced at higher torques. This

behavior of Fuel 4 was noted earlier at the discrete load settings presented (full and part load) and is here seen to be a general behavioral trend.

Thus, a correlation between fuel cetane number and ignition (or combustion) delay would seem to exist at lower operating speeds of the engine but not, due to Fuel 4, at the higher operating speeds.

One interesting outcome of these map sets is that the parameters are highly ordered and mapable. It is also interesting to overlay onset of combustion and onset of rapid combustion. In so doing, the difference between respective curves for the 3GP30 fuel progressively widens with increasing load, whereas Fuels 3 and 4 show virtually no difference until loads approach maximum torque.

The maximum cylinder pressure (Fig. 6.9) varies the least and, as concluded earlier, in itself would not give rise to any substantial concerns over fuel compatibility. Fuel 3 provides somewhat lower peak pressures than the reference fuel (Fuel 1) while Fuel 4 gives somewhat higher peak pressures. However, both Fuel 3 and 4 provide higher maximum pressures for most (Fuel 3), all (Fuel 4) of the engine operating range.

The main maps of interest are the maximum pressure rate (Fig. 6.10, based on a 1°CA span) and the maximum instantaneous pressure rate (Fig. 6.11, based on a 0.2°CA span).

The character of these maps are very similar and show the critical region for all fuels to be in the 1600-1700 RPM range at 150-200 ft.lbs. torque. Thus, the critical area for 'knock' and engine-fuel compatibility studies is uniquely located. However, the important shift (fuel-to-fuel) in these curves is in the numerical rate values. Both Fuels 3 and 4 project pressure rates in excess of 300 PSI/°CA with instantaneous rates in the 500 PSI/°CA range. Further, the isoclines show that the engine will be subject to these very high pressure rates when operated on off-specification fuels for a very substantial portion of the engine operating range.

The second important observation is that, if only maximum torque testing were conducted, these results would not be evident. Thus, engine-fuel compatibility and engine durability studies do require part load investigation, if not complete engine mapping.

One final note should be made. The maximum pressure rates recorded and presented in this report are computer searched, every 0.2 degree crank angle step using a one degree crank angle span while instantaneous rates are likewise searched but use the 0.2 degree span directly (i.e. $\Delta P/\Delta \theta$, $\Delta \theta = 0.2$ degrees). Further, all values used for the map grids are the average result of thirty-two single-shot pressure curves which,

together with the statistical data (standard deviations, see Chapter 5), suggest that a high confidence level can be placed on the numerical data presented.

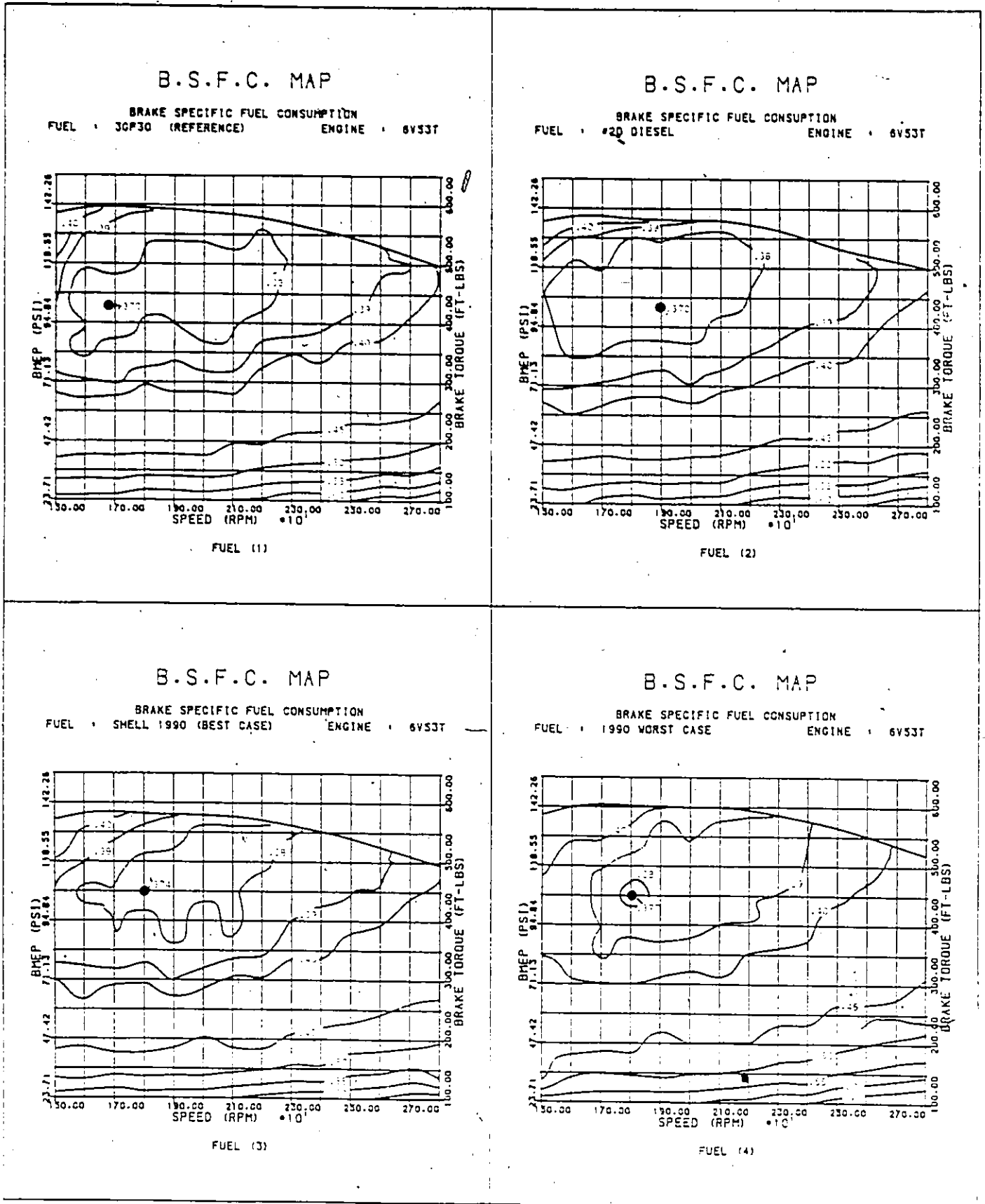


Fig. 6.1: B.S.F.C. Map Comparison.

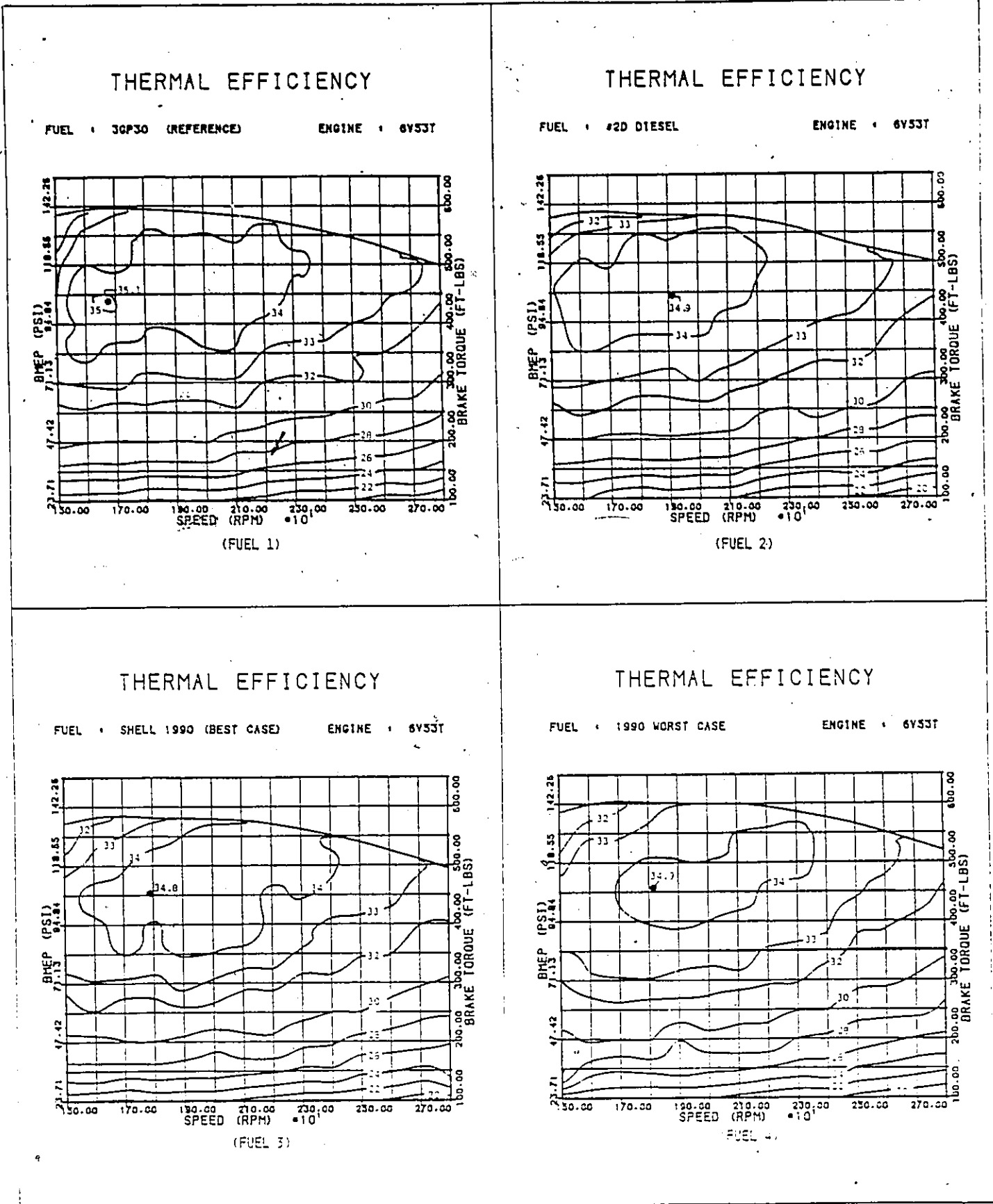


Fig. 6.2; Brake Thermal Efficiency Map Comparison

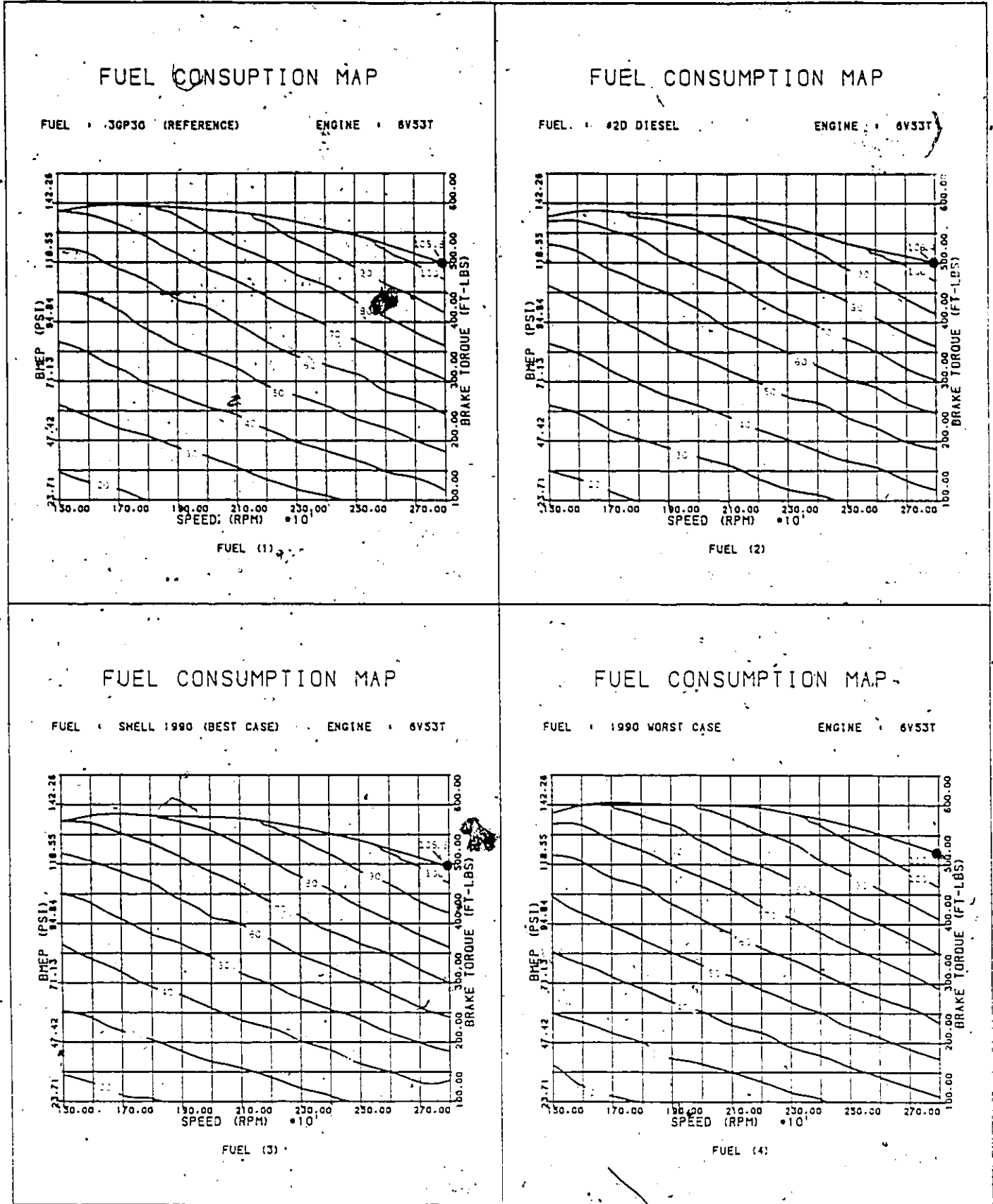


Fig. 6.3: Fuel Consumption Map Comparison.

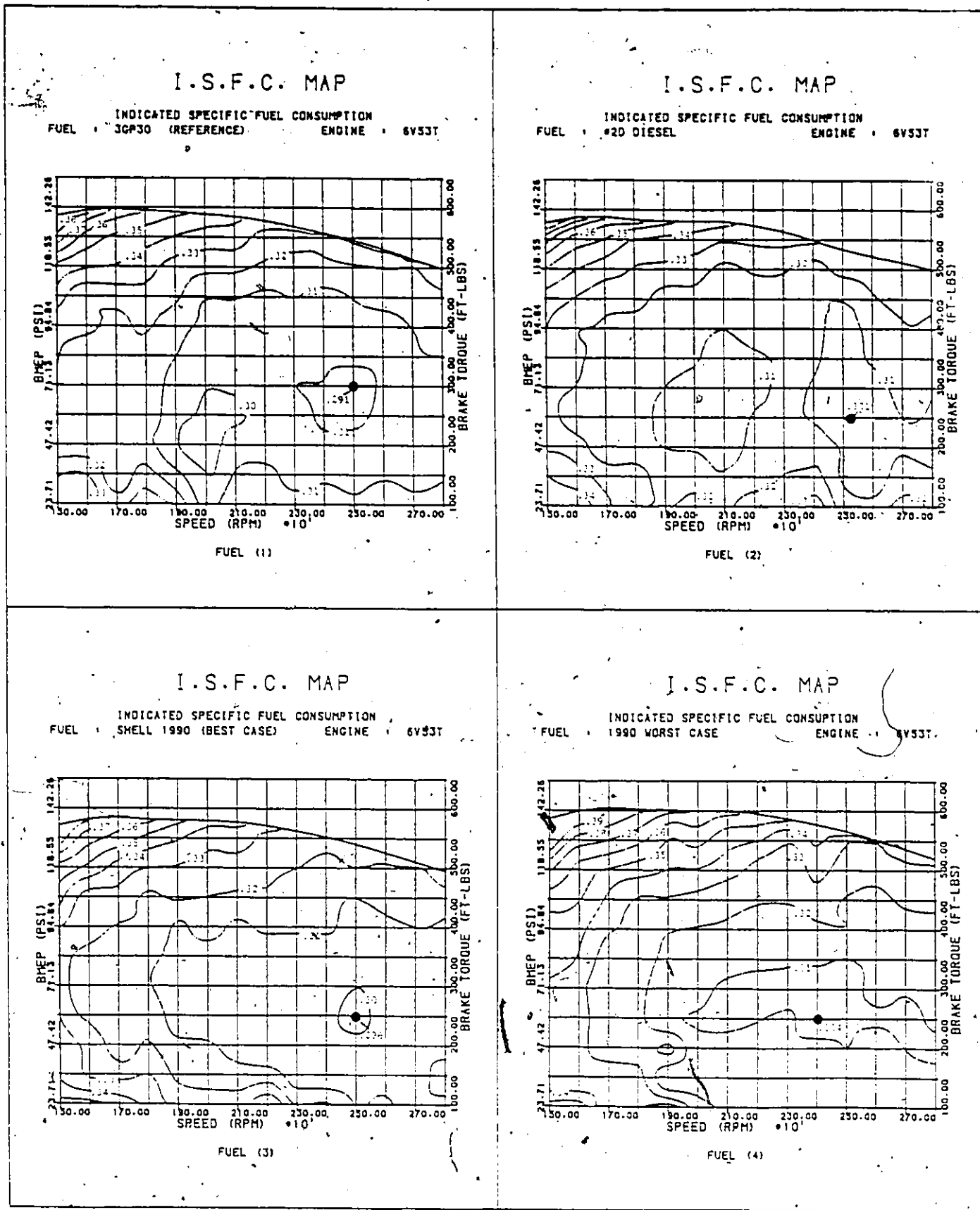
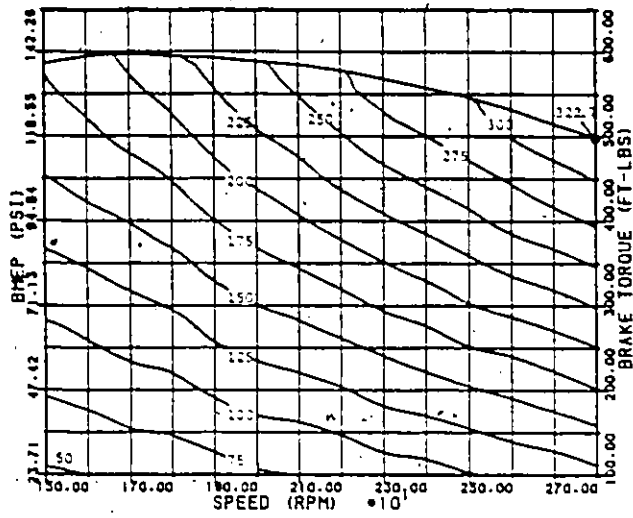


Fig. 6.4: Indicated Specific Fuel Consumption Map Comparison

I.H.P. MAP

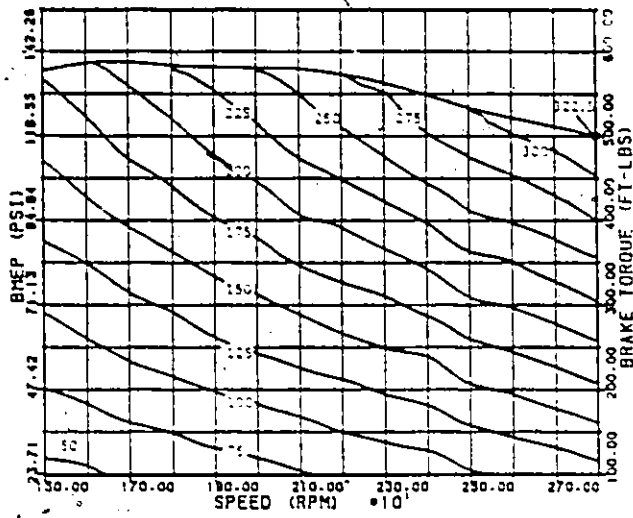
INDICATED HORSEPOWER
FUEL : JCP30 (REFERENCE) ENGINE : 6V53T



(FUEL 1)

I.H.P. MAP

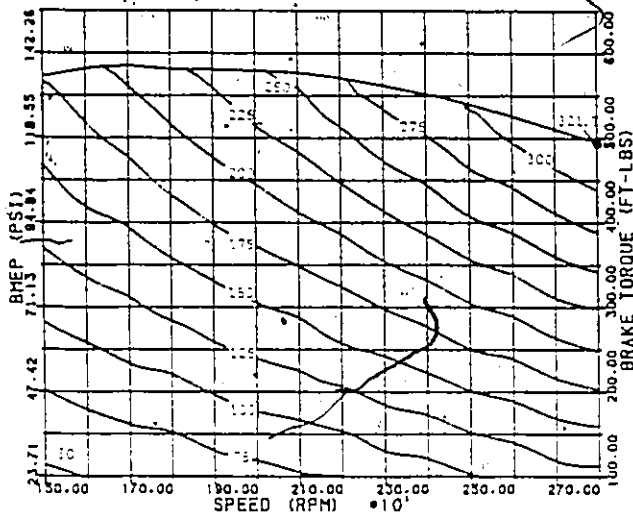
INDICATED HORSEPOWER
FUEL : #20 DIESEL ENGINE : 6V53T



(FUEL 2)

I.H.P. MAP

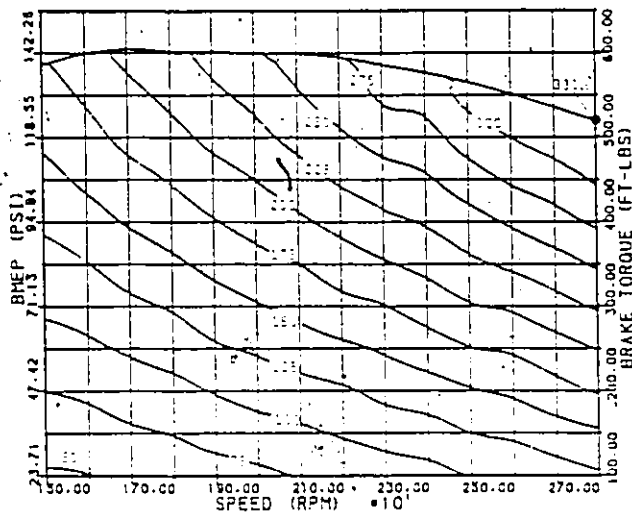
INDICATED HORSEPOWER
FUEL : SHELL 1990 (BEST CASE) ENGINE : 6V53T



(FUEL 3)

I.H.P. MAP

INDICATED HORSEPOWER
FUEL : 1990 WORST CASE ENGINE : 6V53T

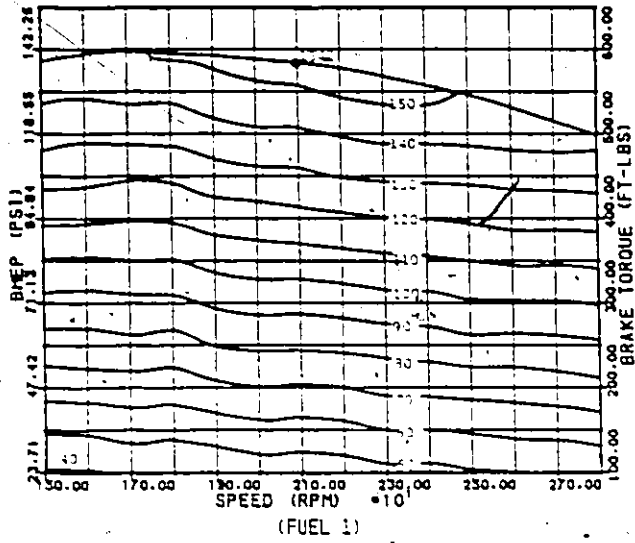


FUEL -

Fig. 6.5: Indicated Horsepower Map Comparison

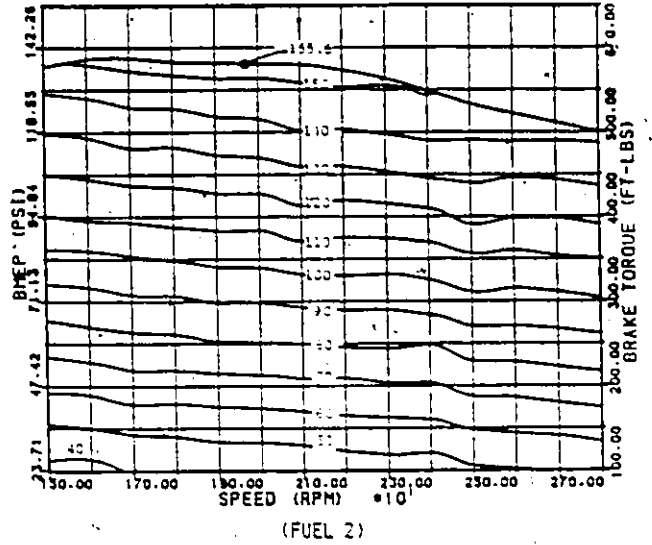
I.M.E.P. MAP

INDICATED MEAN EFFECTIVE PRESSURE
FUEL : 3GP30 (REFERENCE) ENGINE : 6V53T



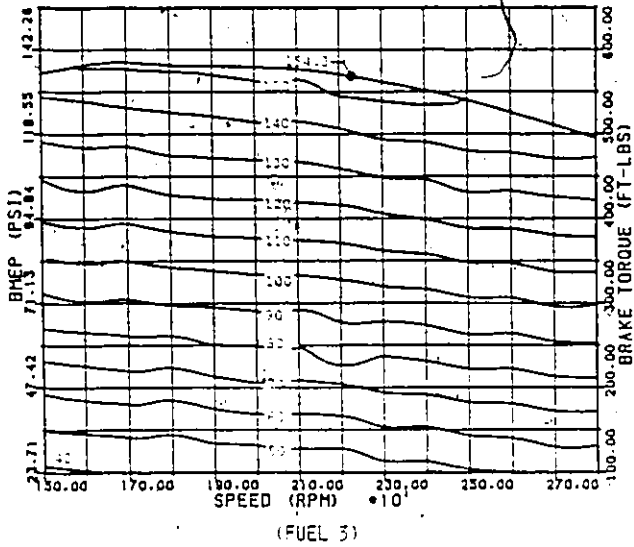
I.M.E.P. MAP

INDICATED MEAN EFFECTIVE PRESSURE
FUEL : #20 DIESEL ENGINE : 6V53T



I.M.E.P. MAP

INDICATED MEAN EFFECTIVE PRESSURE
FUEL : SHELL 1990 (BEST CASE) ENGINE : 6V53T



I.M.E.P. MAP

INDICATED MEAN EFFECTIVE PRESSURE
FUEL : 1990 WORST CASE ENGINE : 6V53T

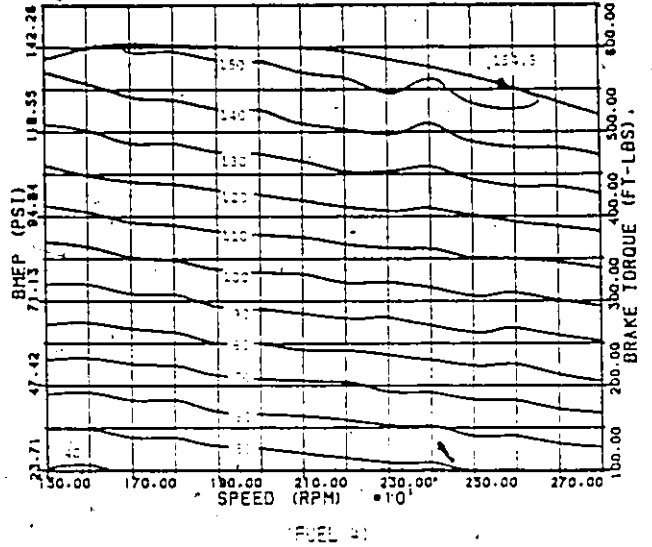


Fig. 6.6: Indicated Mean Effective Pressure Map Comparison

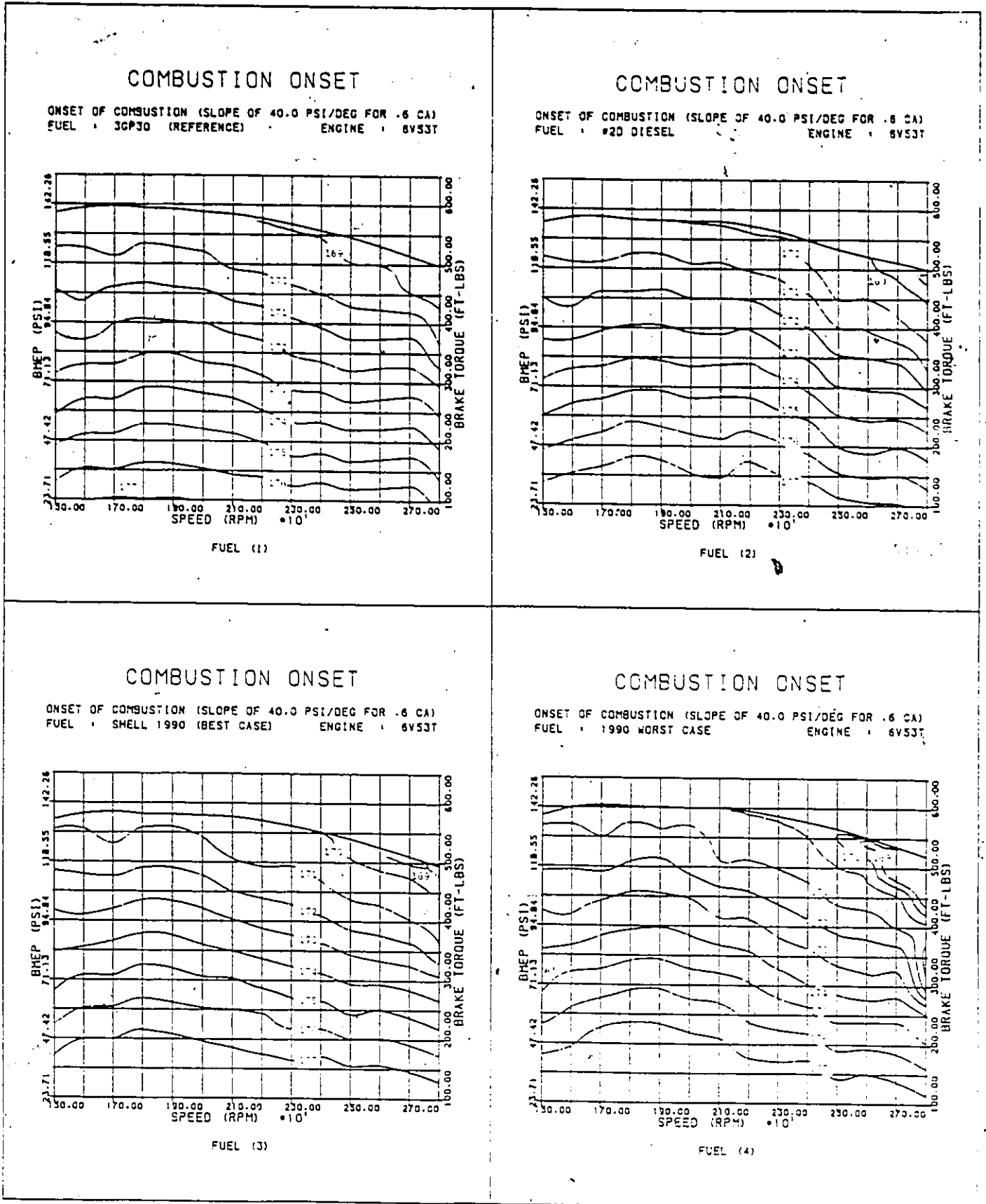


Fig. 6.7: Onset of Combustion Map Comparison

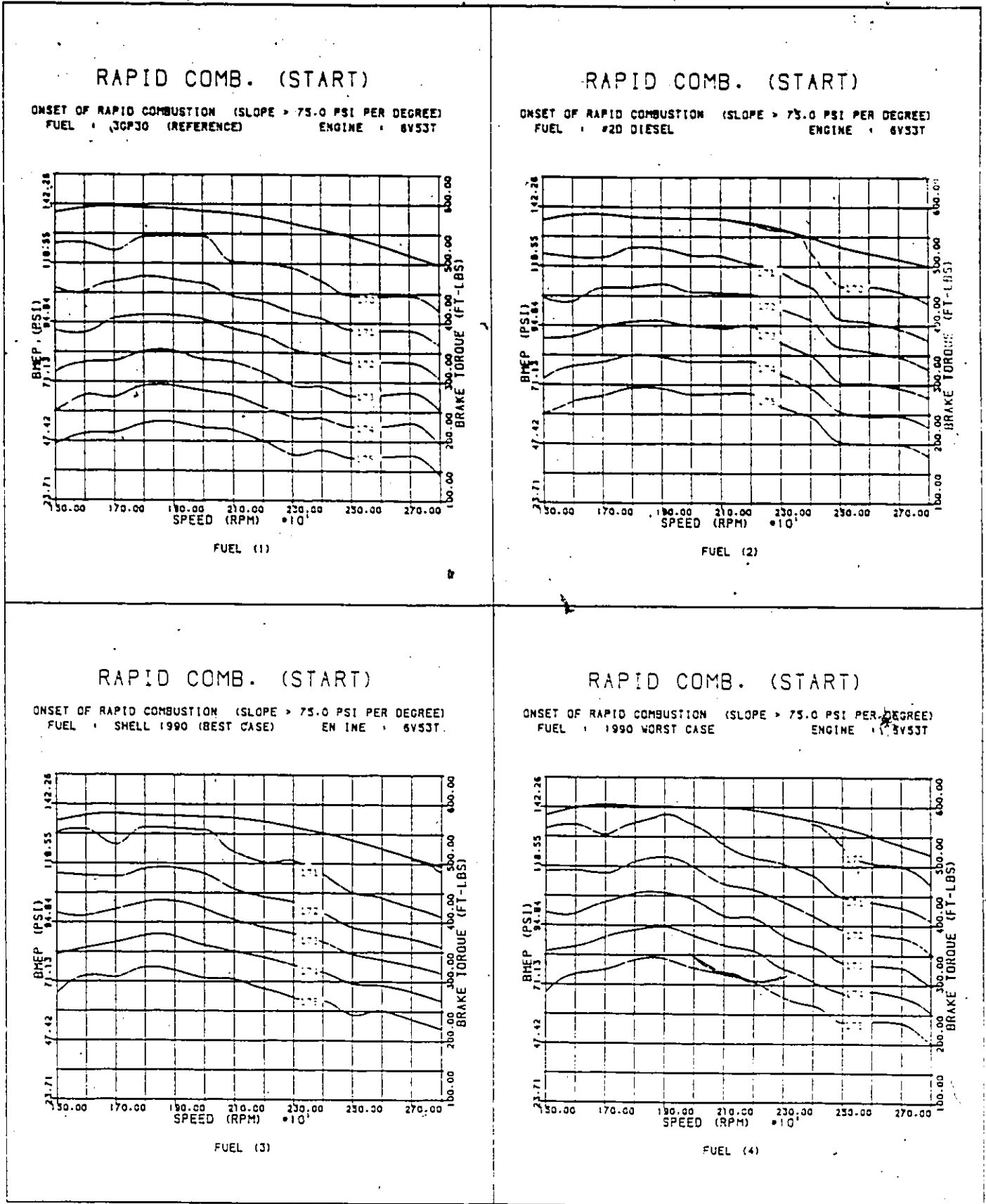
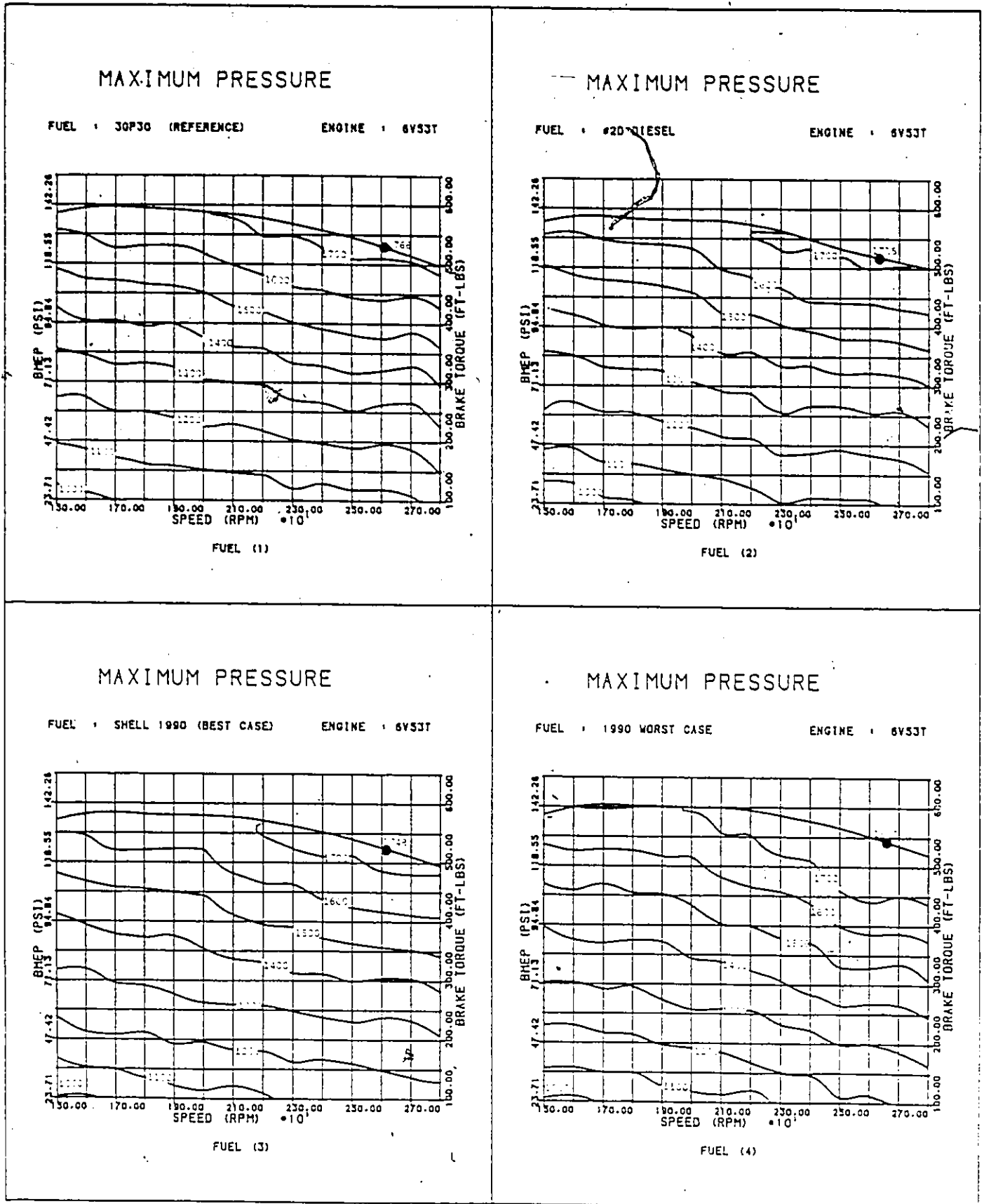


Fig. 6.8: Onset of Rapid Combustion Map Comparison



Fig/ 6.9: Maximum Cylinder Pressure Map Comparison

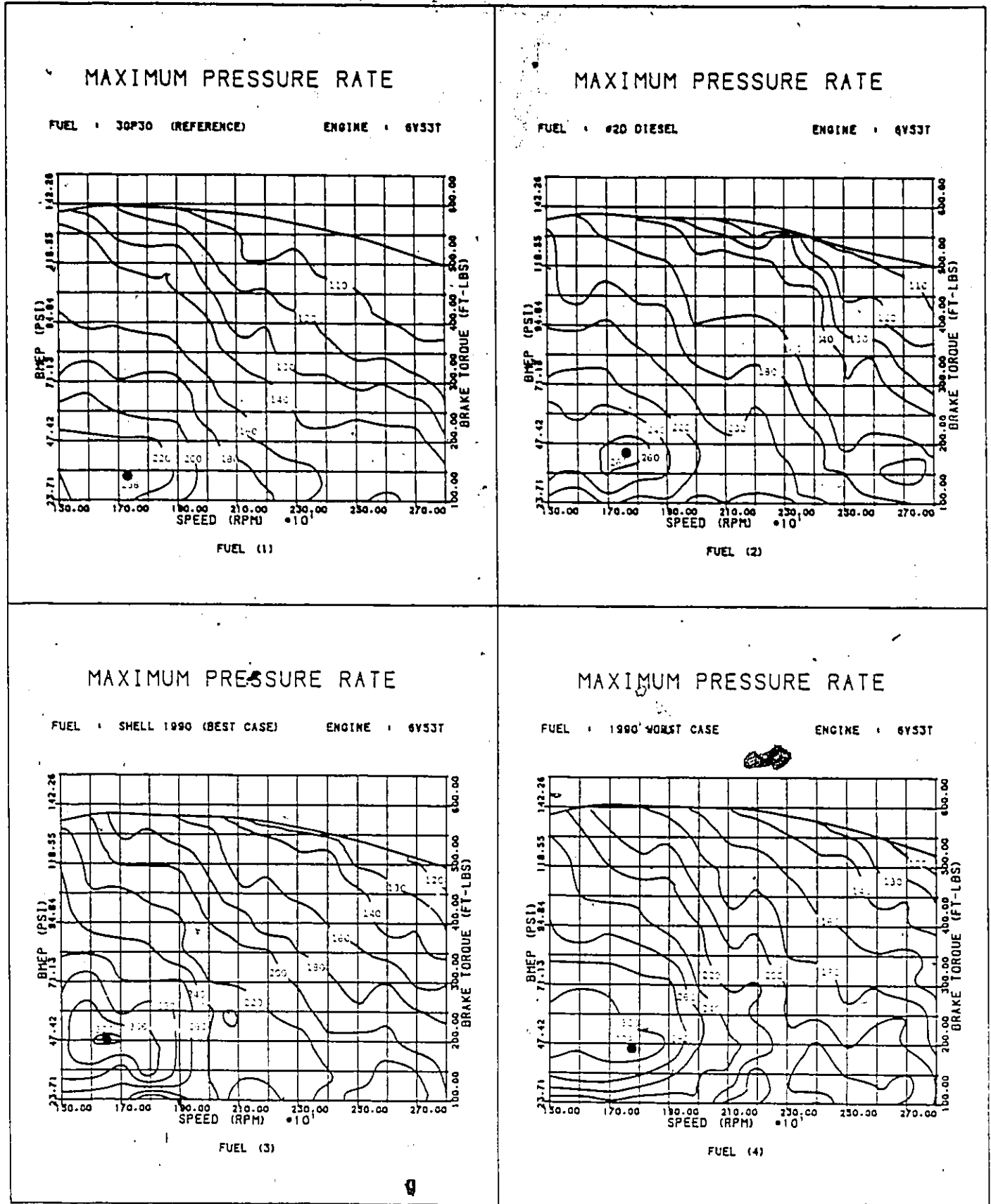


Fig. 6.10: Maximum Pressure Rate Map Comparison

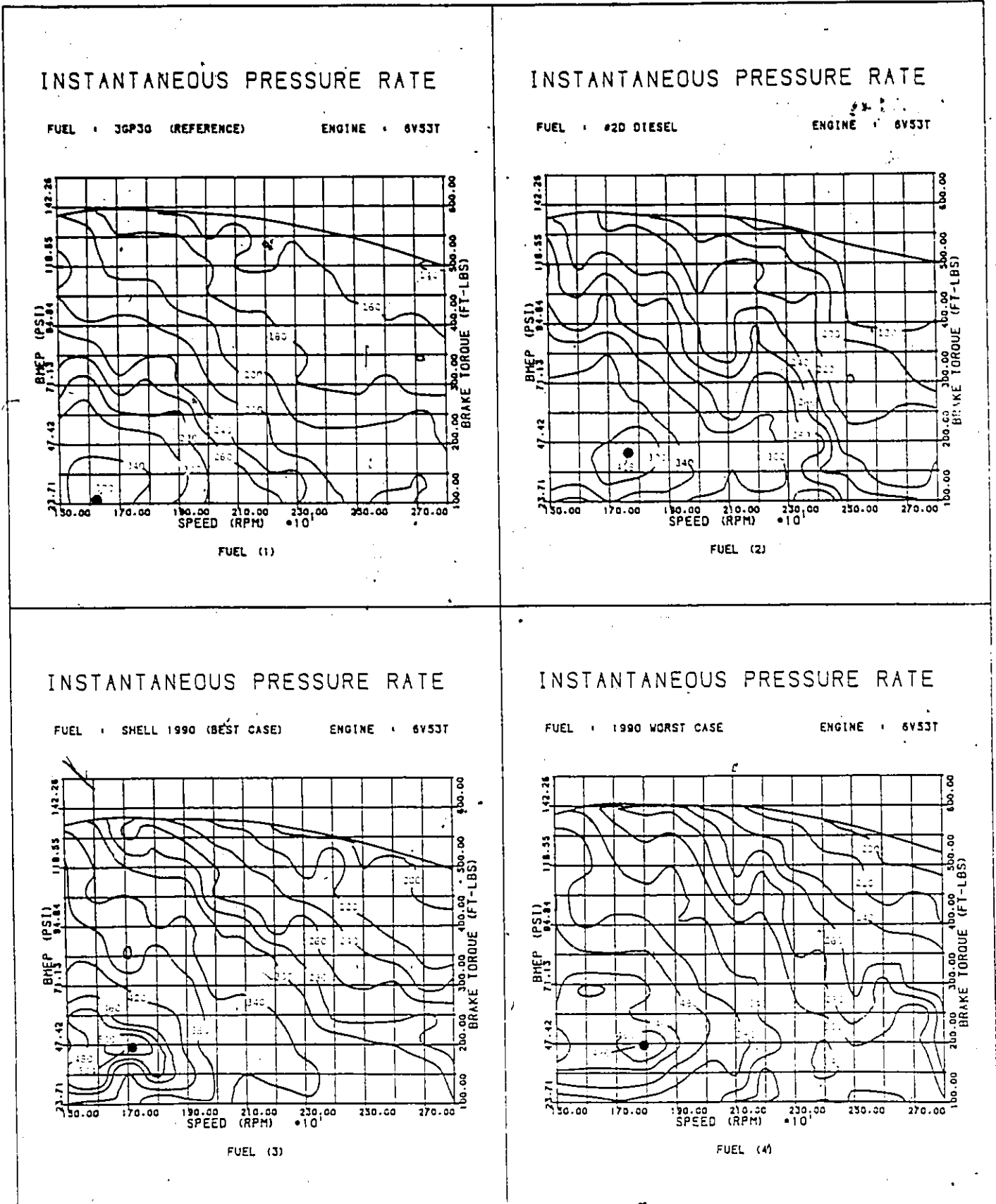


Fig. 6.11: Maximum Instantaneous Pressure Rate Map Comparison

CHAPTER 7

CONCLUSIONS

Throughout this thesis, specific conclusions particular to each section were presented. As such, a set of general overview comments will be given together with an engine-fuel assessment.

7.1 OVERVIEW COMMENTS

1. The University of Ottawa Facility, together with the computerized data acquisition, engine control and data reduction software systems developed, meet the required precision and test repeatability needed for fuel-to-fuel comparisons.
2. TDC was accurately located for the engine tests. Further, it was found that location of TDC must be within ± 0.1 crank angle degrees for accurate indicated horsepower or indicated parameter calculations. From the 107 TDC measurements made, the standard deviation was 0.08, thus the above locational precision is achievable.

For the 6V53T engine, a ± 1.0 degree error in locating TDC would result in a calculated IHP error of from 31.5 to 32.5 IHP, or approximately 10%. For fuel-to-fuel comparisons, it was judged that a 1% error was the maximum that could be tolerated, thus the TDC locational accuracy of ± 0.1 crank angle degrees was required.

3. A digitizing rate of 0.2 crank angle degrees (1800 points/revolution) was found, through a number of cross-correlation and repeat test studies, to be adequate for IHP calculations even on rough combustion fuels. However, this rate was judged to be the minimum requirement as it just barely characterized pressure waves adequately for integral evaluation. Further, averaged P-CA curves were found to be very desirable, if not necessary. However, this digitizing rate was not adequate to characterize explosive detonation or knock.
4. Maximum torque brake characteristic curves (standard engine test procedure), as well as part load brake characteristics, were found to provide valued information. However, such information did not provide any significant insight into engine/fuel compatibility and could, in fact, promote misleading judgements in this area.

5. Indicated parameters were judged to provide a better insight into engine-fuel behaviour, as they represent in-cylinder or combustion space monitoring. They too were unable to provide any objective assessment of engine/fuel compatibility or a preliminary judgement of engine durability. Like brake characteristics, they also could promote misleading judgements in these areas.

Unlike brake parameters however, indicated parameters are difficult to measure and do require sophisticated instrumentation, numerical evaluation and precise knowledge of both the engine under test and the location of TDC. Such measurements do require computerized systems and a very high digitizing rate capability.

6. For fuel-to-fuel comparisons, combustion parameter characterization was judged to be necessary and the only parameters which provided some direct insight into engine/fuel compatibility and perhaps engine durability. Both maximum cylinder pressures and pressure rates were judged to be important in such an assessment. For the 6V53T, pressure rates were judged to be the major concern for the off-specification fuels.

7. In general, it was found that evaluation of pressure rates was not defined (i.e. a standard of measurement with respect to crank angle span must be identified) nor is the interpretation of pressure rates well understood.

However, it is well understood that maximum pressure rates will occur during the early stages of diesel combustion with high rates roughly correlating with ignition delays or fuel cetane numbers.

In this study a 'combustion delay' was defined which was judged (for the engine and fuels tested) to be more tractable and applicable than ignition delay. It further showed an independence from engine speed.

The strongest correlation found was between pressure rates and the combustion development period (time from onset to well established combustion in °CA or the difference between combustion and ignition delays). The correlation applied to all fuels at all engine speed/load settings.

8. The concept of parameter mapping proved to be the most informative data presentation format of all. Optimum or critical engine operating areas became highly visible and definable and engine-fuel trends were easily identified, none of which could be determined or confirmed from conventional characteristic performance curves.

The concept of mapping these parameters is new, thus, reading and interpreting the wealth of information contained in these maps requires development. Computerized interpretation and especially map-to-map comparison techniques deserve consideration and investigation.

However, development of a complete engine-fuel map set (brake, indicated and combustion parameters) requires massive data compilation and handling as well as sophisticated software for reduction and presentation. For these studies, approximately 10,000,000 samples of data per fuel were recorded. This compilation of data is not considered to be excessive for this task and could easily increase substantially if higher digitizing rates are invoked.

7.2 ENGINE-FUEL ASSESSMENT

Although further studies directed at knock evaluation are recommended, the evidence developed to date strongly suggests:

1. Fuels 3 and 4 (both off-specification fuels) result in very high pressure rates which occur over large portions of the operating range of the engine. These rates were observed to give rise to substantial pressure waves and gas vibrations. It is the opinion of the author that such combustion behaviour could result in premature engine failure.

This concern was briefly reviewed with the engine manufacturer who did not share the same degree of concern. Cylinder pressures were seen to be the key factor and the manner in which pressure built to that level (i.e. the pressure rate profile) was not too important.

Again, the author does not share that opinion. While pressure rates per se may not be the factor, they do give rise to gas vibrations which will fatigue engine components and, equally important, result in high metal temperatures and heat transfer.

Certainly, considerably more research has to be done in this area before definitive pressure rate thresholds can be established. The author does believe that the acceptable pressure rate threshold is being exceeded by these off-specification fuels.

2. However, both Fuels 3 and 4 gave good characteristic performance and would not result in a lower power response from the engine. Indeed, for Fuel 4, the reverse is true, increases in power were judged to be sufficient to be discernable by a vehicle operator and could be the selected or preferred fuel. (Engine transient studies, i.e. operation over a prescribed duty cycle, were not conducted but should be considered).
3. The pressure rate problems occur in the early combustion development period and an easy (obvious) 'fix' is not to be expected. It is, however, the opinion of the author that a physical (engine) 'fix' is not to be eliminated. Research should centre about controlled fuel injection timing and injection schedules.

In general, based on the experimental evidence to date, the author would advise caution against any extended or wide spread field use of these fuels prior to both transient and durability studies being conducted. As a minimum, the author recommends a thorough review of these findings with the engine manufacturer regarding engine design limits (re. pressure rates, cylinder peak pressures, etc.) and engine warranties when using these off-specification fuels.

BIBLIOGRAPHY

1. Olree, R.M., Lenane, D.L., "Diesel Combustion Cetane Number Effects"; Ethyl Corporation Research Laboratories, International Congress & Exposition, Detroit, Michigan, February 27-March 2, 1984.
2. Krage, M.K., Lienesch, J.W., Violetta, D.M., "Dynamic Diesel Engine Timing with Microwaves - The General Motor Approach"; SAE 820053, International Congress & Exposition, Detroit, Michigan, Feb. 22-26, 1982.
3. Wood, B.C., "Alternate Fuels in Diesel Engines - A Review"; Southwest Research Institute, Pit & Quarry, Aug. 1981.
4. Baker, Q.A., "Alternate Fuels for Medium-Speed Diesel Engines"; SAE 800330, Congress and Exposition, Cobo Hall, Detroit, Michigan, Feb. 25-29, 1980.
5. Tuteja, A.D., Clark, D.W., "Comparative Performance and Emission Characteristics of Petroleum, Oil Shale and Tar Sands Derived Diesel Fuels"; Detroit Diesel Allison, SAE 800331, 1980.
6. "Improving the Diesel Engine"; Automotive Eng. Vol. 83, Num. 8, Aug. 1983.
7. Robert, N., "Etude de Quelques Sources D'Erreurs Dans La Determination du Point Mort Haut des Moteurs a Pistons"; Journal de Mecanique Appliquee, 0399-0842, Vol. 3, No. 1, 1979.
8. Moore, S.L., Hamilton, G.M., "The Piston Ring at Top Dead Centre"; University of Reading, Tribology Group, Proc. Instn. Mech. Engrs., Vol. 194, No. 1, 1980.
9. Anders, U.W.P., "Influence of the Air Condition in the Combustion Space - Pressure and Temperature in TDC Position of the Piston - As Well As Cetane Number of Fuel on Pressure Rise at Moment of Ignition of Diesel Engine"; Daimler-Benz, ASME, 73-DGP-15, 1974.
10. Bascom, R.C., Wen, S.C., Padd, R.J., "Measurement and Evaluation of Diesel Smoke"; Cummins Engine Co., SAE 780211, 1978.

11. Bolis, D.A., Johnson, J.W., Callen, R., "A Study of the Effect of Oil and Coolant Temperatures on Diesel Engine Brake Specific Fuel Consumption"; Michigan Technological University, SAE 770313, 1977.
12. Russell, F.R., Wilson, J.A., Lewis, O.G., "Complete Automation of a Single Cylinder Diesel Test Engine", Esso Research and Engineering Co., SAE 710817.
13. Bloxham, T.F., Jones, T.F., Murgatroyd, W., Wing, R.D., "Computer Control for IC Engines Development"; CME, Oct. 1972.
14. Benson, R.S., Pick, R., "Recent Advances in Internal Combustion Engine Instrumentation with Particular Reference to High-Speed Data Acquisition and Automated Test Bed"; The University of Manchester Institute of Science and Technology (England), SAE 740695, 1974.
15. Verdonch, I.W., "A Data Acquisition and Processing System for Engine Tests"; State University of Genoa.; SAE 800411, 1980.
16. Sanda, S., Toda, T., Nohira, H., Konomi, T., "Statistical Analysis of Pressure Indicator Data of an Internal Combustion Engine"; Toyota Motor Company, SAE 770882, Passenger Car Meeting Detroit Plaza, Detroit, Michigan, September 26-30, 1977.
17. Lancaster, D.R., Krieger, R.B., Lienesch, J.W., "Measurements and Analysis of Engine Pressure Data"; General Motor Research Lab., SAE 750025, Automotive Engineering Congress and Exposition, Detroit, Michigan, Feb. 24-28, 1975.
18. Steiger, H.A., "Digitalized Measuring Technique Yields Exact Cylinder Pressure Indicator Cards", Int. Symp. on Mar. Eng., Tokyo, Japan, 1973.
19. Williams, H.T., Harper, P.D., Kasonoff, H.A., "Data Acquisition System for Diesel Engine Testing"; Keppers Company, SAE 710819, National Combined Fuels and Lubricants, Powerplant and Truck Meetings, St. Louis, Mo., Oct. 26-29, 1971.
20. Walker, K.L., Warman, E.A., "Data Acquisition and Testing Study", Perkins Engines Co.; SAE 710818, SAE Meeting Oct. 26-29, 1971.
21. Alyea, J.W., Uyehara, O.A., Myers, P.S., "The Development and Evaluation of an Electronic Indicated Horsepower Meter"; SAE 690181, 1969.
22. Brown, W.L., "Methods for Evaluating Requirements and Errors in Cylinder Pressure Measurements", Caterpillar Tractor Co., SAE 670008, 1967.

23. Whyte, R.B., Moyes, B.W., "Effects of Low Cetane Fuels on Diesel Engine Operation: 1- Preliminary Runs on Detroit Diesel 3-71-Engine"; National Research Council of Canada, SAE 821233, 1982.
24. Webster, G.D., Chiappetta, S.J., Ho, J., "Tar Sands Derived Fuels Tested in an Air Cooled High Speed Diesel"; National Defence, Canada, SAE 831206, 1983.
25. Chan, D.Y., Grimsey, R.G., Stoneman, R.T., Webster, G.D., "Canadian Alternative Fuels Tested in a Bombardier Medium Speed Diesel"; SAE 831207, 1983.
26. Currie, T., Whyte, R.B., "Broad Cut Fuels for Automotive Diesels"; SAE 811182, Fuels and Lubricant Meeting, Tulsa, Oklahoma, Oct. 19-22, 1981.
27. Karim, G.A., Burn, K.S., "The Combustion of Gaseous Fuels in a Dual Fuel Engine of the Compression Ignition Type with Particular Reference to Cold Intake Temperature Conditions"; University of Calgary, SAE 800263, Congress and Exposition Cobo Hall, Detroit, Michigan, Feb. 25-29, 1980.
28. Anderton, D., Waters, P.E., "Effect of Fuel Composition on Diesel Engine Noise and Performance"; SAE 820235, 1982.
29. Fisher, R.V., Macey, J.P., "Digital Data Acquisition with Emphasis on Measuring Pressure Synchronously with Crank Angle"; General Motor Co., SAE 750028, Automotive Engineering Congress & Exposition, Detroit, Michigan, Feb. 24-28, 1975.
30. Young, M.B., Lienesh, J.H., "An Engine Diagnostic Package (EDPAC) - Software for Analyzing Cylinder Pressure-Time Data"; General Motors Research Lab., SAE 780967, 1976.
31. Lienesch, J.W., Krage, M.K., "Using Microwaves to Phase Cylinder Pressure to Crankshaft Position"; General Motors Research Labs, SAE 790103, Congress & Exposition Cobo Hall, Detroit, Michigan, Feb. 26-Mar. 2, 1979.
32. Marzouk, M., Watson, M., "Some Problems in Diesel Engine Research with Special Reference to Computer Control and Data Acquisition"; Imperial College of Science and Technology, Combustion Engine Group, 1976.

33. Douaud, A., Eyzat, P., "Digitap - An On-line Acquisition and Processing System for Instantaneous Engine Data - Applications"; Instiut Francais du Petrole, SAE 770218, International Automotive Engineering Congress & Exposition Cobo Hall, Detroit, Michigan, Feb. 28-Mar. 4, 1977.
34. Bennethum, J.E., Mattavi, J.N., Toepel, R.R., "Diesel Combustion Chamber Sampling - Hardware Procedure, and Data Interpretation", General Motors Labs., SAE 750849, SAE Off-Highway Vehicle Meeting Milwaukee, Wisconsin, Sept. 8-11, 1975.
35. Kockanowski, H.A., "The Influence of Top Dead Centre Errors on the Determination of the Indicated Mean Effective Pressure in Internal Combustion Engines"; Journal of Engine Technology, Vol. 37, No. 1/2, 1976.
36. Part of the software used in this thesis was written by Mr. M. Morin as a research assistant at the University of Ottawa engine research team.
The following software packages are included:
 - . The online 1800 point pressure trace storage, calculation of pressure rates, and statistical program.
 - . The map files generation program was corrected and modified to suit the requirements of this work.
 - . The mapping (isocline) program used to produce engine maps in chapter six was modified to produce four plots on one page.
 - . An HP graphics/indicated parameter and data transfer program is also part of these packages.
37. Flanagan, R.C. and Salcudean, M., "Combustion Modelling for Diesel Engines", Contract Report 2SUS2-000396, Department of National Defence, DREO, Ottawa, Canada, 1984, 194 pp.